Characterization of lung tumor-propagating cells reveals a role for CD24 and Yap/Taz in lung cancer progression and metastasis

A dissertation presented

by

Allison Nicole Lau

to

The Division of Medical Sciences

in partial fulfillment of requirements

for the degree of

Doctor of Philosophy

In the subject of

Genetics

Harvard University

Cambridge, Massachusetts

March 2014

Dissertation Advisor: Dr. Carla F. Kim Allison Nicole Lau

Characterization of lung tumor-propagating cells reveals a role for CD24 and Yap/Taz in lung cancer progression and metastasis

ABSTRACT

Lung cancer is the leading cause of cancer deaths worldwide. A large part of this high mortality rate is due to the onset of metastatic disease prior to diagnosis. Advances in treatment for metastatic disease may be achieved by understanding more about the identity of metastatic tumor cells and the mechanisms those cells employ to spread throughout the body. This thesis examined the relationship between cells capable of tumor propagation upon serial transplantation (tumor-propagating cells, or TPCs) and those with metastatic potential.

An orthotopic transplantation assay, in which tumor formation and metastatic growth were measured, revealed the relationship between lung TPCs and metastasis. First, CD24 was identified as a TPC marker in murine lung adenocarcinomas. CD24 expression status was not sufficient to identify lung cancer cells with enhanced metastatic capacity. Selection of tumors cells expressing both TPC markers Sca1 and CD24 enabled enrichment for TPCs with metastatic potential. Knockdown of CD24 in murine lung adenocarcinoma cells resulted in reduced migration *in vitro* and less metastatic tumor formation *in vivo*, demonstrating a functional role for CD24 in lung cancer cell metastasis.

Gene expression analysis demonstrated that many genes in the Hippo pathway and targets of the Hippo mediators Yap and Taz were differentially expressed in lung

TPCs. A gene signature of Yap/Taz targets was significantly associated with worse lung adenocarcinoma patient survival and metastasis. Knockdown of Yap and Taz in murine lung adenocarcinoma cells showed that Yap and Taz are important for lung cancer cell migration. Taz was especially important for metastatic properties of these cells *in vivo*. Activation of Yap in a mouse model of lung adenocarcinoma increased tumor progression and number. These results show that Yap and Taz play an important role in lung tumor migration, progression and metastasis.

The work described here provides insight into the relationship between TPCs and metastasis and identifies pathways utilized by metastatic lung cancer cells. Future studies defining the detailed mechanisms by which CD24 and Yap/Taz activity affect lung cancer metastasis may lead to new treatment options for this deadly disease.

ACKNOWLEDGEMENTS

First, I'd like to thank my advisor Carla Kim. I am so grateful for her support and for her confidence in me and this project. She gave me the flexibility to pursue my own interests and ideas while still giving scientific guidance and direction. Her enthusiasm was so great that I left almost every one of our meetings with a renewed sense of inspiration and purpose. Carla was also extremely supportive of me figuring out my future career goals and was encouraging when I wanted to explore my interest in teaching. I learned so much from her and I cannot thank her enough for all she has done as my advisor. She has been such a wonderful mentor and role model to me.

I would like to thank my Dissertation Advisory Committee members Paola Arlotta, Hanno Hock, and Len Zon. They were more than willing to make time for me and I am very grateful for their insightful suggestions and encouragement. All three of them provided both scientific and professional guidance. I would also like to thank my defense committee members Bill Hahn, Sandy McAllister, and Bob Varelas.

There have been several other faculty members who have been very generous with their time and mentorship. Maria Kontaridis has been my mentor through the Harvard Graduate Women in Science and Engineering mentorship program for the past four years. I am grateful to have had another successful scientist and role model to meet with to discuss science, lab dynamics, professional development, and personal life. Fernando Camargo was generous with reagents and technical advice; I was very lucky to have such an expert on the Hippo pathway in our department. He also gave me the opportunity to be a teaching fellow for a course that he taught, and was a source of inspiration for my interest in teaching. Fred Winston and Sarah Wojiski also mentored

me in my teaching efforts and were always willing to watch my practice lectures and provide feedback to help me improve.

I'd like to thank all of the Kim Lab members both past and present. Their kindness and friendship have been very important to me during my graduate school years. I especially want to thank Juliana Barrios and Alex Beede who helped manage the large mouse colony necessary to complete this work and also provided technical assistance. Kerstin Sinkevicius was my rotation supervisor and taught me most of the techniques I used in this project. She has been a great friend and mentor, providing both technical and professional advice. In addition to Kerstin, I'd also like to thank all of the other postdocs who have helped and advised me over the years: Christine Fillmore, Joo-Hyeon Lee, Kristen Leeman, Sam Rowbotham, and Sima Zacharek. The other graduate students who came before me were extremely welcoming and helpful colleagues: Steve Curtis, Dave Raiser, and Arven Saunders. There have been many others as well who have been important parts of the lab community. I will especially miss eating lunch together, celebrating birthdays, traveling to conferences and retreats, and dressing up for Halloween.

My friends and family have been a great source of support and inspiration for the past five years. I am very thankful that my friends have remained so close throughout our graduate school years. They have been a unique, fun, and close-knit support group. I would like to thank my parents Andy and Elaine Lau and my brother Jeffrey Lau for all of their love and support, even though coming to graduate school meant moving away from them for the first time. I hope that I have given all of my friends and family members the love and encouragement that they all have bestowed upon me.

Lastly, I'd like to thank my fiancé Tim Calamaras. It has been truly rewarding to share my graduate school experience with someone who was going through the same process and understood all of the frustrations, joys, and accomplishments along the way. I am incredibly grateful for all of the encouragement, support, friendship, and love that he has given me. It is hard for me to express how thankful I am to have him in my life, and I'm so excited to see what is next for us.

TABLE OF CONTENTS

Abstract..... iii

Acknowledgements..... v

Table of Contents..... viii

Chapter 1: Introduction..... 1

Cancer and metastasis..... 2

Lung Cancer..... 4

Tumor Heterogeneity and Cancer Stem Cells..... 7

Endogenous Lung Progenitor Cells and

Cells of Origin for Lung Cancers..... 12

Evidence for Lung Cancer Stem Cells..... 21

Metastasis and Cancer Stem Cells..... 24

Summary of the Dissertation..... 26

References..... 28

Chapter 2: Tumor-propagating cells and Yap/Taz activity contribute to lung tumor progression and metastasis..... 39

Abstract..... 42

Introduction..... 43

Results..... 45

Discussion..... 85

Materials and Methods..... 89

Acknowledgements..... 95

References..... 96

Chapter 3: Discussion..... 101

Summary..... 103

Lung TPCs and Metastasis..... 105

The Role of CD24 in Lung Cancer Metastasis..... 110

The Role of Yap/Taz in Lung Cancer Metastasis..... 121

Conclusions..... 142

References..... 144

Appendix..... 154

Mice Used in Tumor Transplants……..……..... 155

Sca1 Gene Signature..... 157

Genes Down in Sca1+ Cells..... 170

Genes Down in shTaz Cells..... 183

GSEA in shGFP vs shTaz cells..... 189

Transcription Factors Differentially Expressed

in Lung and Lung Stem Cells..... 202

Testing of CCSP and SPC knock-in mice for lineage tracing…….. 210

CHAPTER 1:

Introduction

At the time of submission of this dissertation, excerpts from the work presented in this chapter have been published in *Molecular Therapy* as a review entitled *Stem cells and regenerative medicine in lung biology and diseases.* All writing and figures in this chapter were created by ANL.

Cancer and Metastasis

In the United States, roughly one in three women and one in two men will develop cancer in his or her lifetime (Siegel et al., 2013). One in four deaths in the United States is due to cancer; within Hispanic and Asian Americans, cancer has overcome heart disease to become the most common cause of death (McCracken et al., 2007; Siegel et al., 2012). Despite the "war on cancer" that was declared in 1971, the survival of patients with metastatic disease has scarcely changed (Leaf, 2004).

Because of the rise of cancer incidence and death in the 20th century many of us think of cancer as a modern disease (Jones et al., 2012). Since cancer increases with prevalence as we age, this increase in incidence is largely due to the fact that life expectancy in the U.S. has increased by about 30 years in the last century (Arias et al., 2008). However, evidence of cancer has been around for thousands of years. The ancient Greek physician Hippocrates first introduced the term *karkinos (or carcinos, carcinoma),* the Greek word for crab, to describe the image of a tumor surrounded with its blood vessels and projections around 400 BC (Sakorafas and Safioleas, 2009). However, there are records and evidence of cancers dating back many thousands of years. The first known recording of cancer was written on what is known as The Edwin Smith Papyrus in the seventeenth century BC, and is thought to be the teachings of

Imhotep, an Egyptian physician who lived around 2635 BC (Sakorafas and Safioleas, 2009). Scientists have uncovered mummified remains of malignant tissue dating to around 400 AD, as well as skeletons with signs of metastatic tumors growing in the bones from much more ancient relics (Aufderheide, 2003; Prates et al., 2011; Schultz et al., 2007). In fact, cancer may be one of the oldest human diseases.

There are several properties or “hallmarks” that all cancers are purported to share. These include genome instability and mutation, resisting cell death, deregulating cellular energetics, sustaining proliferative signaling, evading growth suppressors, avoiding immune destruction, enabling replicative immortality, tumor-promoting inflammation, inducing angiogenesis, and activating invasion and metastasis (Hanahan and Weinberg, 2011).

This thesis will focus on the last hallmark of cancer: invasion and metastasis. Metastasis is estimated to be responsible for 90% of cancer-associated mortality (Chaffer and Weinberg, 2011). The term “metastasis” for the spread of cancer was coined by the French physician Joseph Recamier in 1829 (Carr and Carr, 2005). In 1889, Stephen Paget was the first to attempt to identify which organs that breast cancers metastasized to, and developed what is known as the “seed and soil” hypothesis (Paget, 1989; Talmadge and Fidler, 2010). Paget wrote, “When a plant goes to seed, its seeds are carried in all directions, but they can only live and grow if they fall on congenial soil” (Paget, 1989). Ewing later challenged this hypothesis, proposing that mechanical forces and circulatory patterns were responsible for organ specificity in metastasis (Ewing, 1928). Fidler and colleagues later showed using parabiosis experiments that the pattern of metastasis formation was dependent on tumor cell

properties and host factors, further supporting the seed and soil hypothesis (Hart and Fidler, 1980).

Today, it is understood that metastasis is made up of a “cascade”, or sequence of events (Chaffer and Weinberg, 2011; Hanahan and Weinberg, 2011). This cascade can also be thought of as two distinct phases: dissemination and colonization. First, cancer cells must locally invade the surrounding tissue and intravasate into the vasculature of the blood vessels or lymph. Next, cells must survive and migrate through the vessels and then extravasate into the new metastatic site. Finally, the tumor cells must be able to survive and grow in the new microenvironment to form a new tumor.

Lung Cancer

Lung cancer is an ideal system to study metastasis since ~85% of patients present with metastatic disease; the five year survival rate for lung cancer is ~15% (Siegel et al., 2013). Lung cancer is the leading cause of cancer-related death for both men and women worldwide; over 1.3 million people die of this disease every year (Ferlay et al., 2010; Siegel et al., 2013). This is largely due to the carcinogenic affects of cigarette smoke, yet about 10-25% of lung cancer cases worldwide occur in never-smokers (Ferlay et al., 2010). Air pollution such as radon, household fumes such as coal and wood burning fumes or cooking oil vapors, as well as industrial hazards such as asbestos and radiation exposure are also known to play a role in lung cancer risk (Hammond et al., 1979; Mumford et al., 1987; National Research Council, 1999; Neugut et al., 1994). There are two histological subtypes of lung cancer: small cell lung cancer (SCLC) making up about 20% of lung cancer cases, and non-small cell lung cancer

(NSCLC), 80% of cases. Non-small cell lung cancer is further subdivided into three groups: large cell carcinoma, squamous cell carcinoma, and adenocarcinoma (Travis et al., 1999).

Lung adenocarcinoma is characterized by glandular differentiation and mucin production, as well as formation in the peripheral lung (Travis et al., 1999). Adenocarcinoma is the most prevalent subtype of lung cancer overall and is the most common form of lung cancer seen in never-smokers (Toh et al., 2006). Conversely, smoking has historically been associated with small cell lung cancer and squamous cell carcinoma, although more smokers are now developing adenocarcinoma, thought to be due to the changes in cigarettes over the past few decades (Hoffmann et al., 2001). Common mutations in lung adenocarcinoma are activating mutations in the genes *KRAS* (~30%), *BRAF*, *ERBB2 (HER2)*, and *PIK3CA*, and loss of function mutations in *TP53* (~50%), *STK11* (*LKB1)* (over 15%), *RB1*, *NF1*, *CDKN2A*, *SMARCA4*, and *KEAP1* (Ding et al., 2008; Imielinski et al., 2012). Other common mutations include alterations in *EGFR* (over 15%) and *ALK* (Ding et al., 2008; Imielinski et al., 2012). There are now mouse models of lung adenocarcinoma that incorporate mutations in many of these genes as oncogenic drivers.

KRAS is member of the Ras family of proto-oncogenes that encode a membrane- bound GTPase signaling protein important for proliferation, differentiation, and survival (Karnoub and Weinberg, 2008). When bound to GDP, Ras proteins are inactive. Activation of upstream growth factor receptors results in a switch to a GTP-bound Ras protein, which then activates downstream pathways such as MAPK or PI3-K. Oncogenic mutations in Ras proteins can affect the GTPase activity of the proteins,

blocking inactivation of the protein back to its GDP-bound state. The mouse model of adenocarcinoma developed by Tyler Jacks and colleagues carries a knock-in allele at the endogenous *Kras* locus, allowing for endogenous expression levels of a mutant Kras protein (Jackson et al., 2001). The sequence contains a stop cassette flanked on either side by LoxP sites followed by an activating mutation in Kras at amino acid 12, a glycine to aspartic acid substitution (LSL-KrasG12D, Kras hereafter). This Kras mutation results in decreased GTPase activity and therefore constitutive signaling. Tumorigenesis can be initiated in a lung specific manner by delivering an adenovirus or lentivirus expressing Cre recombinase to the lungs via either intranasal or intratracheal administration. In the Kras model, tumors develop 6-8 months after Cre administration, and metastases have not been reported in these mice by us or others.

This Kras lung tumor model can also be combined with loss of the cell cycle regulator and tumor suppressor gene *Tp53* to yield more aggressive lung tumors. *TP53* is the most commonly mutated gene in human lung cancer, and is mutated in over 50% of lung adenocarcinomas (Imielinski et al., 2012). In these mice, the LSL-KrasG12D knock-in is combined with two floxed p53 alleles: loxP sites flank exons 2 and 10 of the *Tp53* gene, Kras;p53-flox hereafter (Jackson et al., 2005). Advanced adenocarcinomas form within 15-19 weeks after Cre administration, and approximately 50% of mice develop metastases (between 30-50% in our hands).

Studies of mouse models of lung adenocarcinoma have been used to help further identify genes important for lung cancer metastasis. Loss of the tumor suppressor *Lkb1* in Kras-driven lung cancers was found to confer metastatic ability as well as squamous differentiation (Carretero et al., 2010; Ji et al., 2007). A study using

lentiviral Cre integration sites to track metastatic tumors the Kras;p53-flox model found that tumors that metastasized downregulated the transcription factor *Nkx2-1* (Winslow et al., 2011). In addition to identification of genes and pathways important for lung cancer metastasis, another main focus of cancer research has been to study the heterogeneity present in lung tumors to identify tumor subsets with enhanced tumorigenic properties, often referred to as cancer stem cells.

Tumor Heterogeneity and Cancer Stem Cells

Current cancer stem cell hypotheses propose that a subpopulation of cells within a tumor possesses characteristics of stem cells and can give rise to the heterogeneity of cell types often found in many tumor types. Cancer stem cells are typically identified by dissociating tumor cells, using fluorescence-activated cell sorting to select tumor subpopulations, and transplanting these cells *in vivo*. In some cases, the cancer stem cell population shares marker expression with normal tissue-specific stem cells. Importantly, cancer stem cells are thought to be resistant to available treatment strategies including radiation and chemotherapeutics.

The idea that tumors were made up of cells with stem cell-like properties has been around for over 150 years, postulated in the early-mid 1800s by Recamier and Virchow (Sell, 2004; Wicha et al., 2006). This theory was then formalized by Durante and Virchow's student Conheim in the late 1800s as the "embryonal rest" theory of cancer (Sell, 2004). The embryonal rest theory held that adult tissues contained rare, dormant embryonic remnants that can become reactivated to form cancers. However, this theory fell out of favor by the early 1900s (Sell, 2010).

In the 1960s and 70s there was a resurgence in studies on tumor heterogeneity. In 1961, Till and McCulloch proposed that tissue-specific stem cells could be the cells of origin for cancer, and in 1967, Pierce proposed the idea that cancers were a result of the maturation arrest of stem cells (Till and McCulloch, 1961; Pierce, 1967). Several groups reported that murine and human tumor cells had low colony forming ability in culture, anywhere from 0.001-1% of cells (Hamburger and Salmon, 1977; Messner and McCulloch, 1973; Park et al., 1971); additionally, it was reported that less than 1% of murine lymphoma cells could generate spleen colonies *in vivo* (Bruce and van der Gaag, 1963), lending support to the idea that tumors contained heterogeneous populations. Possible explanations for this heterogeneity were that (1) each cell had a similarly low chance of colony/tumor formation, or that (2) only a certain subset of cells within the tumor population had this ability. However, tumor subpopulations had not been identified that were more or less able to form tumors.

In the mid-late 1990s, John Dick's laboratory performed the seminal experiments that for the first time prospectively isolated a subset of what are referred to today as "cancer stem cells." Dick and colleagues identified a rare population of CD34+CD38- cells within human acute myeloid leukemias capable of tumor formation after transplantation, which they termed "leukemia-initiating cells" (Bonnet and Dick, 1997; Dick, 1996; Lapidot et al., 1994). The leukemia-initiating cells shared cell-surface marker expression (CD24+CD38-) with normal hematopoietic stem cells, had the ability to self-renew, as they had the ability to generate leukemias upon serial transplantation, and also had the ability to form differentiated tumor progeny.

Cancer stem cell populations have since been identified in a wide variety of cancers, including brain (Singh et al., 2004), breast (Al-Hajj et al., 2003), colon (O'Brien et al., 2007; Ricci-Vitiani et al., 2007), liver (Yamashita and Wang, 2013), melanoma (Boiko et al., 2010), ovarian (Foster et al., 2013), pancreatic (Li et al., 2009), and prostate (Patrawala et al., 2006) cancers. However, the cancer stem cell hypothesis has been frequently challenged. Much of this debate has centered on the fact that to identify cancer stem cell populations, human cell populations were transplanted into immunocompromised, mostly NOD/SCID mice to test for serial transplantation or self-renewal ability. Criticism of the cancer stem cell hypothesis focused on the idea that this artificial xenotransplantation assay selects for cells that are able to survive in this foreign microenvironment, and is not representative of the human tumor biology.

The first major study to test this experimentally was by Strasser and colleagues in 2007 (Kelly et al., 2007). Instead of using human tumor cells, they transplanted mouse lymphomas and leukemias into histocompatible mice and found that at least 10% of tumor cells could propagate the disease. These results suggested that cells with tumor propagating ability were more abundant than previously reported, and that some of the differences in tumor propagation ability were due to sub-optimal transplantation assays.

Another major challenge to the cancer stem cell hypothesis came from Sean Morrison's laboratory in 2008. This study again challenged the assays that were being used to identify cancer stem cell populations (Quintana et al., 2008). Instead of NOD/SCID mice, they used a new strain of mice with a NOD/SCID background combined with loss of the interleukin-2 receptor gamma chain, Il2rg-/- (NSG) mice.

These mice are more highly immunocompromised since they lack natural killer cells, T, and B cells whereas NOD/SCID mice only have impaired T and B cell maturation. In addition to the new mouse model, Morrison and colleagues also mixed matrigel extracellular matrix proteins with the cells upon transplantation to increase engraftment rates. They found that 25% of cells from human melanoma patients could form tumors when transplanted using their optimized transplantation assay. Most impressively, they performed single cell transplantations and found that 27% of single cells were able to form melanomas upon transplantation. They tested many markers previously reported to mark cancer stem cell populations and were unable to find any subpopulations that lacked tumorigenic potential (Quintana et al., 2008; Quintana et al., 2010).These results indicated that there are cancers such as melanoma that do not follow the cancer stem cell hierarchy.

Technical advances in the past few years have now made it possible to perform tumor clonal analysis *in vivo* to test cancer stem cell hypotheses. The first study showing evidence for cancer stem cells during unperturbed solid tumor growth was performed by Cedric Blanpain's lab in 2012 in murine squamous skin tumors (Driessens et al., 2012). They used a CreER/Lox lineage tracing and clonal analysis strategy that enabled them to label ~1% of basal tumor epithelial cells by titrating a low dose of tamoxifen administration. The authors found that invasive squamous cell carcinomas, unlike benign papillomas, contained a geometric expansion of a single cancer stem cell population. This study was the first to demonstrate that there were tumor cells with stem cell-like qualities in an unperturbed solid tumor.

Another cell labeling study by Luis Parada's lab identified a putative glioma stem cell population that was resistant to chemotherapy and responsible for tumor regrowth in an *in vivo* mouse model (Chen et al., 2012). The authors used a Nestin-TK-IRES-GFP mouse to label endogenous glioma tumor cells, and treated the mice with the chemotherapeutic agent temozolomide to transiently arrest tumor growth. Tumor regrowth occurred in the Nestin+ GFP marked population. The TK allele then enabled them to treat the mice with ganciclovir in order to kill off this population and show that ablation of GFP+ cells impeded tumor development. This study was the first to provide genetic evidence that there were cells at the top of a cellular hierarchy that were left behind after chemotherapy treatment, and that killing off these cells could have therapeutic benefit.

Another recent study of clonal analysis and tumor heterogeneity from John Dick's laboratory used DNA copy-number alteration profiling, sequencing, and lentiviral lineage tracking to trace the fate of singe cell-derived clones from 10 different human primary colorectal tumors over multiple serial transplantations in mouse renal capsule xenografts (Kreso et al., 2013). Some xenografts remained very similar to the parent tumor, while in others the first transplant and the parental tumor differed drastically, indicating clonal selection during xenograft growth. The authors found that there were clones that persisted through multiple passages, clones that became extinct, clones that remained below the detection threshold initially but then reemerged in later transplantations, and clones that disappeared and later reemerged. Treatment with chemotherapeutic agents eliminated persistent clones and increased those dormant clones initially below the detection threshold.

This study supports the idea that cancer stem cells and non- cancer stem cells are not “black and white” states, but that cellular heterogeneity is more of a “shades of grey” phenomenon (Marusyk and Polyak, 2013). It is possible that tumor cells have a gradient of tumor-propagating ability, or that the cancer stem cell state is reversible (Meacham and Morrison, 2013). Furthermore, it is thought that cancer stem cells no longer need be a rare subpopulation within the tumor. It is likely that many processes are co-existing within tumors that contribute to tumor heterogeneity, including the cancer stem cell model, clonal evolution, and inherent genetic or environmental properties (Magee et al., 2012) (Figure 1-1).

Endogenous Lung Progenitor Cells and Cells of Origin for Lung Cancers

It is important to differentiate the “cancer stem cell” population from the “cell of origin” of cancers. While cancer stem cells refer to a self-renewing cell in the fully formed tumor, the cell of origin refers to the normal cell from which a tumor arises (Visvader, 2011). These ideas are often confused since stem cells, with their quiescence and self-renewal ability, are thought to be susceptible to transformation into cancers. However, there is also evidence that more differentiated cells are able to give rise to cancers as well. In the lung, cancers are hypothesized to originate from endogenous stem and/or progenitor cells.

Endogenous lung stem and progenitor cells are thought to contribute to epithelial maintenance and injury repair. These cells can self-renew and differentiate into progenitors or other more differentiated cells. Since the adult lung is a tissue that has a very low turnover rate, murine lung injury models have been used to identify

Figure 1-1: Models of Tumor Heterogeneity

A. The cancer stem cell model hypothesizes that a subpopulation of cells (blue) has the inherent ability to self-renew and give rise to the heterogeneity of cell types found in the tumor (blue, red, green). Cancer stem cells are typically identified by dissociating tumor cells, using fluorescence-activated cell sorting to select tumor subpopulations, and transplanting these cells *in vivo* to test serial transplantation ability. **B.** The clonal evolution model describes the process by which different tumor cell clones can acquire tumorigenic properties that enable them to contribute to tumor progression. Some clones will acquire greater tumorigenic abilities (blue), while other clones become less tumorigenic (red). **C.** Tumor heterogeneity is likely influenced by a combination of the cancer stem cell model, the clonal evolution model, and other environmental factors not depicted here. Adapted from (Magee et al., 2012).

Figure 1-1: (continued)

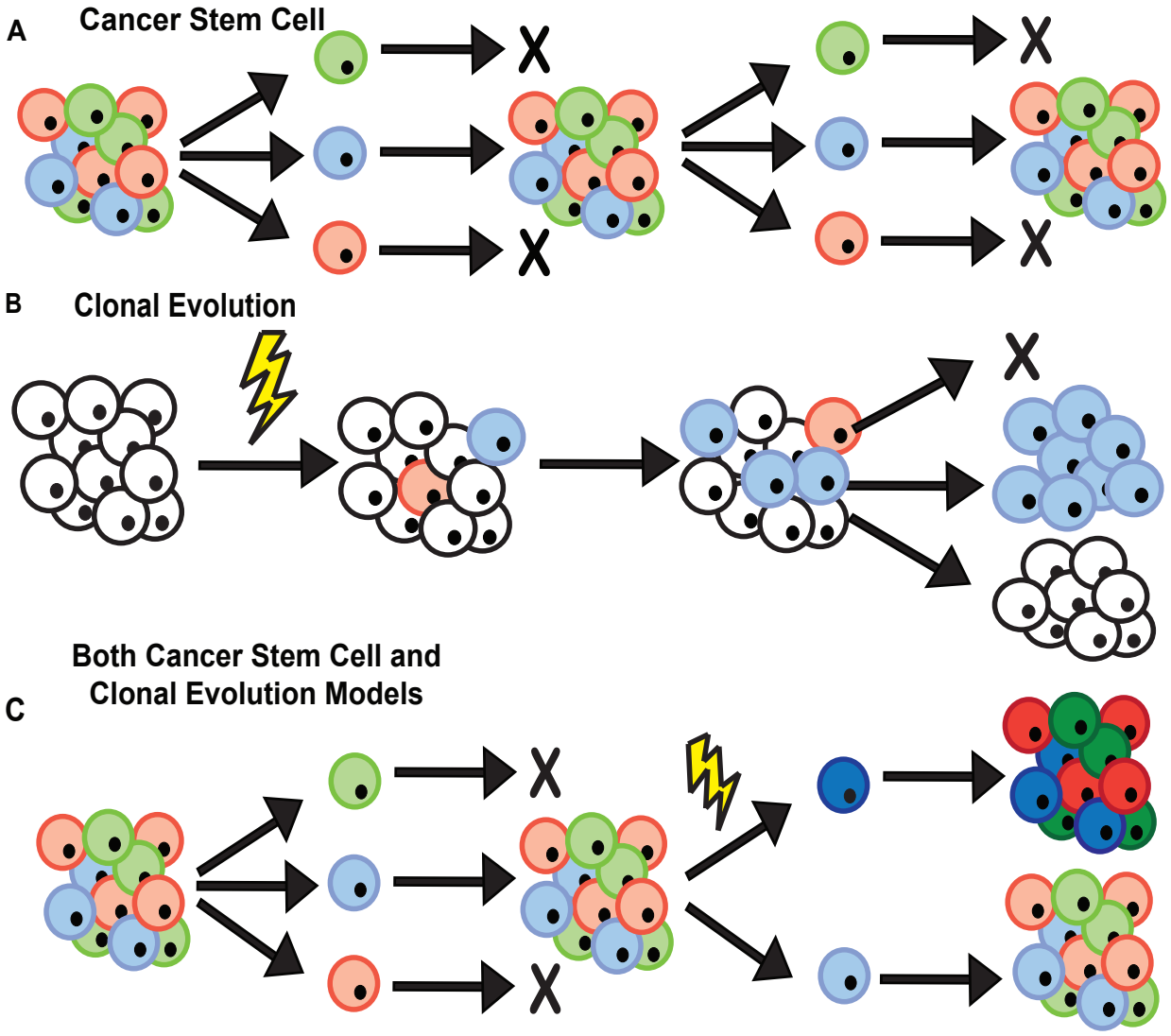

stem/progenitor cells by inducing cellular proliferation and repopulation of the lung epithelium (Rawlins and Hogan, 2006). What these studies have detailed is a complex heterogeneity of putative endogenous stem/progenitor cells with different candidates located in different regions of the mouse lung. This is depicted in schematic form in Figure 1-2.

Basal epithelial cells are a stem/progenitor cell population important in tissue homeostasis and injury repair in the trachea and proximal airways in mice and throughout the airways in humans (Borthwick et al., 2001; Daniely et al., 2004; Rock et al., 2009; Schoch et al., 2004). Lineage tracing studies in the mouse have revealed that basal cells can give rise to club (Clara) cells and ciliated cells in the proximal airways during homeostasis as well as after sulfur dioxide injury in mice (Hong et al., 2004a; Hong et al., 2004b). Basal cells are hypothesized to be the cells of origin for lung squamous cell carcinoma, since squamous cell carcinomas more frequently occur in the proximal lung and often express basal cell markers (Davidson et al., 2013).

The distal bronchiolar epithelium includes non-ciliated columnar club cells which produce surfactants (Massaro et al., 1994) and ciliated cells which propel these surfactants across the bronchiolar wall (van der Schans, 1997). In the airways, the areas surrounding neuroepithelial bodies (NEB) and the bronchioalveolar duct junction (BADJ) represent two different stem/progenitor cell niches. Variant club cells resistant to naphthalene injury were identified near the NEB in the proximal airways and at the BADJ in distal airways (Giangreco et al., 2002; Hong et al., 2001; Reynolds et al., 2000). These cells survive severe injury and can re-epithelialize the airways. As demonstrated by a lineage-tracing study, club cells are stem/progenitor cells that have

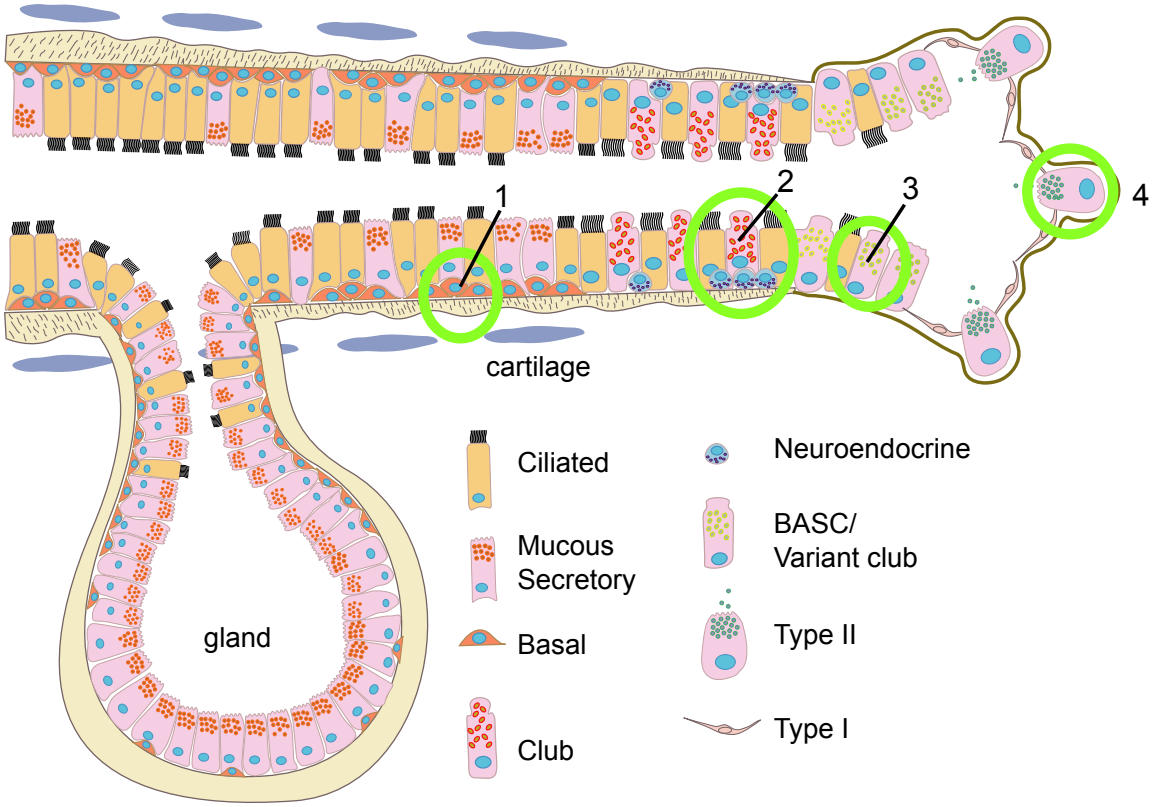

Figure 1-2: Schematic of putative lung stem/progenitor cells in the mouse lung.

1) Basal cells in the tracheobronchial region; 2) variant club cells associated with pulmonary neuroendocrine cell bodies; 3) variant club cells/BASCs present at the bronchioalveolar duct junction; 4) alveolar type II (AT2) cells present in the alveolar space. (Lau et al., 2012) originally adapted from (Randell, 2006).

long-term self-renewal ability and can also generate ciliated cells during epithelial homeostasis (Rawlins et al., 2009).

The epithelium at the air interface of the alveoli consists of flat alveolar type I (AT1) cells and cuboidal alveolar type II (AT2) cells, which produce surfactant to lower surface tension and aid in AT1 cell-mediated gas exchange (Fehrenbach, 2001; Herzog et al., 2008). In the alveolar epithelium, repopulation after bleomycin injury is due to proliferation of AT2 cells, which act as stem/progenitor cells for AT1 cells (Aso et al., 1976; Barkauskas et al., 2013; Desai et al., 2014; Isakson et al., 2001; Kawamoto and Fukuda, 1990).

Bronchioalveolar stem cells (BASCs) are another naphthalene-resistant progenitor cell population located at the BADJ, identified based on their co-expression of the club cell marker, club cell secretory protein (CCSP), and the alveolar type II (AT2) cell marker, pro-surfactant protein C (pro-SP-C) (Kim et al., 2005). BASCs can be isolated using FACS to select for cell expression of the stem cell marker Sca1 after elimination of hematopoietic cells and endothelial cells (CD45-CD31-Sca1+). Importantly, more recent studies have shown that the CD45-CD31-Sca1+ population is more heterogeneous than previously appreciated (Raiser and Kim, 2009; McQualter et al., 2010). Based on our own observations that BASCs are contained in the $Sca1^{low}$ population and express low levels of CD24, a robust marker profile for enriching for BASCs utilizes CD45-CD31-EpCAM+$Sca1^{low}CD24^{low}$ (Zacharek et al., 2011).

BASCs can self-renew in a 3-dimensional (3D) co-culture matrigel assay with primary lung endothelial cells and differentiate into colonies expressing airway and/or alveolar lineage markers and morphology (Lee et al., 2014). Importantly, single murine

CD45- CD31- EpCAM+ Sca1+ cells were able to form both bronchiolar and alveolar colonies *in vitro*, supporting the hypothesis that BASCs represent a true lung stem cell population. BASCs have also been implicated in injury repair after bleomycin-induced injury due to their proliferation after treatment and the *in vitro* data showing their ability to differentiate into alveolar cells in culture (Kim et al., 2005; Lee et al., 2014). A lineage-tracing study using CCSP-CreER mice showed that the percentage of lineage-labeled cells did not increase in the alveolar space during homeostasis or following hyperoxia injury, suggesting that CCSP-expressing cells did not give rise to alveolar cells (Rawlins et al., 2009). However, other lineage-tracing studies using the same CCSP-CreER mice found that CCSP+ cells can give rise to both AT1 and AT2 cells following bleomycin injury (Rock et al., 2011; Tropea et al., 2012). These studies suggest that bronchiolar cells may be able to form alveolar structures under certain conditions.

BASCs have been proposed as a cell of origin in murine models of lung adenocarcinoma, as BASC expansion has been observed after oncogenic Kras induction, and increased tumor number and area was also observed in these mice after injury-induced BASC expansion (Kim et al., 2005). In addition to oncogenic Kras, BASC expansion has been observed after oncogenic stimulation or loss of tumor suppression in other adenocarcinoma models (Besson et al., 2007; Pei et al., 2007). BASC-like cells co-expressing SPC and CCSP can be found within murine lung adenocarcinomas (Curtis et al., 2010; Kim et al., 2005).

Others have proposed that AT2 cells are cells of origin for lung adenocarcinoma (Desai et al., 2014; Mainardi et al., 2014; Xu et al., 2012). Hogan and colleagues used CCSP-CreER and SPC-CreER knock-in mice in combination with the LSL-KrasG12D

allele to drive tumorigenesis in CCSP-expressing (club or BASC, low levels in AT2) or SPC-expressing (BASC or AT2) cells (Xu et al., 2012). They found that both cells near the BADJ and in the alveoli proliferate after KrasG12D induction by either driver, but that adenocarcinomas preferentially formed in the alveoli versus hyperplasia near the BADJ. Similar results were found by Krasnow and colleagues (Desai et al., 2014). These results suggest that AT2 cells can serve as the cells of origin for adenocarcinomas, but due to expression of SPC and CCSP in other cell types does not definitely show that they are the only cell type to be able to do so.

Another study by Barbacid and colleagues supports the AT2 cell being the cell of origin of adenocarcinomas (Mainardi et al., 2014). In this study, Kras-G12V was driven by *RERT* mice, a knock in strain that expresses Cre-ER under the control of the locus encoding the large subunit of RNA polymerase II. It was found that large clusters of cells that led to adenocarcinomas were only found in the alveolar region. At 4 weeks after treatment, they identified large clusters that were SPC+, as well as some BADJ clusters that were CCSP+ and SPC+, suggesting their origin from BASCs. However, at 8 weeks, all of the lesions were located in the alveoli and were SPC+ suggesting that the advanced lesions originated from SPC+ AT2 cells. The authors also looked at intratracheal infection with AdCre in the LSL-KrasG12V mice and found similar results; bronchiolar or BADJ lesions never progressed to high-grade lesions, while those in the alveoli progressed to large stage adenocarcinomas.

A recent study by Berns and colleagues supports the idea that there are multiple cells of origin for lung adenocarcinoma (Sutherland et al., 2014). Using Ad-CCSP-Cre and Ad-SPC-Cre viruses to drive Kras and delete p53 in club cells, BASCs, or AT2

cells, the authors concluded that both CCSP+ (club or BASC) cells and SPC+ (AT2 or BASC) cells can form adenocarcinomas. They also used a confetti reporter mouse to show that after infection with Ad-CCSP-Cre, lesions arise from CCSP+ cells in the BADJ, suggesting their origin from BASCs. Without drivers that are more cell-type restricted, it is difficult to rule out contribution of multiple cell types to tumor initiation. A main issue in the lung field is the lack of restrictive markers for each cell type, as CCSP and SPC are expressed in both BASCs and other epithelial cells.

The above studies demonstrate a rich network of endogenous stem and progenitor populations in mouse lungs. Although there may be overlap between cells identified in different investigations, an important concept is that there appears to be regional specificity of the progenitors. Overall, the available literature demonstrates a complex hierarchy of endogenous progenitors that appear specific to different lung regions. In addition to lineage tracing and other techniques to better identify and study the homeostasis of these cells, other *in vivo* assays such as cell transplantation are needed to assess the ability of putative lung stem/progenitor cells to reconstitute lung epithelial cell lineages within damaged or diseased tissue. To conclusively show which cells are true stem cell populations and which are cells of origin for lung cancers, cell type-restricted promoters are needed. In this way oncogenic Kras can be driven in various lung epithelial cell types proposed to be cells of origin for lung adenocarcinoma including club cells, BASCs, AT2, and AT1 cells.

Evidence for Lung Cancer Stem Cells

In addition to cells of origin, accumulating data has provided evidence for the existence of cancer stem cells in some lung cancers. The first study to look at stem cell characteristics in lung cancer cells was performed over 30 years ago by Carney and colleagues, describing a rare population of cells in patient lung cancer samples with the ability to form colonies in soft agar which could recapitulate the original tumor phenotype when transplanted into nude mice (Carney et al., 1982).

Since then, many studies have been done, largely looking at potential cancer stem cell populations in human lung cancer cell lines or cultured cells. Side population cells, which efflux Hoechst dye, have been shown to be resistant to chemotherapy, express increased levels of drug transporters, and show increased invasiveness *in vitro* (Ho et al., 2007). This study of six human non-small cell lung cancer cell lines also showed that side population cells were tumorigenic in a subcutaneous transplant assay in mice (Ho et al., 2007). CD133, originally a cell surface marker of brain and colon cancer stem cells, has also been used to identify lung cancer cells with tumorigenic properties. CD133+ cells from human lung tumors formed self-renewing spheres *in vitro* that could propagate tumors when transplanted subcutaneously in mice, and CD133+ cells from xenografts were enriched for tumorigenicity (Bertolini et al., 2009; Eramo et al., 2008; Tirino et al., 2009). However, other studies looking at lung cancer cell lines have shown that CD133 does not mark a cancer stem cell population (Meng et al., 2009a; 2009b). Another cell surface marker, CD44, marked tumorigenic cells in lung cancer cell lines transplanted subcutaneously (Leung et al., 2010). Expression of aldehyde dehydrogenase (ALDH) has also been used to isolate putative cancer stem

cells in leukemia, brain, breast, colon, prostate, liver, bladder, pancreatic, thyroid, and head and neck cancers (Bar et al., 2007; Chen et al., 2009; Cheung et al., 2007; Ginestier et al., 2007; Huang et al., 2009; Li et al., 2010; Ma et al., 2008; Rasheed et al., 2010; Su et al., 2010; Todaro et al., 2010). ALDH1+ cells from primary human lung tumor cells and from lung cancer cells lines were enriched for tumor initiating ability in subcutaneous transplant assays (Jiang et al., 2009; Liang and Shi, 2012; Sullivan et al., 2010).

Many of these above studies were done using cell lines, cultured primary cells, and/or subcutaneous transplantation. Previous work in our lab has developed an orthotopic transplantation assay for delivering tumor cells to the murine lung. Sca1, one of the cell surface markers used to isolate bronchioalveolar stem cells from the normal mouse lung, was found to enrich for cells with tumor-propagating ability in primary mouse adenocarcinomas from the Kras;p53-flox mouse model using this assay (Curtis et al., 2010). However, in the same study Sca1 did not enrich for tumor-propagating cells in other mouse tumor models carrying different oncogenic mutations. This study using genetically distinct mouse models suggests that those seeking to identify human lung cancer propagating cells should consider the genotype of their human tumor samples.

A recent study also using this orthotopic transplantation assay in the Kras;p53-flox model identified a CD24+ITGB4+Notch^{hi} tumor propagating cell population (Zheng et al., 2013). Although the findings of this study have some overlap with the work presented here, there are a few important differences in the two studies. The work of Sweet-Cordero and colleagues focused on the role of the Notch pathway in tumor

propagation, while our work focuses on the Hippo pathway. The sorting strategy used in the study uses mice that have a Rosa26-LSL-YFP allele as a marker of Cre-infected Kras;p53-flox tumor cells. Last, the metastatic capacity of the tumor propagating CD24+ITGB4+Notch^{hi} population was not studied.

Within human lung cancer, a CD166+ cancer stem cell population has been identified by serial transplantation of primary human NSCLC tumor cells subcutaneously into NSG mice (Zhang et al., 2012). The authors tested the markers CD166, CD44, CD133, and EpCAM and found that only CD166 was able to distinguish a population of tumor propagating and non-tumor propagating cells via serial transplantation. All of the other markers tested were able to form tumors from both positive and negative populations.

However, a population of human lung cancer stem cells serially transplanted in the lung microenvironment that recapitulates the lung tumor phenotype is yet to be described. In fact, at the time this work was started, our lab was the only one to identify a tumor propagating cell population in autochthonous mouse models of lung cancer using an orthotopic transplantation assay. Thus, while several lung cancer stem cell candidates have emerged, ongoing studies to further characterize lung tumor propagating cells will further identify and target important lung cancer cells.

Similarly, there has yet to be published work prospectively identifying subsets of metastatic lung cancer cells. The low five-year survival rate for patients diagnosed with lung cancer is largely due to the fact that most patients already have metastatic disease at time of diagnosis (Siegel et al., 2013). One way to develop therapies for metastatic

cancer is to examine possible links to cancer stem cells, although little has been done in this field.

Metastasis and Cancer Stem Cells

The first studies to examine tumor heterogeneity with regards to metastasis were performed by Fidler and colleagues in the mid-late 1970s. Fidler was first able to select for more metastatic cancer cells through repeated *in vivo* selection in animal models (Fidler, 1973). Fidler and colleagues next did a series of experiments where they first grew melanoma in culture and then either the parent cells or individual cell clones were transplanted via tail vein into mice (Fidler and Kripke, 1977). They found that in contrast to when bulk tumor cells were transplanted, transplanting various cell clones resulted in large differences in the number of resulting lung tumors that formed. The authors interpreted this result to mean that the parent tumor was heterogeneous and contained "highly metastatic tumor cell variants." To determine whether the heterogeneity in tumors was preexisting or whether it was due to random differences in cell survival, they did another set of experiments where a parent cell line and 21 clones produced from this line were injected via tail vein or subcutaneously and examined at different time points (Kripke et al., 1978). The authors concluded that the heterogeneity was preexisting since clones tended to have similar metastatic capability regardless of transplantation type. These were the first experiments to suggest such a metastatic heterogeneity in cancer, and that such heterogeneity should be taken into account when developing cancer therapies (Fidler, 1978).

The first study to demonstrate the existence of a metastatic cancer stem cell population was performed by Heeschen and colleagues (Hermann et al., 2007). The authors identified a CD133+CXCR4+ cancer stem cell population that was essential for metastasis. First, the authors identified CD133+CXCR4+ cells at the leading edge of patient tumors, and showed that CD133+ cells from pancreatic cell lines were enriched for tumor propagating activity and resistant to chemotherapy. From orthotopic pancreatic transplants of pancreatic cancer cell lines, only CD133+CXCR4+ cells were found in the circulating blood and were later able to seed liver metastases, while the CD133+CXCR4- population was not. Treatment with a CXCR4 inhibitor reduced these metastases. Although this was the first study to link cancer stem cells and metastasis, this study used cell lines instead of primary human or mouse tumor cells. Other notable studies utilizing cell lines and xenograft models have been done in breast cancer, identifying cells with aldehyde dehydrogenase activity as metastatic cancer stem cells (Charafe-Jauffret et al., 2009; 2010; Croker et al., 2009; Korkaya et al., 2008).

Another approach to link cancer stem cells and metastasis used a lentiviral barcoding strategy (Dieter et al., 2011). They grew primary human colon cancer tumors as spheres in culture, infected them with lentivirus, and then serially transplanted these spheres under the kidney capsule in immunodeficient mice. Using the lentiviral integration sites as “barcodes,” the authors identified three types of tumor initiating cells (TICs): tumor transit-amplifying cells (T-TACs) with limited self-renewal ability, delayed-contributing tumor initiating cells (DC-TICs) with activity in secondary or tertiary mice, and self-renewing long-term tumor initiating cells (LT-TICs) which were responsible for tumor formation in serial transplants. Only the LT-TICs were responsible for metastasis.

Wong and colleagues identified a CD26+ cancer stem cell population in colon cancer enriched for metastatic capability using primary human colorectal tumors (Pang et al., 2010). In patients, CD26 expression was higher in liver metastases than in primary tumors, and primary tumors with CD26 expression were more likely to metastasize. The authors then transplanted tumor subpopulations in the cecal wall of mice. Both CD26+ and CD26- cells were able to form primary tumors, but only CD26+ cells were able to form liver metastases. These results are interesting because while CD26 doesn't enrich for tumor propagating ability, it does enrich for metastatic ability.

To date, only these few studies have shown a causal relationship between cancer stem cells and metastasis, the majority of which were published in the past 5 years since this thesis work had begun. Prior to this work, a link between lung cancer stem cells and metastasis had yet to be shown.

Summary of the Dissertation

My thesis work will prospectively identify a population of lung tumor propagating cells that is enriched for metastatic potential. In Chapter 2, I will detail our work looking at CD24 and Sca1 as markers of a murine lung tumor-propagating cell population with enriched metastatic capacity. We also found that CD24 function was important for lung cancer cell migration and metastasis. Next, we used a microarray of TPC and non-TPC cells to create a TPC gene signature that is predictive of survival and metastasis in lung adenocarcinoma patients. Members and targets of the Hippo pathway were found to be enriched in this population by Gene Set Enrichment Analysis (GSEA). We found that the Hippo mediators Yap and Taz were important for lung cancer cell migration, metastasis,

and lung tumor progression. This study is the first to prospectively isolate lung tumor propagating cells with metastatic potential, and also highlights the utility of tumor propagating cells for identifying molecules contributing to metastatic lung cancer and potentially enabling therapeutic targeting. It is also the first to identify the importance of Yap/Taz in lung cancer progression in a mouse model of lung cancer *in vivo*. In Chapter 3, I will further discuss the significance of these findings in the context of the field. Unanswered questions and future directions for this project will also be explored. My hope is that these studies of tumor heterogeneity and metastasis will contribute to our understanding and help enable targeting of metastatic lung cancer cells.

References

Al-Hajj, M., Wicha, M.S., Benito-Hernandez, A., Morrison, S.J., and Clarke, M.F. (2003). Prospective identification of tumorigenic breast cancer cells. Proc. Natl. Acad. Sci. U.S.a. *100*, 3983–3988.

Arias, E., Curtin, L.R., Wei, R., and Anderson, R.N. (2008). U.S. decennial life tables for 1999-2001, United States life tables. Natl Vital Stat Rep *57*, 1–36.

Aso, Y., Yoneda, K., and Kikkawa, Y. (1976). Morphologic and biochemical study of pulmonary changes induced by bleomycin in mice. Lab. Invest. *35*, 558–568.

Aufderheide, A.C. (2003). The Scientific Study of Mummies (Cambridge University Press).

Bar, E.E., Chaudhry, A., Lin, A., Fan, X., Schreck, K., Matsui, W., Piccirillo, S., Vescovi, A.L., DiMeco, F., Olivi, A., et al. (2007). Cyclopamine-mediated hedgehog pathway inhibition depletes stem-like cancer cells in glioblastoma. Stem Cells *25*, 2524–2533.

Barkauskas, C.E., Cronce, M.J., Rackley, C.R., Bowie, E.J., Keene, D.R., Stripp, B.R., Randell, S.H., Noble, P.W., and Hogan, B.L.M. (2013). Type 2 alveolar cells are stem cells in adult lung. J. Clin. Invest. *123*, 3025–3036.

Sutherland, K.D., Song, J.Y., Kwon, M.C., Proost, N., Zevenhoven, J., and Berns, A. (2014). Multiple cells of origin of mutant K-Ras-induced mouse lung adenocarcinoma. Proc. Natl. Acad. Sci. U.S.A. *111*, 4952-4957.

Bertolini, G., Roz, L., Perego, P., Tortoreto, M., Fontanella, E., Gatti, L., Pratesi, G., Fabbri, A., Andriani, F., Tinelli, S., et al. (2009). Highly tumorigenic lung cancer CD133+ cells display stem-like features and are spared by cisplatin treatment. Proc. Natl. Acad. Sci. U.S.A. *106*, 16281–16286.

Besson, A., Hwang, H.C., Cicero, S., Donovan, S.L., Gurian-West, M., Johnson, D., Clurman, B.E., Dyer, M.A., and Roberts, J.M. (2007). Discovery of an oncogenic activity in p27Kip1 that causes stem cell expansion and a multiple tumor phenotype. Genes Dev. *21*, 1731–1746.

Boiko, A.D., Razorenova, O.V., van de Rijn, M., Swetter, S.M., Johnson, D.L., Ly, D.P., Butler, P.D., Yang, G.P., Joshua, B., Kaplan, M.J., et al. (2010). Human melanoma-initiating cells express neural crest nerve growth factor receptor CD271. Nature *466*, 133–137.

Bonnet, D., and Dick, J.E. (1997). Human acute myeloid leukemia is organized as a hierarchy that originates from a primitive hematopoietic cell. Nat. Med. *3*, 730–737.

Borthwick, D.W., Shahbazian, M., Krantz, Q.T., Dorin, J.R., and Randell, S.H. (2001). Evidence for stem-cell niches in the tracheal epithelium. Am. J. Respir. Cell Mol. Biol. *24*, 662–670.

BRUCE, W.R., and van der GAAG, H. (1963). A QUANTITATIVE ASSAY FOR THE NUMBER OF MURINE LYMPHOMA CELLS CAPABLE OF PROLIFERATION IN VIVO. Nature *199*, 79–80.

Carney, D.N., Gazdar, A.F., Bunn, P.A., and Guccion, J.G. (1982). Demonstration of the stem cell nature of clonogenic tumor cells from lung cancer patients. Stem Cells *1*, 149–164.

Carr, J., and Carr, I. (2005). The origin of cancer metastasis. Can. Bull. Med. Hist. *22*, 353-358.

Carretero, J., Shimamura, T., Rikova, K., Jackson, A.L., Wilkerson, M.D., Borgman, C.L., Buttarazzi, M.S., Sanofsky, B.A., McNamara, K.L., Brandstetter, K.A., et al. (2010). Integrative genomic and proteomic analyses identify targets for Lkb1-deficient metastatic lung tumors. Cancer Cell *17*, 547–559.

Chaffer, C.L., and Weinberg, R.A. (2011). A perspective on cancer cell metastasis. Science *331*, 1559–1564.

Charafe-Jauffret, E., Ginestier, C., Iovino, F., Tarpin, C., Diebel, M., Esterni, B., Houvenaeghel, G., Extra, J.-M., Bertucci, F., Jacquemier, J., et al. (2010). Aldehyde dehydrogenase 1-positive cancer stem cells mediate metastasis and poor clinical outcome in inflammatory breast cancer. Clin. Cancer Res. *16*, 45–55.

Charafe-Jauffret, E., Ginestier, C., Iovino, F., Wicinski, J., Cervera, N., Finetti, P., Hur, M.H., Diebel, M.E., Monville, F., Dutcher, J., et al. (2009). Breast cancer cell lines contain functional cancer stem cells with metastatic capacity and a distinct molecular signature. Cancer Res. *69*, 1302–1313.

Chen, J., Li, Y., Yu, T.-S., McKay, R.M., Burns, D.K., Kernie, S.G., and Parada, L.F. (2012). A restricted cell population propagates glioblastoma growth after chemotherapy. Nature *488*, 522–526.

Chen, Y.-C., Chen, Y.-W., Hsu, H.-S., Tseng, L.-M., Huang, P.-I., Lu, K.-H., Chen, D.-T., Tai, L.-K., Yung, M.-C., Chang, S.-C., et al. (2009). Aldehyde dehydrogenase 1 is a putative marker for cancer stem cells in head and neck squamous cancer. Biochem. Biophys. Res. Commun. *385*, 307–313.

Cheung, A.M.S., Wan, T.S.K., Leung, J.C.K., Chan, L.Y.Y., Huang, H., Kwong, Y.L., Liang, R., and Leung, A.Y.H. (2007). Aldehyde dehydrogenase activity in leukemic blasts defines a subgroup of acute myeloid leukemia with adverse prognosis and superior NOD/SCID engrafting potential. Leukemia *21*, 1423–1430.

Croker, A.K., Goodale, D., Chu, J., Postenka, C., Hedley, B.D., Hess, D.A., and Allan, A.L. (2009). High aldehyde dehydrogenase and expression of cancer stem cell markers selects for breast cancer cells with enhanced malignant and metastatic ability. J. Cell. Mol. Med. *13*, 2236–2252.

Curtis, S.J., Sinkevicius, K.W., Li, D., Lau, A.N., Roach, R.R., Zamponi, R., Woolfenden, A.E., Kirsch, D.G., Wong, K.-K., and Kim, C.F. (2010). Primary tumor genotype is an important determinant in identification of lung cancer propagating cells. Cell Stem Cell *7*, 127–133.

Daniely, Y., Liao, G., Dixon, D., Linnoila, R.I., Lori, A., Randell, S.H., Oren, M., and Jetten, A.M. (2004). Critical role of p63 in the development of a normal esophageal and tracheobronchial epithelium. Am. J. Physiol., Cell Physiol. *287*, C171–C181.

Davidson, M.R., Gazdar, A.F., and Clarke, B.E. (2013). The pivotal role of pathology in the management of lung cancer. J Thorac Dis *5*, S463–S478.

Desai, T.J., Brownfield, D.G., and Krasnow, M.A. (2014). Alveolar progenitor and stem cells in lung development, renewal and cancer. Nature.

Dick, J.E. (1996). Normal and leukemic human stem cells assayed in SCID mice. Semin. Immunol. *8*, 197–206.

Dieter, S.M., Ball, C.R., Hoffmann, C.M., Nowrouzi, A., Herbst, F., Zavidij, O., Abel, U., Arens, A., Weichert, W., Brand, K., et al. (2011). Distinct types of tumor-initiating cells form human colon cancer tumors and metastases. Cell Stem Cell *9*, 357–365.

Ding, L., Getz, G., Wheeler, D.A., Mardis, E.R., McLellan, M.D., Cibulskis, K., Sougnez, C., Greulich, H., Muzny, D.M., Morgan, M.B., et al. (2008). Somatic mutations affect key pathways in lung adenocarcinoma. Nature *455*, 1069–1075.

Driessens, G., Beck, B., Caauwe, A., Simons, B.D., and Blanpain, C. (2012). Defining the mode of tumour growth by clonal analysis. Nature *488*, 527–530.

Eramo, A., Lotti, F., Sette, G., Pilozzi, E., Biffoni, M., Di Virgilio, A., Conticello, C., Ruco, L., Peschle, C., and De Maria, R. (2008). Identification and expansion of the tumorigenic lung cancer stem cell population. Cell Death Differ. *15*, 504–514.

Ewing, J. (1928). Neoplastic diseases: a treatise on tumors.

Fehrenbach, H. (2001). Alveolar epithelial type II cell: defender of the alveolus revisited. Respir. Res. *2*, 33–46.

Ferlay, J., Shin, H.-R., Bray, F., Forman, D., Mathers, C., and Parkin, D.M. (2010). Estimates of worldwide burden of cancer in 2008: GLOBOCAN 2008. Int. J. Cancer *127*, 2893–2917.

Fidler, I.J. (1973). Selection of successive tumour lines for metastasis. Nature New Biol. *242*, 148–149.

Fidler, I.J. (1978). Tumor heterogeneity and the biology of cancer invasion and metastasis. Cancer Res. *38*, 2651–2660.

Fidler, I.J., and Kripke, M.L. (1977). Metastasis results from preexisting variant cells within a malignant tumor. Science *197*, 893–895.

Foster, R., Buckanovich, R.J., and Rueda, B.R. (2013). Ovarian cancer stem cells: working towards the root of stemness. Cancer Lett. *338*, 147–157.

Giangreco, A., Reynolds, S.D., and Stripp, B.R. (2002). Terminal bronchioles harbor a unique airway stem cell population that localizes to the bronchoalveolar duct junction. Am. J. Pathol. *161*, 173–182.

Ginestier, C., Hur, M.H., Charafe-Jauffret, E., Monville, F., Dutcher, J., Brown, M., Jacquemier, J., Viens, P., Kleer, C.G., Liu, S., et al. (2007). ALDH1 is a marker of normal and malignant human mammary stem cells and a predictor of poor clinical outcome. Cell Stem Cell *1*, 555–567.

Hamburger, A.W., and Salmon, S.E. (1977). Primary bioassay of human tumor stem cells. Science *197*, 461–463.

Hammond, E.C., Selikoff, I.J., and Seidman, H. (1979). Asbestos exposure, cigarette smoking and death rates. Annals of the New York Academy of Sciences *330*, 473-490.

Hanahan, D., and Weinberg, R.A. (2011). Hallmarks of cancer: the next generation. Cell *144*, 646–674.

Hart, I.R., and Fidler, I.J. (1980). Role of organ selectivity in the determination of metastatic patterns of B16 melanoma. Cancer Res. *40*, 2281–2287.

Hermann, P.C., Huber, S.L., Herrler, T., Aicher, A., Ellwart, J.W., Guba, M., Bruns, C.J., and Heeschen, C. (2007). Distinct populations of cancer stem cells determine tumor growth and metastatic activity in human pancreatic cancer. Cell Stem Cell *1*, 313–323.

Herzog, E.L., Brody, A.R., Colby, T.V., Mason, R., and Williams, M.C. (2008). Knowns and unknowns of the alveolus. Proc Am Thorac Soc *5*, 778–782.

Ho, M.M., Ng, A.V., Lam, S., and Hung, J.Y. (2007). Side population in human lung cancer cell lines and tumors is enriched with stem-like cancer cells. Cancer Res. *67*, 4827–4833.

Hoffmann, D., Hoffmann, I., and El-Bayoumy, K. (2001). The less harmful cigarette: a controversial issue. a tribute to Ernst L. Wynder. Chem. Res. Toxicol. *14*, 767–790.

Hong, K.U., Reynolds, S.D., Giangreco, A., Hurley, C.M., and Stripp, B.R. (2001). Clara cell secretory protein-expressing cells of the airway neuroepithelial body microenvironment include a label-retaining subset and are critical for epithelial renewal after progenitor cell depletion. Am. J. Respir. Cell Mol. Biol. *24*, 671–681.

Hong, K.U., Reynolds, S.D., Watkins, S., Fuchs, E., and Stripp, B.R. (2004a). Basal cells are a multipotent progenitor capable of renewing the bronchial epithelium. Am. J. Pathol. *164*, 577–588.

Hong, K.U., Reynolds, S.D., Watkins, S., Fuchs, E., and Stripp, B.R. (2004b). In vivo differentiation potential of tracheal basal cells: evidence for multipotent and unipotent subpopulations. Am. J. Physiol. Lung Cell Mol. Physiol. *286*, L643–L649.

Huang, E.H., Hynes, M.J., Zhang, T., Ginestier, C., Dontu, G., Appelman, H., Fields, J.Z., Wicha, M.S., and Boman, B.M. (2009). Aldehyde dehydrogenase 1 is a marker for normal and malignant human colonic stem cells (SC) and tracks SC overpopulation during colon tumorigenesis. Cancer Res. *69*, 3382–3389.

Imielinski, M., Berger, A.H., Hammerman, P.S., Hernandez, B., Pugh, T.J., Hodis, E., Cho, J., Suh, J., Capelletti, M., Sivachenko, A., et al. (2012). Mapping the hallmarks of lung adenocarcinoma with massively parallel sequencing. Cell *150*, 1107–1120.

Isakson, B.E., Lubman, R.L., Seedorf, G.J., and Boitano, S. (2001). Modulation of pulmonary alveolar type II cell phenotype and communication by extracellular matrix and KGF. Am. J. Physiol., Cell Physiol. *281*, C1291–C1299.

Jackson, E.L., Willis, N., Mercer, K., Bronson, R.T., Crowley, D., Montoya, R., Jacks, T., and Tuveson, D.A. (2001). Analysis of lung tumor initiation and progression using conditional expression of oncogenic K-ras. Genes Dev. *15*, 3243–3248.

Jackson, E.L., Olive, K.P., Tuveson, D.A., Bronson, R., Crowley, D., Brown, M., and Jacks, T. (2005). The differential effects of mutant p53 alleles on advanced murine lung cancer. Cancer Res. *65*, 10280–10288.

Ji, H., Ramsey, M.R., Hayes, D.N., Fan, C., McNamara, K., Kozlowski, P., Torrice, C., Wu, M.C., Shimamura, T., Perera, S.A., et al. (2007). LKB1 modulates lung cancer differentiation and metastasis. Nature *448*, 807–810.

Jiang, F., Qiu, Q., Khanna, A., Todd, N.W., Deepak, J., Xing, L., Wang, H., Liu, Z., Su, Y., Stass, S.A., et al. (2009). Aldehyde dehydrogenase 1 is a tumor stem cell-associated marker in lung cancer. Mol. Cancer Res. *7*, 330–338.

Jones, D.S., Podolsky, S.H., and Greene, J.A. (2012). The burden of disease and the changing task of medicine. N. Engl. J. Med. *366*, 2333–2338.

Karnoub, A.E., and Weinberg, R.A. (2008). Ras oncogenes: split personalities. Nat. Rev. Mol. Cell Biol. *9*, 517–531.

Kawamoto, M., and Fukuda, Y. (1990). Cell proliferation during the process of bleomycin-induced pulmonary fibrosis in rats. Acta Pathol. Jpn. *40*, 227–238.

Kelly, P.N., Dakic, A., Adams, J.M., Nutt, S.L., and Strasser, A. (2007). Tumor growth need not be driven by rare cancer stem cells. Science *317*, 337.

Kim, C.F.B., Jackson, E.L., Woolfenden, A.E., Lawrence, S., Babar, I., Vogel, S., Crowley, D., Bronson, R.T., and Jacks, T. (2005). Identification of bronchioalveolar stem cells in normal lung and lung cancer. Cell *121*, 823–835.

Korkaya, H., Paulson, A., Iovino, F., and Wicha, M.S. (2008). HER2 regulates the mammary stem/progenitor cell population driving tumorigenesis and invasion. Oncogene *27*, 6120–6130.

Kreso, A., O'Brien, C.A., van Galen, P., Gan, O.I., Notta, F., Brown, A.M.K., Ng, K., Ma, J., Wienholds, E., Dunant, C., et al. (2013). Variable clonal repopulation dynamics influence chemotherapy response in colorectal cancer. Science *339*, 543–548.

Kripke, M.L., Gruys, E., and Fidler, I.J. (1978). Metastatic heterogeneity of cells from an ultraviolet light-induced murine fibrosarcoma of recent origin. Cancer Res. *38*, 2962–2967.

Lapidot, T., Sirard, C., Vormoor, J., Murdoch, B., Hoang, T., Caceres-Cortes, J., Minden, M., Paterson, B., Caligiuri, M.A., and Dick, J.E. (1994). A cell initiating human acute myeloid leukaemia after transplantation into SCID mice. Nature *367*, 645–648.

Lau, A.N., Goodwin, M., Kim, C.F., and Weiss, D.J. (2012). Stem cells and regenerative medicine in lung biology and diseases. Mol. Ther. *20*, 1116–1130.

Leaf, C. (2004). Why we're losing the war on cancer (and how to win it). Fortune *149*, 76–82–84–6–88passim.

Lee, J.-H., Bhang, D.H., Beede, A., Huang, T.L., Stripp, B.R., Bloch, K.D., Wagers, A.J., Tseng, Y.-H., Ryeom, S., and Kim, C.F. (2014). Lung Stem Cell Differentiation in Mice Directed by Endothelial Cells via a BMP4-NFATc1-Thrombospondin-1 Axis. Cell *156*, 440–455.

Leung, E.L.-H., Fiscus, R.R., Tung, J.W., Tin, V.P.-C., Cheng, L.C., Sihoe, A.D.-L., Fink, L.M., Ma, Y., and Wong, M.P. (2010). Non-small cell lung cancer cells expressing CD44 are enriched for stem cell-like properties. PLoS ONE *5*, e14062.

Li, C., Lee, C.J., and Simeone, D.M. (2009). Identification of human pancreatic cancer stem cells. Methods Mol. Biol. *568*, 161–173.

Li, T., Su, Y., Mei, Y., Leng, Q., Leng, B., Liu, Z., Stass, S.A., and Jiang, F. (2010). ALDH1A1 is a marker for malignant prostate stem cells and predictor of prostate cancer patients' outcome. Lab. Invest. *90*, 234–244.

Liang, D., and Shi, Y. (2012). Aldehyde dehydrogenase-1 is a specific marker for stem cells in human lung adenocarcinoma. Med. Oncol. *29*, 633–639.

Ma, S., Chan, K.W., Lee, T.K.-W., Tang, K.H., Wo, J.Y.-H., Zheng, B.-J., and Guan, X.-Y. (2008). Aldehyde dehydrogenase discriminates the CD133 liver cancer stem cell populations. Mol. Cancer Res. *6*, 1146–1153.

Magee, J.A., Piskounova, E., and Morrison, S.J. (2012). Cancer stem cells: impact, heterogeneity, and uncertainty. Cancer Cell *21*, 283–296.

Mainardi, S., Mijimolle, N., Francoz, S., Vicente-Dueñas, C., Sánchez-García, I., and Barbacid, M. (2014). Identification of cancer initiating cells in K-Ras driven lung adenocarcinoma. Proc. Natl. Acad. Sci. U.S.a. *111*, 255–260.

Marusyk, A., and Polyak, K. (2013). Cancer. Cancer cell phenotypes, in fifty shades of grey. Science *339*, 528–529.

Massaro, G.D., Singh, G., Mason, R., Plopper, C.G., Malkinson, A.M., and Gail, D.B. (1994). Biology of the Clara cell. pp. L101–L106.

McCracken, M., Olsen, M., Chen, M.S., Jemal, A., Thun, M., Cokkinides, V., Deapen, D., and Ward, E. (2007). Cancer incidence, mortality, and associated risk factors among Asian Americans of Chinese, Filipino, Vietnamese, Korean, and Japanese ethnicities. CA Cancer J Clin *57*, 190–205.

McQualter, J.L., Yuen, K., Williams, B., and Bertoncello, I. (2010). Evidence of an epithelial stem/progenitor cell hierarchy in the adult mouse lung. Proc. Natl. Acad. Sci. U.S.a. *107*, 1414–1419.

Meacham, C.E., and Morrison, S.J. (2013). Tumour heterogeneity and cancer cell plasticity. Nature *501*, 328–337.

Meng, X., Li, M., Wang, X., Wang, Y., and Ma, D. (2009a). Both CD133+ and CD133- subpopulations of A549 and H446 cells contain cancer-initiating cells. Cancer Sci. *100*, 1040–1046.

Meng, X., Wang, X., and Wang, Y. (2009b). More than 45% of A549 and H446 cells are cancer initiating cells: evidence from cloning and tumorigenic analyses. Oncol. Rep. *21*, 995–1000.

Messner, H.A., and McCULLOCH, E.A. (1973). Interacting cell populations affecting granulopoietic colony formation by normal and leukemic human marrow cells. Blood *42*, 701–710.

Mumford, J.L., He, X.Z., Chapman, R.S., Cao, S.R., Harris, D.B., Li, X.M, Xian, Y.L., Jiang, W.Z., Xu, C.W., Chuang, J.C., et al. (1987). Lung cancer and indoor air pollution in Xuan Wei, China. Science *23,* 217–220.

National Research Council (NRC), Committee on Health Risks of Exposure to Radon, Board on Radiation Effects Research and Commission on Life Sciences. (1999). Health effects of exposure to radon. (BEIR IV). In: NRC, editor. Washington: National Academy Press.

Neugut, A.I., Murray, T., Santos, J., Amols, H., Hayes, M.K., Flannery, J.T., Robinson, E. (1994). Increased risk of lung cancer after breast cancer radiation therapy in cigarette smokers. Cancer *73*,1615–1620.

O'Brien, C.A., Pollett, A., Gallinger, S., and Dick, J.E. (2007). A human colon cancer cell capable of initiating tumour growth in immunodeficient mice. Nature *445*, 106–110.
Paget, S. (1989). The distribution of secondary growths in cancer of the breast. 1889.

Pang, R., Law, W.L., Chu, A.C.Y., Poon, J.T., Lam, C.S.C., Chow, A.K.M., Ng, L., Cheung, L.W.H., Lan, X.R., Lan, H.Y., et al. (2010). A subpopulation of CD26+ cancer stem cells with metastatic capacity in human colorectal cancer. Cell Stem Cell *6*, 603–615.

Park, C.H., Bergsagel, D.E., and McCULLOCH, E.A. (1971). Mouse myeloma tumor stem cells: a primary cell culture assay. J. Natl. Cancer Inst. *46*, 411–422.

Patrawala, L., Calhoun, T., Schneider-Broussard, R., Li, H., Bhatia, B., Tang, S., Reilly, J.G., Chandra, D., Zhou, J., Claypool, K., et al. (2006). Highly purified CD44+ prostate cancer cells from xenograft human tumors are enriched in tumorigenic and metastatic progenitor cells. Oncogene *25*, 1696–1708.

Pei, X.-H., Bai, F., Smith, M.D., and Xiong, Y. (2007). p18Ink4c collaborates with Men1 to constrain lung stem cell expansion and suppress non-small-cell lung cancers. Cancer Res. *67*, 3162–3170.

Pierce, G.B. (1967). Teratocarcinoma: model for a developmental concept of cancer. Curr. Top. Dev. Biol. *2*, 223–246.

Prates, Sousa, Oliveira, Ikram (2011). Prostate metastatic bone cancer in an Egyptian Ptolemaic mummy, a proposed radiological diagnosis. International Journal of Paleopathology *1*, 6–6.

Quintana, E., Shackleton, M., Foster, H.R., Fullen, D.R., Sabel, M.S., Johnson, T.M., and Morrison, S.J. (2010). Phenotypic heterogeneity among tumorigenic melanoma cells from patients that is reversible and not hierarchically organized. Cancer Cell *18*, 510–523.

Quintana, E., Shackleton, M., Sabel, M.S., Fullen, D.R., Johnson, T.M., and Morrison, S.J. (2008). Efficient tumour formation by single human melanoma cells. Nature *456*, 593–598.

Raiser, D.M., and Kim, C.F. (2009). Commentary: Sca-1 and Cells of the Lung: A matter of Different Sorts. Stem Cells *27*, 606–611.

Randell, S.H. (2006). Airway epithelial stem cells and the pathophysiology of chronic obstructive pulmonary disease. Proc Am Thorac Soc *3*, 718–725.

Rasheed, Z.A., Yang, J., Wang, Q., Kowalski, J., Freed, I., Murter, C., Hong, S.-M., Koorstra, J.-B., Rajeshkumar, N.V., He, X., et al. (2010). Prognostic significance of tumorigenic cells with mesenchymal features in pancreatic adenocarcinoma. J. Natl. Cancer Inst. *102*, 340–351.

Rawlins, E.L., and Hogan, B.L.M. (2006). Epithelial stem cells of the lung: privileged few or opportunities for many? Development *133*, 2455–2465.

Rawlins, E.L., Okubo, T., Xue, Y., Brass, D.M., Auten, R.L., Hasegawa, H., Wang, F., and Hogan, B.L.M. (2009). The role of Scgb1a1+ Clara cells in the long-term maintenance and repair of lung airway, but not alveolar, epithelium. Cell Stem Cell *4*, 525–534.

Reynolds, S.D., Giangreco, A., Power, J.H., and Stripp, B.R. (2000). Neuroepithelial bodies of pulmonary airways serve as a reservoir of progenitor cells capable of epithelial regeneration. Am. J. Pathol. *156*, 269–278.

Ricci-Vitiani, L., Lombardi, D.G., Pilozzi, E., Biffoni, M., Todaro, M., Peschle, C., and De Maria, R. (2007). Identification and expansion of human colon-cancer-initiating cells. Nature *445*, 111–115.

Rock, J.R., Barkauskas, C.E., Cronce, M.J., Xue, Y., Harris, J.R., Liang, J., Noble, P.W., and Hogan, B.L.M. (2011). Multiple stromal populations contribute to pulmonary fibrosis without evidence for epithelial to mesenchymal transition. Proc. Natl. Acad. Sci. U.S.a. *108*, E1475–E1483.

Rock, J.R., Onaitis, M.W., Rawlins, E.L., Lu, Y., Clark, C.P., Xue, Y., Randell, S.H., and Hogan, B.L.M. (2009). Basal cells as stem cells of the mouse trachea and human airway epithelium. Proc. Natl. Acad. Sci. U.S.a. *106*, 12771–12775.

Sakorafas, G.H., and Safioleas, M. (2009). Breast cancer surgery: an historical narrative. Part I. From prehistoric times to Renaissance. Eur J Cancer Care (Engl) *18*, 530–544.

Schoch, K.G., Lori, A., Burns, K.A., Eldred, T., Olsen, J.C., and Randell, S.H. (2004). A subset of mouse tracheal epithelial basal cells generates large colonies in vitro. Am. J. Physiol. Lung Cell Mol. Physiol. *286*, L631–L642.

Schultz, M., Parzinger, H., Posdnjakov, D.V., Chikisheva, T.A., and Schmidt-Schultz, T.H. (2007). Oldest known case of metastasizing prostate carcinoma diagnosed in the skeleton of a 2,700-year-old Scythian king from Arzhan (Siberia, Russia). Int. J. Cancer *121*, 2591–2595.

Sell, S. (2004). Stem cell origin of cancer and differentiation therapy. Crit. Rev. Oncol. Hematol. *51*, 1–28.

Sell, S. (2010). On the stem cell origin of cancer. Am. J. Pathol. *176*, 2584–2494.

Siegel, R., Naishadham, D., and Jemal, A. (2012). Cancer statistics for Hispanics/Latinos, 2012. CA Cancer J Clin *62*, 283–298.

Siegel, R., Naishadham, D., and Jemal, A. (2013). Cancer statistics, 2013. CA Cancer J Clin *63*, 11–30.

Singh, S.K., Hawkins, C., Clarke, I.D., Squire, J.A., Bayani, J., Hide, T., Henkelman, R.M., Cusimano, M.D., and Dirks, P.B. (2004). Identification of human brain tumour initiating cells. Nature *432*, 396–401.

Su, Y., Qiu, Q., Zhang, X., Jiang, Z., Leng, Q., Liu, Z., Stass, S.A., and Jiang, F. (2010). Aldehyde dehydrogenase 1 A1-positive cell population is enriched in tumor-initiating cells and associated with progression of bladder cancer. Cancer Epidemiol. Biomarkers Prev. *19*, 327–337.

Sullivan, J.P., Spinola, M., Dodge, M., Raso, M.G., Behrens, C., Gao, B., Schuster, K., Shao, C., Larsen, J.E., Sullivan, L.A., et al. (2010). Aldehyde dehydrogenase activity selects for lung adenocarcinoma stem cells dependent on notch signaling. Cancer Res. *70*, 9937–9948.

Talmadge, J.E., and Fidler, I.J. (2010). AACR centennial series: the biology of cancer metastasis: historical perspective. Cancer Res. *70*, 5649–5669.

TILL, J.E., and McCULLOCH, E.A. (1961). A direct measurement of the radiation sensitivity of normal mouse bone marrow cells. Radiat. Res. *14*, 213–222.

Tirino, V., Camerlingo, R., Franco, R., Malanga, D., La Rocca, A., Viglietto, G., Rocco, G., and Pirozzi, G. (2009). The role of CD133 in the identification and characterisation of tumour-initiating cells in non-small-cell lung cancer. Eur J Cardiothorac Surg *36*, 446–453.

Todaro, M., Iovino, F., Eterno, V., Cammareri, P., Gambara, G., Espina, V., Gulotta, G., Dieli, F., Giordano, S., De Maria, R., et al. (2010). Tumorigenic and metastatic activity of human thyroid cancer stem cells. Cancer Res. *70*, 8874–8885.

Toh, C.K., Gao, F., Lim, W.T., Leong, S.S., Fong, K.W., Yap, S.P., Hsu, A.A., Eng, P., Koong, H.N., Thirugnanam, A., et al. (2006). Never-smokers with lung cancer: epidemiologic evidence of a distinct disease entity. J. Clin. Oncol. *24,* 2245–2251.

Travis WD, Colby TV, Corrin B, Shimosato Y, Brambilla E. In Collaboration with Sobin LH and Pathologists from 14 Countries. (1999). World Health Organization International Histological Classification of Tumours. Histological Typing of Lung and Pleural Tumours. 3rd Edn Springer-Verlag.

Tropea, K.A., Leder, E., Aslam, M., Lau, A.N., Raiser, D.M., Lee, J.-H., Balasubramaniam, V., Fredenburgh, L.E., Alex Mitsialis, S., Kourembanas, S., et al. (2012). Bronchioalveolar stem cells increase after mesenchymal stromal cell treatment in a mouse model of bronchopulmonary dysplasia. Am. J. Physiol. Lung Cell Mol. Physiol. *302*, L829–L837.

van der Schans, C.P. (1997). Forced expiratory manoeuvres to increase transport of bronchial mucus: a mechanistic approach. Monaldi Arch Chest Dis *52*, 367–370.

Visvader, J.E. (2011). Cells of origin in cancer. Nature *469*, 314–322.

Wicha, M.S., Liu, S., and Dontu, G. (2006). Cancer stem cells: an old idea--a paradigm shift. Cancer Res. *66*, 1883–90–discussion1895–6.

Winslow, M.M., Dayton, T.L., Verhaak, R.G.W., Kim-Kiselak, C., Snyder, E.L., Feldser, D.M., Hubbard, D.D., DuPage, M.J., Whittaker, C.A., Hoersch, S., et al. (2011). Suppression of lung adenocarcinoma progression by Nkx2-1. Nature *473*, 101–104.

Xu, X., Rock, J.R., Lu, Y., Futtner, C., Schwab, B., Guinney, J., Hogan, B.L.M., and Onaitis, M.W. (2012). Evidence for type II cells as cells of origin of K-Ras-induced distal lung adenocarcinoma. Proc. Natl. Acad. Sci. U.S.A. *109*, 4910–4915.

Yamashita, T., and Wang, X.W. (2013). Cancer stem cells in the development of liver cancer. J. Clin. Invest. *123*, 1911–1918.

Zacharek, S.J., Fillmore, C.M., Lau, A.N., Gludish, D.W., Chou, A., Ho, J.W.K., Zamponi, R., Gazit, R., Bock, C., Jäger, N., et al. (2011). Lung stem cell self-renewal relies on BMI1-dependent control of expression at imprinted loci. Cell Stem Cell *9*, 272–281.

Zhang, W.C., Shyh-Chang, N., Yang, H., Rai, A., Umashankar, S., Ma, S., Soh, B.S., Sun, L.L., Tai, B.C., Nga, M.E., et al. (2012). Glycine decarboxylase activity drives non-small cell lung cancer tumor-initiating cells and tumorigenesis. Cell *148*, 259–272.

Zheng, Y., la Cruz, de, C.C., Sayles, L.C., Alleyne-Chin, C., Vaka, D., Knaak, T.D., Bigos, M., Xu, Y., Hoang, C.D., Shrager, J.B., et al. (2013). A rare population of CD24(+)ITGB4(+)Notch(hi) cells drives tumor propagation in NSCLC and requires Notch3 for self-renewal. Cancer Cell *24*, 59–74.

CHAPTER 2:

Tumor-propagating cells and Yap/Taz activity contribute to lung tumor progression and metastasis

Author Contributions

ANL, SJC, SPR, MM, DEW, DTM, KWS, and JB performed experiments and analyzed results. CMF performed bioinformatic analyses. ANL, AMB and JB managed mouse colony. ZEW, DJW, KKW, and FDC generated mice and/or reagents. ANL, SJC, DEW and CFK designed experiments. ANL and CFK wrote the article.

At the time of submission of this dissertation, much of the work presented in this chapter has been published in *The EMBO Journal* as a manuscript entitled:

Tumor-propagating cells and Yap/Taz activity contribute to lung tumor progression and metastasis

Allison N. Lau,[1,2] Stephen J. Curtis,[1,2] Christine M. Fillmore,[1,2] Samuel P. Rowbotham,[1,2] Morvarid Mohseni,[1,3] Darcy E. Wagner, [4] Alexander M. Beede,[1,2] Daniel T. Montoro,[1,2] Kerstin W. Sinkevicius,[1,2] Zandra E. Walton,[5] Juliana Barrios,[1,2] Daniel J. Weiss, [4] Fernando D. Camargo,[1,3] Kwok-Kin Wong,[5] and Carla F. Kim [1,2,6]

[1] Stem Cell Program, Boston Children's Hospital, Boston MA 02115 and the Harvard Stem Cell Institute, Cambridge, MA 02138 USA

[2] Department of Genetics, Harvard Medical School, Boston, MA 02115, USA

[3] Department of Stem Cell and Regenerative Biology, Harvard University, Cambridge, MA 02138, USA

[4]Department of Medicine, University of Vermont, Burlington, Vermont, USA 05405

[5] Department of Medical Oncology, Dana-Farber Cancer Institute, Boston, MA 02115 USA, Department of Medicine, Brigham and Women's Hospital, Harvard Medical School, Boston, MA 02115, USA, Ludwig Center at Dana-Farber/Harvard Cancer Center, Boston, MA 02115, USA

[6] Corresponding author

Contact information:
Email: carla.kim@childrens.harvard.edu
Phone: 617-919-4644
Fax: 617-730-0222

Running title: TPCs and Taz in metastatic lung cancer

Abstract

Metastasis is the leading cause of morbidity for lung cancer patients. Here we demonstrate that murine tumor propagating cells (TPCs) with the markers Sca1 and CD24 are enriched for metastatic potential in orthotopic transplantation assays. In lung cancer patient data sets, metastatic spread and patient survival could be stratified with a murine lung TPC gene signature. The TPC signature was enriched for genes in the Hippo signaling pathway. In cell lines resembling TPCs, knockdown of CD24 or the Hippo mediators Yap1 or Taz decreased *in vitro* cellular migration and transplantation of metastatic disease. Furthermore, constitutively active Yap was sufficient to drive lung tumor progression *in vivo*. These results demonstrate functional roles for CD24 and Yap/Taz in lung tumor propagation and metastasis. This study demonstrates the utility of TPCs to identify molecules contributing to metastatic lung cancer, potentially enabling the therapeutic targeting of this devastating disease.

Introduction

The average five-year survival rate for patients diagnosed with lung cancer remains at a strikingly low 16%. The predominant contributor to this statistic is the fact that the vast majority (~85%) of patients are diagnosed when their cancer has already progressed beyond a localized state (Siegel et al., 2013). Even for those patients who undergo resection of localized lung cancer, 72% will later develop lethal metastatic disease (Pisters et al., 2000). In the absence of novel early detection modalities, it is essential to better understand the mechanisms that control progression and metastasis in order to offer new therapeutic options for lung cancer patients.

The mucin-like cell surface adhesion molecule, CD24, has been implicated as a marker and a key regulator of advanced disease in multiple types of cancer, yet with some possibly conflicting results (Lee et al., 2011; Liu et al., 2012; Overdevest et al., 2011). High levels of CD24 detected by immunohistochemistry had a significantly increased likelihood of disease progression and cancer-related death for lung cancer patients (Kristiansen et al., 2003; Lee et al., 2010). Disseminated lung tumor cells from malignant pleural effusions also express CD24 (Yao et al., 2013). On the other hand, CD24-negative/low membrane expression was significantly correlated with poor differentiation and worse survival in lung cancers (Damelin et al., 2011). In breast cancers, the links between CD24 expression and tumor progression have also differed between studies (Al-Hajj et al., 2003; Shipitsin et al., 2007).

Tumor-propagating cells (TPCs) are tumor cells capable of serially transplanting and recapitulating the tumor phenotype and may contribute to tumor progression and metastasis, yet few studies have directly tested this idea. Notable examples have

utilized cancer cell lines and xenograft models in breast cancer (Charafe-Jauffret et al., 2010; Charafe-Jauffret et al., 2009; Croker et al., 2009; Korkaya et al., 2008), pancreatic (Hermann et al., 2007), and colorectal cancer (Pang et al., 2010) to link metastasis to TPCs. Murine CD24+ CD90+ TPCs play a key role in breast cancer metastasis through cell autonomous and microenvironmental requirements (Malanchi et al., 2011). However, differentiated, non-tumor propagating cancer cells can also facilitate metastasis in embryonal rhabdomyosarcoma (Ignatius et al., 2012). A CD24-expressing population (CD24+ITGB4+Notch^{hi}) was shown to be enriched for tumor propagation in a mouse model of lung cancer (Zheng et al, 2013), yet the metastatic potential of this CD24+ cell population has not been reported.

The Hippo signaling cascade, most noted for its role in organ size control and development, has been posited to play a role in cancer progression (reviewed in Pan, 2010), and emerging evidence supports this concept in lung cancer. Expression of the canonical effector of the Hippo pathway, Yes associated protein 1 (Yap1), has been correlated with poor prognosis in non-small cell lung cancer patients and was shown to modulate the tumorigenicity of human lung cancer cell lines (Wang et al., 2010). Overexpression of WW domain-containing transcription regulator protein 1 (Wwtr1, more commonly referred to as Taz), a paralog of Yap1, was capable of transforming immortalized human bronchial epithelial cells, while knockdown of Taz in non-small cell lung cancer cell lines decreased tumorigenicity, validating Taz as an oncogene in the lung (Zhou et al., 2011).

Metastatic lung adenocarcinomas, the most common form of lung cancer in patients, can be initiated in mice harboring *Lox-Stop-Lox-KrasG12D* and *p53flox/flox*

alleles (hereafter, Kras;p53-flox) upon intranasal instillation of adenovirus expressing Cre-recombinase (Jackson et al., 2005). Using this model, we have shown that the Sca1+ population of tumor cells is enriched for tumor-propagating potential (Curtis et al., 2010). In the present study, we determined that CD24a (the mouse homolog of human CD24, CD24 hereafter) is an additional lung TPC marker and a key mediator of lung cancer cell line migration and subcutaneous tumor propagation. We also show that Sca1+CD24+ cells are enriched for metastatic potential after orthotopic delivery of tumor cells. Lung TPCs exhibit transcriptional profiles correlating with metastatic potential and poor patient prognosis. Finally, our data point to a functional role for YAP and TAZ in lung cancer progression and metastasis.

Results

CD24 expression marks cells with tumor-propagating capacity

We sought to identify additional cell surface markers of the Sca1+ Kras;p53-flox cancer cells we previously identified as lung TPCs. DAPI- CD31- CD45- Sca1+ (Sca1+ hereafter) and DAPI- CD31- CD45- Sca1- (Sca1- hereafter) cell populations from four primary Kras;p53-flox lung tumors were isolated via fluorescence activated cell sorting (FACS) as previously described (Curtis et al., 2010) and their transcriptional profiles were analyzed by Affymetrix microarray (Appendix).

Expression levels of cell surface markers were examined followed by quantitative real-time PCR (qPCR) and FACS analysis to identify candidate lung TPC markers. Differential expression of Sca1 (LY6A) in TPCs was confirmed (fold change in Sca1+ vs. Sca1-, 30.77) in this data set. CD133, a putative marker of human lung cancer cells with increased tumorigenicity (Bertolini et al., 2009; Chen et al., 2008; Eramo et al.,

2008; Levina et al., 2008), was highly expressed in Sca1+ TPCs by microarray and qPCR analysis (fold change, 23.63) (Curtis et al., 2010), yet flow cytometry for CD133 failed to show enrichment within the Sca1+ fraction (unpublished observations). Several other markers of aggressive cancer stem cells in other tissues, including CD44 and CXCR4, were not significantly differentially expressed in Sca1+ and Sca1- cells. Interestingly, CD24 was upregulated in lung TPCs (fold change, 1.8). qPCR confirmed that CD24 was overexpressed more than 3-fold in Sca1+ TPCs from Kras;p53-flox lung tumors compared to Sca1- cells (p=0.0057) (Figure 2-1A). Flow cytometric analysis of Kras;p53-flox lung tumor cell preparations revealed that 87.1% +/- 5.44% of Sca1+ cells were CD24+ (Figure 2-1B, n=7).

We utilized our orthotopic intratracheal transplantation model (Curtis et al., 2010) to verify that CD24 expressing cells were lung TPCs. Primary Kras;p53-flox lung tumors were isolated for digestion, FACS, and transplantation. We first compared the activity of DAPI- CD31- CD45- CD24+ cells (hereafter CD24+) with the activity of DAPI- CD31- CD45- CD24- cells (CD24-). 10,000 CD24+ or CD24- cells were transplanted intratracheally into immunocompromised *Foxn1*$^{nu/nu}$ (nude) mice. Recipient mice were observed until they exhibited labored breathing, when mice were euthanized for analysis of lung tumors (22 ± 3 weeks for CD24+ cells, 25 ± 4 weeks for CD24- cells). The CD24+ and CD24- populations both propagated lung adenocarcinomas that accurately recapitulated primary Kras;p53-flox tumors (Figure 2-1C,D). 100% of recipient mice developed at least one lung tumor after transplantation of 10,000 CD24+ or CD24- cells (10/10 for CD24+ and 12/12 for CD24-) (Appendix). Histological

Figure 2-1: CD24 marks cells enriched for tumor-propagating ability.

A. Real Time RT-PCR analysis for CD24 in sorted Sca1+ and Sca1- Kras;p53-flox lung tumor cells. **B.** A representative flow cytometry plot showing CD24 and Sca1 expression in Kras;p53-flox lung tumor cells. Cells shown were gated on the single, live (DAPI-negative), CD31-negative, CD45-negative population. **C and D.** H&E image showing a secondary Kras;p53-flox lung adenocarcinoma from the transplantation of CD24+ tumor cells (C) or CD24- tumor cells (D). 200x magnification, scale bar = 100μm. **E. and F.** Quantification of tumors from transplantation of 10,000 CD24+ or CD24- cells. **E.** Average tumor number per recipient mouse. N = 7 for each cell type transplanted. **F.** Average tumor burden in secondary mice calculated as the percentage of lung area filled with tumors. N = 6 for CD24+, N=7 for CD24-. **G.** Table showing tertiary tumor formation ability of CD24+ and CD24- Kras;p53-flox lung tumor cells from secondary transplants. 1,000 or 10,000 CD24+ or CD24- cells were intratracheally transplanted into immunocompromised mice. The percentage of recipient mice with at least one lung tumor after 13-28 weeks is shown. p=0.0063, Fisher's Exact Test, two tailed. **H**. H&E image showing a tertiary Kras;p53-flox lung adenocarcinoma from the transplantation of CD24+ tumor cells. *, $p < 0.05$.

Figure 2-1: (continued)

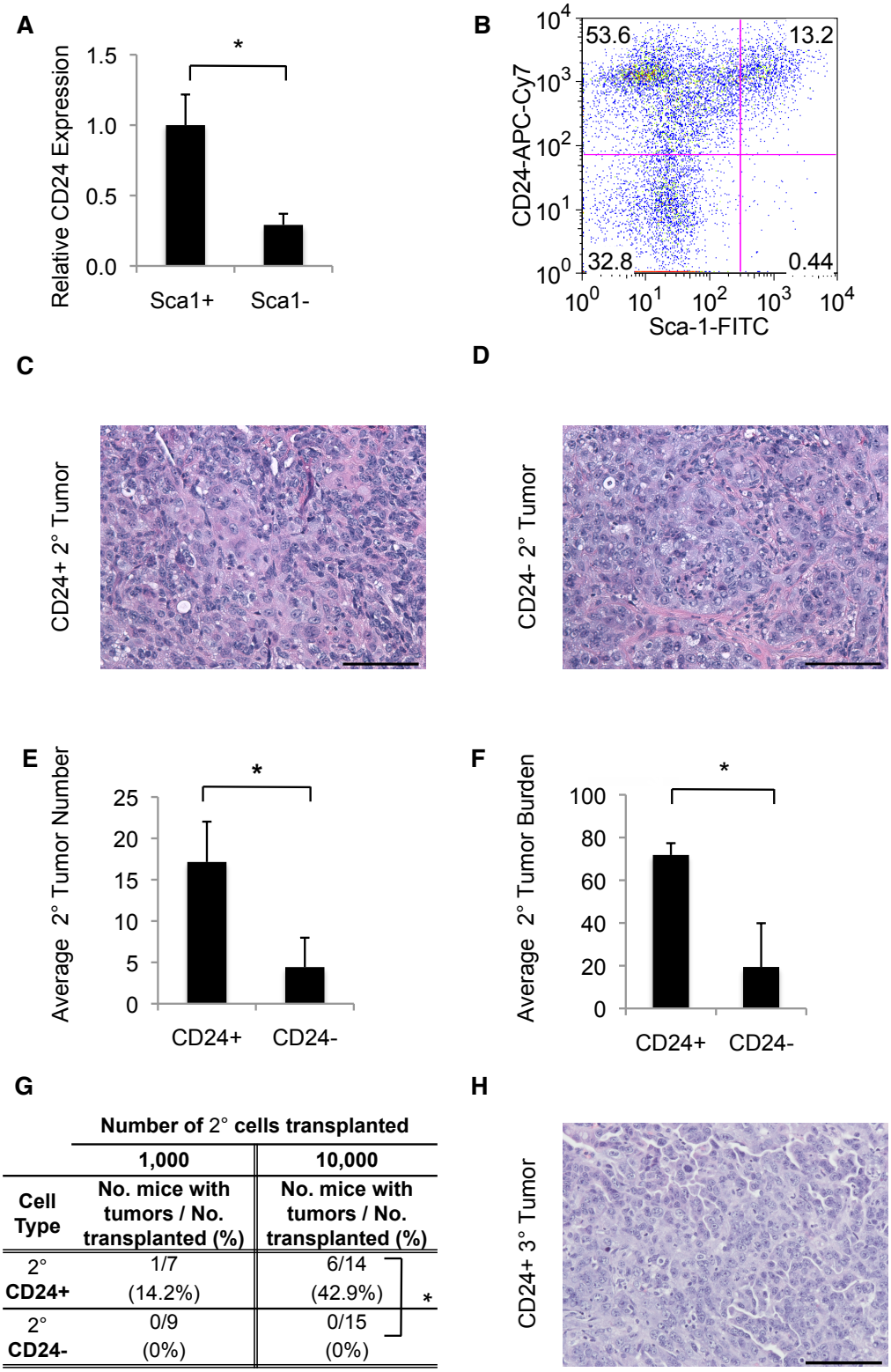

	Number of 2° cells transplanted		
	1,000	10,000	
Cell Type	No. mice with tumors / No. transplanted (%)	No. mice with tumors / No. transplanted (%)	
2° CD24+	1/7 (14.2%)	6/14 (42.9%)	*
2° CD24-	0/9 (0%)	0/15 (0%)	

analysis revealed that while CD24+ recipient mice had an average of 17 tumors, CD24- recipients had only 4 ($p=1.2x10-4$), and likewise CD24+ recipients showed 72% tumor burden (lung area filled with tumor) in contrast to 19% tumor burden observed for CD24- recipients ($p=8.3x10-5$) (Figure 2-1E,F).

We next tested the ability of cell populations separated by CD24 expression to serially passage tumors. Interestingly, lung tumors in recipient mice contained a CD24+ population regardless of whether CD24+ or CD24- cells were transplanted despite ~95% cell purity at the time of tumor cell isolation (Figure 2-2A,B). 1,000 or 10,000 CD24+ or CD24- cells from secondary tumors were FACS-sorted and transplanted orthotopically to test for serial tumor formation ability. Recipients of CD24- cells from secondary tumors did not develop lung tumors (0/9 and 0/15 for 1,000 and 10,000 cells, respectively). In contrast, CD24+ cells from secondary tumors could form tertiary tumors. CD24+ cells from secondary tumors yielded tumors in 1/7 mice after transplantation of 1,000 cells and in 6/14 mice after transplantation of 10,000 cells, $p=0.0063$) (Figure 2-1G,H, Figure 2-2C,D, Appendix). These data supported our hypothesis that CD24 is a marker of lung cancer cells with tumor-propagating capacity.

We next used the combination of Sca1 and CD24 to further delineate Kras;p53-flox TPCs. Limiting dilution transplantation experiments were used to compare TPC activity in the Sca1+CD24+, Sca1-CD24+, Sca1+CD24- and Sca1-CD24- fractions. Recipients of Sca1+CD24+ and Sca1-CD24+ tumor cells had higher rates of tumor formation than Sca1-CD24- and Sca1+CD24- recipients, further showing CD24 is a TPC marker (Sca1-CD24+ vs Sca1-CD24-, $p=0.0429$, Sca1-CD24+ vs Sca1+CD24-, $p=0.0290$) (Figure 2-3A, Appendix).

Figure 2-2: Characterization of CD24+ TPCs. A-B. Representative FACS plot of a lung tumor from a secondary mouse transplanted with CD24+ cells (A) or CD24- cells (B)**.** Cells shown were gated on the single, live (DAPI-negative), CD31-negative, CD45-negative population. **C-D.** Tables showing tertiary tumor formation ability of CD24+ and CD24- Kras;p53-flox lung tumor cells from CD24+ (C) or CD24- (D) secondary transplants. 1,000 or 10,000 CD24+ or CD24- cells were intratracheally transplanted into immunocompromised mice. The percentage of recipient mice with at least one lung tumor after 28 weeks is shown. CD24+ CD24- p=0.0108, Fisher's Exact Test, two tailed. **E.** Table of metastatic incidence in secondary mice from transplantation of 10,000 CD24+ or CD24- cells. The number and (percentage) of recipient mice with at least one metastatic lesion are shown in the first column. Location columns show the number and (percentage) of recipient mice with metastases in the noted site. **F.** H&E images showing metastases from the transplantation of CD24+ tumor cells (left column images) or CD24- tumor cells (right column images). Top, chest cavity metastases; Middle, lymph node metastases; Bottom, heart metastasis from CD24+ recipient, normal heart from CD24- recipient. All H&E images 200x magnification. Scale bars represent 100μm. **G.** The average tumor size of secondary tumors from transplantation of CD24+ (N=8) or CD24- (N=10) cells. **H.** The percentage of recipient mice bearing lung tumors from transplantation of CD24+ (N=10) or CD24- (N=10) cells with the indicated tumor grade (Scale 1-4) is shown. Grade 1 lesions were not observed in recipient mice

Figure 2-2: (continued)

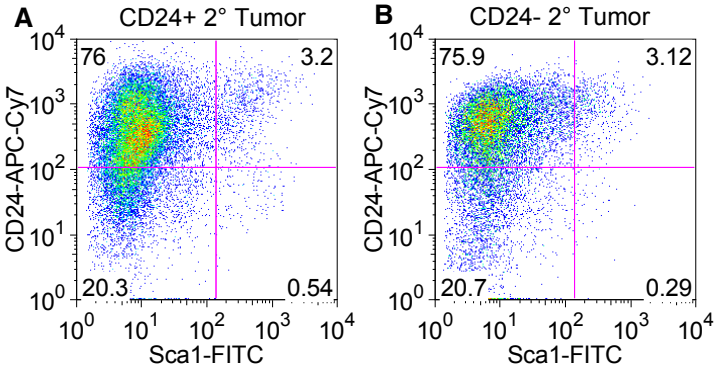

C

Cells from CD24+ derived tumors		
	Number of cells transplanted	
	1,000	10,000
Cell Type	No. mice with tumors / No. transplanted (%)	No. mice with tumors / No. transplanted (%)
CD24+	0/2 (0%)	1/5 (20%)
CD24-	0/2 (0%)	0/5 (0%)

D

Cells from CD24- derived tumors		
	Number of cells transplanted	
	1,000	10,000
Cell Type	No. mice with tumors / No. transplanted (%)	No. mice with tumors / No. transplanted (%)
CD24+	1/5 (20%)	5/9 (55.6%)
CD24-	0/7 (0%)	0/10 (0%)

*

E

		Location of Metastasis		
Cell Type	No. mice with mets. / No. mice with tumors (%)	Pleural Lining/ Chest Cavity	Lymph node	Heart
CD24+	7/7 (100%)	7/7 (100%)	3/7 (43%)	3/7 (43%)
CD24-	6/8 (75%)	6/6 (100%)	2/6 (33%)	0/6 (0%)

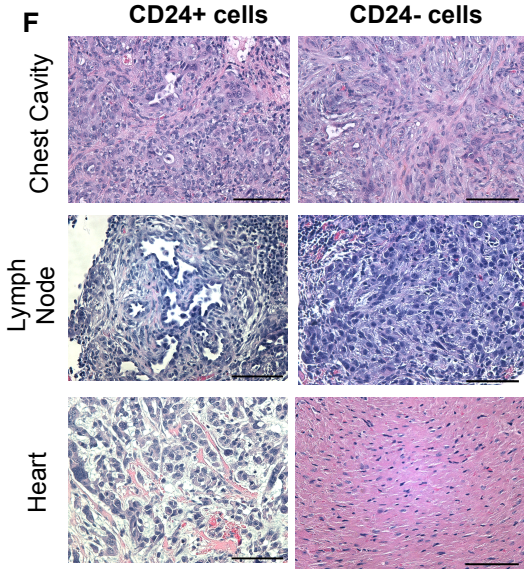

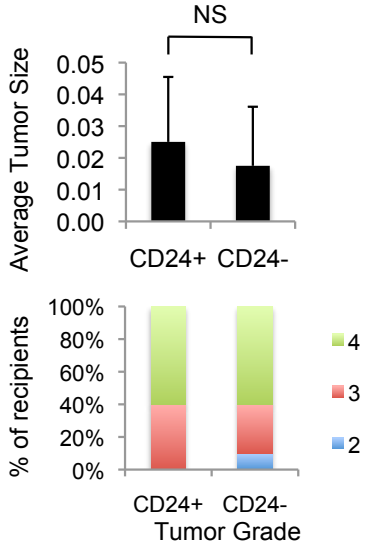

Figure 2-3: Sca1 and CD24 mark cells in Kras;p53-flox tumors with metastatic potential after orthotopic transplantation. A. Table showing tumor propagation ability of Sca1+CD24+, Sca1-CD24+, Sca1+CD24- and Sca1-CD24- Kras;p53-flox lung tumor cells. 100-10,000 cells were intratracheally transplanted into immunocompromised mice. The percentage of recipient mice with at least one lung tumor after 17-33 weeks is shown. **B.** Table showing tertiary tumor formation ability of Sca1+CD24+, Sca1-CD24+,and Sca1-CD24- Kras;p53-flox lung tumor cells from secondary transplants. 10,000 cells were intratracheally transplanted into immunocompromised mice. The percentage of recipient mice with at least one lung tumor after 20-29 weeks is shown. **C.** H&E images showing a lung tumor (left) and kidney metastasis (right) from the transplantation of Sca1+CD24+ tumor cells. 200x magnification, scale bars = 100μm. **D.** H&E images showing a lung tumor (left) and chest cavity metastasis (right) from the transplantation of Sca1-CD24+ tumor cells. 200x magnification, scale bars = 100μm. **E**. Table of metastatic incidence in secondary mice from transplantation of 6000-10,000 Sca1+CD24+, Sca1-CD24+, Sca1+CD24- and Sca1-CD24- Kras;p53-flox lung tumor cells. The number and (percentage) of recipient mice with at least one metastatic lesion are shown in the first column. Location columns show the number and (percentage) of recipient mice with metastases in the noted site. **F**. The percentage of recipient mice bearing lung tumors from transplantation of Sca1+CD24+ (N=7) or Sca1-CD24+ (N=9) cells with the indicated tumor grade (Scale 1-4) is shown. Grade 1 or 2 lesions were not observed in recipient mice.

Figure 2-3: (continued)

A

Cell Type	Number of cells transplanted: 100	1,000-6,000	6,000-10,000
	No. mice with tumors / No. transplanted (%)		
Sca1+/ CD24+	3/18 (17%)	2/14 (14%)	9/19 (47%)
Sca1-/ CD24+	0/17 (0%)	4/13 (31%)	12/20 (60%) *
Sca1+/ CD24-	1/18 (6%)	0/7 (0%)	1/8 (13%) *
Sca1-/ CD24-	0/18 (0%)	2/12 (17%)	6/21 (29%)

B

Cell Type	Number of 2° cells transplanted: 1,000-6,000	6,000-10,000
	No. mice with tumors / No. transplanted (%)	
Sca1+/ CD24+	3/5 (60%)	7/17 (41%)
Sca1-/ CD24+	1/7 (14%)	6/19 (32%) *
Sca1+/ CD24-	0/2 (0%)	1/6 (17%) *
Sca1-/ CD24-	2/9 (22%)	0/18 (0%)

C

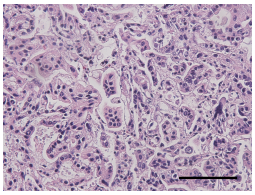

Sca1+CD24+ Lung Tumor, Grade 4

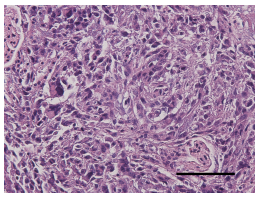

Sca1+CD24+ Kidney Metastasis

D

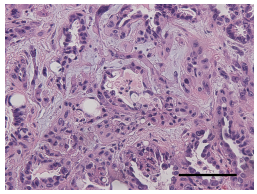

Sca1-CD24+ Lung Tumor, Grade 4

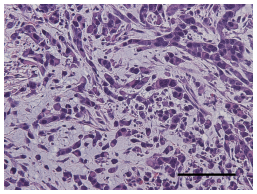

Sca1-CD24+ Chest Metastasis

E

Cell Type	No. mice with mets. / No. mice with tumors (%)	6,000 - 10,000 cells, Location: Pleural Lining/ Chest Cavity	Lymph node	Distant
Sca1+/ CD24+	6/7 (86%) *	6/6 (100%)	3/6 (50%)	1/6 kidney (17%)
Sca1-/ CD24+	3/10 (30%)	3/3 (100%)	0/3 (0%)	0/3 (0%)

F

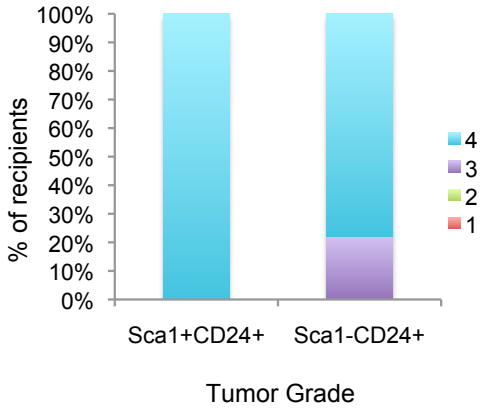

Similar to our results using CD24 alone, Sca1+CD24+ and Sca1-CD24+ also had higher rates of tumor propagation in secondary transplantation (Figure 2-3B). Importantly, cytospin and qPCR showed the four Sca1/CD24-sorted populations had similar epithelial cell content (Figure 2-4A,B,C,D). Thus, Sca1+CD24+ and Sca1-CD24+ cells are enriched for Kras;p53-flox TPCs.

Sca1+ CD24+ status correlates with metastatic potential

Orthotopically transplanted Kras;p53-flox tumor cell populations also produced metastases in recipient mice, allowing us to also test the role of TPCs in metastasis. First, a cohort of CD24+ and CD24- cell recipients were euthanized for collection of tissues from common metastatic sites for lung cancer, including connective tissue in the pleural cavity, lymph nodes, heart, liver, spleen and adrenal glands. To more fairly compare metastatic capacity, we analyzed CD24- cell recipients 26-29 weeks after transplantation, when they had primary tumors of similar size and grade as tumors in CD24+ cell recipients analyzed at 22 weeks (Figure 2-2G,H). With these parameters, there was no significant difference in metastasis in recipients of CD24+ cells versus CD24- cells (Figure 2-2E). CD24+ cell recipients developed metastatic lesions in the chest wall, local lymph nodes, and the heart (Figure 2-2E, F). Similarly, mice that received CD24- cells developed small chest cavity lesions and local lymph node metastases yet did not have metastatic lesions in the heart. Thus, CD24 status alone is not sufficient as a metastatic marker.

Sca1+ and Sca1- cells from Kras;p53-flox tumors were also transplanted via intratracheal transplantation to test for metastatic potential, since previous studies only examined the role of Sca1 in tumor propagation (Curtis et al., 2010) (Figure 2-5A,B,

Figure 2-4: Characterization of Sca1+CD24+ TPCs

A. Percent of Kras;p53-flox lung tumors cells with SPC expression determined after cytospin and staining. Representative images of SPC+ and SPC- cells are shown. N= 3 mice. **B.** qPCR analysis of Vimentin expression in Sca1+CD24+, Sca1-CD24+, Sca1+CD24- and Sca1-CD24- Kras;p53-flox lung tumor cells. Normal lung EpCAM+ and EpCAM- cells were used as negative and positive controls. **C.** qPCR analysis of SMA (Acta2) expression in Sca1+CD24+, Sca1-CD24+, Sca1+CD24- and Sca1-CD24- Kras;p53-flox lung tumor cells. **D.** qPCR analysis of ECadherin (ECad) expression in Sca1+CD24+, Sca1-CD24+, Sca1+CD24- and Sca1-CD24- Kras;p53-flox lung tumor cells. **E.** Average tumor size in Sca1+CD24+ (N=4) and Sca1-CD24+ recipients. (N =8).

Figure 2-4: (continued)

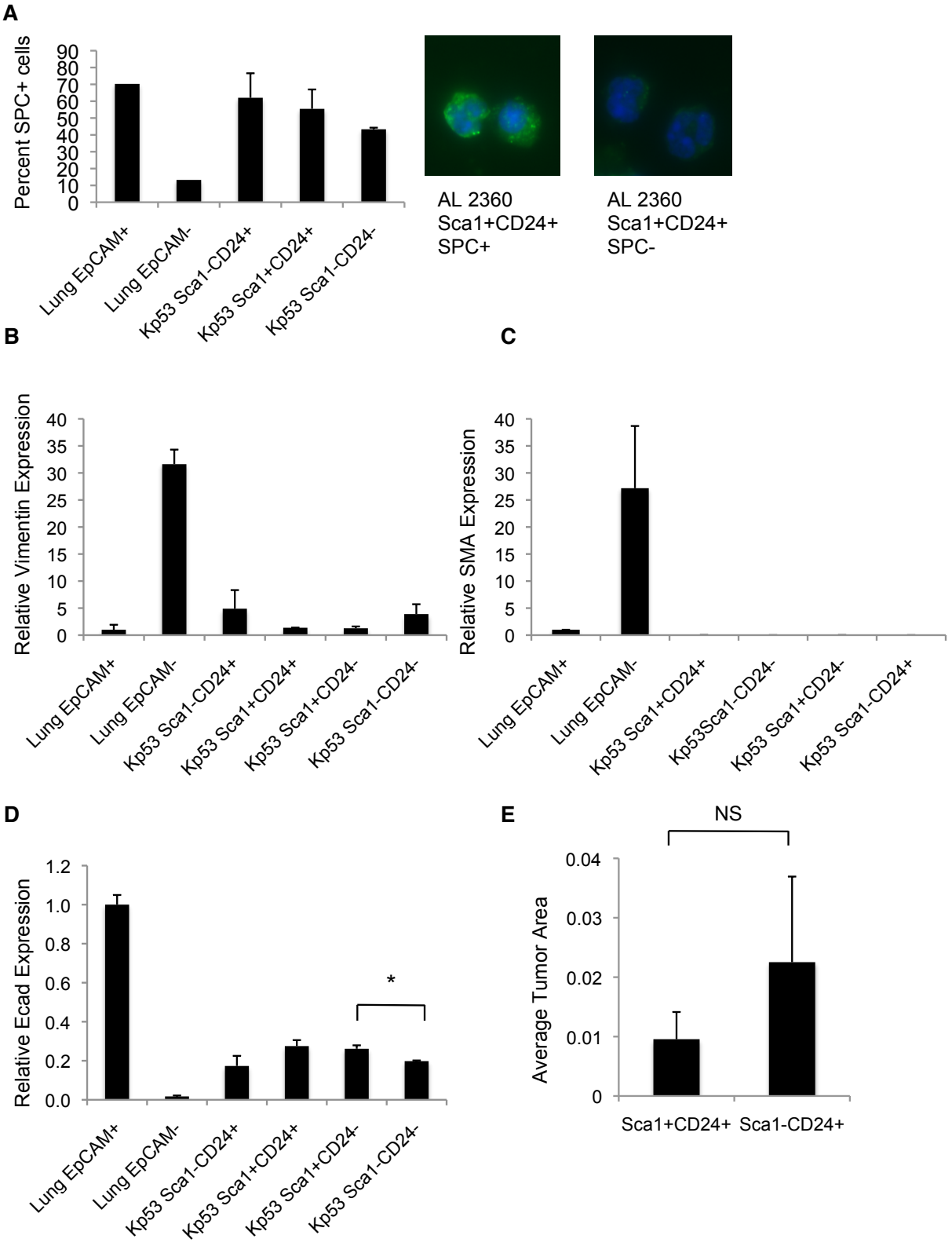

Figure 2-5: Tumor transplants using Sca1. A. Table showing tumor propagation ability of Sca1+ and Sca1- Kras;p53-flox lung tumor cells. 1,000-10,000 cells were intratracheally transplanted into immunocompromised mice. The percentage of recipient mice with at least one lung tumor after 17-29 weeks is shown. **B**. Table of metastatic incidence in secondary mice from transplantation of 6,000-10,000 Sca1+ or Sca1- Kras;p53-flox lung tumor cells. The number and (percentage) of recipient mice with at least one metastatic lesion are shown in the first column. Location columns show the number and (percentage) of recipient mice with metastases in the noted site.

Figure 2-5: (continued)

A

	Number of cells transplanted	
	1,000-6,000	**6,000-10,000**
Cell Type	**No. mice with tumors / No. transplanted (%)**	**No. mice with tumors / No. transplanted (%)**
Sca1+	3/5 (60%)	3/3 (100%)
Sca1-	2/5 (40%)	2/2 (100%)

B

		Location		
Cell Type	**No. mice with mets. / No. mice with tumors (%)**	**Pleural Lining/ Chest Cavity**	**Lymph node**	**Distant**
Sca1+	2/3 (66.7%)	2/2 (100%)	0/2 (0%)	0/2 (0%)
Sca1-	1/2 (50%)	1/1 (100%)	0/1 (0%)	0/1 (0%)

Appendix). More mice are needed to make definitive conclusions about the role of Sca1 as a metastatic marker (2/3 mice developed metastases in Sca1+ transplants vs. 1/2 mice in Sca1- transplants) (Figure 2-5B).

Having identified the Sca1+CD24+ and Sca1-CD24+ populations as TPC-enriched, we tested their relative metastatic capability. Recipients of Sca1+CD24+ or Sca1-CD24+ populations developed high-grade lung tumors and metastases (Figure 2-3C,D). When we compared mice bearing lung tumors of equal size and comparable grades that arose from either of the TPC populations, recipients of Sca1+CD24+ cells (6/7) were significantly more likely to have metastases than the Sca1-CD24+ recipients (3/10) ($p=0.0498$, Figure 2-3E, F, Figure 2-4E). Thus, at least two TPC populations can be identified with Sca1 and CD24 staining, and the Sca1+CD24+ phenotype is most highly associated with metastatic activity.

CD24 plays a functional role in metastatic activity

To further probe the role of CD24 in the metastatic spread of lung cancer, we generated a series of cell lines from the Kras;p53-flox lung adenocarcinoma model. The CK1750 and SC241 cell lines exhibit many properties of metastatic lung tumor cells. Firstly, CK1750 cells robustly formed adenocarcinomas when transplanted intratracheally (10/12 recipients formed tumors when 1,000-10,000 cells were injected) (Figure 2-6A). Furthermore, these recipient animals developed metastases in multiple sites including the chest wall (5/10), lymph nodes (4/10), adrenal glands (2/10), and liver (1/10), with approximately 50% of recipients exhibiting metastasis to one or more sites (Figure 2-6A). Nearly all CK1750 and SC241 cells expressed CD24 and Sca1 (Figure 2-

Figure 2-6: CD24 expression is required for migration and ectopic growth of murine lung adenocarcinoma cells. A. H&E images of a lung tumor (left) and adrenal gland metastasis (right) from intratracheal transplantation from the Kras;p53-flox CK1750 cell line. Images are 200x magnification, scale bars represent 100μM. **B.** FACS plot from CK1750 cells showing expression of CD24 and Sca1. Cells shown were gated on the single, live (DAPI-negative), CD31-negative, CD45-negative population. **C.** Analysis of cellular migration from in vitro transwell migration assays, determined by scoring cells migrating towards serum-containing (10% FBS) media with CK1750 CD24 knockdown cells (shCD24-Low-1 & Low-5, n=3) or control CK1750 shGFP cells (shGFP n=6,). Results shown are the average of three independent experiments. **D.** Average number of lung metastases after tail vein injection of CK1750 shGFP cells (circles), CK1750 shCD24-Low-1 cells (squares), or CK1750 shCD24-Low-5 cells (triangles). Lungs were analyzed for metastases two weeks after injection of 500,000 cells. Each symbol represents an individual mouse analyzed. **E.** Table showing the number of recipient mice with lung tumor formation after intratracheal injection with 100,000 shGFP cells or shCD24-Low-1 cells out of the total injected mice (percentage). *, $p < 0.05$.

Figure 2-6: (continued)

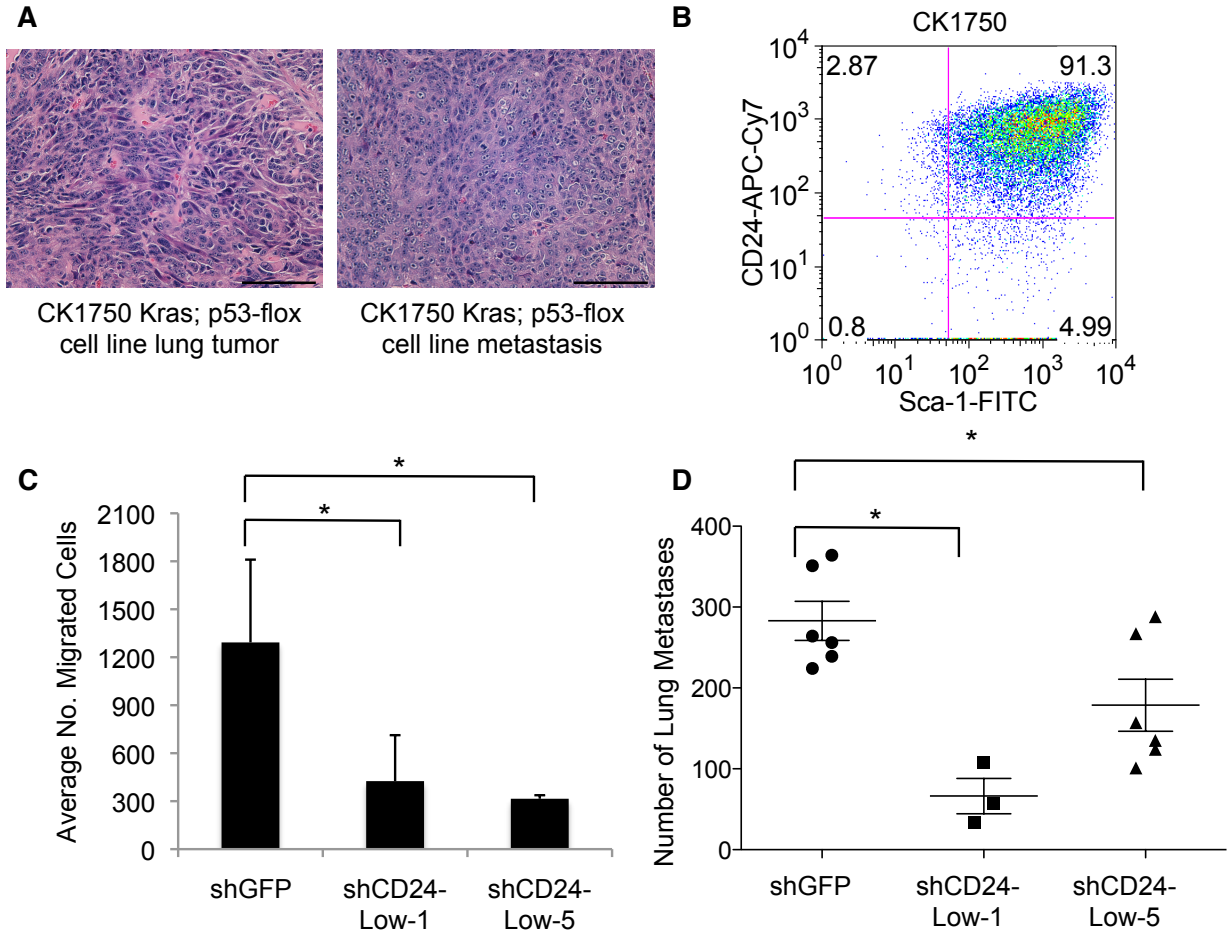

E

Treatment	Lung Tumor Incidence	
shGFP IT	4/6 (66.7%)	*
shCD24-Low-1 IT	0/5 (0%)	

6B). Thus, the cell lines functionally and phenotypically resembled the most metastatic Kras;p53-flox lung TPCs.

Utilizing two different shRNA constructs against CD24 (shCD24-1 targets the 3'UTR, while shCD24-5 targets the coding region) we diminished CD24 expression to ~20-30% of normal transcript levels compared to shGFP control cells after selection for CK1750 and SC241 cells expressing the lowest levels of CD24 (termed "Low") (Figure 2-7A). Importantly, knockdown of CD24 in the CK1750 cell line did not affect the growth of the cells in standard cell culture conditions (Figure 2-7B). However, in transwell *in vitro* migration assays, the CD24 knockdown lines showed markedly less migration compared with control shGFP cells (Figure 2-6C); the shCD24-Low-1 and shCD24-Low-5 lines showed a 3-fold and 4-fold reductions in migration, respectively ($p=0.033$ & $p=0.015$). CD24 knockdown in SC241 cells showed similar results; the shCD24-Low-1 and shCD24-Low-5 lines also showed 3-fold and 4-fold reductions in migration, respectively ($p=0.013$ & $p=0.0024$) (Figure 2-6C). To assess metastatic capacity *in vivo*, shGFP and shCD24 cells were injected into the tail vein of nude mice. Transplantation of the shCD24-Low-1 and shCD24-Low-5 lines resulted in a significantly lower number of lung metastases ($p = 0.7x10^{-4}$, & $p=0.027$) and smaller tumor burden for shCD24-Low-1 transplants (Figure 2-6D, Figure 2-7D,E). However, average tumor size was not significantly different between the shGFP control and shCD24 groups, suggesting engraftment rather than proliferation is affected by knockdown of CD24 in this tail vein assay (Figure 2-7F). Intratracheal injections showed that shCD24 cells were devoid of TPC activity compared with shGFP controls; shCD24-Low-1 cells produced lung tumors

Figure 2-7: CD24 knockdown in CK1750 and SC241 cells. A. qPCR for CD24 expression levels after knockdown of of CD24 in CK1750 (see also Figure 3) **B.** A growth curve analysis of CD24 knockdown and control (shGFP) CK1750 cell line derivatives. No time points showed significant differences. **C.** The average number of migratory cells observed in transwell migration assays, determined by the number of cells migrating towards serum-containing (10% FBS) media in control or CD24 knockdown SC241 cells. *p= 0.013 shCD24-Low-1, p= 0.0024, shCD24-Low-5. Results shown are from one representative experiment. **D**. H&E images of lung metastasis after tail vein injection of 500,000 CK170 shGFP, shCD24-Low-1, and shCD24-Low-5 cells. Images are 40x magnification, scale bars represent 1000μM. **E.** Average tumor burden in tumors from tail vein transplantation of shGFP or shCD24 CK1750 cells calculated as the percentage of lung area filled with tumors. N = 6 mice for shGFP, N=3 for shCD24-Low-1, N=6 for shCD24-Low-5. *, shCD24-Low-1 p=0.048. **F.** Average tumor area in tumors from tail vein transplantation shGFP or shCD24 CK1750 cells. N = 6 mice for shGFP, N=3 for shCD24-Low-1, N=6 for shCD24-Low-5. **G**. Cell line derivatives (10,000 cells) were transplanted subcutaneously and resulting tumors were measured.

Figure 2-7: (continued)

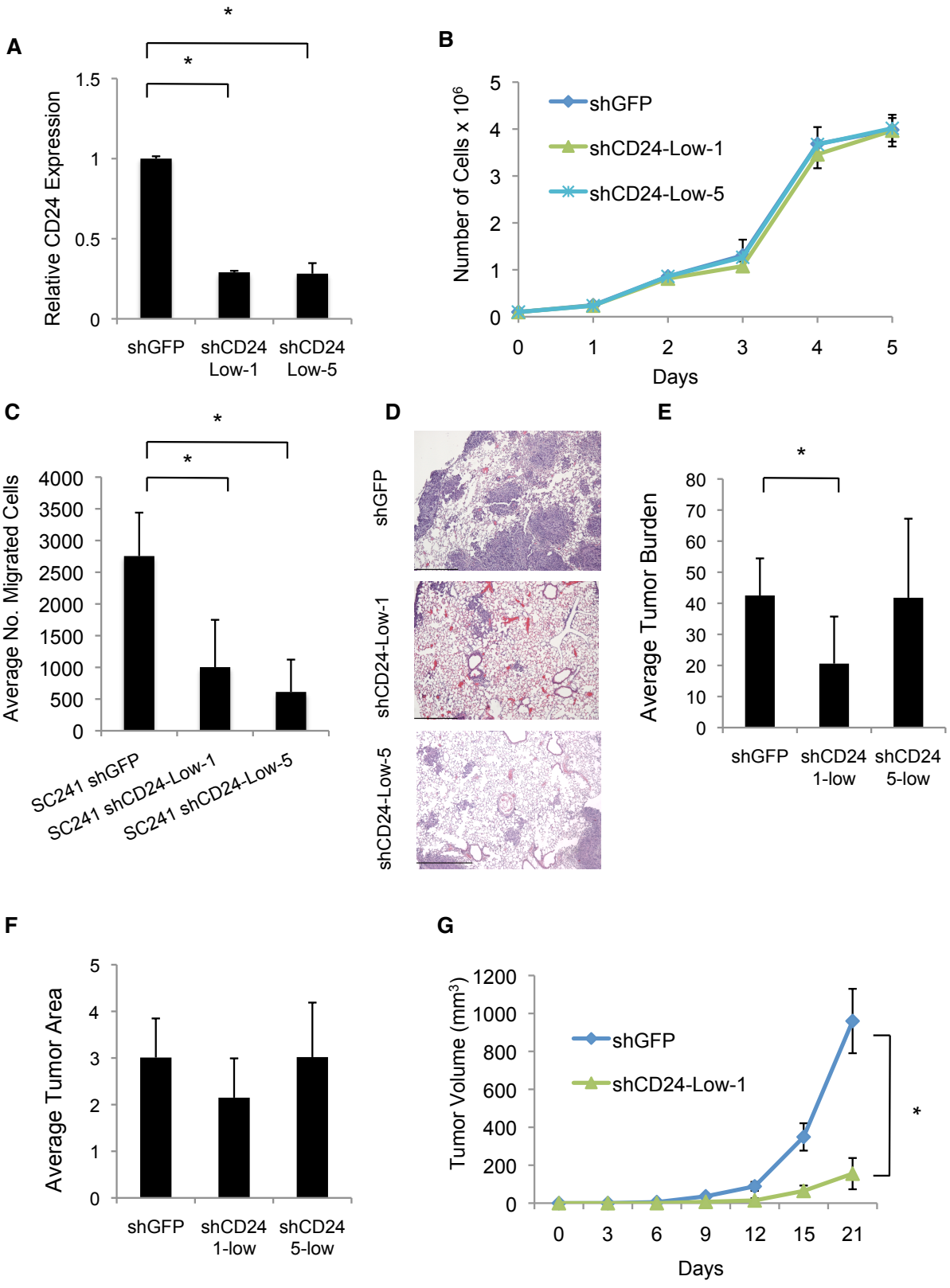

after IT administration in 0/5 recipients whereas shGFP cells yielded tumors in 4/6 recipients (p= 0.04, Figure 2-6E). While CD24 knockdown cells were capable of subcutaneous tumor formation, the shCD24-Low-1 line showed a longer latency to first palpable tumor (p=0.04) and yielded smaller tumors 3 weeks post-transplant (p=0.001) (Figure 2-7G). These findings strongly suggest that CD24 plays a functional role in TPC activity and in promoting lung cancer metastasis.

To further probe the mechanism of CD24 function in metastasis, we bred CD24 knockout mice to the Kras;p53-flox mice and we have started to compare tumor development and metastasis in Kras;p53-flox CD24 KO/KO and CD24 WT/WT mice (Figure 2-8A,B). To date, the percentage of Kras;p53; CD24 KO mice with metastasis was not significantly different compared to wild-type controls (8/29=28% of CD24KO mice had metastasis and 7/15=47% of CD24WT/WT mice developed metastases, Figure 2-8B). Interestingly, we observed a trend for reduced metastases in the pleural lining or chest cavity in CD24 KO mice (3/8=38%) compared to CD24 WT mice (5/7=71%). These data are still preliminary due to low numbers of WT/WT mice, yet they do demonstrate that CD24 is not required for metastasis per se. CD24 may prove to have a role in metastatic development in particular locations. It is also important to note that CD24 is deleted in these mice from development and at the time of tumor initiation, so that any CD24-dependent activity that may occur specifically during the course of tumor progression and metastasis cannot be assessed.

Murine lung TPCs exhibit clinically relevant, metastatic gene expression profiles

To better understand the connections between TPCs and metastatic potential, we next took an unbiased gene expression profiling approach. Microarray data from the

Figure 2-8: Kras;p53-flox CD24WT and CD24KO mice have similar rates of tumor formation and metastases. Tumor development and metastasis formation was examined 17 weeks following Cre administration, unless mice exhibited signs of distress earlier. **A.** The number and percentage of mice with that developed lung tumors are shown. **B**. The number and percentage of mice with at least one metastatic lesion are shown in the first column. Location columns show the number and percentage of mice with metastases in the noted site.

Figure 2-8: (continued)

A

	No. mice with tumors / No. mice infected (%)
Kras; p53fl/fl; CD24 WT/WT	15/15 (100%)
Kras; p53fl/fl; CD24 KO/KO	29/30 (97%)

B

		Location		
	No. mice with mets. / No. mice with tumors (%)	**Pleural Lining/ Chest Cavity**	**Lymph node or lymphatic**	**Distant**
Kras; p53fl/fl; CD24 WT/WT	7/15 (47%)	5/7 (71%)	4/7 (57%)	0/7 (0%)
Kras; p53fl/fl; CD24 KO/KO	8/29 (28%)	3/8 (38%)	6/8 (75%)	0/8 (0%)

Kras;p53-flox TPCs were further interrogated by bioinformatics. 278 differentially expressed, upregulated probes corresponding to 250 unique genes (log_2 fold-change > 1.53 and p-value <= 0.02) were used in this analysis (Figure 2-9A) (Appendix). Gene set enrichment analysis (GSEA) on the expression data revealed that gene sets involved in processes such as cytoskeletal rearrangement, cell motility/migration, and invasion, all of which are associated with metastatic capacity, were significantly overrepresented in TPCs (Figure 2-9B). Sca1+ and Sca1- populations had equally low levels of vimentin *(Vim)* expression and high levels of E-cadherin *(Cdh1)* (Figure 2-10A,B), confirming that enrichment for these gene sets was not a result of stromal contamination. These results supported the idea that lung TPCs are involved in metastatic spread of Kras;p53-flox lung tumors, and that this activity is not related to an epithelial-to-mesenchymal transition as observed in other tumor types (Cordenonsi et al., 2011).

As we had found increasing evidence that TPCs contributed to metastasis, we sought to determine a relationship between murine TPCs and lung adenocarcinoma patient data. We generated a gene signature consisting of 126 human orthologs corresponding to the significantly upregulated genes in Kras;p53-flox TPCs (Appendix). The TPC gene signature was examined in the Director's Challenge cohort of lung adenocarcinoma patients and was found to be significantly associated with decreased overall survival (p=0.0006) and with metastasis (p=0.049) (Figure 2-9C). These data indicated that our results using murine models to study tumor propagation and metastasis are applicable to human lung cancer.

Figure 2-9: Lung tumor-propagating cells exhibit clinically relevant gene expression profiles that suggest metastatic potential. **A.** Heatmap showing the 250 genes significantly upregulated in Sca1+ TPCs compared to Sca1- non-TPCs from Kras;p53-flox lung tumors as assessed by Affymetrix Mouse 430 2.0 gene expression microarray. Red indicates upregulated expression, green is downregulated expression. **B.** Table of the top 5 most significantly enriched gene sets (based on GSEA enrichment and False Discovery Rate (FDR) q-value less than 0.25) in the TPC cell population. Hippo conserved signature genes found in the indicated gene set are listed in the last column. **C**. The Director's Challenge collection of lung cancer data sets was interrogated for expression of a gene signature upregulated in murine TPCs. Higher expression of the TPC signature (red) versus lower expression of the TPC signature (blue) was compared for patient metastasis (left) and overall survival (right). **D-G.** Expression of indicated genes by qPCR in sorted TPC or non-TPC cells from Kras;p53-flox lung tumors. N=8 samples each. **D**. Yap1 expression, **E.** Taz (Wwtr1) expression, **F.** Nf2 expression, **G.** Cyr61 expression. **H**. The Director's Challenge collection of lung cancer data sets was interrogated for expression of the Hippo conserved signature. Higher expression of the Hippo signature (red) versus lower expression of the Hippo signature (blue) was compared for patient metastasis (left) and overall survival (right). *, $p < 0.05$

Figure 2-9: (continued)

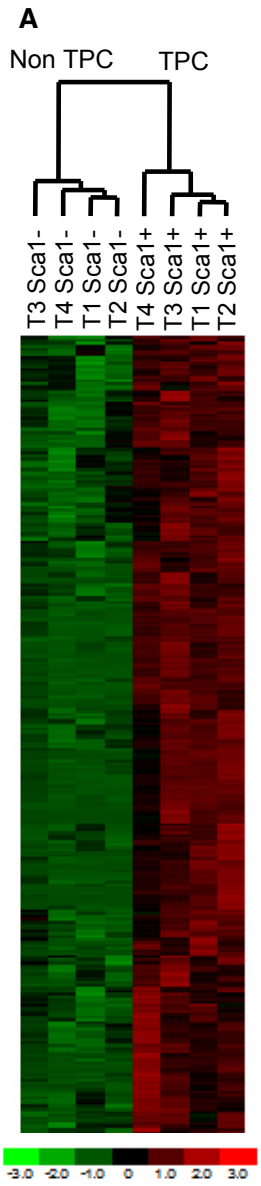

B

Gene Set	Enrichment Score	FDR Q-Value	Hippo Genes
Cell Projection	0.564	0.0147	TGFB2
Actin Filament Based Process	0.550	0.0148	LATS1, NF2, TNNT2
Actin Cytoskeleton Organization and Biogenesis	0.555	0.0154	LATS1, NF2, FLNA, FSCN1
Regulation of Cell Migration	0.671	0.0205	NF2
Regulation of Cell Morphogenesis	0.752	0.0208	N/A

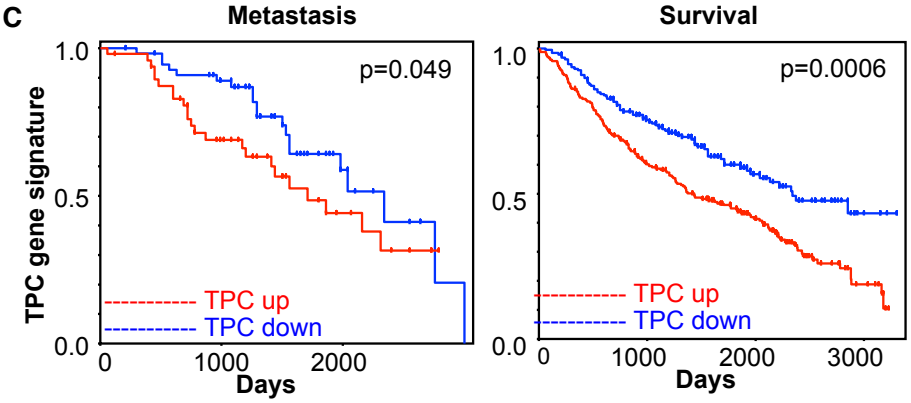

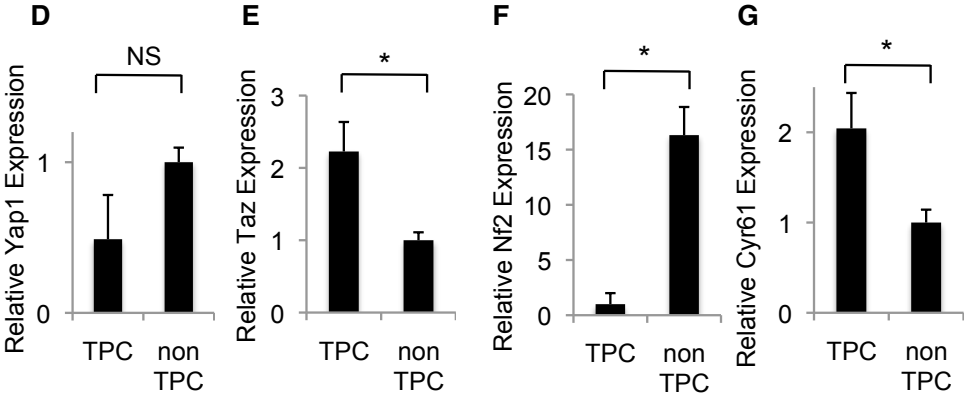

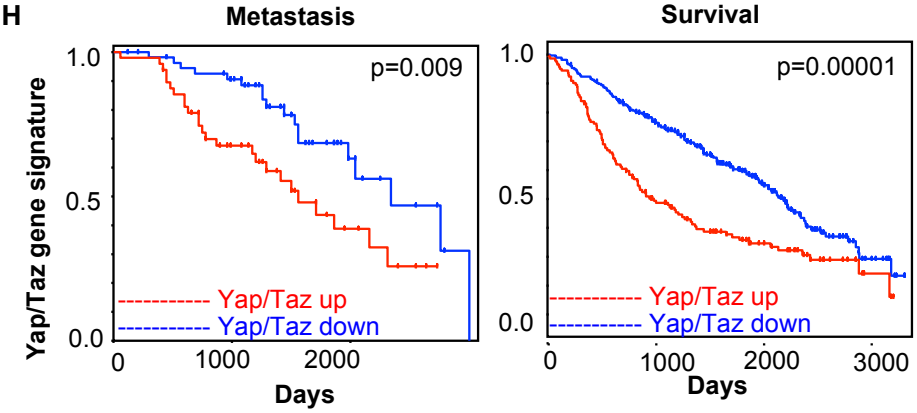

Figure 2-10. Kras;p53-flox Sca1+ TPCs and Sca1- non-TPCs. A. qPCR analysis of Vimentin (*Vim*) expression in lung TPCs and non-TPC cells. **B**. qPCR analysis of expression of E-Cadherin (*Cdh1*) in lung TPCs and non-TPC cells. **C.** Enrichment plot from GSEA of Yap/Taz Signature enrichment in TPCs. NES = Normalized Enrichment score, P value = nominal P value.

Figure 2-10: (continued)

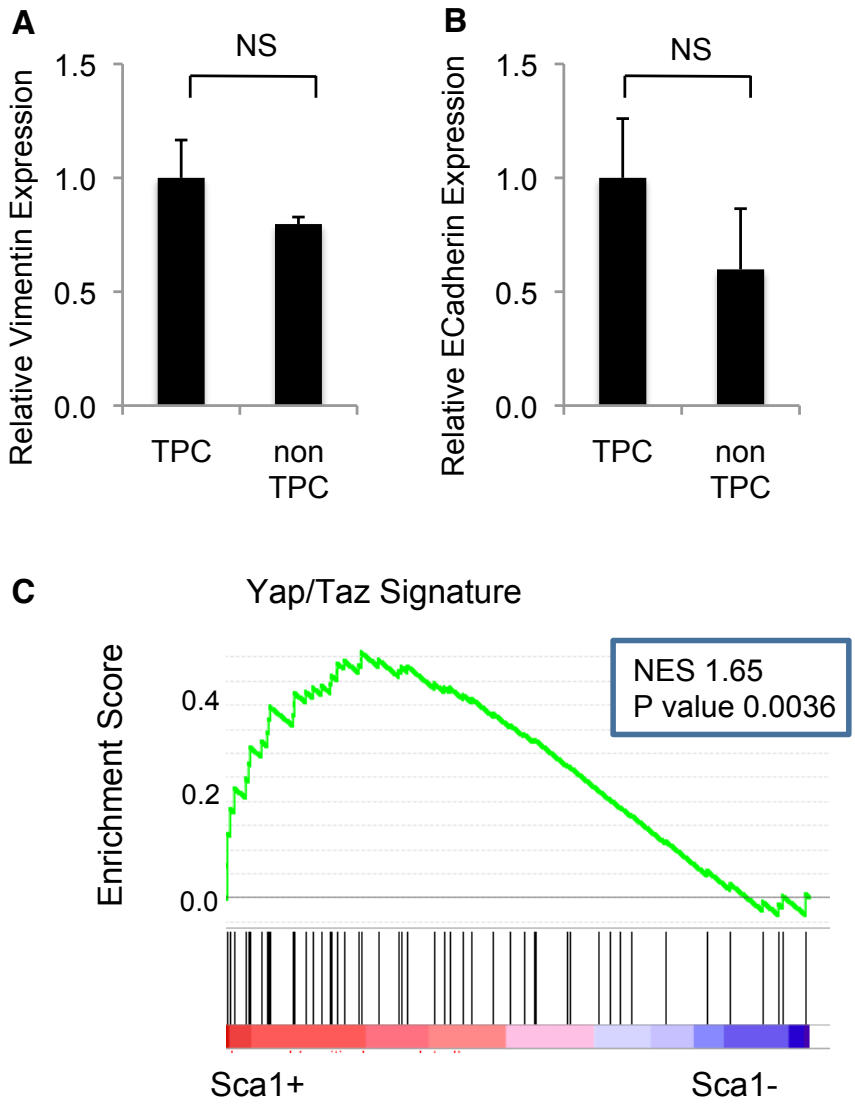

Yap/Taz in metastatic lung TPCs

We next used the gene expression analyses to identify molecules other than CD24 that may be crucial for lung tumor propagation and metastatic potential. The gene sets enriched in lung TPCs, including Actin Filament Based Processes, Actin Cytoskeleton Organization and Biogenesis, and Regulation of Cell Migration, included members of the Hippo signaling cascade (Figure 2-9B). Furthermore, GSEA with a Yap/Taz Gene Signature (Cordenonsi et al., 2011) revealed that Sca1+ TPCs were significantly enriched for this gene set; 25 out of 52 genes in the Yap/Taz gene set exhibited core enrichment in lung TPCs (Figure 2-10C).

We validated expression differences in Hippo pathway components in lung TPCs. *Yap1* was not significantly differentially expressed between the Sca1+ and Sca1- cells by Real Time RT-PCR analysis (Figure 2-9D, p=0.10). However, *Wwtr1 (Taz)*, which has been shown to be important in lung development (Mitani et al., 2009), was over 2-fold overexpressed in the Sca1+ TPCs compared to Sca1- cells (Figure 2-9E, p=0.0087). Importantly, the potent negative regulator of the Hippo pathway, *Nf2*, was greater than 15-fold down-regulated in the Sca1+ cell population (Figure 2-9F, p=0.0001), while a known downstream target of activated Hippo signaling, *cysteine-rich angiogenic inducer 61 (Cyr61),* was over 2-fold up-regulated in the Sca1+ cell population (Figure 2-9G, p=0.021). In the Director's Challenge cohort of lung adenocarcinoma patients, the Yap/Taz signature was significantly associated with worse overall survival (p=0.00001) and with metastasis (p=0.009) (Figure 2-9H). We have also stained a human lung tumor tissue microarray for YAP (Figure 2-11). Slides

Figure 2-11: Human Lung Tumor Tissue Microarray Stained for YAP. Slides were stained for YAP and scored for both nuclear and cytoplasmic expression level scores (1-3) and percentages of positive cells (0-100%). H-Score is the score x percent tumor nuclei (0-300). **A.** Kaplan-Meier survival curve using H-Score, patients grouped into terciles. **B.** Kaplan-Meier Survival curve using YAP nuclear percentage, patients grouped by nuclear score and nuclear percent. **C.** Median YAP Nuclear Percent by N-stage. **D.** Median YAP Nuclear Percent by T-stage. **E.** Median YAP Nuclear Percent by Final Stage. **F.** MedianYAP H-Score by N-stage. **G.** Median YAP H-Score by T-stage. **H.** Median YAP H-Score by Final Stage.

Figure 2-11: (continued)

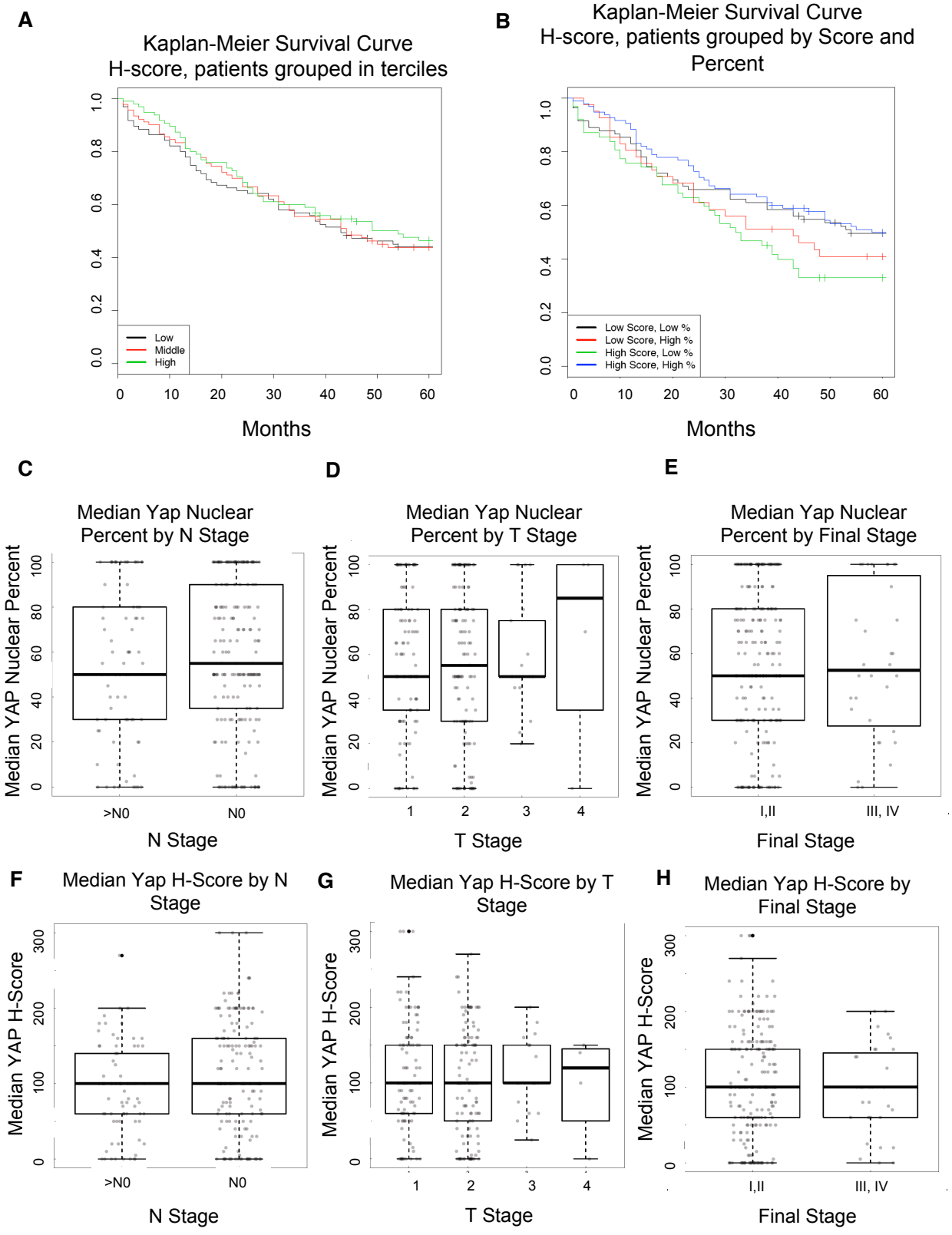

were stained for YAP and scored for both nuclear and cytoplasmic expression level scores (1-3) and percentages of positive cells (0-100%). There was a trend of higher YAP nuclear percentage with higher T stage (Figure 2-11D). Although no significant associations with survival or stage were found, this could be due to staining difficulties (one slide of samples could not be scored due to poor staining) or to insufficient sample size. These data implicated Yap/Taz in TPCs and human lung cancer progression.

We next examined Yap1/Taz protein levels in tissue sections from murine lung cancer models, since differences in protein levels and localization of the Hippo transcriptional controllers may be more important than overall expression levels detected at the RNA level. Yap1/Taz activity is tightly controlled at the protein level: phosphorylated Yap1/Taz is sequestered in the cytoplasm and inactive, but dephosphorylated Yap1/Taz can translocate into the nucleus to activate target gene transcription. Using an antibody that recognizes both Yap1 and Taz proteins, we performed immunostaining of tumors from the non-metastatic Kras model (Jackson et al., 2001) and the Kras;p53-flox metastatic tumors. Interestingly, Yap1/Taz expression in Kras tumors was very weak and almost exclusively cytoplasmic (Figure 2-12A, n=4). In stark contrast, in Kras;p53-flox tumors (n=4) ~30-50% of tumor cells expressed nuclear Yap1/Taz, and in lymph node metastases from Kras;p53-flox mice, almost all cells expressed nuclear Yap1/Taz (n=3) (Figure 2-12A). These results supported the concept that Yap1/Taz expression and activity is correlated with more aggressive disease in lung cancer.

To determine if Yap activity is sufficient to affect lung tumor progression, we used a doxycycline-inducible, constitutively active allele of Yap1 in combination with

Figure 2-12: Yap/Taz function contributes to lung tumor progression and metastatic potential. A. Representative Yap1/Taz IHC (brown staining) in a Kras primary lung tumor (top), Kras;p53-flox tumor (middle), and Kras;p53-flox lymph node metastasis (bottom). 400x magnification, with zoom as shown, approximately 75 μm. **B.** Percentage of mice of each genotype with tumors of grade 0-4 scored from paraffin sections. Grade shown is the highest tumor grade present in each mouse. Grade 0 indicates no tumors present. **C.** Number of lung tumors per mouse was scored from paraffin sections and averaged for each genotype. N = 15 Kras mice, 14 Kras;Yap mice. **D.** Tumor burden was measured as the percentage of lung filled with tumors. *$p<0.05$. Mice were euthanized 7 months after Cre or earlier if symptoms of lung tumors were apparent. N = 15 Kras mice, 14 Kras;Yap mice. **E**. Percentage of Ki67+ cells per 200x field. **F.** The average number of migratory cells observed in transwell migration assays, determined by the number of cells migrating towards serum-containing (10% FBS) media in control, Yap1 or Taz knockdown CK1750 cells. Results shown are the average of three independent experiments. **G.** Average number of lung metastases after tail vein injection of CK1750 shGFP cells (circles), CK1750 shYap1 cells (squares, up triangles), or CK1750 shTaz cells (down triangles, diamonds). Lungs were analyzed for metastases two weeks after injection of 100,000 cells. Each symbol represents an individual mouse analyzed. Data shown are the combination of two independent experiments. *$p < 0.05$, one tailed t test, n=6.

Figure 2-12: (continued)

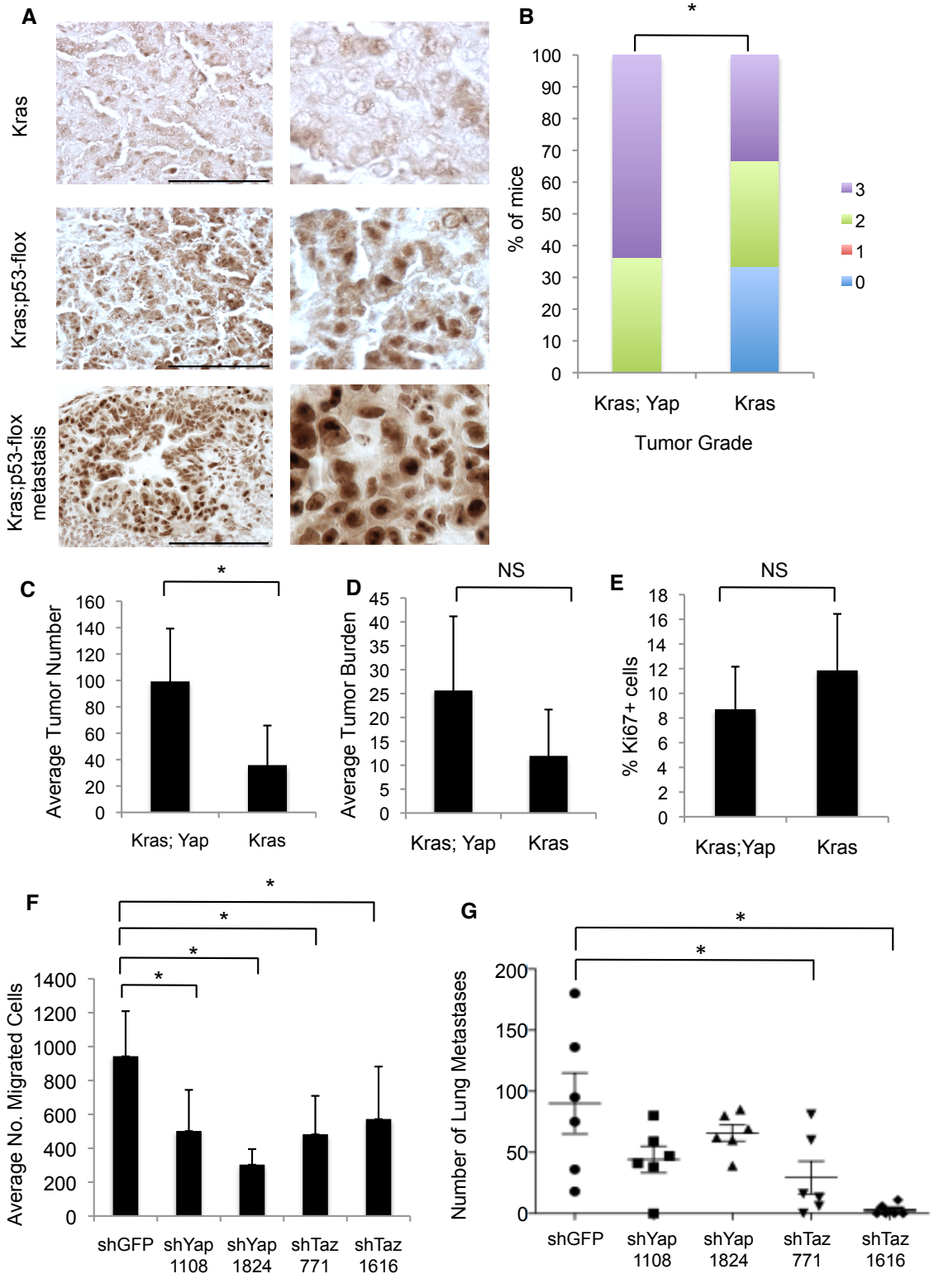

oncogenic Kras *in vivo*. In *tetO-YapS127A* mice, a mutated version of Yap1 exhibits enhanced nuclear localization of Yap1 and constitutive signaling activity (Schlegelmilch et al, 2011). In a binary genetic approach, we activated Yap1 activity in lung tumor cells by treating *Kras; LSL-rtTA; tetO-YapS127A* mice with Adeno-Cre to initiate lung tumorigenesis, followed by treatment with doxycycline to activate Yap signaling concomitant with tumor initiation. Mice were euthanized when they showed signs of distress, seven months after Adeno-Cre and doxycycline administration. Histological analysis showed that tumors of *Kras; LSL-rtTA; tetO-YapS127A* mice were significantly higher grade than those in Kras controls (Cochran-Armitage test, $p = 0.04$, Figure 2-12B). *Kras; LSL-rtTA; tetO-YapS127A* mice had significantly more tumors than Kras controls (Figure 2-12C), but no difference in overall tumor burden, average tumor size, or Ki67 staining index (Figure 2-12D,E, Figure 2-13A,B,C). These results indicated that Yap activation is sufficient to promote lung tumor progression in vivo.

We interrogated the role of Yap/Taz in metastatic capacity using in vitro migration and in vivo tail vein assays in the Kras;p53-flox cell lines after knockdown of *Yap1/Taz*. Two different shRNAs were used to reduce *Yap1* or *Taz* levels to 40-80% of control levels (Figure 2-13D,E). A significant reduction (1.5-3-fold compared to shGFP) in migration was observed in the shYap1 or shTaz cells exhibiting knockdown ($p < 0.05$) compared with the negative control shGFP (Figure 2-12F). To examine whether YAP knockdown in the human lung cancer cell line A549 would yield similar results, we interrogated the ability of two different doxycycline-inducible YAP shRNAs to affect cell migration. Dox-induced YAP knockdown resulted in significantly fewer migrated cells using both hairpins ($p=0.023$ and $p=0.020$); migration was over 2-fold decreased in

Figure 2-13: Yap/Taz knockdown and CK1750, SC241, Tmet, and A549 cells. **A.** qPCR analysis of human Yap1 levels in Kras;LSL-rtTA; tetO-YapS127A (Kras; Yap) mice and littermate controls **B.** Average tumor size in Kras;Yap mice and Kras controls. N = 6 Kras mice, 11 Kras;Yap mice. **C.** Representative images of Ki67 staining in a Kras;Yap tumor (top) and a Kras tumor (bottom). Images are 200x magnification. **D.** qPCR analysis of Yap1 levels after knockdown of Yap1 in CK1750 cells. **E.** qPCR analysis of Taz levels after knockdown of Taz in CK1750 cells. **F.** The average number of migratory cells observed in transwell migration assays, determined by the number of cells migrating towards serum-containing (10% FBS) media in control or YAP1 knockdown A549 cells. +DOX cells were treated with 1ug/mL doxycycline for two days prior to migration experiment to induce knockdown. A and B are two different YAP1 shRNAs. Results shown are the average of two independent experiments. *, p = 0.023, shYAPA, p= 0.020, shYAPB. **G.** H&E images of lung metastasis after tail vein injection of 100,000 CK170 shGFP, shYap1 or shTaz cells. Images are 40x magnification, scale bars represent 1000μM. **H.** Average tumor burden in tumors from tail vein transplantation of shGFP or shTaz CK1750 cells calculated as the percentage of lung area filled with tumors. N=6 mice. shTaz1616, p=0.0096. **I**. Average tumor size in tumors from shGFP or shTaz CK1750 cells. N=6 mice. p= 0.00031 shTaz 771, $p=5.9x10^{-5}$ shTaz16

Figure 2-13: (continued)

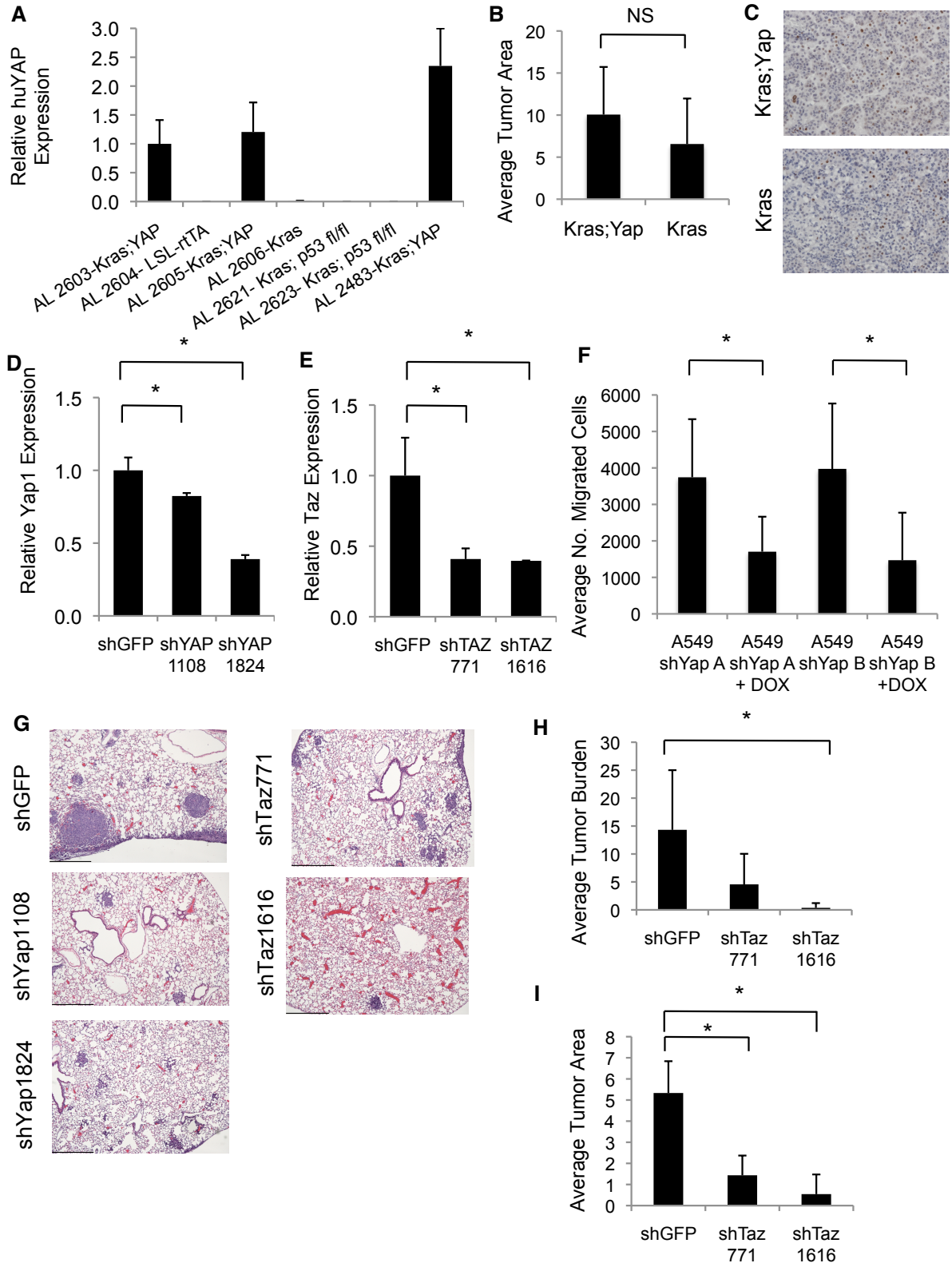

A549 YAP knockdown cells (Figure 2-13F). Finally, tail vein injection was performed to assess the impact of knockdown on metastatic capacity in vivo. Lung metastases were significantly less frequent in recipients of shTaz cell lines compared to shGFP or shYap cells (shYap1108 p=0.061, shYap1824 p=0.18, shTaz771 p=0.029, shTaz1616 p=0.0029), and recipients of shTaz1616 cell lines in particular showed very few or no metastases or tumor burden (Figure 2-12G, Figure 2-13G,H). Average tumor size was also smaller in shTaz recipients (Figure 2-13I). These data indicated that Yap/Taz is necessary and sufficient to drive key steps in advanced lung tumorigenesis, including progression, migration, and metastasis.

To investigate the mechanism of Yap/Taz activity and to discover potential Taz targets in lung cancer cells, gene expression microarray analysis was performed. 3 paired shGFP or shTaz Kras;p53-flox murine lung tumor cell lines (CK1750, SC241, and Tmet) were compared; differentially expressed genes are listed in the Appendix (Figure 2-14A). Gene Set Enrichment Analysis of the shTaz vs shGFP data was used to identify gene sets with negative enrichment scores, indicating cellular processes possibly impacted by *Taz* knockdown (Figure 2-14B). The Yap/Taz gene signature (Cordenonsi et al., 2011) and genes differentially expressed in the *Taz* knockout mouse lungs (Mitani et al, 2009) were significantly enriched in the shTaz data set, validating our approach. qPCR confirmed differential expression of *Cyr61*, a known Yap/Taz target, and *Ltbp4*, a mediator of the TGF-β pathway and possible Yap/Taz target, in SC241 shGFP and shTaz cells (Figure 2-14C), further validating our gene expression data set. Published data sets connected to migration and metastasis (Lung Cancer

Figure 2-14: Gene Set Enrichment Analysis in shGFP vs shTaz cells A. qPCR analysis of Taz levels after knockdown of Taz in CK1750, SC241, and Tmet cells used for microarray analysis. **B**. Enrichment plots from GSEA showing enrichment in shGFP vs shTaz cells. NES = Normalized Enrichment score, P value = nominal P value. See manuscript text for references. **C.** qPCR analysis of Ltbp4 levels after knockdown of Taz in SC241 cells. **D**. qPCR analysis of Cyr61 levels after knockdown of Taz in SC241 cells. **E.** qPCR analysis of Bcl2 levels after knockdown of Taz in SC241 cells.

Figure 2-14: (continued)

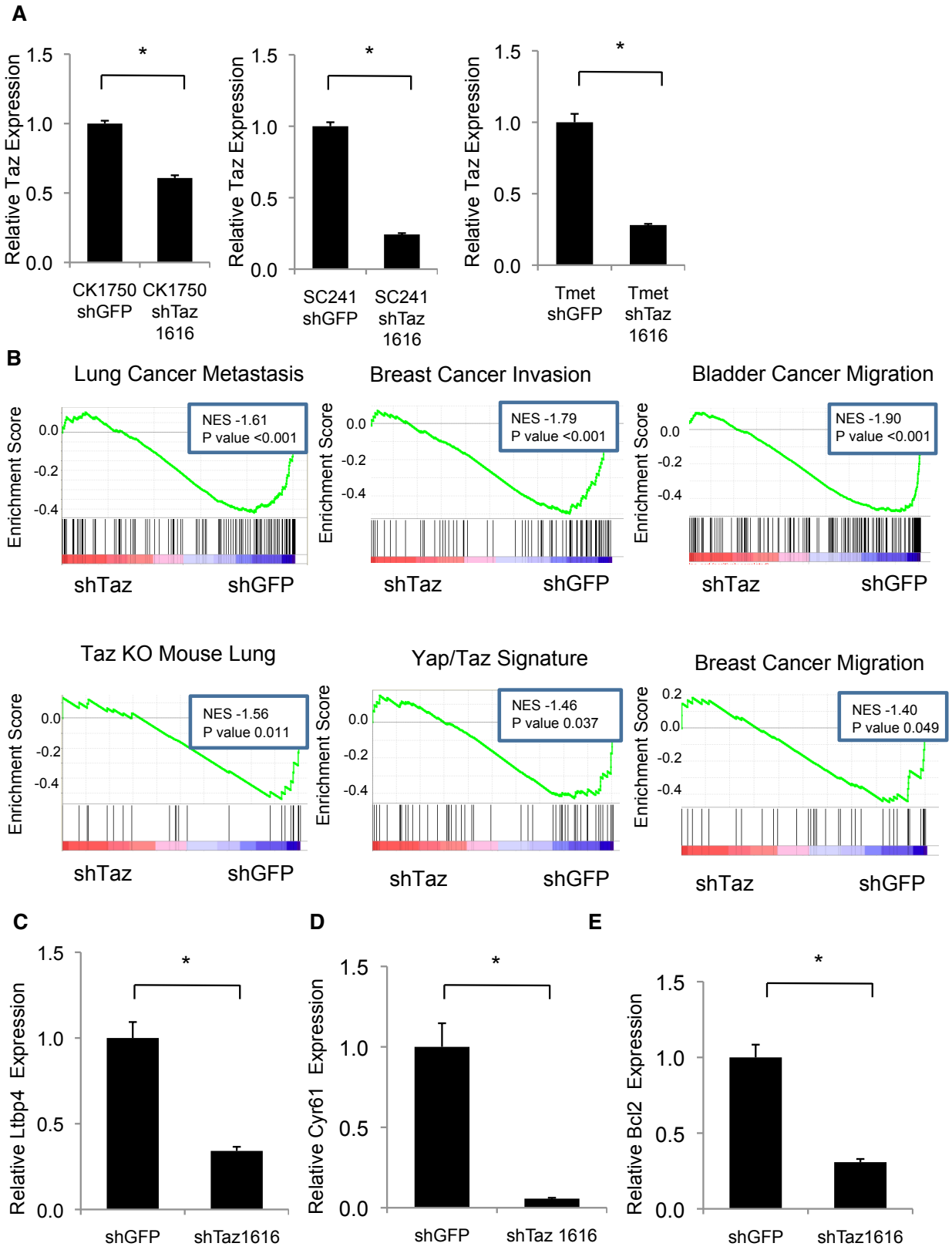

Metastasis- Nguyen et al., 2009, Breast Cancer Invasion- Patsialou et al., 2012, Breast Cancer Migration- Gunawardane et al., 2005, Bladder Cancer Migration- Wu et al., 2008) were also enriched, validating the metastatic capacity associated with Yap/Taz activity.

Gene sets of interest that were significantly enriched in shTaz cells revealed several pathways and activities that may be critical for Yap/Taz function in lung cancer progression and metastasis. Several gene sets associated with NF Kappa B signaling were significantly enriched: I KappaB Kinase NF KappaB Cascade, Regulation of I KappaB Kinase NF KappaB Cascade, and Positive Regulation of I KappaB Kinase NF KappaB Cascade (Appendix). Expression of *Bcl2*, an NF-KB target that inhibits apoptosis, was validated for significantly decreased expression in shTaz cells (Figure 2-14E). Gene sets corresponding to actin cytoskeletal processes were also highly decreased after Taz knockdown, including Actin Cytoskeleton, Cytoskeletal Protein Binding, Actin Binding, Actin Filament Binding, and Actin Filament Based Processes. These pathways and activities may be critical for cancer progression and metastasis.

Discussion

Our results provide novel insight into the cells and pathways that drive the progression and metastasis of lung adenocarcinoma using TPCs as a discovery platform. TPCs expressing Sca1 and CD24 were enriched for metastatic activity after orthotopic transplantation. CD24 knockdown impaired metastatic processes including migration and ectopic tumor growth. Our findings also implicate a role for the Hippo signaling mediators Yap and Taz in lung TPCs and the progression and metastasis of

lung cancer. Importantly, expression of TPC and Yap/Taz gene signatures predicted metastasis and patient survival, demonstrating the relevance of our findings in mouse models to human disease. These results delineate new ways to uncover clinically relevant mechanisms in advanced lung cancer.

Our data provide new understanding of the links between tumor-propagating cells and metastasis, an idea that has been postulated for at least a decade with limited experimental backing (reviewed in (Adhikari et al., 2011)). The significant correlation of our TPC gene expression signature with both metastasis and patient survival adds new support for this proposition. Lung TPCs also exhibited downregulation of *Nkx2.1*, a mechanism known to correspond with increased metastatic potential (Curtis et al., 2010; Winslow et al., 2011). We show that several TPC populations can produce metastatic lesions, albeit with differing degrees of activity; Sca1+CD24+ cells were more metastatic than Sca1-CD24+ cells. Differing from our work, tumor cell barcoding studies in colon cancer showed that only one TPC fraction, long-term TPCs, contributed to metastases (Dieter et al., 2011). Therefore, in some tumor types one unique metastasis-propagating cell population may exist, whereas our data suggest a gradient of metastatic capacity exists within lung tumors.

CD24 appears to be required for lung TPCs to propagate tumors and possibly to drive a metastatic cascade. CD24 expression levels were similar in lung tumors arising in recipient mice after transplantation of CD24+ or CD24- cells; it is possible that activation of CD24 expression is critical during a particular stage of tumorigenesis or metastatic progression. Furthermore, results in bladder (Overdevest et al., 2011) and liver (Lee et al., 2011) cancer, in combination with the present study, make a strong

argument for CD24 being a marker and functional mediator of metastatic potential in multiple tumor types. As proliferation and apoptosis were not significantly altered in CD24 knockdown cells, the mechanism by which CD24 affects tumorigenesis remains to be determined.

We demonstrate for the first time that Yap/Taz are active in lung-tumor propagating cells with metastatic potential, and that Yap activation affects lung tumor progression in a mouse model *in vivo*. Interestingly, the Yap/Taz gene signature predicted lung cancer patient metastasis and survival. Taz expression was also found to be significantly associated with poor differentiation, poor survival, and metastasis in patients with non-small cell lung cancer (Xie et al., 2012). Previously, Yap1 and Taz have both been implicated in different processes of lung development and disease (see also Introduction). Taz interacts with the master transcription factor Nkx2.1 during mouse lung development to promote alveolarization (Mitani et al., 2009). These and our own observations of elevated Taz expression in TPCs and decreased lung metastases from tail vein injections after knockdown of Taz tempt us to speculate that Taz, rather than Yap1, is primarily utilized by lung tumors to promote metastasis. Supporting this idea, Taz may regulate the cancer stem cell phenotype in breast cancers (Cordenonsi et al., 2011). In our studies, constitutive mutant Yap was sufficient to significantly impact Kras-driven lung tumor progression, yet metastasis did not develop in Kras;Yap mice. Notably, the presence of more high grade tumors in Kras;Yap mice required euthanasia and may have precluded our ability to assess later metastatic progression. It is also possible that further activation of Yap1 through mutation at more than one site is

necessary to drive metastases. It remains possible that both Yap1 and Taz play important and complementary roles in lung TPC function and metastatic potential.

Yap/Taz may control lung cancer cell migration and metastasis through a number of mechanisms implicated in this study. In tail vein assays, the average tumor size was significantly less in recipients of shTaz cells vs shGFP cells, pointing to the potential importance of Taz regulation of proliferation in advanced lung tumors. Supporting this idea, we found many gene sets enriched for cell growth in shTaz cells. GSEA also suggested a role for Taz regulation of the NF-KappaB pathway, which has been shown to be required for Kras;p53-flox lung tumorigenesis (Meylan et al, 2009; Xue et al., 2011). Further studies are needed to which, if any, of the cellular activities identified in our expression analyses are critical for Yap/Taz contribution to aggressive lung cancer.

It will be important to understand the cellular markers and mechanistic drivers of metastatic cancer cells in each tumor type of interest. In bladder cancer, CD24+ cells rely on the STAT3/NANOG network to promote metastasis (Lee et al., 2011), whereas CD24+ cells utilize the SRC-family kinase YES in metastatic melanoma (Liu et al., 2012). Additionally, we show here that Yap/Taz activity may mediate lung cancer metastasis in lung TPCs. It remains to be determined if there is a direct interaction between CD24 and Yap1/Taz regulation in lung tumorigenesis, since we found that these molecules were all required for lung cancer cell metastatic behavior. Interestingly, Hippo signaling has been implicated in regulation of expression of CD44, another surface marker of tissue-specific TPCs such as in breast cancer (Cordenonsi et al., 2011; Xu et al., 2010). Although there may be overlap between the markers and

pathways responsible for metastasis in different tumor types, many combinations are likely utilized by aggressive cancer cells. Synergistic investigations into the phenotype of cells that are responsible for metastatic spread of lung cancer and the pathways that mediate this progression should ultimately lead to new ways to target the most functionally important and deadly lung cancer cells.

Materials and Methods

Generation of Cell Lines and *in vitro* Assays

CK1750 and SC241 cells were generated by culturing tumor cells from a Kras;p53-flox donor mouse in DMEM+10%FBS. Tmet cells were obtained from Monte Winslow (Winslow et al, 2011). These cells were infected with lentiviral constructs from The RNAi Consortium, pLKO.1 based system. The two hairpins directed at CD24a were TRCN0000077028 (shCD24a-1) and TRCN0000077032 (shCD24a-5), the two hairpins directed at Yap1 were TRCN0000095866 (Yap1108) and TRCN0000095864 (Yap1824), the two hairpins directed at Taz were TRCN0000095949 (Taz1616) and TRCN0000095951 (Taz771), with a non-targeting hairpin directed against GFP (Sigma SHC005) as a control. Transduced cells were selected with 3μg/ml puromycin for 1-2 weeks. Knockdown was confirmed by quantitative RT-PCR and flow cytometry. To generate shCD24-Low-1 and shcD24-Low-5 cell lines, sorts for the lowest CD24 expressing cells were completed. All lines were maintained in DMEM+10%FBS. 24-well format cell migration assays (Corning) were performed as per the manufacturer's instructions. Briefly, cells were serum-starved overnight, harvested with Accutase (Millipore) and counted. Cells were plated in serum-free conditions (30,000 cells per

well) on the top chambers and the bottom chambers contained either serum-free DMEM or DMEM+10%FBS. After a 24 hour incubation, non-migratory cells were removed using a cotton swab, migratory cells were stained with DAPI for imaging and nuclei were counted using ImageJ. All conditions were completed with three to four replicates and averaged.

Mice and Tissues

Lox-Stop-Lox-Kras^{G12D};*p53*$^{fl/fl}$ and *Lox-Stop-Lox-Kras*^{G12D} mice (Jackson et al., 2005; Jackson et al., 2001) were maintained in virus-free conditions on 129 SvJae background. *Lox-Stop-Lox-Kras*^{G12D};*Lox-Stop-Lox-rtTA;tetO-YapS127A* mice were maintained in virus-free conditions on a mixed 129/C57Bl6 background. All mouse experiments were approved by the BCH Animal Care and Use Committee and by the Dana-Farber Cancer Institute Institutional Animal Care and Use Committee, both accredited by AAALAC, and were performed in accordance with relevant institutional and national guidelines and regulations. Lung tissue preparation was as described (Curtis et al., 2010) and sections were analyzed for tumors by at least two investigators including a pathologist with expertise in murine lung cancer. Tumor burden, the percentage of lung filled with tumor, was calculated using ImageJ to measure total lung and tumor area from H&E stained paraffin sections from each mouse. Tumor size was measured using ImageJ to quantify tumor area from paraffin sections and the average area of all lung tumors per mouse was calculated. For metastases, heart, liver, spleen, kidneys, lymph nodes, and chest wall were also analyzed. Immunohistochemistry was performed as described (Schlegelmilch et al., 2011) with anti- Yap1 (1:50, Cell Signaling #4912) or anti-Ki67 (1:10,000, Novocastra) antibodies and developed using Vectastain

Elite ABC kit (Vector Labs). Immunofluorescent staining for pro-SPC was performed with anti-pro-SPC (1:500, Chemicon). Imaging was performed with a Nikon 90i camera and NIS-Elements software and processed with NIS-Elements and Adobe Photoshop.

FACS Analysis and Sorting

Mice were euthanized with avertin overdose and lungs were dissected and examined grossly for tumor formation. Tumors were dissected from the lungs of primary mice and tumor tissue was prepared as described (Curtis et al., 2010). Briefly, tumors were isolated, minced, digested rotating for 1h at 37°C with 2mg/ml Collagenase/Dispase (Roche) and then filtered twice (100 μm, then 40 μm) after a 5 minute incubation with 0.025 mg/mL DNase. Cell lines were trypsinized and then filtered (40 μm). Single cell suspensions were stained using Sca1-FITC, –PE, or APC-Cy7, CD45-APC, CD31-APC, CD24-Biotin (with Streptavidin-APC/Cy7) or –FITC (BD Pharmingen) with 7AAD (Molecular Probes) or DAPI (Sigma) staining to visualize dead cells. All antibodies were incubated for 15-20 minutes at 1:100 dilutions for primaries and 1:200 for secondaries. Cell sorting was performed with a Beckman Coulter/Cytomation MoFlo or a BD FACS Aria, and data were analyzed with FloJo software (Tree Star, Inc.).

Tumor Transplants

Intratracheal transplants were performed as described (Curtis et al., 2010). Mice were monitored for signs of lung tumor onset and euthanized for gross and histological analysis upon signs of distress. Cells for tail vein injections were resuspended in PBS and mice were sacrificed two weeks after injection for analysis of lung metastasis. Cells for subcutaneous injections were resuspended in a 1:1 mixture of PBS and matrigel (BD

Biosciences), and subcutaneous tumor volume was measured (volume = length x width x depth).

Quantitative RT-PCR Gene Expression Analysis

RNA from sorted cell populations was extracted from 8-12 tumors using the Stratagene Absolutely RNA Nanoprep Kit. cDNA was made using the SuperScript III kit (Invitrogen) and analyzed using TaqMan Assays (Applied Biosystems) for *Acta2* (Mm00725412_s1), *Bcl2* (Mm00477631_m1*), Cd24a* (Mm00782538_sH), *Cdh1* (Mm01247357_m1), *Cyr61* (Mm00487498_m1), *Ltbp4* (Mm00723631_m1*), Nf2* (Mm00477771_m1), *Vim* (Mm01333430_m1), *Wwtr1* (Mm01289583_m1), *Yap1* (Mm01143263_m1), or *YAP1* (Hs00902712_g1), with a BioRad iQ5 iCycler or StepOnePlus™ Real-Time PCR System (Applied Biosystems) and software as per the manufacturer's recommendations. Mouse *Actb* (B-actin, 4352341E) or *Gapdh* (4352339E) was used as an endogenous control for normalization.

Microarray Analysis

For Sca1+/Sca1- arrays, four primary tumors from Kras;p53-flox mice were dissociated and sorted into CD31-/CD45-/Sca1- and CD31-/CD45-/Sca1+ populations. RNA was isolated as above and subsequently amplified using the WT-Ovation Pico kit (NuGEN). The amplified cDNA was fragmented and biotin labeled using the FL-Ovation Biotin V2 kit (NuGEN). The Children's Hospital Boston Molecular Genetics Core Facility performed the hybridization and data acquisition using an Affymetrix Mouse Genome 430 2.0 expression array. Array normalization, expression value calculation

and clustering analysis were performed using DNA-Chip Analyzer (www.dchip.org, Schadt et al., 2001). The Invariant Set Normalization method was used to normalize arrays at probe cell level to make them comparable, and the model-based method was used for probe-selection and computing expression values. These expression levels were attached with standard errors as measurement accuracy, which were subsequently used to compute 90% confidence intervals of fold changes between the Sca1+ and Sca1- groups. The lower confidence bounds of fold changes were conservative estimate of the real fold changes. Genes with more than 2 fold increased expression in Sca1+ cells relative to Sca1- cells and an associated p value of 0.02 were selected for further study (Sca1+ up gene signature, Appendix). The Affymetrix probe match tool was used for matching the Sca1+ up gene list to human U133A probes. Gene set enrichment analysis (GSEA) was performed by the Center for Computational Cancer Biology at the Dana Farber Cancer Institute with the pre-ranked implementation of the GSEA software package (Subramanian et al., 2005) using the moderated t-statistic from limma to determine rank order (Smyth, 2004).

shGFP/shTaz Arrays were performed in the Boston Children's Hospital Molecular Genetics Core facility on Affymetrix mouse Gene2.0ST slides. Array quality was assessed using the R/Bioconductor package (http://www.bioconductor.org/). Raw CEL files from U133A Affymetrix arrays were processed using the robust multi-array average (RMA) algorithm (Irizarry et al., 2003). To identify genes correlating with the phenotypic groups, we used limma (Smyth, 2004) to fit a statistical linear model to the data and then tested for differential gene expression in the two groups: shTaz (SC241, CK1750

and Tmet) vs shGFP (SC241, CK1750 and Tmet). GSEA (Subramanian et al., 2005) was performed using the javaGSEA desktop application on pre-ranked gene lists constructed from RMA normalized expression data.

Human tumor data Kaplan-Meier analysis

Raw gene expression data from human lung adenocarcinoma samples were obtained from publications (Director's Challenge, 2008, Chitale et al., 2009, http://cbio.mskcc.org/Public/lung_array_data/). Among these datasets, 3 are annotated for survival post biopsy while 1 dataset is annotated for both survival and metastatic spread of disease. Probes intensities from the Affymetrix U133A platform used in these studies were normalized and modeled using dChip software. Kaplan-Meier survival analyses were implemented after the samples were hierarchically clustered using centroid linkage into two risk groups using either the human orthologues of the Sca1+ up gene set or the Yap/Taz conserved gene set (Cordenonsi et al., 2011). Differences of the survival risk between the two risk groups were assessed using the Mantel-Haenszel log rank test. The larger area between the two risk groups and its associated smaller p value from the Mantel-Haenszel log rank test implicate a better classification model. For the dataset for which metastatic spread was annotated, both survival and metastatic spread of the two risk groups were queried.

Statistical Analysis

Except where indicated, Student's t-test was used to compare measurements between 2 conditions. For tumor cell transplants, data organized in tables was analyzed using Fisher's exact test. GraphPad Prism (GraphPad Software, Inc.), Excel and Mstat (McArdle Laboratory for Cancer Research, University of Wisconsin) were used for

graphing and statistical analyses. Unless noted otherwise, pooled data is represented by the mean and standard deviation. p-values less than 0.05 with a one-tailed distribution were considered significant.

Acknowledgements

We thank the DFCI, BIDMC, and CHB HemOnc FACS facilities, M. Correll and S. Duan of the DFCI Center for Computational Cancer Biology, and members of the Kim Lab for technical assistance and discussions, R. Bronson for histopathology, L. Zon, C. Cepko, S. Armstrong, and W. Hahn for helpful discussions. This work was supported by DoD, Air Force Office of Scientific Research, National Defense Science and Engineering Graduate Fellowships, 32 CFR 168a (to S.J.C. and A.N.L.), PF-09-121-01-DDC and PF-12-151-01-DMC from the American Cancer Society (to K.W.S. and C.M.F., respectively), the Ladies Auxilliary to the Veterans of Foreign Wars (to C.M.F.), Dana Farber Harvard Cancer Center Lung Cancer SPORE grant P50 CA090578, R01 AG2400401, R01 CA122794, R01 CA140594 (to K-K.W.), the V Foundation for Cancer Research, American Cancer Society Research Scholar Grant #RSG-08-082-01-MGO, the Freeman Trust, the Harvard Stem Cell Institute, NIH/NHLBI U01 HL100402 and R01 HL090136 and The Lung Cancer Alliance (to C.F.K.).

References

Adhikari, A.S., Agarwal, N., Iwakuma, T. (2011). Metastatic potential of tumor-initiating cells in solid tumors. Front. Biosci. *16*, 1927-1938.

Al-Hajj, M., Wicha, M.S., Benito-Hernandez, A., Morrison, S.J., and Clarke, M.F. (2003). Prospective identification of tumorigenic breast cancer cells. Proc. Natl. Acad. Sci. U.S.A. *100*, 3983–3988.

Bertolini, G., Roz, L., Perego, P., Tortoreto, M., Fontanella, E., Gatti, L., Pratesi, G., Fabbri, A., Andriani, F., Tinelli, S., et al. (2009). Highly tumorigenic lung cancer CD133+ cells display stem-like features and are spared by cisplatin treatment. Proc. Natl. Acad. Sci. U.S.A. *106*, 16281–16286.

Charafe-Jauffret, E., Ginestier, C., Iovino, F., Tarpin, C., Diebel, M., Esterni, B., Houvenaeghel, G., Extra, J.-M., Bertucci, F., Jacquemier, J., et al. (2010). Aldehyde dehydrogenase 1-positive cancer stem cells mediate metastasis and poor clinical outcome in inflammatory breast cancer. Clin. Cancer Res. *16*, 45–55.

Charafe-Jauffret, E., Ginestier, C., Iovino, F., Wicinski, J., Cervera, N., Finetti, P., Hur, M.H., Diebel, M.E., Monville, F., Dutcher, J., et al. (2009). Breast cancer cell lines contain functional cancer stem cells with metastatic capacity and a distinct molecular signature. Cancer Res. *69*, 1302–1313.

Chen, Y.C., Hsu, H.S., Chen, Y.W., Tsai, T.H., How, C.K., Wang, C.Y., Hung, S.C., Chang, Y.L., Tsai, M.L., Lee, Y.Y., et al. (2008). Oct-4 expression maintained cancer stem-like properties in lung cancer-derived CD133-positive cells. PLoS One *3*, e2637.

Chitale, D., Gong, Y., Taylor, B.S., Broderick, S., Brennan, C., Somwar, R., Golas, B., Wang, L., Motoi, N., Szoke, J., et al. (2009). An integrated genomic analysis of lung cancer reveals loss of DUSP4 in EGFR-mutant tumors. Oncogene *31*, 2773-2783.

Cordenonsi, M., Zanconato, F., Azzolin, L., Forcato, M., Rosato, A., Frasson, C., Inui, M., Montagner, M., Parenti, A.R., Poletti, A., et al. (2011). The Hippo transducer TAZ confers cancer stem cell-related traits on breast cancer cells. Cell *147*, 759–772.

Croker, A.K., Goodale, D., Chu, J., Postenka, C., Hedley, B.D., Hess, D.A., and Allan, A.L. (2009). High aldehyde dehydrogenase and expression of cancer stem cell markers selects for breast cancer cells with enhanced malignant and metastatic ability. J. Cell. Mol. Med. *13*, 2236–2252.

Curtis, S.J., Sinkevicius, K.W., Li, D., Lau, A.N., Roach, R.R., Zamponi, R., Woolfenden, A.E., Kirsch, D.G., Wong, K.-K., and Kim, C.F. (2010). Primary tumor genotype is an important determinant in identification of lung cancer propagating cells. Cell Stem Cell *7*, 127–133.

Damelin, M., Geles, K.G., Follettie, M.T., Yuan, P., Baxter, M., Golas, J., DiJoseph, J.F., Karnoub, M., Huang, S., Diesl, V., et al. (2011). Delineation of a cellular hierarchy in lung cancer reveals an oncofetal antigen expressed on tumor-initiating cells. Cancer Res. *71*, 4236–4246.

Dieter, S.M., Ball, C.R., Hoffmann, C.M., Nowrouzi, A., Herbst, F., Zavidij, O., Abel, U., Arens, A., Weichert, W., Brand, K., et al. (2011). Distinct types of tumor-initiating cells form human colon cancer tumors and metastases. Cell Stem Cell *9*, 357–365.

Director's Challenge Consortium for the Molecular Classification of Lung Adenocarcinoma, Shedden, K., Taylor, J.M., Enkemann, S.A., Tsao, M., Yeatman, T.J., Gerald, W.L., Eschrich, S., Jurisica, I., Giodano, T.J., et al. (2008). Gene expression-based survival prediction in lung adenocarcinoma: a multi-site, blinded validation study. Nat. Med. *14*, 822-827.

Eramo, A., Lotti, F., Sette, G., Pilozzi, E., Biffoni, M., Di Virgilio, A., Conticello, C., Ruco, L., Peschle, C., and De Maria, R. (2008). Identification and expansion of the tumorigenic lung cancer stem cell population. Cell Death Differ. *15*, 504–514.

Gunawardane, R.N., Sgroi, D.C., Wrobel, C.N., Koh, E., Daley, G.Q., Brugge, J.S. (2005). Novel role for PDEF in epithelial cell migration and invasion. Cancer Res. *65*, 11572-11580.

Hermann, P.C., Huber, S.L., Herrler, T., Aicher, A., Ellwart, J.W., Guba, M., Bruns, C.J., and Heeschen, C. (2007). Distinct populations of cancer stem cells determine tumor growth and metastatic activity in human pancreatic cancer. Cell Stem Cell *1*, 313–323.

Ignatius, M.S., Chen, E., Elpeck, N.M., Fuller, A.Z., Tenente, I.M., Clagg, R., Liu, S., Blackburn, J.S., Linardic, C.M., Rosenberg, A.E., et al. (2012). In Vivo imaging of tumor-propagating cells, regional tumor heterogeneity, and dynamic cell movements in embryonal rhabdomyosarcoma. Cancer Cell *21*, 680-693.

Irizarry, R.A., Hobbs, B., Collin, F., Beazer-Barclay, Y.D., Antonellis, K.J., Scherf, U., and Speed, T.P. (2003). Exploration, normalization, and summaries of high density oligonucleotide array probe level data. Biostatistics *4*, 249–264.

Jackson, E.L., Olive, K.P., Tuveson, D.A., Bronson, R., Crowley, D., Brown, M., and Jacks, T. (2005). The differential effects of mutant p53 alleles on advanced murine lung cancer. Cancer Res. *65*, 10280–10288.

Jackson, E.L., Willis, N., Mercer, K., Bronson, R.T., Crowley, D., Montoya, R., Jacks, T., and Tuveson, D.A. (2001). Analysis of lung tumor initiation and progression using conditional expression of oncogenic K-ras. Genes Dev. *15*, 3243–3248.

Korkaya, H., Paulson, A., Iovino, F., and Wicha, M.S. (2008). HER2 regulates the mammary stem/progenitor cell population driving tumorigenesis and invasion. Oncogene *27*, 6120–6130.

Kristiansen, G., Schlüns, K., Yongwei, Y., Denkert, C., Dietel, M., and Petersen, I. (2003a). CD24 is an independent prognostic marker of survival in nonsmall cell lung cancer patients. Br. J. Cancer *88*, 231–236.

Lee, H.J., Choe, G., Jheon, S., Sung, S.-W., Lee, C.-T., and Chung, J.-H. (2010). CD24, a novel cancer biomarker, predicting disease-free survival of non-small cell lung carcinomas: a retrospective study of prognostic factor analysis from the viewpoint of forthcoming (seventh) new TNM classification. J Thorac Oncol *5*, 649–657.

Lee, T.K., Castilho, A., Cheung, V.C., Tang, K.H., Ma, S., and Ng, I.O. (2011). CD24(+) liver tumor-initiating cells drive self-renewal and tumor initiation through STAT3-mediated NANOG regulation. Cell Stem Cell *9*, 50-63.

Levina, V., Marrangoni, A.M., DeMarco, R., Gorelik, E., and Lokshin, A.E. (2008). Drug-selected human lung cancer stem cells: cytokine network, tumorigenic and metastatic properties. PLoS One *3*, e3077.

Liu, W., Monahan, K.B., Pfefferle, A.D., Shimamura, T., Sorrentiono, J., Chan, K., Roadcap, D.W., Ollila, D.W., Thomas, N.E., Castrillon, D.H., et al. (2012). LKB1/STK11 inactivation leads to expansion of a pro-metastatic tumor sub-population in melanoma. Cancer Cell *21*, 751-764.

Malanchi, I., Santamaria-Martínez, A., Susanto, E., Peng, H., Lehr, H.-A., Delaloye, J.-F., and Huelsken, J. (2012). Interactions between cancer stem cells and their niche govern metastatic colonization. Nature *481*, 85–89.

Meylan, E., Dooley, A.L., Feldser, D.M., Shen, L., Turk, E., Ouyang, C., and Jacks, T. (2009). Requirement for NF-KappaB signaling in a mouse model of lung adenocarcinoma. Nature *46*, 104-107.

Mitani, A., Nagase, T., Fukuchi, K., Aburatani, H., Makita, R., and Kurihara, H. (2009). Transcriptional coactivator with PDZ-binding motif is essential for normal alveolarization in mice. Am. J. Respir. Crit. Care Med. *180*, 326–338.

Nguyen, D.X., Chiang, A.C., Zhang, X.H., Kim, J.Y., Kris, M.G., Ladanyi, M., Gerald, W.L., and Massague, J. (2009). WNT/TCF signaling through LEF1 and HOXB9 mediates lung adenocarcinoma metastasis. Cell *138*, 51-62.

Overdevest, J.B., Thomas, S., Kristiansen, G., Hansel, D.E., Smith, S.C., and Theodorescu, D. (2011). CD24 offers a therapeutic target for control of bladder cancer metastasis based on a requirement for lung colonization. Cancer Res. *71*, 3802–3811.

Patsialou, A., Wang, Y., Lin, J., Whitney, K., Goswami, S., Kenny, P.A., and Condeelis, J.S. (2012). Selective gene-expression profiling of migratory tumor cells in vivo predicts clinical outcome in breast cancer patients. Breast Cancer Res. *14*, R129.

Pan, D. (2010). The hippo signaling pathway in development and cancer. Dev. Cell *19*, 491-505.

Pang, R., Law, W.L., Chu, A.C.Y., Poon, J.T., Lam, C.S.C., Chow, A.K.M., Ng, L., Cheung, L.W.H., Lan, X.R., Lan, H.Y., et al. (2010). A subpopulation of CD26+ cancer stem cells with metastatic capacity in human colorectal cancer. Cell Stem Cell *6*, 603–615.

Pisters, K.M., Ginsberg, R.J., Giroux, D.J., Putnam, J.B., Kris, M.G., Johnson, D.H., Roberts, J.R., Mault, J., Crowley, J.J., and Bunn, P.A. (2000). Induction chemotherapy before surgery for early-stage lung cancer: A novel approach. Bimodality Lung Oncology Team. J. Thorac. Cardiovasc. Surg. *119*, 429-439.

Schadt, E.E., Li, C., Ellis, B., and Wong, W.H. (2001). Feature extraction and normalization algorithms for high-density oligonucleotide gene expression array data. J. Cell. Biochem. Suppl. *37*, 120-125.

Schlegelmilch, K., Mohseni, M., Kirak, O., Pruszak, J., Rodriguez, J.R., Zhou, D., Kreger, B.T., Vasioukhin, V., Avruch, J., Brummelkamp, T.R., et al. (2011). Yap1 acts downstream of α-catenin to control epidermal proliferation. Cell *144*, 782–795.

Shipitsin, M., Campbell, L.L., Argani, P., Weremowicz, S., Bloushtain-Qimron, N., Yao, J., Nikolskaya, T., Serebryiskaya, T., Beroukhim, R., Hu, M., et al. (2007). Molecular definition of breast tumor heterogeneity. Cancer Cell *11*, 259-273.

Siegel, R., Naishadham, D., and Jemal, A. (2013). Cancer statistics, 2013. CA Cancer. J. Clin. *63*, 11–30.

Smyth, G.K. (2004). Linear models and empirical bayes methods for assessing differential expression in microarray experiments. Stat. Appl. Genet. Mol. Biol. *3*, Article3.

Subramanian, A., Tamayo, P., Mootha, V.K., Mukherjee, S., Ebert, B.L., Gillette, M.A., Paulovich, A., Pomeroy, S.L., Golub, T.R., Lander, E.S., et al. (2005). Gene set enrichment analysis: a knowledge-based approach for interpreting genome-wide expression profiles. Proc. Natl. Acad. Sci. U.S.A. *102*, 15545-15550.

Wang, Y., Dong, Q., Zhang, Q., Li, Z., Wang, E., and Qiu, X. (2010). Overexpression of yes-associated protein contributes to progression and poor prognosis of non-small-cell lung cancer. Cancer Sci. *101*, 1279–1285.

Winslow, M.M., Dayton, T.L., Verhaak, R.G.W., Kim-Kiselak, C., Snyder, E.L., Feldser, D.M., Hubbard, D.D., DuPage, M.J., Whittaker, C.A., Hoersch, S., et al. (2011). Suppression of lung adenocarcinoma progression by Nkx2-1. Nature *473*, 101–104.

Wu, Y., Siadaty, M.S., Berens, M.E., Hampton, G.M., and Theodorescu, D. (2008). Overlapping gene expression profiles of cell migration and tumor invasion in human bladder cancer identify metallothionein 1E and nicotinamide N-methyltransferase as novel regulators of cell migration. Oncogene *27*, 6679-6689.

Xie, M., Zhang, L., He, C.-S., Hou, J.-H., Lin, S.-X., Hu, Z.-H., Xu, F., and Zhao, H.-Y. (2012). Prognostic significance of TAZ expression in resected non-small cell lung cancer. J Thorac Oncol *7*, 799–807.

Xu, Y., Stamenkovic, I., and Yu, Q. (2010). CD44 attenuates activation of the hippo signaling pathway and is a prime therapeutic target for glioblastoma. Cancer. Res. *70*, 2455-2464.

Xue, W., Meylan, E., Oliver, T.G., Feldser, D.M., Winslow, M.M., Bronson, R., and Jacks, T. (2011). Response and resistance to NF-kB inhibitors in mouse models of lung adenocarcinoma. Cancer Discov. *1*, 236-247.

Yao, X., Labelle, M., Lamb, C.R., Dugan, J.M., Williamson, C.A., Spencer, D.R., Christ, K.R., Keating, R.O., Lee, W.D., Paradis, G.A., et al. (2013). Determination of 35 cell surface antigen levels in malignant pleural effusions identifies CD24 as a marker of disseminated tumor cells. Int. J. Cancer *133*, 2925–2933.

Zheng, Y., la Cruz, de, C.C., Sayles, L.C., Alleyne-Chin, C., Vaka, D., Knaak, T.D., Bigos, M., Xu, Y., Hoang, C.D., Shrager, J.B., et al. (2013). A rare population of CD24(+)ITGB4(+)Notch(hi) cells drives tumor propagation in NSCLC and requires Notch3 for self-renewal. Cancer Cell *24*, 59–74.

Zhou, Z., Hao, Y., Liu, N., Raptis, L., Tsao, M.-S., and Yang, X. (2011). TAZ is a novel oncogene in non-small cell lung cancer. Oncogene *30*, 2181–2186.

CHAPTER 3:

Discussion

Author Contributions

Several people contributed to the work presented in this chapter. **Allison N. Lau** and **Carla F. Kim** developed hypotheses and designed experiments. **Kerstin W. Sinkevicius** provided human lung tumor RNA samples and performed CD24 staining in human lung tumors**.** Pathologists **Lucian Chirieac** and **Lynette Sholl** analyzed CD24 staining in human tumors. **Samuel P. Rowbotham** contributed to phospho-Yap western blot experiments as well as Yap/Taz and CD24 qPCR experiments. **Darcy E. Wagner** performed F-actin staining experiments. **Enhua Zhou** performed cell contractility studies. **Kevin Chou** and **Masaki Mori** provided assistance with TEAD reporter experiments**.**

Summary

The work presented in this thesis identifies key molecules and pathways important for lung cancer metastasis. These findings are summarized in Figure 3-1. First, studies of murine lung adenocarcinoma tumors led to prospective isolation of TPC populations with metastatic potential. When fractionating murine lung tumors into four populations based on expression of the TPC markers Sca1 and CD24, two populations were capable of tumor propagation and metastasis, Sca1+CD24+ and Sca1-CD24+. However, metastatic capability was enriched in the Sca1+CD24+ population. CD24 function was also found to be important for migration and metastatic properties of murine lung adenocarcinoma cells. In addition to identification of CD24 as a molecule important for metastasis, further study of the double positive population will be valuable in understanding more about metastatic lung cancer cells. Gene expression analysis of murine lung TPCs identified the Hippo pathway as an important pathway involved in lung cancer metastasis. Mediators of their signaling mechanism, Yap and Taz, were found to be important for tumor progression and metastases of lung adenocarcinoma cells. The advances described here will lead to future studies regarding the mechanism of CD24 and Yap/Taz in metastatic lung cancer, which will hopefully lead to treatments for this deadly disease.

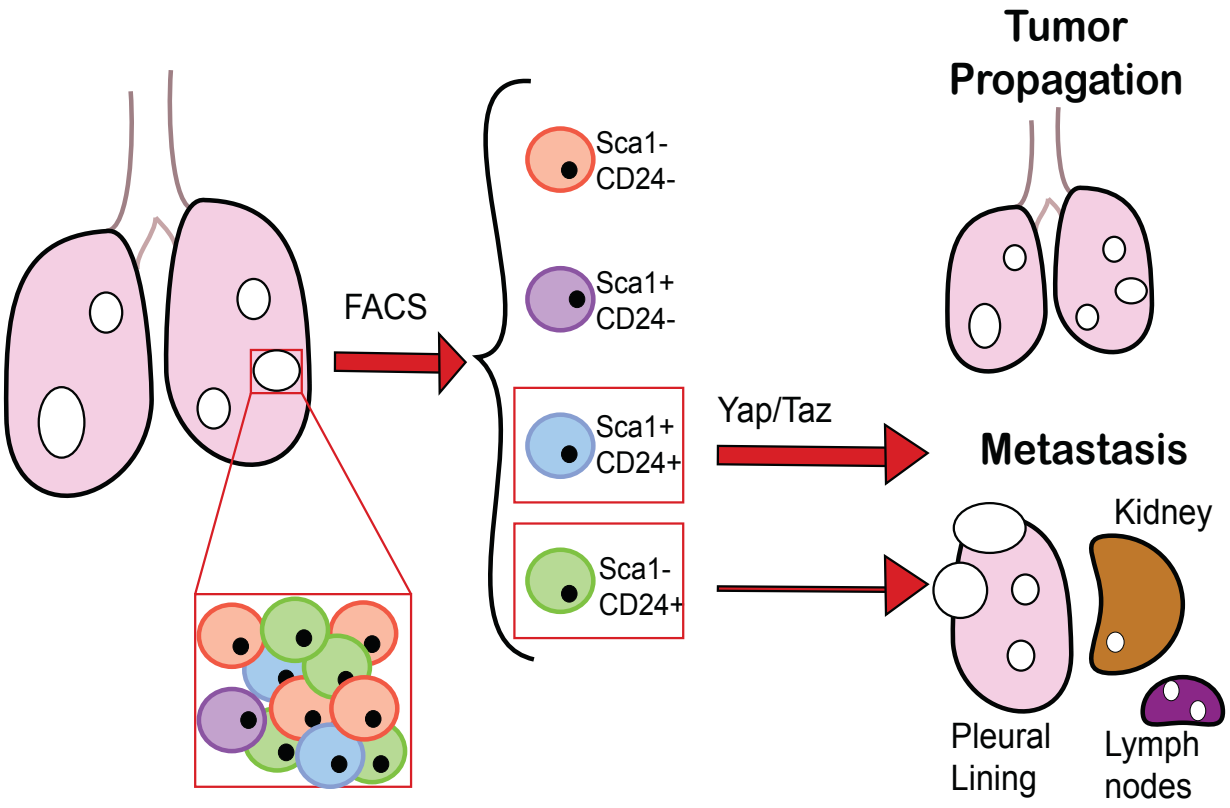

Figure 3-1: Model of murine lung TPCs and metastasis. Murine lung adenocarcinoma tumors were fractionated into four populations based on expression of the TPC markers Sca1 and CD24. Two populations were capable of tumor propagation, Sca1+CD24+ and Sca1-CD24+, but metastatic ability was enriched in the Sca1+CD24+ population.

Lung TPCs and Metastasis

Although a few previous studies have linked TPCs with metastasis in other cancer types, the work presented here is the first to link lung TPCs and metastasis. The results of this study bring up several intriguing questions regarding the relationship between tumor propagating ability and metastatic ability. First, our work provides evidence that there are multiple TPC populations within murine Kras;p53-flox lung adenocarcinomas, and that these various TPCs have different degrees of metastatic capacity. Second, our work highlights differences in TPC frequency based on tumor subfractionation using single markers or combinations of markers to enrich for different populations.

Many studies of CSCs, clonal evolution, and metastasis raise the issue of whether metastatic potential is limited to one population of tumorigenic cells or whether it can arise through genetic or epigenetic changes in many populations of cancer cells (Magee et al., 2012). Today, it is generally thought within the field that some combination of the cancer stem cell hypothesis, clonal evolution, and microenvironmental influence is at work within tumors, with different tumor types leaning more towards a hierarchy than others (Magee et al., 2012; Meacham and Morrison, 2013). Our results support the idea that multiple populations within lung adenocarcinoma may be capable of tumor propagation and metastasis. It would be interesting to test whether multiple tumor clones within Kras-driven lung tumors have different tumor propagating and metastatic abilities at various time points during tumor progression or after therapy. Ongoing work in our lab is examining this hypothesis using

a LSL-YFP lineage tag to sort and transplant tumor cells at various time points (K Bellaria, SJ Curtis, C Kriegel, CF Kim, unpublished data).

Others have suggested that there are multiple TPC clones within a tumor and that these TPCs compete with each other for tumor repopulation or metastatic ability (Baccelli and Trumpp, 2012; Magee et al., 2012; Visvader and Lindeman, 2012). Our results support this hypothesis, showing that Sca1+CD24+ TPCs are best able to seed metastases, but that Sca1-CD24+ TPCs are also able to metastasize at a lower frequency. While some studies have identified one TPC population that is capable of metastasis (Dieter et al., 2011; Hermann et al., 2007; Pang et al., 2010), other studies show that there are multiple tumor clones (not necessarily TPCs) that are responsible for metastasis (Campbell et al., 2010; Gerlinger et al., 2012; 2014; Wu et al., 2012; Yachida et al., 2010).

Two studies by Iacobuzio-Donahue, Futreal and colleages showed that there are clonal populations within pancreatic tumors that give rise to distant metastases, but that these metastatic clones are distinct and evolve from the original parental clones which are non-metastatic (Campbell et al., 2010; Yachida et al., 2010). Similar work in renal cell carcinoma and medulloblastoma found that there were metastatic clones which branched off from the parental tumor clone (Gerlinger et al., 2012; 2014; Wu et al., 2012). These studies provide evidence for parallel evolution of multiple mutations in different tumor subclones. In contrast, a study of tumor clones in breast cancer showed evidence for a single metastatic clone that arose late in tumor development (Navin et al., 2011). Similar to our findings, two studies of acute lymphoblastic leukemia (ALL) showed that there were several CSC clones that existed in patients (Anderson et al.,

2011; Notta et al., 2011). During progression, after therapy, and in serial xenotransplantation different clones could take over and initiate new tumors (Anderson et al., 2011; Notta et al., 2011).

Another interesting implication of the work presented here is that the TPC frequency was lower when comparing more purified populations than it was for bulk populations (Table 3-1) (Chapter 2) (Curtis et al., 2010). TPC frequency was similar in the total epithelial tumor cell population (CD31-CD45-) and in Sca1+ TPCs (~1/ 1,400), whereas TPC frequency in Sca1+CD24+ and Sca1-CD24+ was much lower (~1/ 8,000-10,000).

This raises the interesting idea that tumor cell populations influence each other's tumor propagation ability, and more importantly, regulate each other's role in driving tumor maintenance or progression. Little has been studied about the effect of separating smaller and smaller subfractions of tumor cells from their surrounding microenvironment. It is possible that there are supporting cells in more heterogeneous TPCs that are lost upon further selection of Sca1+CD24+ cells, and this explains the difference in TPC frequency in these populations. In the normal lung, Sca1 has been shown to also mark fibroblasts and other stromal cells (McQualter et al., 2009), while CD24 marks epithelial populations such as ciliated cells, BASCs, and other lung progenitors (McQualter et al., 2010; Zacharek et al., 2011). It is possible that either stromal cells and/or other epithelial cells within Kras;p53-flox tumors are present within the Sca1+ TPC population and interact with tumor propagating cells to enhance their function, and that further selection of Sca1+CD24+ and Sca1-CD24+ cells reduces the

Table 3-1. Frequency of tumor-propagating cells in multiple populations of Kras;p53-flox lung tumors. TPC frequency was determined by limiting dilution analysis of tumor transplants and calculated using the L-CALC software.

Kras; p53-flox tumor cells transplanted		
Population	**TPC Frequency**	**Source**
CD31-CD45-	1/ 1,400	(Curtis et al., 2010)
Sca1+	1/ 1,489	(Curtis et al., 2010)
Sca1-	1/ 7,567	(Curtis et al., 2010)
Sca1+ CD24+	1/ 10,284	(Lau et al., 2014)
Sca1- CD24+	1/ 8,153	(Lau et al., 2014)
Sca1+ CD24-	1/ 37,838	(Lau et al., 2014)
Sca1- CD24-	1/ 22,289	(Lau et al., 2014)

ability of these cells to interact. For example, the non-TPC tumor cells such as the CD24- and Sca1- populations may produce paracrine signaling molecules that support TPCs. Work in breast cancer has shown that paracrine factors produced by non-cancer stem cells can influence and expand cancer stem cell populations (Fillmore et al., 2010; Harrison et al., 2013; Scheel et al., 2011; Yamamoto et al., 2013).

Other work in our lab has shown that interaction with endothelial cells enhances both bronchioalveolar stem cell function (Lee et al., 2014), as well as Kras lung tumor cell growth in subcutaneous transplants (JH Lee and CF Kim, unpublished data). It is known that Kras;p53-flox tumors contain a significant amount of desmoplastic stroma (Jackson et al., 2005). Studies in other cancers such as brain, colorectal, and head and neck cancers have shown that stromal cells such as endothelial cells or myofibroblasts within the tumor can enhance CSC numbers or function (Borovski et al., 2009; Calabrese et al., 2007; Krishnamurthy et al., 2010; Lu et al., 2013; Vermeulen et al., 2010). In trying to sort out the most purified, enriched TPC population, it is possible that we have abrogated important interactions of these TPCs with their stromal cell and non-TPC partners.

Cancer stem cell therapies have focused on targeting the cancer stem cells themselves. However, if the signals regulating cancer stem cell function are originating in the microenvironment, then disrupting the cancer stem cell niche may be an important strategy for cancer therapy. The work of several groups suggests that anti-angiogenic therapies aimed at disrupting the vascular niche of cancer stem cells could be used to treat brain tumors (Borovski et al., 2009; Calabrese et al., 2007; Folkins et al., 2007). Targeting secreted factors produced by stromal cells or other tumor cells that

induce cancer stemness could also be an important strategy for cancer stem cell therapy.

It would be interesting to see if transplanting the Sca1+CD24+ and Sca1-CD24+ populations along with different tumor stromal cell types such as endothelial cells or fibroblasts would enhance their tumor propagating ability. Another interesting experiment would be to isolate tumor cell subpopulations, uniquely label each, and then transplant mixed populations to determine how they influence each other. We could also perform lineage tracing experiments within unperturbed tumors to track different tumor cell subpopulations simultaneously and watch how they influence tumor progression.

The Role of CD24 in Lung Cancer Metastasis

Although the CD24 gene has been cloned for over 20 years, the function of CD24 is still being elucidated. CD24 is a glycosyl phosphatidylinositol (GPI) –linked cell surface adhesion molecule with multiple *N*- and *O*- glycosylation sites (Fang et al., 2010). CD24 was first identified in 1978 as part of screen to identify leukocyte differentiation antigens and was first named “heat-stable antigen,” or HSA, due to its heat resistance ability (Springer et al., 1978). Mouse CD24 was cloned in 1990, and the human CD24 was identified in 1991 (Kay et al., 1990; Kay et al., 1991). Unlike the mouse protein, human CD24 also contains additional serine and threonine residues, making the molecule more mucin-like (Kay et al., 1991). This difference in structure could possibly lead to differences in mouse CD24 versus human CD24 function, as will be further discussed.

CD24 knockout mice have a defect in B cell maturation (Wenger et al., 1995; Nielsen et al., 1997). In B cells, CD24 acts as a co-stimulatory molecule that activates T cells (Hubbe and Altevogt, 1994; Liu et al., 1997). In other contexts and in cancer cells, CD24 has been shown to bind to P-selectin to mediate cell rolling along endothelial cells (Aigner et al., 1997; Friederichs et al., 2000; Sammar et al., 1994). CD24 has also been shown to signal through the Src family kinases (SFKs) to activate mitogen-activated protein kinase (MAPK) signaling (Bretz et al., 2012a; 2012b; Liu et al., 2012; Mierke et al., 2011; Sammar et al., 1997; Wang et al., 2010a; Zarn et al., 1996).

In addition to hematopoietic cells, CD24 is expressed on a wide variety of epithelial cells and cancers, and has been well studied in mammary stem cells and breast cancer stem cells. Murine mammary stem cells are found in the $CD49f^{hi}CD29^{hi}$CD24+Sca1- population, while in human breast cancer, the cancer stem cell phenotype is thought to be CD44+CD24-/low (Al-Hajj et al., 2003; Shackleton et al., 2006; Stingl et al., 2006). Murine CD24+ CD90+ breast cancer cells were shown to be TPCs that also played a role in metastasis (Malanchi et al., 2012).

In the lung, the CD24 high expressing population is thought to contain ciliated cells, while BASCs or other lung progenitors are $CD24^{low}$ (McQualter et al., 2010; (Zacharek et al., 2011). In lung cancer, patients with high expression of CD24 by immunohistochemistry had more advanced disease progression and cancer-related death (Kristiansen et al., 2003a; Lee et al., 2010). Malignant pleural effusions from lung cancers have also been shown to express CD24 (Yao et al., 2013). However, another study showed that lung cancers with CD24-negative/low expression were associated with worse survival and poor differentiation (Damelin et al., 2011). A recent study in the

Kras;p53-flox model showed that the CD24+ITGB4+Notch^{hi} population was enriched for tumor propagation, but metastatic potential in this population was not examined (Zheng et al., 2013).

Since Src phosphorylation is one mechanism by which CD24 controls cell migration and invasion, total Src levels and phosphorylation status of Src family kinases were measured by Western blot in CK1750 shGFP and shCD24 cells in three murine Kras;p53-flox lung tumor cell lines, CK1750, Tmet and SC241 (Figure 3-2). While Src levels were similar, phospho-SFK levels decreased after CD24 knockdown in all three cell lines; decreased SFK activity may impair tumor propagation in CD24 knockdown cells. Further experiments such as immunoprecipitation and western blots for specific SFK members will be needed to identify which SFK member is responsible for the effect on migration and invasion. In addition, treatment of shGFP and shCD24 cells with dasatinib, a SFK inhibitor, would further show that SFK activity is important for migration of CD24-expressing lung cancer cells.

Recent studies also showed that CD24 acts through Src to affect the contractility of cancer cells, leading to their increased invasiveness (Bretz et al., 2012b; Mierke et al., 2011). Contractile forces are one of many physical forces such as hydrostatic pressure, shear stress, and compression and tension forces that cells are exposed to in their microenvironment (Butcher et al., 2009; Halder et al., 2012). Cells respond to these mechanical properties of their environment, including stiffness of the extracellular matrix (ECM) as well as traction or compression forces exerted by other cells. The cells then use these cues to change the stiffness of their cytoskeletons, and actomyosin

Figure 3-2: p-SFK levels decrease after CD24 knockdown. Phospho-Src Family Kinase and total Src levels are shown in shGFP vs shCD24 whole-cell lysates from three Kras;p53-flox lung cancer cell lines. p-SFK and Src blots were stripped and re-probed with a pan-Actin antibody as a loading control. Similar results were obtained in repeat experiments.

Figure 3-2: (continued)

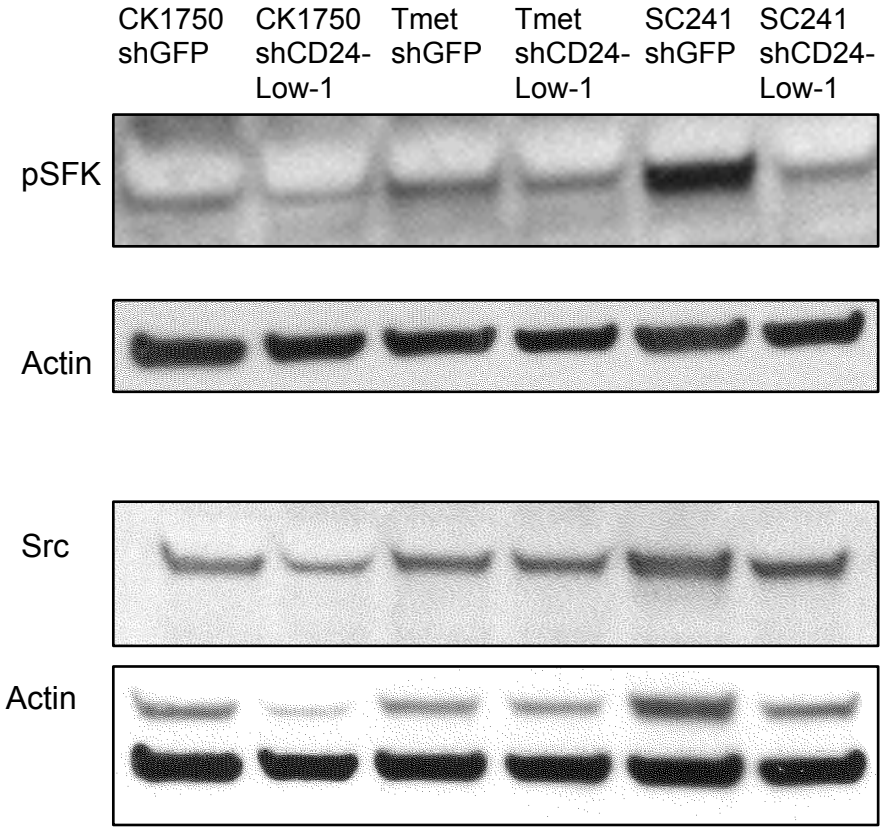

contractility and cytoskeletal remodeling then transmits forces back to the ECM and other cells to induce microenvironmental changes. The disruption of this process of "mechanoreciprocity" has been shown to promote tumorigenesis (Butcher et al., 2009).

We tested whether knockdown of CD24 in CK1750 cells affected cell contractility and found that CD24 knockdown decreased the traction force, net contractile moment, and the contractile strain energy of individual cells (Figure 3-3). Apart from contractility, other cell mechanical properties can be tested such as testing the dynamics of cell spreading. Our current focus is to test whether CD24 (and Taz, discussed later) affects the spreading of cell aggregates on a solid fibronectin-coated substrate in 3 dimensions (Douezan et al., 2011). This spreading is dependent on integrin binding to fibronectin and is thought to mimic *in vitro* the process of EMT observed in metastatic tumors *in vivo*. In this assay, the cells are measured as a population instead of on an individual cell basis as in the contractility experiments. This may be beneficial to rule out variability in single cell experiments based on CD24 knockdown levels. In the future, we also plan to perform these cell spreading experiments on primary Kras;p53-flox CD24+ or CD24- lung tumor cells.

CD24 has been therapeutically targeted in many other studies. In bladder cancer, treatment of mice with an anti-CD24 antibody decreased tumor formation in xenograft models (Overdevest et al., 2011). Anti-CD24 antibody treatment has also been used in models of colorectal and pancreatic cancers (Sagiv et al., 2008). There have also been anti-CD24 clinical treatments for hematopoietic cancers (Benkerrou et al., 1998; Fischer et al., 1991). Treating mice with an anti-CD24 antibody either in Kras;p53-flox mice or in our transplant assay for TPC ability could be useful in terms of testing effectiveness of

Figure 3-3: Contractility measurements in CD24 knockdown cells. A. Root mean squared traction measurements of CK1750 shGFP and shCD24 cells. Cells are plated sparsely on collagen 1-coated gels. N = 39-46 cells per group. Statistical comparisons to control were made using the Kruskal-Wallis nonparametric one-way analysis of variance by ranks. p= 0.0146. **B.** Median traction measurements of CK1750 shGFP and shCD24 cells. p= 0.0224 **C.** Net contractile moment measurements of CK1750 shGFP and shCD24 cells p=0.0300 **D.** Contractile strain energy measurements of CK1750 shGFP and shCD24 cells. p= 0.00300 **E-F.** Example measurement of traction forces exerted by a single shCD24 cell in Pa.

Figure 3-3: (continued)

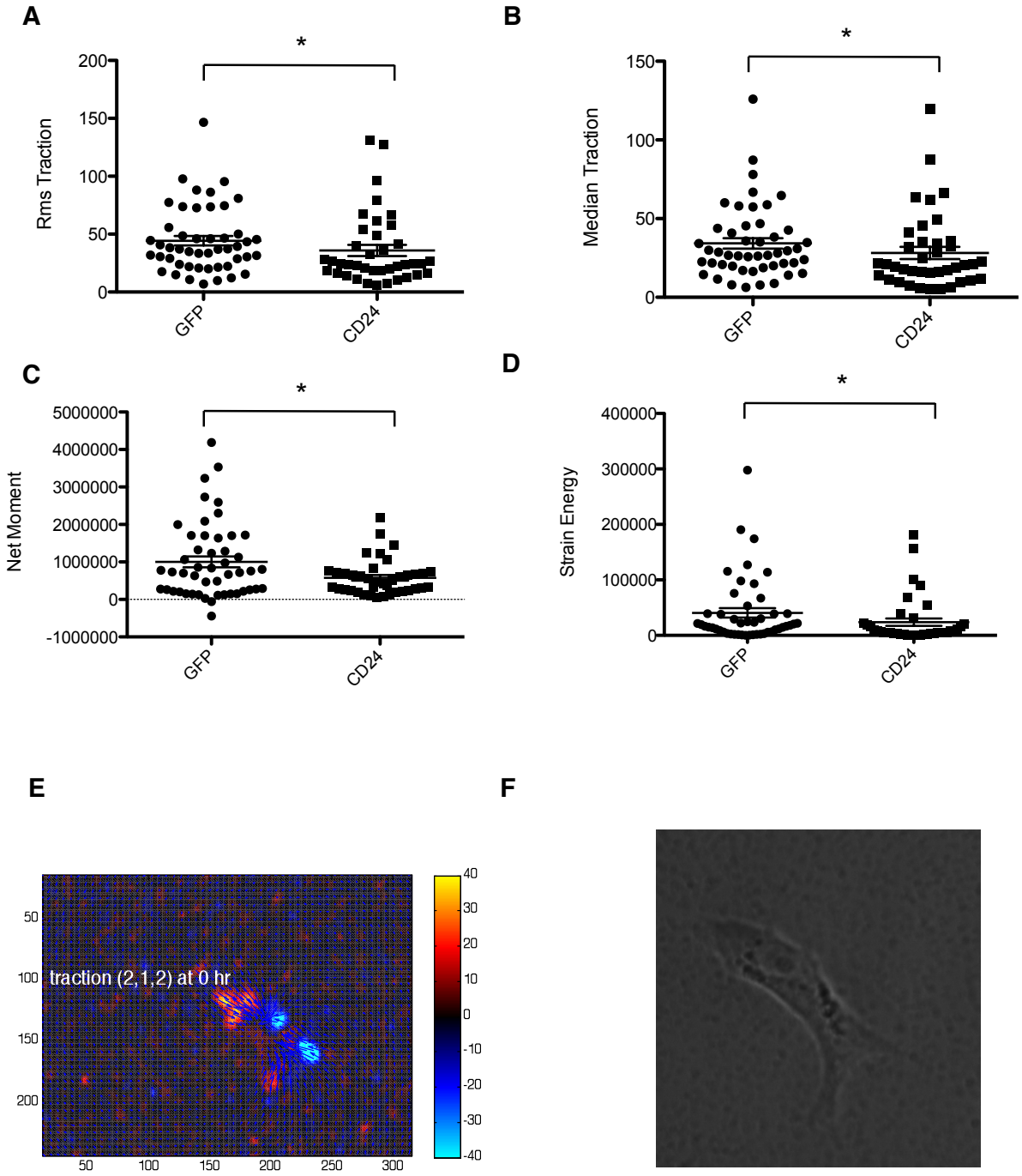

anti-CD24 treatments in lung adenocarcinoma. These experiments would provide a complement to our studies of Kras;p53-flox; CD24 KO mice.

We have also examined the role of CD24 in human lung cancer. By qPCR, CD24 expression in human lung tumors did not differ across tumor stage (Figure 3-4A). In fact, perhaps opposite of what was expected, tumors with higher CD24 mRNA expression were more differentiated (Figure 3-4B). Similarly, immunohistochemistry for CD24 on human lung tumor sections showed that staining was highest in more differentiated cells as determined by a pathologist (Figure 3-4C) (L Chirieac, AN Lau, L Sholl, KW Sinkevicius, CF Kim, unpublished data). In contrast to what has been reported by other studies (Kristiansen et al., 2003a; Lee et al., 2010), staining of a human lung tissue microarray of more than 60 samples failed to show a correlation with patient prognosis (L Chirieac, KW Sinkevicius, CF Kim, unpublished data).

It is possible that the different structure of CD24 in humans compared to mice is responsible for these differences; or, another possibility is that CD24 localization is important to consider in these experiments. It has been reported in breast cancer that CD24 has both apical membranous and membrano-cytoplasmic expression patterns (Abraham et al., 2005; Kristiansen et al., 2003b; Park et al., 2010). Apical membranous expression patterns were found in more differentiated cells, while membrano-cytoplasmic expression was found in more aggressive tumor cells (Park et al., 2010).

In lung cancer, it has been reported that intracellular CD24 is most correlated with patient prognosis (Lee et al., 2010). We noticed that CD24 expression in human matched sets of human lung tumors and metastases also displayed both apical and

Figure 3-4: Human CD24 expression is higher in more differentiated lung tumor cells. A. Quantitative real-time PCR analysis of relative CD24 mRNA levels in human lung tumor samples grouped by tumor stage. N = 25 samples **B.** Quantitative real-time PCR analysis of relative CD24 mRNA levels in human lung tumor samples grouped by tumor differentiation status. N = 25 samples. **C.** Example of CD24 staining in human lung adenocarcinoma tissue.

Figure 3-4: (continued)

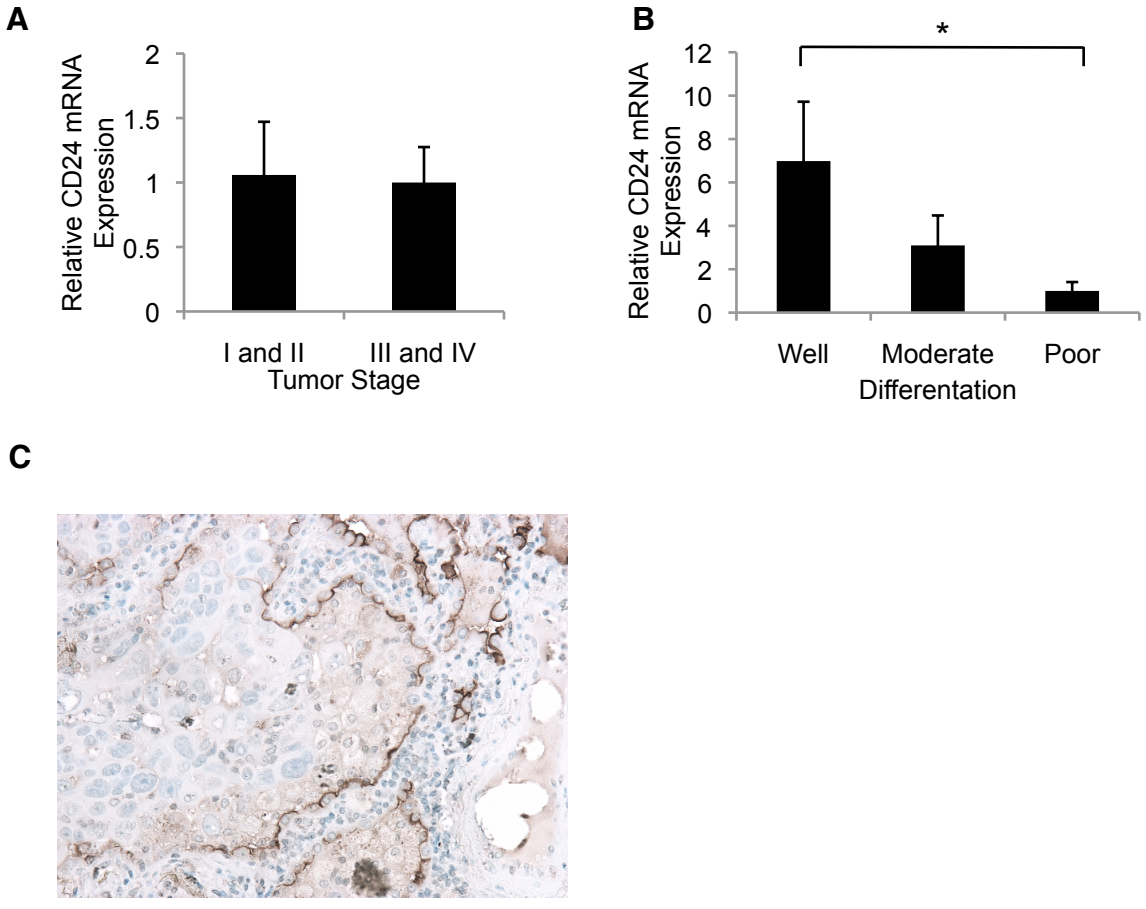

cytoplasmic expression patterns (KW Sinkevicius, CF Kim, unpublished data). Similar to the report in breast cancer, tumors with membrano-cytoplasmic CD24 staining were more poorly differentiated than those with apical CD24 staining. Also, the majority of lymph node metastases had higher CD24 levels than the primary tumors. It is possible that CD24 has dual roles: one to mark EMT/stem-like cells (membrano-cytoplasmic) and the other to mark more differentiated cells (apical membranous). Further staining and analysis of CD24 expression patterns in human tumors will be needed to validate this hypothesis.

The Role of Yap/Taz in Lung Cancer Metastasis

Yap and its paralog Taz are best known as mediators of the Hippo signaling pathway, a pathway first identified in *Drosophila melanogaster* and known for its role in organ size determination, stem cell activity, and tumorigenesis (reviewed in (Johnson and Halder, 2014)). Like other signaling pathways, the Hippo pathway carries signals from the plasma membrane to the nucleus, but unlike other pathways, the Hippo pathway is not known to have specific extracellular signaling proteins. Instead, the pathway is regulated by a large, ever-expanding network of cell adhesion, cytoskeletal, and cell polarity proteins. Like their upstream regulators, additional transcription factor binding partners of Yap and Taz as well as their downstream targets are still being elucidated.

The core Hippo pathway consists of serine threonine kinases Mst1/2 and Lats1/2, the scaffolding proteins Sav1 and Mob1a/1b, and the transcriptional coactivators Yap and Taz. Mst kinases form a complex with Sav1 and then

phosphorylate and activate Lats kinases and Mob1 proteins, which then phosphorylate Yap and Taz. When phosphorylated, Yap and Taz are sequestered in the cytoplasm by 14-3-3 or are degraded. When non-phosphorylated, Yap and Taz translocate into the nucleus where they bind to transcription factors such as the TEAD family of transcription factors to mediate transcription of target genes important for survival, anti-apoptosis, and tumorigenesis.

Higher levels and nuclear localization of Yap and Taz have been found in many human cancers, including breast, colon, liver, lung, ovarian, and skin cancers (Camargo et al., 2007; Chan et al., 2008; Dong et al., 2007; Fernandez-L et al., 2009; Overholtzer et al., 2006; Steinhardt et al., 2008; Xu et al., 2009; Zender et al., 2006; Zhao et al., 2007). Yap expression has been correlated with poor prognosis in non-small cell lung cancer patients and was shown to be tumorigenic in human lung cancer cell lines (Wang et al., 2010b). Overexpression of Taz was able to transform immortalized human bronchial epithelial cells while knockdown in lung cancer cell lines decreased their tumorigenicity (Zhou et al., 2011). Taz expression was found to be significantly associated with poor differentiation, poor survival, and metastasis in lung cancer patients (Xie et al., 2012). Interestingly, although deregulation of Yap and Taz expression levels and nuclear localization have been reported, the mechanism regulating these changes is unknown. Mutations in Hippo pathway members are rare in cancers, as are activating mutations in Yap and Taz. Yap and Taz are amplified in several types of cancer (Baldwin et al., 2005; Fernandez-L et al., 2009; Modena et al., 2006; Overholtzer et al., 2006; Snijders et al., 2005; Zender et al., 2006), while Mst and

Lats kinases have been reported to be silenced via promoter methylation and epigenetic silencing (Jiang et al., 2006; Seidel et al., 2007; Takahashi et al., 2005).

We found that knockdown of either Yap or Taz was able to decrease migration of CK1750 murine lung adenocarcinoma cells in transwell migration assays (Chapter 2). We were able to obtain LSL-rtTA; tetO-YapS127A mice and breed them to our Kras lung adenocarcinoma mouse model (Schlegelmilch et al., 2011). The resulting Kras; LSL-rtTA; tetO-YapS127A (Kras;Yap) mice had more and higher grade tumors than Kras controls (Chapter 2). The LSL-rtTA; tetO-YapS127A mice were also bred to Kras;p53-flox mice to generate Kras;p53-flox;LSL-rtTA;tetO-YapS127A mice; however, these mice died within one month after AdCre administration (AN Lau, CF Kim, unpublished data). Cause of death was unknown, but increased upper airway hyperplasia was observed in these mice, suggesting that loss of p53 in combination with Kras and Yap activation causes overproliferation of airway cells. In the future, intratracheal administration of AdCre could be used to infect only the distal lung, however airway cells will also be targeted with this method. Diluting the AdCre further could also be of use to try and get around this issue, as could driving Cre only in BASCs and alveolar cells with the SPC-CreER mouse (Xu et al., 2012). Conversely, we have also bred Yap fl/fl mice to the Kras;p53-flox mouse model and have infected these mice as well as Kras;p53-flox;Yap WT littermate control mice with AdCre. Mice will be euthanized at 17 weeks post-AdCre administration and the number and size of lung tumors will be measured, as will number and location of metastases. Based on our results from the Kras;Yap mice, we expect that Yap deletion in Kras;p53-flox tumors will

result in decreased numbers of lung tumors, lower grade tumors, and possibly decreased numbers of metastases.

However, knockdown of Taz, and not Yap, led to decreased lung tumor formation after tail vein injection, suggesting that Taz may be the more important factor for metastasis *in vivo* (Chapter 2). Transwell invasion assays also revealed that shTaz cells had significantly fewer invaded cells compared to shGFP cells ($p=0.016$) (Figure 3-5). Therefore, Taz may affect metastasis by regulating invasion as well as migration. Taz, also known as Wwtr1, or WW-domain containing transcription regulator-1, was identified in 2000 as a 14-3-3 interacting protein and shares 45% amino acid identity with Yap (Kanai et al., 2000). Interestingly, Taz knockout mice have partial embryonic lethality, but those that do survive are characterized by a lung developmental phenotype; the adult lungs display enlarged airspaces reminiscent of emphysematous lungs (Mitani et al., 2009). Taz has been shown to directly interact with the master lung transcription factor TTF-1 (Nkx2-1) to regulate differentiation of lung epithelial cells (Park et al., 2004). These data, in combination with our results pointing to Taz as the more important protein in terms of metastatic capability, suggest that perhaps Taz, rather than Yap, is more important for lung cancer metastasis. Similarly, in breast cancer stem cells, Taz was shown to play an important role in metastasis (Cordenonsi et al., 2011).

Since our data suggest a role for Taz in metastasis, Taz deletion in Kras;p53-flox mice would be an important experiment to show that Taz affects tumor progression and metastasis in a mouse model of lung cancer. Since Taz KO/KO mice are difficult to obtain and breed, breeding Taz fl/fl mice which have recently been published (Xin et al., 2013) to our Kras;p53-flox model would be ideal. In lieu of testing the affects of Yap

Figure 3-5: Invasion Assay with CK1750 shTaz cells. The average number of invasive cells observed in transwell invasion assays, determined by the number of cells invading through a matrigel-coated membrane towards serum-containing (10% FBS) media in control or Taz knockdown CK1750 cells. *p=0.016. Results shown are from one independent experiment.

Figure 3-5: (continued)

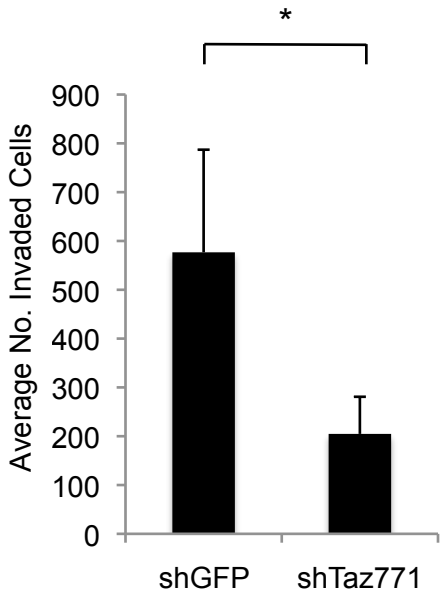

and Taz directly in these mouse models, another future direction will be to determine the more detailed mechanism of Yap and Taz action in lung adenocarcinoma cells. Since Nkx2-1 (Ttf-1) and Hmga2 expression levels have been shown to correlate with metastatic disease, we examined expression levels of these genes in both CD24 and Yap/Taz knockdown cells. Nkx2-1 was found to be down-regulated in tumor progression and not expressed in metastases, while Hmga2 was found to be more highly expressed in metastatic tumors (Winslow et al., 2011). Hmga2 expression decreased after knockdown of CD24 with one out of two hairpins ($p=0.026$), but not after Taz knockdown (Figure 3-6A, B). Nkx2-1 increased after knockdown of Yap with one of two hairpins ($p=0.045$) but was not altered after CD24 or Taz knockdown (Figure 3-6C,D). This indicates that CD24 and Yap/Taz may be affecting migration and metastasis through a mechanism that does not rely on Hmga2/Nkx2-1 regulation.

To address whether CD24 regulated migration and invasion by activating Yap and Taz activity (or vice versa), we used qPCR, FACS, Western blot, and luciferase reporter assays. We have found no consistent changes in the levels of Yap, Taz, or the Yap/Taz targets Cyr61 and Ctgf in CD24 knockdown cells nor vice versa; CD24 was not altered in Yap/Taz knockdown cells (Figure 3-7A,B,C,E). CD24 knockdown did not alter Yap/Taz phosphorylation levels (Figure 3-7D). CK1750 cells overexpressing wildtype human YAP, YAPS127A, or TAZS89A (Figure 3-8A,B) were made to assess the affect on CD24 levels as well as to examine migration and metastatic properties. YAP or TAZ overexpression had no affect on CD24 levels by FACS (Figure 3-8C) and did not have a significant affect on cell migration or tail vein metastases (Figure 3-8D,E). However, CK1750 cells are already highly migratory/metastatic and express very high levels of

Figure 3-6: Hmga2 and Nkx2-1 levels in CD24 and Yap/Taz knockdown cells. A. qPCR analysis of Hmga2 expression levels after CD24 knockdown. shCD24-Low-1 p = 0.026. **B**. qPCR analysis of Hmga2 expression levels after Taz knockdown. **C.** qPCR analysis of Nkx2-1 expression levels after CD24 knockdown. **D.** qPCR analysis of Nkx2-1 expression levels after Taz knockdown. shYap1824 p=0.045**.**

Figure 3-6: (continued)

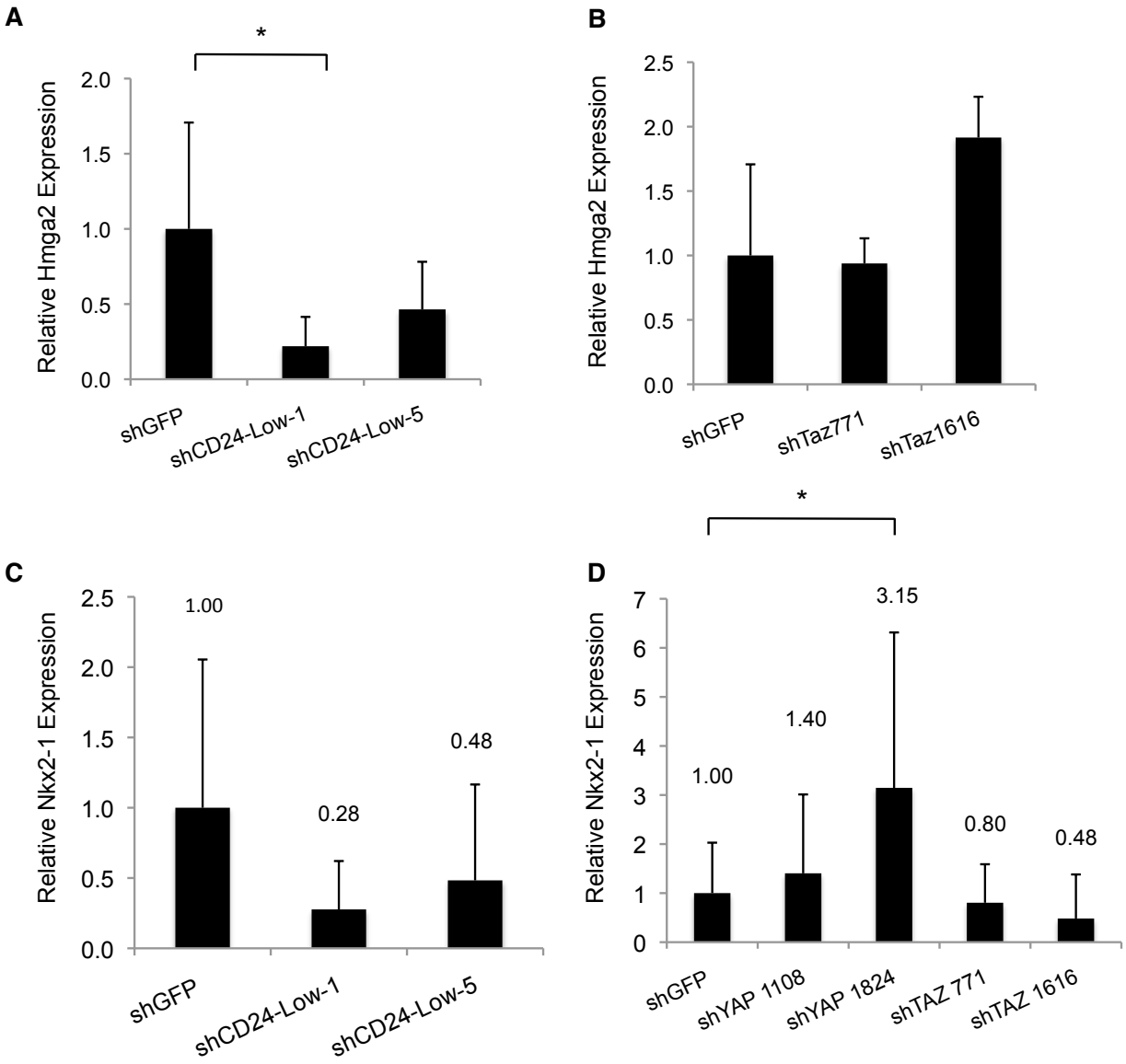

Figure 3-7: Analysis of CD24 and Yap/Taz reciprocal expression levels. A. Quantitative real-time PCR analysis of relative Yap1 and Taz mRNA levels in shCD24 cell lines normalized to expression in shGFP cells. Data represent the mean of four independent experiments, error bars represent the standard deviation of the mean. **B.** Quantitative real-time PCR analysis of relative CD24 mRNA levels in shYap1 and shTaz cell lines normalized to levels in shGFP cells. Data represent the mean of four independent experiments, error bars represent the standard deviation of the mean. **C.** Quantitative real-time PCR analysis of relative mRNA levels of Yap1/Taz targets Cyr61 and CTGF mRNA in shCD24 cell lines normalized to expression in shGFP cells. Data represent the mean of four independent experiments, error bars represent the standard deviation of the mean. **D.** Whole-cell lysate serial dilutions from shGFP and shCD24 cells immunoblotted with the indicated antibodies. Similar results were obtained in repeat experiments. **E.** FACS analysis of CD24 levels in shYap1 and shTaz cell lines compared to levels in shGFP cells.

Figure 3-7: (continued)

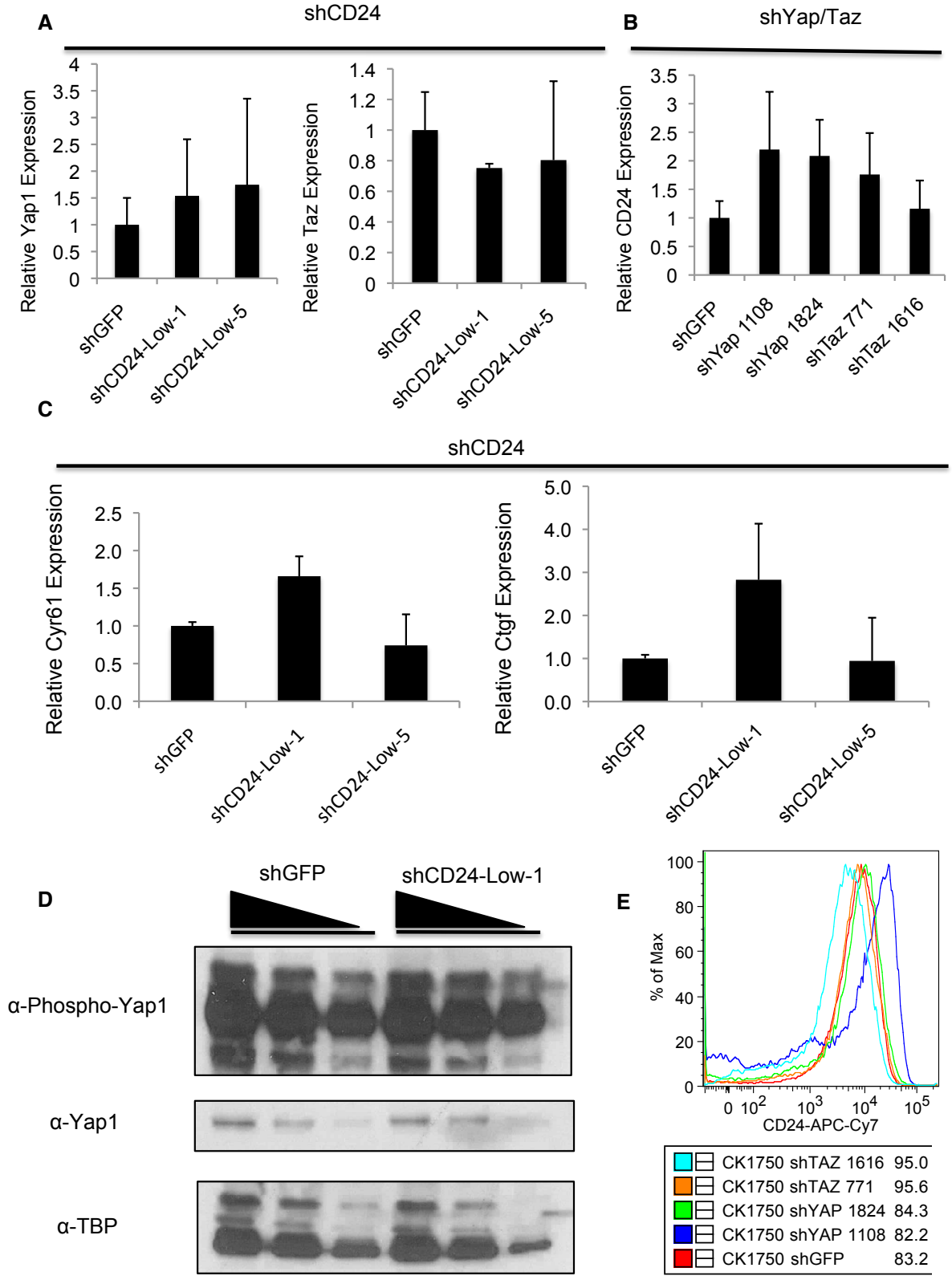

Figure 3-8: YAP and TAZ overexpression in CK1750 cells. A. qPCR analysis of human YAP expression levels in CK1750 cells made to overexpress empty vector, YAP,YAPS127A, or TAZ. **B**. qPCR analysis of human TAZ expression levels in CK1750 cells made to overexpress empty vector, YAP,YAPS127A, or TAZ. **C.** FACS analysis of CD24 levels in CK1750 cell lines overexpressing YAP or TAZ compared to levels in cells expressing empty vector. **D.** The average number of migratory cells observed in transwell migration assays, determined by the number of cells migrating towards serum-containing (10% FBS) media in control or YAP or TAZ overexpressing- CK1750 cells. Results shown are the average of three independent experiments. **E.** Average number of lung metastases after tail vein injection of CK1750 cells expressing empty vector (circles), YAP (squares), YAPS127A (up triangles), or TAZS89A (down triangles). Lungs were analyzed for metastases two weeks after injection of 5000 cells. Each symbol represents an individual mouse analyzed. **F.** Average number of lung metastases after tail vein injection of CK1750 cells expressing empty vector (circles), YAP (squares) or TAZS89A (up triangles). Lungs were analyzed for metastases two weeks after injection of 50,000 cells. Each symbol represents an individual mouse analyzed.

Figure 3-8: (continued)

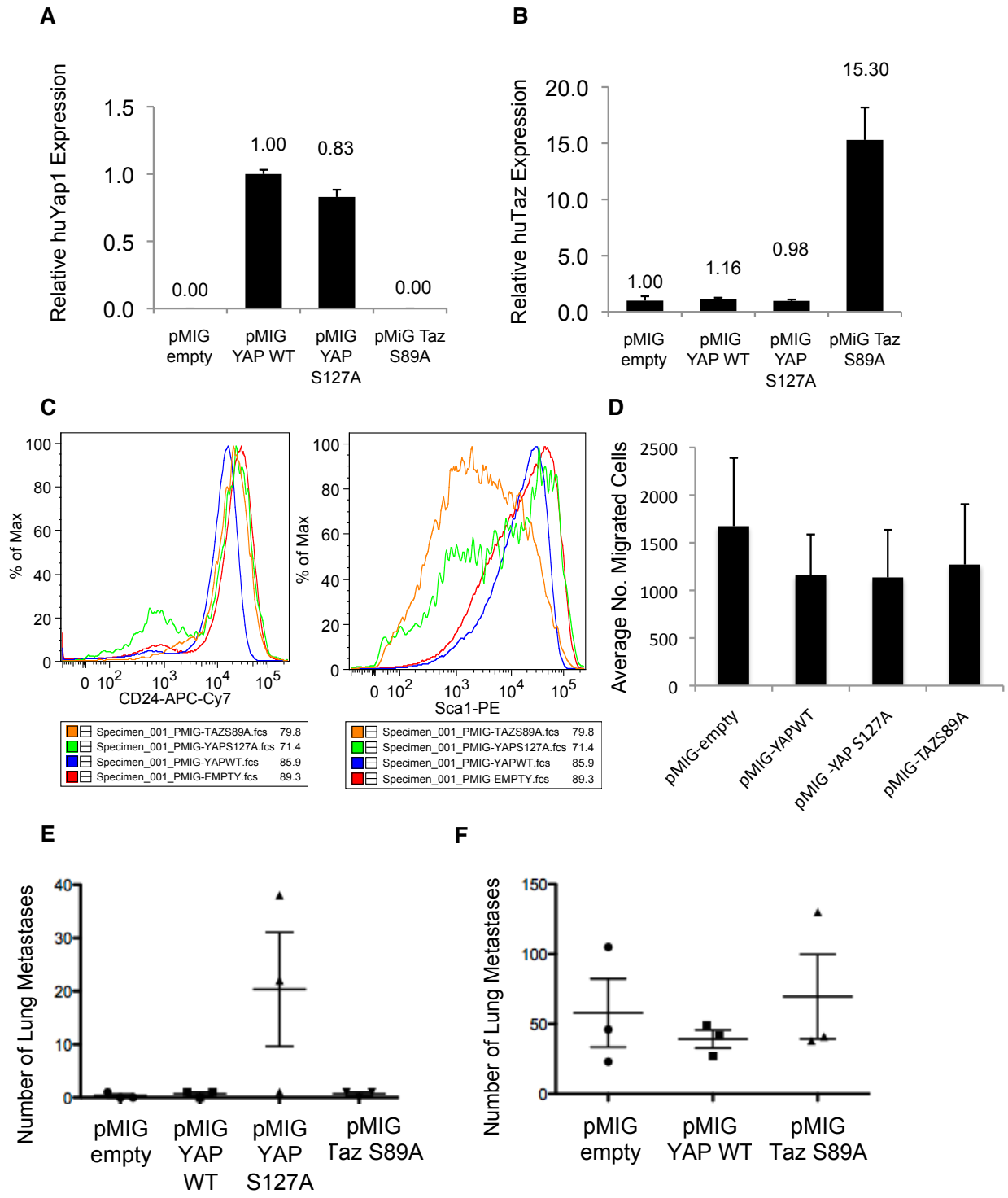

CD24 at baseline and therefore it may be difficult to observe an increase in these properties. Another possibility is that the human version of YAP or TAZ has different effects on migration or metastasis as compared to murine Yap/Taz in these cells.

Two different TEAD-reporter systems were used to measure Yap/Taz activity (Figure 3-9A,B). In one set of experiments, CK1750 shGFP or shCD24 cells were transfected with a plasmid containing a TEAD-binding site cassette 5' of luciferase. In a second set of experiments, CK1750 shGFP or shCD24 cells were infected with a virus containing a TEAD-binding site cassette 5' of an mCherry reporter (Mohseni et al., 2014). shYap/shTaz CK1750 cells were used as controls (Figure 3-9A,B). We observed a decrease in reporter activity after CD24 knockdown using the mCherry TEAD reporter ($p=0.010$ shCD24-Low-1, $p= 0.0064$ shCD24-Low-5). However, with the luciferase TEAD reporter, a decrease in reporter activity was only seen with one of two CD24 hairpins (shCD24-Low-1, $p =0.0038$). Therefore, there is no clear relationship between CD24 and Yap/Taz expression that we can establish with these methods, yet further studies may reveal a connection, possibly through the regulation of the actin cytoskeleton.

As discussed in Chapter 2, we also performed a microarray gene expression comparison of three Kras;p53 murine lung cancer cell lines with shTaz versus a control hairpin (shGFP). Gene sets of interest that were significantly enriched in shTaz cells included several sets associated with NF Kappa B signaling, mitochondria, as well as gene sets corresponding to actin cytoskeletal processes (Appendix). NF Kappa B signaling is known to be required in lung adenocarcinoma (Meylan et al, 2009; Xue et al., 2011), so the genes in this gene set could be interesting to follow up on in TPCs and

Figure 3-9: TEAD-binding site- (TBS)-reporter assays in CD24 and Yap/Taz knockdown cells. A. Relative luciferase units of control, shCD24, or shYap/Yaz CK1750 cells transfected with a TBS-luciferase reporter. Luciferase was measured two days after transfection. Results shown are from three independent experiments. shCD24-Low-1 p =0.0038, shYap1108 p=0.0031, shYap1824 p=0.0078, shTaz771 $p=3.6x10^{-5}$. **B**. Relative mCherry expression of control or shCD24 CK1750 cells infected with a lentivirus containing a TBS-mCherry reporter. Results shown are from two independent experiments shCD24-Low-1 p=0.010, shCD24-Low-5 p= 0.0064, shYap1824 p= 0.046 , shTaz771 p= 0.0010.

Figure 3-9: (continued)

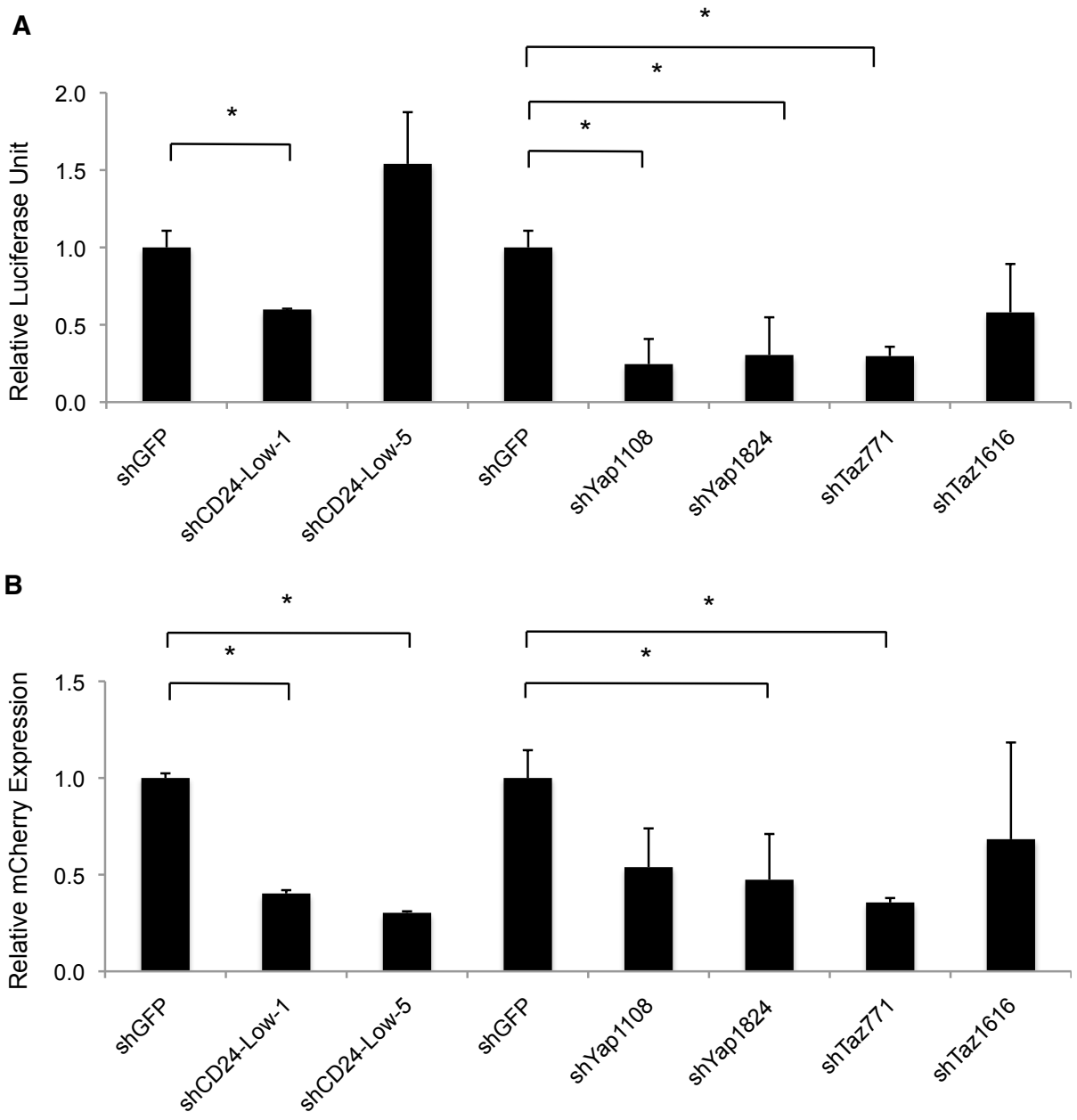

Taz deficient lung cells. In *Drosophila*, Yap was found to regulate mitochondrial structure (Nagaraj et al., 2012), and mitochondrial dysfunction was shown to cooperate with Ras activation to inactivate the Hippo pathway and drive tumor progression (Ohsawa et al., 2012). Mitochodrial dysfunction and metabolism could also be an attractive target to study in lung TPCs and Taz knockdown cells.

Gene sets corresponding to actin cytoskeletal processes were highly decreased after Taz knockdown, including Actin Cytoskeleton, Cytoskeletal Protein Binding, Actin Binding, Actin Filament Binding, and Actin Filament Based Processes. F-actin staining was performed in the CK1750 cell lines to determine if Taz knockdown altered the arrangement of the actin cytoskeleton. Knockdown of Taz significantly decreased anisotropy and alignment indices, two measures of F-actin orientation (Figure 3-10) (Xu et al., 2012). CK1750 cells with Taz knockdown also had fewer lamellapodia and fillipodia, another indicator of migratory potential (AN Lau, DE Wagner, unpublished observations). An intact cytoskeleton is needed to generate sufficient contractile forces for cell movement, therefore disruption of the F-actin network may have contributed to the decreased migration and metastatic capacity of shTaz cells. Previous work in ovarian cancer has shown the degree of actin-alignment was highly correlated to cell stiffness (Xu et al., 2012).

Similar to our work with CD24, we also tested whether contractile forces were affected in measurements of single CK1750 cells after Taz knockdown (Figure 3-11). Taz knockdown did not significantly affect measures of cell contractility in these assays. We also plan to test whether Taz knockdown affects cell spreading dynamics in the 3-D fibronectin-coated substrate assay (Douezan et al., 2011). There is published evidence

Figure 3-10: Actin alignment is altered following knockdown of Taz in CK1750 cells. A, B. Summary of F-actin orientation analysis. The anisotropic and alignment indices were extracted for each cell line (n= at least 6 for each cell line; all experiments performed in replicate). Bars represent means and error bars are standard deviation of the mean. **A.** Alignment index in CK1750 shGFP vs shTaz cells. p = 0.027. **B.** Anisotropy index in CK1750 shGFP vs shTaz cells. The anisotropy index is a measure of how much the cell deviates from isotropy (where there would be no actin alignment). A value of one is isotropic; the closer to one this value is, the less aligned the cells are. p = 0.035. **C.** Representative fluorescent images for F-actin stained with phalloidin in CK1750 shGFP cells. Original images taken at 1000x. **D.** Representative fluorescent images for F-actin stained with phalloidin in CK1750 shTaz1616 cells.

Figure 3-10: (continued)

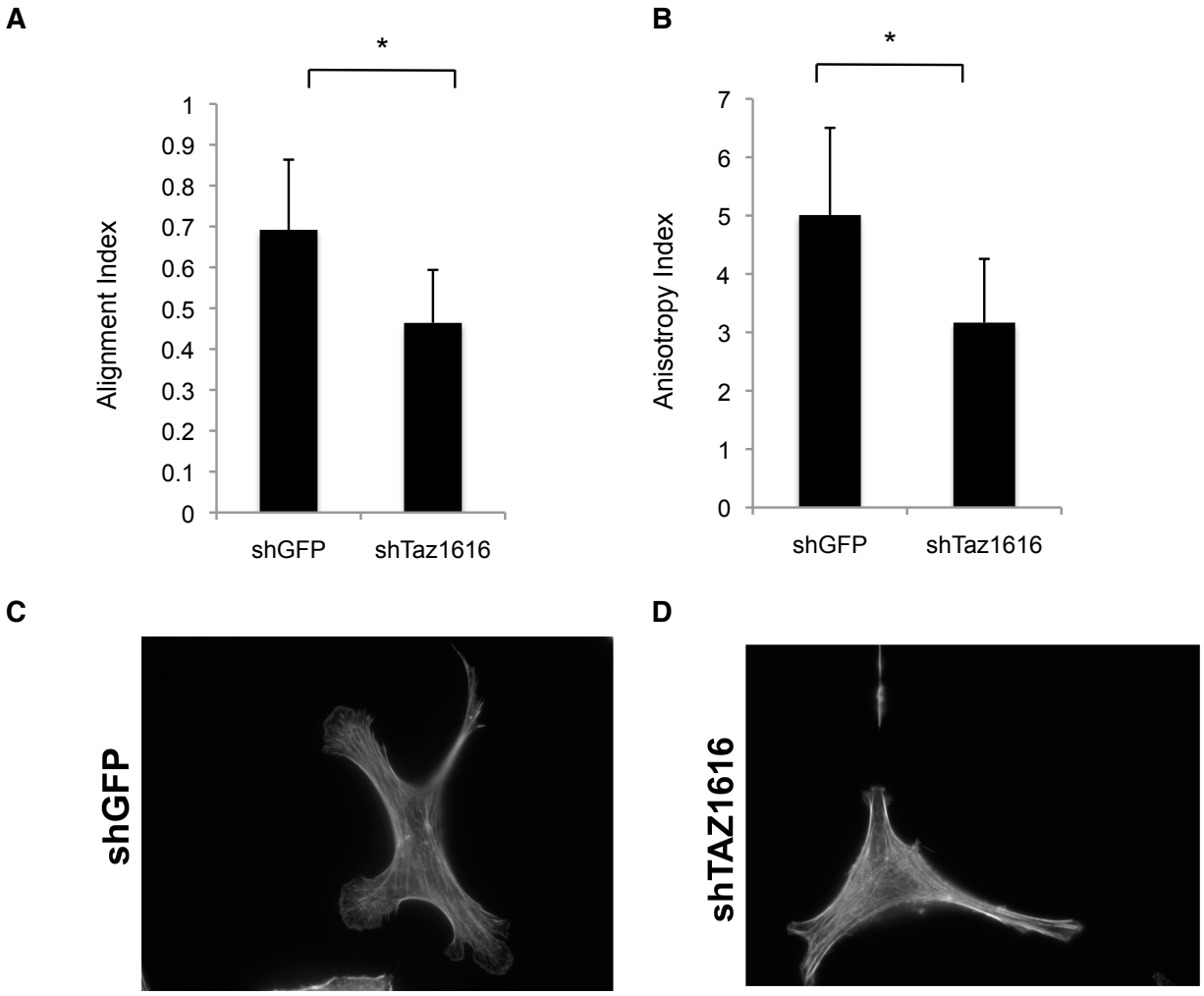

Figure 3-11: Contractility measurements in Taz knockdown cells. A. Root mean squared traction measurements of CK1750 shGFP and shTaz cells. Cells are plated sparsely on collagen 1-coated gels. N = 45-46 cells per group. Statistical comparisons to control were made using the Kruskal-Wallis nonparametric one-way analysis of variance by ranks. p= 0.918. **B.** Median traction measurements of CK1750 shGFP and shTaz cells. p= 0.818 **C.** Net contractile moment measurements of CK1750 shGFP and shTaz cells p=0.611 **D.** Contractile strain energy measurements of CK1750 shGFP and shTaz cells. p= 0.721

Figure 3-11: (continued)

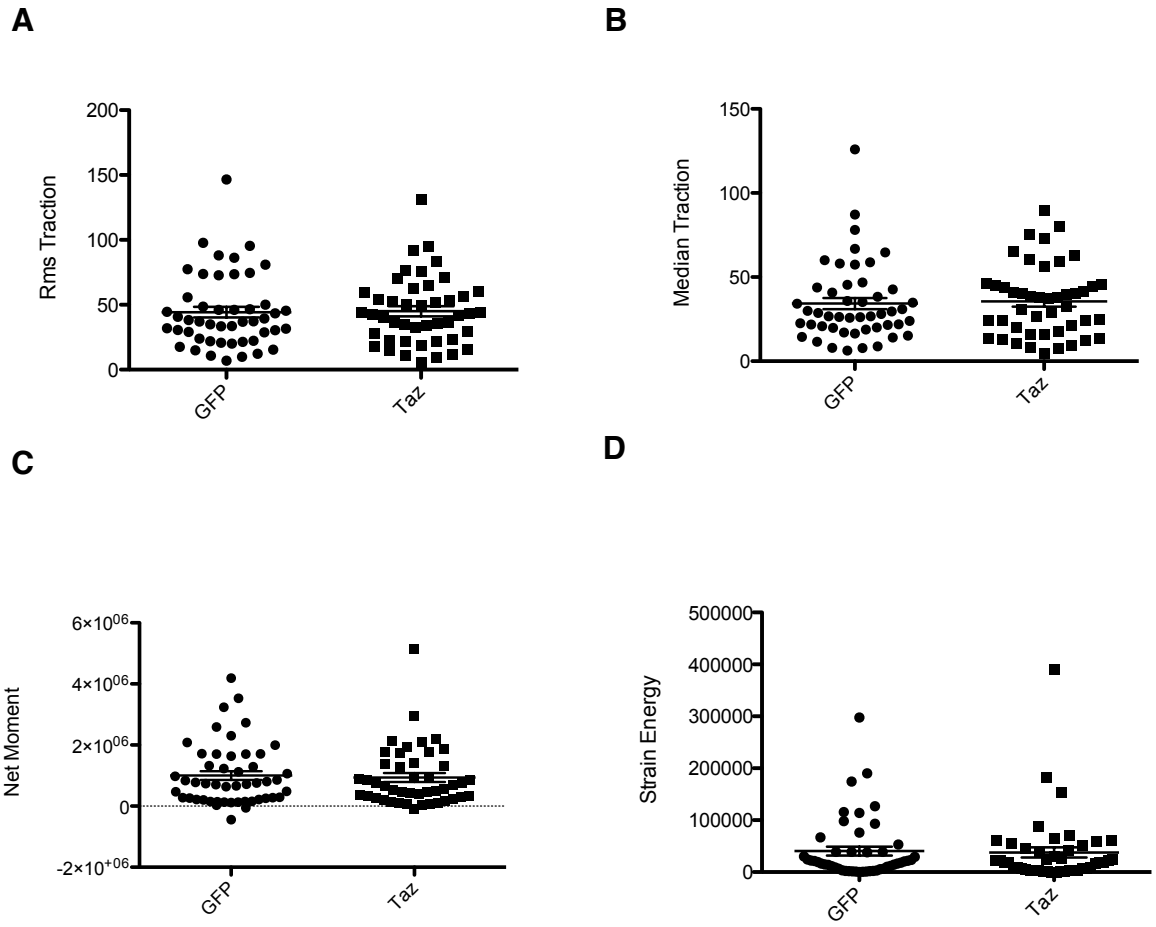

that Yap and Taz both respond to mechanical cues and also mediate mechanotransduction (Halder et al., 2012). Nuclear Yap/Taz localization is regulated by cell spreading; on stiff surfaces, Yap/Taz is nuclear, whereas on soft surfaces, Yap/Taz is cytoplasmic (Dupont et al., 2011). Similarly, when cells are grown on large fibronectin islands and cells spread out, Yap and Taz are nuclear, whereas cells grown on small islands have cytoplasmic and inactive Yap/Taz (Dupont et al., 2011). When F-actin or Rho are inhibited, Yap and Taz are inactivated, and conversely, F-actin polmerization promotes increased Yap/Taz activity (Dupont et al., 2011; Sansores-Garcia et al., 2011; Wada et al., 2011). Inhibition of myosin regulators also inactivates Yap and Taz (Dupont et al., 2011; Wada et al., 2011). Since defects in mechanotransduction are implicated in tumorigenesis and metastasis, future study of the effect of Taz on this process in lung adenocarcinoma should be informative. Further studies are needed to determine which, if any, of the cellular activities identified in our expression analyses are critical for Yap/Taz contribution to aggressive lung cancer.

Conclusions

The work presented in this thesis makes important conclusions about the relationship between lung TPCs and metastasis. We found that there were multiple TPC populations with metastatic ability, but that using two TPC markers enriched for TPCs with metastatic capability. Additionally, cell-cell interactions between TPCs, non-TPCs, and tumor stroma are likely to affect TPC and metastatic ability.

This work opens up many avenues for future study. More work will be necessary to determine if both CD24 and Yap/Taz are important regulators of (or are being acted

upon by) actin dynamics and mechanotransduction in lung adenocarcinoma cells. Our gene expression studies point to the importance of the actin cytoskeleton, and more functional studies of cell spreading dynamics and cellular forces exerted in metastatic cells will be performed to confirm these findings. While our data suggest a role for Taz in lung cancer metastasis, further experiments are needed to elucidate the specific transcription factors and target genes that are mediating Taz function.

Identification of lung tumor cells important for metastatic disease is important for understanding more about the mechanisms of metastasis. The genes and pathways discovered in murine lung TPCs were also shown to be important for lung adenocarcinoma patient survival, and it is my hope that by studying these pathways we can develop targeted therapies to treat metastatic lung cancer.

References

Abraham, B.K., Fritz, P., McClellan, M., Hauptvogel, P., Athelogou, M., and Brauch, H. (2005). Prevalence of CD44+/CD24-/low cells in breast cancer may not be associated with clinical outcome but may favor distant metastasis. Clin. Cancer Res. *11*, 1154–1159.

Aigner, S., Sthoeger, Z.M., Fogel, M., Weber, E., Zarn, J., Ruppert, M., Zeller, Y., Vestweber, D., Stahel, R., Sammar, M., et al. (1997). CD24, a mucin-type glycoprotein, is a ligand for P-selectin on human tumor cells. Blood *89*, 3385–3395.

Al-Hajj, M., Wicha, M.S., Benito-Hernandez, A., Morrison, S.J., and Clarke, M.F. (2003). Prospective identification of tumorigenic breast cancer cells. Proc. Natl. Acad. Sci. U.S.a. *100*, 3983–3988.

Anderson, K., Lutz, C., van Delft, F.W., Bateman, C.M., Guo, Y., Colman, S.M., Kempski, H., Moorman, A.V., Titley, I., Swansbury, J., et al. (2011). Genetic variegation of clonal architecture and propagating cells in leukaemia. Nature *469*, 356–361.

Baccelli, I., and Trumpp, A. (2012). The evolving concept of cancer and metastasis stem cells. J. Cell Biol. *198*, 281–293.

Baldwin, C., Garnis, C., Zhang, L., Rosin, M.P., and Lam, W.L. (2005). Multiple microalterations detected at high frequency in oral cancer. Cancer Res. *65*, 7561-7567.

Benkerrou, M., Jais, J.P., Leblond, V., Durandy, A., Sutton, L., Bordigoni, P., Garnier, J.L., Le Bidois, J., Le Deist, F., Blanche, S., et al. (1998). Anti-B-cell monoclonal antibody treatment of severe posttransplant B-lymphoproliferative disorder: prognostic factors and long-term outcome. Blood *92*, 3137–3147.

Borovski, T., Verhoeff, J.J.C., Cate, ten, R., Cameron, K., de Vries, N.A., van Tellingen, O., Richel, D.J., van Furth, W.R., Medema, J.P., and Sprick, M.R. (2009). Tumor microvasculature supports proliferation and expansion of glioma-propagating cells. Int. J. Cancer *125*, 1222–1230.

Bretz, N.P., Salnikov, A.V., Perne, C., Keller, S., Wang, X., Mierke, C.T., Fogel, M., Erbe-Hofmann, N., Schlange, T., Moldenhauer, G., et al. (2012a). CD24 controls Src/STAT3 activity in human tumors. Cell. Mol. Life Sci. *69*, 3863–3879.

Bretz, N., Noske, A., Keller, S., Erbe-Hofmann, N., Schlange, T., Salnikov, A.V., Moldenhauer, G., Kristiansen, G., and Altevogt, P. (2012b). CD24 promotes tumor cell invasion by suppressing tissue factor pathway inhibitor-2 (TFPI-2) in a c-Src-dependent fashion. Clin. Exp. Metastasis *29*, 27–38.

Butcher, D.T., Alliston, T., and Weaver, V.M. (2009). A tense situation: forcing tumour progression. Nat. Rev. Cancer *9*, 108–122.

Calabrese, C., Poppleton, H., Kocak, M., Hogg, T.L., Fuller, C., Hamner, B., Oh, E.Y., Gaber, M.W., Finklestein, D., Allen, M., et al. (2007). A perivascular niche for brain tumor stem cells. Cancer Cell *11*, 69–82.

Camargo, F.D., Gokhale, S., Johnnidis, J.B., Fu, D., Bell, G.W., Jaenisch, R., and Brummelkamp, T.R. (2007). YAP1 increases organ size and expands undifferentiated progenitor cells. Curr. Biol. *17*, 2054–2060.

Campbell, P.J., Yachida, S., Mudie, L.J., Stephens, P.J., Pleasance, E.D., Stebbings, L.A., Morsberger, L.A., Latimer, C., McLaren, S., Lin, M.-L., et al. (2010). The patterns and dynamics of genomic instability in metastatic pancreatic cancer. Nature *467*, 1109–1113.

Chan, S.W., Lim, C.J., Guo, K., Ng, C.P., Lee, I., Hunziker, W., Zeng, Q., and Hong, W. (2008). A role for TAZ in migration, invasion, and tumorigenesis of breast cancer cells. Cancer Res. *68*, 2592–2598.

Cordenonsi, M., Zanconato, F., Azzolin, L., Forcato, M., Rosato, A., Frasson, C., Inui, M., Montagner, M., Parenti, A.R., Poletti, A., et al. (2011). The Hippo transducer TAZ confers cancer stem cell-related traits on breast cancer cells. Cell *147*, 759–772.

Curtis, S.J., Sinkevicius, K.W., Li, D., Lau, A.N., Roach, R.R., Zamponi, R., Woolfenden, A.E., Kirsch, D.G., Wong, K.-K., and Kim, C.F. (2010). Primary tumor genotype is an important determinant in identification of lung cancer propagating cells. Cell Stem Cell *7*, 127–133.

Damelin, M., Geles, K.G., Follettie, M.T., Yuan, P., Baxter, M., Golas, J., DiJoseph, J.F., Karnoub, M., Huang, S., Diesl, V., et al. (2011). Delineation of a cellular hierarchy in lung cancer reveals an oncofetal antigen expressed on tumor-initiating cells. Cancer Res. *71*, 4236–4246.

Dieter, S.M., Ball, C.R., Hoffmann, C.M., Nowrouzi, A., Herbst, F., Zavidij, O., Abel, U., Arens, A., Weichert, W., Brand, K., et al. (2011). Distinct types of tumor-initiating cells form human colon cancer tumors and metastases. Cell Stem Cell *9*, 357–365.

Dong, J., Feldmann, G., Huang, J., Wu, S., Zhang, N., Comerford, S.A., Gayyed, M.F., Anders, R.A., Maitra, A., and Pan, D. (2007). Elucidation of a universal size-control mechanism in Drosophila and mammals. Cell *130*, 1120–1133.

Douezan, S., Guevorkian, K., Naouar, R., Dufour, S., Cuvelier, D., and Brochard-Wyart, F. (2011). Spreading dynamics and wetting transition of cellular aggregates. Proc. Natl. Acad. Sci. U.S.a. *108*, 7315–7320.

Dupont, S., Morsut, L., Aragona, M., Enzo, E., Giulitti, S., Cordenonsi, M., Zanconato, F., Le Digabel, J., Forcato, M., Bicciato, S., et al. (2011). Role of YAP/TAZ in mechanotransduction. Nature *474*, 179–183.

Fang, X., Zheng, P., Tang, J., and Liu, Y. (2010). CD24: from A to Z. Cell. Mol. Immunol. *7*, 100–103.

Fernandez-L, A., Northcott, P.A., Dalton, J., Fraga, C., Ellison, D., Angers, S., Taylor, M.D., and Kenney, A.M. (2009). YAP1 is amplified and up-regulated in hedgehog-associated medulloblastomas and mediates Sonic hedgehog-driven neural precursor proliferation. Genes Dev. *23*, 2729–2741.

Fischer, A., Blanche, S., Le Bidois, J., Bordigoni, P., Garnier, J.L., Niaudet, P., Morinet, F., Le Deist, F., Fischer, A.M., and Griscelli, C. (1991). Anti-B-cell monoclonal antibodies in the treatment of severe B-cell lymphoproliferative syndrome following bone marrow and organ transplantation. N. Engl. J. Med. *324*, 1451–1456.

Folkins, C., Man, S., Xu, P., Shaked, Y., Hicklin, D.J., and Kerbel, R.S. (2007). Anticancer therapies combining antiangiogenic and tumor cell cytotoxic effects reduce the tumor stem-like cell fraction in glioma xenograft tumors. Cancer Res. *67*, 3560-3564.

Friederichs, J., Zeller, Y., Hafezi-Moghadam, A., Gröne, H.J., Ley, K., and Altevogt, P. (2000). The CD24/P-selectin binding pathway initiates lung arrest of human A125 adenocarcinoma cells. Cancer Res. *60*, 6714–6722.

Gerlinger, M., Horswell, S., Larkin, J., Rowan, A.J., Salm, M.P., Varela, I., Fisher, R., McGranahan, N., Matthews, N., Santos, C.R., et al. (2014). Genomic architecture and evolution of clear cell renal cell carcinomas defined by multiregion sequencing. Nat. Genet. *46*, 225–233.

Gerlinger, M., Rowan, A.J., Horswell, S., Larkin, J., Endesfelder, D., Gronroos, E., Martinez, P., Matthews, N., Stewart, A., Tarpey, P., et al. (2012). Intratumor heterogeneity and branched evolution revealed by multiregion sequencing. N. Engl. J. Med. *366*, 883–892.

Halder, G., Dupont, S., and Piccolo, S. (2012). Transduction of mechanical and cytoskeletal cues by YAP and TAZ. Nat. Rev. Mol. Cell Biol. *13*, 591–600.

Harrison, H., Simoes, B.M., Rogerson L., Howell, S.J., Landberg, G., and Clarke, R.B. (2013). Oestrogen increases the activity of oestrogen receptor negative breast cancer stem cells through paracrine EGFR and Notch signaling. Breast Cancer Res. *15*, R21.

Hermann, P.C., Huber, S.L., Herrler, T., Aicher, A., Ellwart, J.W., Guba, M., Bruns, C.J., and Heeschen, C. (2007). Distinct populations of cancer stem cells determine tumor growth and metastatic activity in human pancreatic cancer. Cell Stem Cell *1*, 313–323.

Hubbe, M., and Altevogt, P. (1994). Heat-stable antigen/CD24 on mouse T lymphocytes: evidence for a costimulatory function. Eur. J. Immunol. *24*, 731–737.

Jackson, E.L., Olive, K.P., Tuveson, D.A., Bronson, R., Crowley, D., Brown, M., and Jacks, T. (2005). The differential effects of mutant p53 alleles on advanced murine lung cancer. Cancer Res. *65*, 10280–10288.

Jiang, Z., Li, X., Hu, J., Zhou, W., Jiang, Y., Li, G., and Lu, D. (2006). Promoter hypermethylation-mediated down-regulation of LATS1 and LATS2 in human astrocytoma. Neurosci Res. *56*, 450-458.

Johnson, R., and Halder, G. (2014). The two faces of Hippo: targeting the Hippo pathway for regenerative medicine and cancer treatment. Nat Rev Drug Discov *13*, 63–79.

Kanai, F., Marignani, P.A., Sarbassova, D., Yagi, R., Hall, R.A., Donowitz, M., Hisaminato, A., Fujiwara, T., Ito, Y., Cantley, L.C., et al. (2000). TAZ: a novel transcriptional co-activator regulated by interactions with 14-3-3 and PDZ domain proteins. Embo J. *19*, 6778–6791.

Kay, R., Rosten, P.M., and Humphries, R.K. (1991). CD24, a signal transducer modulating B cell activation responses, is a very short peptide with a glycosyl phosphatidylinositol membrane anchor. J. Immunol. *147*, 1412–1416.

Kay, R., Takei, F., and Humphries, R.K. (1990). Expression cloning of a cDNA encoding M1/69-J11d heat-stable antigens. J. Immunol. *145*, 1952–1959.

Krishnamurthy, S., Dong, Z., Vodopyanov, D., Imai, A., Helman, J.I., Prince, M.E., Wicha, M.S., and Nor, J.E. (2010). Endothelial cell-initiated signaling promotes the survival and self-renewal of cancer stem cells. Cancer Res. *70*, 9969-9978.

Kristiansen, G., Schlüns, K., Yongwei, Y., Denkert, C., Dietel, M., and Petersen, I. (2003a). CD24 is an independent prognostic marker of survival in nonsmall cell lung cancer patients. Br. J. Cancer *88*, 231–236.

Kristiansen, G., Winzer, K.-J., Mayordomo, E., Bellach, J., Schlüns, K., Denkert, C., Dahl, E., Pilarsky, C., Altevogt, P., Guski, H., et al. (2003b). CD24 expression is a new prognostic marker in breast cancer. Clin. Cancer Res. *9*, 4906–4913.

Lau, A.N., Curtis, S.J., Fillmore, C.M., Rowbotham, S.P., Mohseni, M., Wagner, D.E., Beede, A.M., Montoro, D.T., Sinkevicius, K.W., Walton, Z.E., et al. (2014). Tumor-propagating cells and Yap/Taz activity contribute to lung tumor progression and metastasis. Embo J. *33*, 468-481.

Lee, H.J., Choe, G., Jheon, S., Sung, S.-W., Lee, C.-T., and Chung, J.-H. (2010). CD24, a novel cancer biomarker, predicting disease-free survival of non-small cell lung carcinomas: a retrospective study of prognostic factor analysis from the viewpoint of forthcoming (seventh) new TNM classification. J Thorac Oncol *5*, 649–657.

Lee, J.-H., Bhang, D.H., Beede, A., Huang, T.L., Stripp, B.R., Bloch, K.D., Wagers, A.J., Tseng, Y.-H., Ryeom, S., and Kim, C.F. (2014). Lung Stem Cell Differentiation in Mice Directed by Endothelial Cells via a BMP4-NFATc1-Thrombospondin-1 Axis. Cell *156*, 440–455.

Liu, W., Monahan, K.B., Pfefferle, A.D., Shimamura, T., Sorrentino, J., Chan, K.T., Roadcap, D.W., Ollila, D.W., Thomas, N.E., Castrillon, D.H., et al. (2012). LKB1/STK11 inactivation leads to expansion of a prometastatic tumor subpopulation in melanoma. Cancer Cell *21*, 751–764.

Liu, Y., Wenger, R.H., Zhao, M., and Nielsen, P.J. (1997). Distinct costimulatory molecules are required for the induction of effector and memory cytotoxic T lymphocytes. J. Exp. Med. *185*, 251–262.

Lu, J., Ye, X., Fan, F., Xia, L., Bhattacharya, R., Bellister, S., Tozzi, F., Sceusi E., Zhou, Y., Tachibana, I., et al. (2013). Endothelial cells promote the colorectal cancer stem cell phenotype through a soluble form of Jagged-1. Cancer Cell *23*, 171-185.

Magee, J.A., Piskounova, E., and Morrison, S.J. (2012). Cancer stem cells: impact, heterogeneity, and uncertainty. Cancer Cell *21*, 283–296.

Malanchi, I., Santamaria-Martínez, A., Susanto, E., Peng, H., Lehr, H.-A., Delaloye, J.-F., and Huelsken, J. (2012). Interactions between cancer stem cells and their niche govern metastatic colonization. Nature *481*, 85–89.

McQualter, J.L., Brouard, N., Williams, B., Baird, B.N., Sims-Lucas, S., Yuen, K., Nilsson, S.K., Simmons, P.J., and Bertoncello, I. (2009). Endogenous fibroblastic progenitor cells in the adult mouse lung are highly enriched in the sca-1 positive cell fraction. Stem Cells *27*, 623–633.

McQualter, J.L., Yuen, K., Williams, B., and Bertoncello, I. (2010). Evidence of an epithelial stem/progenitor cell hierarchy in the adult mouse lung. Proc. Natl. Acad. Sci. U.S.a. *107*, 1414–1419.

Meacham, C.E., and Morrison, S.J. (2013). Tumour heterogeneity and cancer cell plasticity. Nature *501*, 328–337.

Meylan, E., Dooley, A.L., Feldser, D.M., Shen, L., Turk, E., Ouyang, C., and Jacks, T. (2009). Requirement for NF-KappaB signaling in a mouse model of lung adenocarcinoma. Nature *46*, 104-107.

Mierke, C.T., Bretz, N., and Altevogt, P. (2011). Contractile forces contribute to increased glycosylphosphatidylinositol-anchored receptor CD24-facilitated cancer cell invasion. J. Biol. Chem. *286*, 34858–34871.

Mitani, A., Nagase, T., Fukuchi, K., Aburatani, H., Makita, R., and Kurihara, H. (2009). Transcriptional coactivator with PDZ-binding motif is essential for normal alveolarization in mice. Am. J. Respir. Crit. Care Med. *180*, 326–338.

Modena, P., Lualdi, E., Facchinetti, F., Veltman, J., Reid, J.F., Minardi, S., Janssen, I., Giangaspero, F., Forni, M., Finocchiaro, G., et al. (2006). Identification of tumor-specific molecular signatures in intracranial ependymoma and association with clinical characteristics. J. Clin. Oncol. *24*, 5223-5233.

Mohseni, M., Sun, J., Lau, A., Curtis, S., Goldsmith, J., Fox, V.L., Wei, C., Frazier, M., Samson, O., Wong, K.-K., et al. (2014). A genetic screen identifies an LKB1-MARK signalling axis controlling the Hippo-YAP pathway. Nat. Cell Biol. *16*, 108–117.

Nagaraj R., Gururaja-Rao, S., Jones, K.T., Slattery, M., Negre, N., Braas, D., Christofk, H., White, K.P., Mann, R., and Banerjee, U. (2012). Control of mitochondrial structure and function by the Yorkie/YAP oncogenic pathway. Genes Dev. *26*, 2027-2-37.

Navin, N., Kendall, J., Troge, J., Andrews, P., Rodgers, L., McIndoo, J., Cook, K., Stepansky, A., Levy, D., Esposito, D., et al. (2011). Tumour evolution inferred by single-cell sequencing. Nature *472*, 90–94.

Nielsen, P.J., Lorenz, B., Müller, A.M., Wenger, R.H., Brombacher, F., Simon, M., Weid, von der, T., Langhorne, W.J., Mossmann, H., and Köhler, G. (1997). Altered erythrocytes and a leaky block in B-cell development in CD24/HSA-deficient mice. Blood *89*, 1058–1067.

Notta, F., Mullighan, C.G., Wang, J.C.Y., Poeppl, A., Doulatov, S., Phillips, L.A., Ma, J., Minden, M.D., Downing, J.R., and Dick, J.E. (2011). Evolution of human BCR-ABL1 lymphoblastic leukaemia-initiating cells. Nature *469*, 362–367.

Ohsawa, S., Sato, Y., Enomoto, M., Nakamura, M., Betsumiya, A., and Igaki, T. (2012). Mitochondrial defect drives non-autonomous tumour progression through Hippo signalling in Drosophila. Nature *490*, 547-551.

Overdevest, J.B., Thomas, S., Kristiansen, G., Hansel, D.E., Smith, S.C., and Theodorescu, D. (2011). CD24 offers a therapeutic target for control of bladder cancer metastasis based on a requirement for lung colonization. Cancer Res. *71*, 3802–3811.

Overholtzer, M., Zhang, J., Smolen, G.A., Muir, B., Li, W., Sgroi, D.C., Deng, C.-X., Brugge, J.S., and Haber, D.A. (2006). Transforming properties of YAP, a candidate oncogene on the chromosome 11q22 amplicon. Proc. Natl. Acad. Sci. U.S.a. *103*, 12405–12410.

Pang, R., Law, W.L., Chu, A.C.Y., Poon, J.T., Lam, C.S.C., Chow, A.K.M., Ng, L., Cheung, L.W.H., Lan, X.R., Lan, H.Y., et al. (2010). A subpopulation of CD26+ cancer stem cells with metastatic capacity in human colorectal cancer. Cell Stem Cell *6*, 603–615.

Park, K.-S., Whitsett, J.A., Di Palma, T., Hong, J.-H., Yaffe, M.B., and Zannini, M. (2004). TAZ interacts with TTF-1 and regulates expression of surfactant protein-C. J. Biol. Chem. *279*, 17384–17390.

Park, S.Y., Lee, H.E., Li, H., Shipitsin, M., Gelman, R., and Polyak, K. (2010). Heterogeneity for stem cell-related markers according to tumor subtype and histologic stage in breast cancer. Clin. Cancer Res. *16*, 876–887.

Rosen, J.M., and Roarty, K. (2014). Paracrine signaling in mammary gland development: what can we learn about intratumoral heterogeneity? Breast Cancer Res. *16*, 202.

Sagiv, E., Starr, A., Rozovski, U., Khosravi, R., Altevogt, P., Wang, T., and Arber, N. (2008). Targeting CD24 for treatment of colorectal and pancreatic cancer by monoclonal antibodies or small interfering RNA. Cancer Res. *68*, 2803–2812.

Sammar, M., Aigner, S., Hubbe, M., Schirrmacher, V., Schachner, M., Vestweber, D., and Altevogt, P. (1994). Heat-stable antigen (CD24) as ligand for mouse P-selectin. Int. Immunol. *6*, 1027–1036.

Sammar, M., Gulbins, E., Hilbert, K., Lang, F., and Altevogt, P. (1997). Mouse CD24 as a signaling molecule for integrin-mediated cell binding: functional and physical association with src-kinases. Biochem. Biophys. Res. Commun. *234*, 330–334.

Sansores-Garcia, L., Bossuyt, W., Wada, K.-I., Yonemura, S., Tao, C., Sasaki, H., and Halder, G. (2011). Modulating F-actin organization induces organ growth by affecting the Hippo pathway. Embo J. *30*, 2325–2335.

Schlegelmilch, K., Mohseni, M., Kirak, O., Pruszak, J., Rodriguez, J.R., Zhou, D., Kreger, B.T., Vasioukhin, V., Avruch, J., Brummelkamp, T.R., et al. (2011). Yap1 acts downstream of α-catenin to control epidermal proliferation. Cell *144*, 782–795.

Seidel, C., Schagdarsurengin, U., Blumke, K., Wurl, P., Pfeifer, G.P., Hauptmann, S., Taubert, H, and Dammann, R. (2007). Frequent hypermethylation of MST1 and MST2 in soft tissue sarcoma. Mol. Carcinog. *46*, 865-871.

Shackleton, M., Vaillant, F., Simpson, K.J., Stingl, J., Smyth, G.K., Asselin-Labat, M.-L., Wu, L., Lindeman, G.J., and Visvader, J.E. (2006). Generation of a functional mammary gland from a single stem cell. Nature *439*, 84–88.

Snijders, A.M., Schmidt, B.L., Fridlyand, J., Dekker, N., Pinkel, D., Jordan, R.C., and Albertson, D.G. (2005). Rare amplicons implicate frequent deregulation of cell fate specification pathways in oral squamous cell carcinoma. Oncogene *24*, 4232-4242.

Springer, T., Galfrè, G., Secher, D.S., and Milstein, C. (1978). Monoclonal xenogeneic antibodies to murine cell surface antigens: identification of novel leukocyte differentiation antigens. Eur. J. Immunol. *8*, 539–551.

Steinhardt, A.A., Gayyed, M.F., Klein, A.P., Dong, J., Maitra, A., Pan, D., Montgomery, E.A., and Anders, R.A. (2008). Expression of Yes-associated protein in common solid tumors. Hum. Pathol. *39*, 1582–1589.

Stingl, J., Eirew, P., Ricketson, I., Shackleton, M., Vaillant, F., Choi, D., Li, H.I., and Eaves, C.J. (2006). Purification and unique properties of mammary epithelial stem cells. Nature *439*, 993–997.

Takahashi, Y., Miyoshi, Y., Takahata, C., Irahara, N., Taguchi, T., Tamaki, Y., and Noguchi, S. (2005). Down-regulation of LATS1 and LATS2 mRNA expression by promoter hypermethylation and its association with biologically aggressive phenotype in human breast cancers. Clin. Cancer Res. *11*, 1380-1385.

Vermeulen, L., De Sousa E Melo, F., van der Heijden, M., Cameron, K., de Jong, J.H., Borovski, T., Tuynman, J.B., Todaro, M., Merz, C., Rodermond, H., et al. (2010). Wnt activity defines colon cancer stem cells and is regulated by the microenvironment. Nat. Cell Biol. *12*, 468–476.

Visvader, J.E., and Lindeman, G.J. (2012). Cancer stem cells: current status and evolving complexities. Cell Stem Cell *10*, 717–728.

Wada, K.-I., Itoga, K., Okano, T., Yonemura, S., and Sasaki, H. (2011). Hippo pathway regulation by cell morphology and stress fibers. Development *138*, 3907–3914.

Wang, W., Wang, X., Peng, L., Deng, Q., Liang, Y., Qing, H., and Jiang, B. (2010a). CD24-dependent MAPK pathway activation is required for colorectal cancer cell proliferation. Cancer Sci. *101*, 112–119.

Wang, Y., Dong, Q., Zhang, Q., Li, Z., Wang, E., and Qiu, X. (2010b). Overexpression of yes-associated protein contributes to progression and poor prognosis of non-small-cell lung cancer. Cancer Sci. *101*, 1279–1285.

Wenger, R.H., Kopf, M., Nitschke, L., Lamers, M.C., Köhler, G., and Nielsen, P.J. (1995). B-cell maturation in chimaeric mice deficient for the heat stable antigen (HSA/mouse CD24). Transgenic Res. *4*, 173–183.

Wu, X., Northcott, P.A., Dubuc, A., Dupuy, A.J., Shih, D.J.H., Witt, H., Croul, S., Bouffet, E., Fults, D.W., Eberhart, C.G., et al. (2012). Clonal selection drives genetic divergence of metastatic medulloblastoma. Nature *482*, 529–533.

Xie, M., Zhang, L., He, C.-S., Hou, J.-H., Lin, S.-X., Hu, Z.-H., Xu, F., and Zhao, H.-Y. (2012). Prognostic significance of TAZ expression in resected non-small cell lung cancer. J Thorac Oncol *7*, 799–807.

Xin, M., Kim, Y., Sutherland, L.B., Murakami, M., Qi, X., McAnally, J., Porrello, E.R., Mahmoud, A.I., Tan, W., Shelton, J.M., et al. (2013). Hippo pathway effector Yap promotes cardiac regeneration. Proc. Natl. Acad. Sci. U.S.a. *110*, 13839–13844.

Xu, M.Z., Yao, T.-J., Lee, N.P.Y., Ng, I.O.L., Chan, Y.-T., Zender, L., Lowe, S.W., Poon, R.T.P., and Luk, J.M. (2009). Yes-associated protein is an independent prognostic marker in hepatocellular carcinoma. Cancer *115*, 4576–4585.

Xu, W., Mezencev, R., Kim, B., Wang, L., McDonald, J., and Sulchek, T. (2012). Cell stiffness is a biomarker of the metastatic potential of ovarian cancer cells. PLoS ONE *7*, e46609.

Xu, X., Rock, J.R., Lu, Y., Futtner, C., Schwab, B., Guinney, J., Hogan, B.L.M., and Onaitis, M.W. (2012). Evidence for type II cells as cells of origin of K-Ras-induced distal lung adenocarcinoma. Proc. Natl. Acad. Sci. U.S.A. *109*, 4910–4915.

Xue, W., Meylan, E., Oliver, T.G., Feldser, D.M., Winslow, M.M., Bronson, R., and Jacks, T. (2011). Response and resistance to NF-kB inhibitors in mouse models of lung adenocarcinoma. Cancer Discov. *1*, 236-247.

Yachida, S., Jones, S., Bozic, I., Antal, T., Leary, R., Fu, B., Kamiyama, M., Hruban, R.H., Eshleman, J.R., Nowak, M.A., et al. (2010). Distant metastasis occurs late during the genetic evolution of pancreatic cancer. Nature *467*, 1114–1117.

Yamamoto, M., Taguchi, Y., Ito-Kureha, T., Semba, K., Yamaguchi, N., Inoue, J. (2013). NF-kappaB non-cell-autonomously regulates cancer stem cell populations in the basal-like breast cancer subtype. Nat. Commun. *4*, 2299.

Yao, X., Labelle, M., Lamb, C.R., Dugan, J.M., Williamson, C.A., Spencer, D.R., Christ, K.R., Keating, R.O., Lee, W.D., Paradis, G.A., et al. (2013). Determination of 35 cell surface antigen levels in malignant pleural effusions identifies CD24 as a marker of disseminated tumor cells. Int. J. Cancer *133*, 2925–2933.

Zacharek, S.J., Fillmore, C.M., Lau, A.N., Gludish, D.W., Chou, A., Ho, J.W.K., Zamponi, R., Gazit, R., Bock, C., Jäger, N., et al. (2011). Lung stem cell self-renewal relies on BMI1-dependent control of expression at imprinted loci. Cell Stem Cell *9*, 272–281.

Zarn, J.A., Zimmermann, S.M., Pass, M.K., Waibel, R., and Stahel, R.A. (1996). Association of CD24 with the kinase c-fgr in a small cell lung cancer cell line and with the kinase lyn in an erythroleukemia cell line. Biochem. Biophys. Res. Commun. *225*, 384–391.

Zender, L., Spector, M.S., Xue, W., Flemming, P., Cordon-Cardo, C., Silke, J., Fan, S.-T., Luk, J.M., Wigler, M., Hannon, G.J., et al. (2006). Identification and validation of oncogenes in liver cancer using an integrative oncogenomic approach. Cell *125*, 1253–1267.

Zhao, B., Wei, X., Li, W., Udan, R.S., Yang, Q., Kim, J., Xie, J., Ikenoue, T., Yu, J., Li, L., et al. (2007). Inactivation of YAP oncoprotein by the Hippo pathway is involved in cell contact inhibition and tissue growth control. Genes Dev. *21*, 2747–2761.

Zheng, Y., la Cruz, de, C.C., Sayles, L.C., Alleyne-Chin, C., Vaka, D., Knaak, T.D., Bigos, M., Xu, Y., Hoang, C.D., Shrager, J.B., et al. (2013). A rare population of CD24(+)ITGB4(+)Notch(hi) cells drives tumor propagation in NSCLC and requires Notch3 for self-renewal. Cancer Cell *24*, 59–74.

Zhou, Z., Hao, Y., Liu, N., Raptis, L., Tsao, M.-S., and Yang, X. (2011). TAZ is a novel oncogene in non-small cell lung cancer. Oncogene *30*, 2181–2186.

APPENDIX

Mice Used in Tumor Transplants

Table A1: CD24 primary transplants

Table 1		CD24+	CD24-
Donor Mouse	**No. of Kras;p53-flox cells transplanted**	**Number of Mice with tumors/ Number Transplanted**	
SC 625	10,000	4/4	2/2
SC 879	10,000	ND	3/3
SC 880	10,000	2/2	3/3
SC 881	10,000	4/4	4/4

Table A2: CD24 secondary transplants

Table 2			CD24+	CD24-
Donor Mouse	**Original Donor**	**No. of 2° cells transplanted**	**Number of Mice with tumors/ Number Transplanted**	
NU 1920	SC 881 CD24-	1,000	0/2	0/2
NU 1921	SC 880 CD24-	1,000	ND	0/1
NU 1922	SC 881 CD24+	1,000	0/2	0/2
NU 1983	SC 881 CD24-	1,000	1/1	0/2
NU 1984	SC 879 CD24-	1,000	0/2	0/2
NU 1920	SC 881 CD24-	10,000	0/2	0/2
NU 1921	SC 880 CD24-	10,000	1/1	0/2
NU 1922	SC 881 CD24+	10,000	0/2	0/2
NU 1885	SC 881 CD24+	10,000	1/3	0/3
NU 1886	SC 879 CD24-	10,000	3/3	0/3
NU 1983	SC 881 CD24-	10,000	1/1	0/1
NU 1984	SC 879 CD24-	10,000	0/2	0/2

Table A3: Sca1/CD24 primary transplants

Table 3		Sca1+CD24+	Sca1-CD24+	Sca1+CD24-	Sca1-CD24-
Donor Mouse	**No. of Kras;p53-flox cells transplanted**	**Number of Mice with tumors/ Number Transplanted**			
SC 1051	100	0/3	0/3	0/3	0/3
SC 1132	100	1/3	0/2	1/3	0/3
AL 1149	100	1/3	0/3	0/3	0/3
AL 1150	100	1/3	0/3	0/3	0/3
AL 1265	100	0/3	0/3	0/3	0/3
AL 1323	100	0/3	0/3	0/3	0/3
SC 1052	1,000	0/2	0/1	0/2	0/2
SC 1078	1,000	0/3	1/3	0/2	1/3
DR 1091 + DR 1093 + DR 1099	1,100	0/3	1/3	0/3	0/1
AL 1532	2,992	0/3	0/3	ND	0/3
AL 1633 + AL 1674 + AL 1670	3,621	2/3	2/3	ND	1/3
AL 1476	6,000	1/3	2/4	ND	1/3
AL 1534	6,997	2/3	1/3	ND	0/3
AL 1945, 1532, 1531	7,272	1/2	3/3	0/3	3/3
AL 1668 + AL 1672	9,167	2/3	4/4	ND	0/3
AL 1784 + AL 1785 + AL 1787	10,000	2/3	2/2	1/2	1/3
AL 2041 + AL 2043	10,000	1/2	0/1	ND	1/3
AL 2224	10,000	0/3	0/3	0/3	0/3

Table A4: Sca1/CD24 secondary transplants

Table 4			Sca1+CD24+	Sca1-CD24+	Sca1+CD24-	Sca1-CD24-
Donor Mouse	**Original Donor**	**No. of 2° cells transplanted**	**Number of Mice with tumors/ Number Transplanted**			
NU 2764	AL 1784 + AL 1785 + AL 1787 Sca1-CD24+	3883	ND	0/3	ND	1/3
NU 2737	AL 1668 + AL 1672 Sca1-CD24+	5070	1/2	0/2	ND	0/3
NU 2745	AL 1668 + AL 1672 Sca1-CD24+	5499	2/3	1/2	0/2	1/3
NU 2740	AL 1784 + AL 1785 + AL 1787 Sca1+CD24+	7650	2/2	2/3	1/2	0/2
NU 2733	AL 1945, 1532, 1531 Sca1-CD24+	10,000	2/2	0/3	0/2	0/3
NU 2691	AL 1476 Sca1-CD24+	10,000	1/3	2/2	ND	0/2
NU 2692	AL 1476 Sca1-CD24+	10,000	1/2	1/2	ND	0/3
NU 2726	AL 1784 + AL 1785 + AL 1787 Sca1+CD24+	10,000	0/2	0/3	ND	0/3
NU 2732	AL 1945, 1532, 1531 Sca1-CD24+	10,000	0/3	0/3	0/2	0/2
NU 2766	AL 1784 + AL 1785 + AL 1787 Sca1-CD24-	10,000	1/3	1/3	ND	0/3

Table A5: Sca1 Gene Signature

Human Orthologues of Sca1+ up genes - U133a probe list	
Probe Set ID	**Gene Symbol**
219693_at	AGPAT4
228667_at	AGPAT4
1553734_at	AK7
1569699_at	AK7
1569700_s_at	AK7
241326_at	AK7
202759_s_at	AKAP2 /// PALM2-AKAP2
202760_s_at	AKAP2 /// PALM2-AKAP2
226694_at	AKAP2 /// PALM2-AKAP2
205633_s_at	ALAS1
212224_at	ALDH1A1
228817_at	ALG9
219374_s_at	ALG9 /// FDXACB1
243151_at	ANKRD42
201012_at	ANXA1
233011_at	ANXA1
1568126_at	ANXA2
201590_x_at	ANXA2
210427_x_at	ANXA2
213503_x_at	ANXA2
201686_x_at	API5
201687_s_at	API5
214959_s_at	API5
214960_at	API5
233078_at	API5
218218_at	APPL2
210066_s_at	AQP4
210067_at	AQP4
210068_s_at	AQP4
210906_x_at	AQP4
226228_at	AQP4
205239_at	AREG
215564_at	AREG
1557285_at	AREGB
206030_at	ASPA
228807_at	ASPA
1568743_at	ATP10A
214255_at	ATP10A
214256_at	ATP10A
221484_at	B4GALT5
221485_at	B4GALT5

206232_s_at	B4GALT6
206233_at	B4GALT6
235333_at	B4GALT6
222643_s_at	BBS1 /// DPP3
204378_at	BCAS1
234221_at	BCAS1
234780_at	BCAS1
224435_at	C10orf58
228155_at	C10orf58
232662_x_at	C10orf58
218925_s_at	C11orf1
222785_x_at	C11orf1
231530_s_at	C11orf1
231538_at	C11orf1
1552950_at	C15orf26
229238_at	C17orf97
1555111_at	C1orf114
1555112_a_at	C1orf114
206721_at	C1orf114
231077_at	C1orf192
237131_at	C1orf230
228100_at	C1orf88
218123_at	C21orf59
244369_at	C21orf59
1553761_at	C22orf30
1558097_at	C22orf30
216555_at	C22orf30
236941_at	C22orf30
231133_at	C2orf39
220149_at	C2orf54
230273_at	C6orf165
1554919_s_at	C7orf63
219455_at	C7orf63
221946_at	C9orf116
59437_at	C9orf116
229012_at	C9orf24
1553433_at	C9orf93
1556516_at	C9orf93
1558082_at	C9orf93
1558160_at	C9orf93
1559672_a_at	C9orf93
236945_at	C9orf93
239712_at	C9orf93
242821_at	C9orf93

1566149_at	CALML4
1566150_at	CALML4
1568600_at	CALML4
221879_at	CALML4
64408_s_at	CALML4
236085_at	CAPSL
1553886_at	CCDC108
1556969_at	CCDC108
239508_x_at	CCDC108
222890_at	CCDC113
230807_at	CCDC151
240293_at	CCDC153
1563563_at	CCDC40
220592_at	CCDC40
220593_s_at	CCDC40
229918_at	CCDC40
239254_at	CCDC40
219644_at	CCDC41
239282_at	CCDC41
211173_at	CCKAR
211174_s_at	CCKAR
203593_at	CD2AP
236257_at	CD2AP
205288_at	CDC14A
210440_s_at	CDC14A
210441_at	CDC14A
210742_at	CDC14A
210743_s_at	CDC14A
225081_s_at	CDCA7L
227742_at	CLIC6
242913_at	CLIC6
221900_at	COL8A2
52651_at	COL8A2
1558034_s_at	CP
204846_at	CP
227253_at	CP
228143_at	CP
202551_s_at	CRIM1
202552_s_at	CRIM1
228496_s_at	CRIM1
205081_at	CRIP1
207030_s_at	CSRP2
211126_s_at	CSRP2
200661_at	CTSA

223454_at	CXCL16
226960_at	CXCL17
223294_at	CXorf26
224177_s_at	CXorf26
206755_at	CYP2B6
217133_x_at	CYP2B6
206754_s_at	CYP2B6 /// CYP2B7P1
207913_at	CYP2F1
223385_at	CYP2S1
1555497_a_at	CYP4B1
210096_at	CYP4B1
1007_s_at	DDR1
207169_x_at	DDR1
208779_x_at	DDR1
210749_x_at	DDR1
202480_s_at	DEDD
211255_x_at	DEDD
215158_s_at	DEDD
208250_s_at	DMBT1
205186_at	DNALI1
227081_at	DNALI1
1553976_a_at	DPCD
226009_at	DPCD
218567_x_at	DPP3
232510_s_at	DPP3
1553105_s_at	DSG2
217901_at	DSG2
238116_at	DYNLRB2
201999_s_at	DYNLT1
1564630_at	EDN1
218995_s_at	EDN1
222802_at	EDN1
1568930_at	EFCAB1
220156_at	EFCAB1
239500_at	EFCAB1
201842_s_at	EFEMP1
201843_s_at	EFEMP1
228421_s_at	EFEMP1
219833_s_at	EFHC1
225656_at	EFHC1
231026_at	EFHC1
219850_s_at	EHF
222932_at	EHF
224189_x_at	EHF

225645_at	EHF
232360_at	EHF
232361_s_at	EHF
201510_at	ELF3
210827_s_at	ELF3
229842_at	ELF3
225156_at	ELOF1
204975_at	EMP2
225078_at	EMP2
225079_at	EMP2
238500_at	EMP2
237314_at	ENKUR
204160_s_at	ENPP4
204161_s_at	ENPP4
208156_x_at	EPPK1
232164_s_at	EPPK1
232165_at	EPPK1
234552_at	EPPK1
234555_at	EPPK1
202609_at	EPS8
208621_s_at	EZR
208622_s_at	EZR
208623_s_at	EZR
217230_at	EZR
217234_s_at	EZR
204363_at	F3
223058_at	FAM107B
223059_s_at	FAM107B
1557385_at	FAM161A
1564467_at	FAM161A
239090_at	FAM161A
242584_at	FAM161A
232968_at	FANK1
1557771_at	FHAD1
1560097_at	FHAD1
1563639_a_at	FHAD1
1563830_a_at	FHAD1
1563961_at	FHAD1
1564635_a_at	FHAD1
201539_s_at	FHL1
201540_at	FHL1
210298_x_at	FHL1
210299_s_at	FHL1
214505_s_at	FHL1

205906_at	FOXJ1
239275_at	FRMPD2 /// FRMPD2P1 /// FRMPDP2
205044_at	GABRP
203397_s_at	GALNT3
203398_s_at	GALNT3
204224_s_at	GCH1
211020_at	GCNT2
230788_at	GCNT2
206917_at	GNA13
224761_at	GNA13
227539_at	GNA13
206681_x_at	GP2
208473_s_at	GP2
214324_at	GP2
214325_at	GP2
240856_at	GPR120
202831_at	GPX2
239595_at	GPX2
205770_at	GSR
225609_at	GSR
205752_s_at	GSTM5
1557915_s_at	GSTO1
201470_at	GSTO1
1552515_at	HIPK1
1552516_a_at	HIPK1
212291_at	HIPK1
212293_at	HIPK1
207764_s_at	HIPK3
210148_at	HIPK3
213697_at	HIPK3
226297_at	HIPK3
208429_x_at	HNF4A
214832_at	HNF4A
214851_at	HNF4A
216889_s_at	HNF4A
230914_at	HNF4A
205543_at	HSPA4L
202438_x_at	IDS
202439_s_at	IDS
206342_x_at	IDS
210666_at	IDS
211782_at	IDS
212221_x_at	IDS
212223_at	IDS

213821_s_at	IDS
217432_s_at	IDS
236823_at	IDS
218100_s_at	IFT57
222519_s_at	IFT57
222520_s_at	IFT57
218516_s_at	IMPAD1
222654_at	IMPAD1
222655_s_at	IMPAD1
224743_at	IMPAD1
224744_at	IMPAD1
227774_s_at	IMPAD1
204989_s_at	ITGB4
204990_s_at	ITGB4
211905_s_at	ITGB4
214292_at	ITGB4
230704_s_at	ITGB4
201124_at	ITGB5
201125_s_at	ITGB5
214020_x_at	ITGB5
214021_x_at	ITGB5
1568619_s_at	ITPRIPL2
227514_at	ITPRIPL2
227792_at	ITPRIPL2
227954_at	ITPRIPL2
227956_at	ITPRIPL2
228074_at	ITPRIPL2
226003_at	KIF21A
231875_at	KIF21A
212101_at	KPNA6
212102_s_at	KPNA6
212103_at	KPNA6
226976_at	KPNA6
224534_at	KREMEN1
227250_at	KREMEN1
234843_s_at	KREMEN1
235370_at	KREMEN1
243029_at	KREMEN1
200923_at	LGALS3BP
204272_at	LGALS4
217892_s_at	LIMA1
222456_s_at	LIMA1
222457_s_at	LIMA1
1558469_at	LPP

202821_s_at	LPP
202822_at	LPP
224811_at	LPP
230996_at	LPP
235000_at	LPP
241879_at	LPP
243874_at	LPP
206076_at	LRRC23
217609_at	LRRC23
1554584_at	LRRC48
208140_s_at	LRRC48
215173_at	LRRC50
222068_s_at	LRRC50
202018_s_at	LTF
206276_at	LY6D
212233_at	MAP1B
214577_at	MAP1B
226084_at	MAP1B
201668_x_at	MARCKS
201669_s_at	MARCKS
201670_s_at	MARCKS
213002_at	MARCKS
225897_at	MARCKS
213045_at	MAST3
226238_at	MCEE
220990_s_at	MIR21 /// TMEM49
204783_at	MLF1
204784_s_at	MLF1
207565_s_at	MR1
207566_at	MR1
210223_s_at	MR1
210224_at	MR1
210528_at	MR1
235352_at	MR1
1552364_s_at	MSI2
225233_at	MSI2
225237_s_at	MSI2
225238_at	MSI2
225240_s_at	MSI2
239232_at	MSI2
243010_at	MSI2
243579_at	MSI2
220953_s_at	MTMR12
225232_at	MTMR12

202180_s_at	MVP
204798_at	MYB
215152_at	MYB
206197_at	NME5
1553994_at	NT5E
1553995_a_at	NT5E
203939_at	NT5E
227486_at	NT5E
201173_x_at	NUDC
210574_s_at	NUDC
210575_at	NUDC
209925_at	OCLN
227492_at	OCLN
231022_at	OCLN
235937_at	OCLN
228577_x_at	ODF2L
230926_s_at	ODF2L
231909_x_at	ODF2L
237420_at	ODF2L
209626_s_at	OSBPL3
209627_s_at	OSBPL3
202780_at	OXCT1
244134_at	OXCT1
215823_x_at	PABPC1 /// RLIM
214204_at	PACRG
215472_at	PACRG
218736_s_at	PALMD
222725_s_at	PALMD
232187_at	PALMD
202336_s_at	PAM
212958_x_at	PAM
214620_x_at	PAM
203242_s_at	PDLIM5
203243_s_at	PDLIM5
211680_at	PDLIM5
211681_s_at	PDLIM5
212412_at	PDLIM5
213684_s_at	PDLIM5
216803_at	PDLIM5
216804_s_at	PDLIM5
221994_at	PDLIM5
241208_at	PDLIM5
215718_s_at	PHF3
217951_s_at	PHF3

217952_x_at	PHF3
217953_at	PHF3
217954_s_at	PHF3
204213_at	PIGR
226147_s_at	PIGR
207469_s_at	PIR
202430_s_at	PLSCR1
202446_s_at	PLSCR1
244315_at	PLSCR1
202075_s_at	PLTP
233454_at	POLN
242804_at	POLN
204304_s_at	PROM1
1554997_a_at	PTGS2
204748_at	PTGS2
203223_at	RABEP1
214552_s_at	RABEP1
225064_at	RABEP1
225092_at	RABEP1
231002_s_at	RABEP1
210335_at	RASSF9
1554003_at	RGNEF
1554004_a_at	RGNEF
1559706_at	RGNEF
1560348_at	RGNEF
219610_at	RGNEF
232994_s_at	RGNEF
1553318_at	RIBC1
235946_at	RIBC1
222815_at	RLIM
225416_at	RLIM
244470_at	RLIM
221523_s_at	RRAGD
221524_s_at	RRAGD
230093_at	RSPH1
1556049_at	RTN4
210968_s_at	RTN4
211509_s_at	RTN4
214629_x_at	RTN4
219684_at	RTP4
1569433_at	SAMD5
228653_at	SAMD5
242626_at	SAMD5
205725_at	SCGB1A1

230378_at	SCGB3A1
202082_s_at	SEC14L1
202083_s_at	SEC14L1
202084_s_at	SEC14L1
240036_at	SEC14L1
206941_x_at	SEMA3E
210083_at	SEMA7A
230345_at	SEMA7A
200986_at	SERPING1
209090_s_at	SH3GLB1
209091_s_at	SH3GLB1
210101_x_at	SH3GLB1
203123_s_at	SLC11A2
203124_s_at	SLC11A2
203125_x_at	SLC11A2
210047_at	SLC11A2
237106_at	SLC11A2
219911_s_at	SLCO4A1
229239_x_at	SLCO4A1
206874_s_at	SLK
206875_s_at	SLK
208127_s_at	SOCS5
209647_s_at	SOCS5
209648_x_at	SOCS5
205406_s_at	SPA17
216119_s_at	SPEF1
1552716_at	SPEF2
232745_x_at	SPEF2
233429_at	SPEF2
1552630_a_at	SRCAP
1569138_a_at	SRCAP
212275_s_at	SRCAP
213667_at	SRCAP
215053_at	SRCAP
38766_at	SRCAP
1555427_s_at	SYNCRIP
209024_s_at	SYNCRIP
209025_s_at	SYNCRIP
217832_at	SYNCRIP
217833_at	SYNCRIP
217834_s_at	SYNCRIP
236146_at	SYNCRIP
202796_at	SYNPO
235128_at	SYNPO

235914_at	SYNPO
206161_s_at	SYT5
206162_x_at	SYT5
207662_at	TBX1
211273_s_at	TBX1
211274_at	TBX1
236926_at	TBX1
242941_x_at	TBX1
202396_at	TCERG1
205217_at	TIMM8A
210800_at	TIMM8A
209386_at	TM4SF1
209387_s_at	TM4SF1
215033_at	TM4SF1
215034_s_at	TM4SF1
238168_at	TM4SF1
217016_x_at	TMEM212
1558177_at	TMEM229B
227544_at	TMEM229B
238820_at	TMEM229B
219503_s_at	TMEM40
222892_s_at	TMEM40
1569003_at	TMEM49
1556116_s_at	TNPO1
1557278_s_at	TNPO1
207657_x_at	TNPO1
209225_x_at	TNPO1
209226_s_at	TNPO1
212635_at	TNPO1
221829_s_at	TNPO1
225765_at	TNPO1
225766_s_at	TNPO1
243324_x_at	TNPO1
217853_at	TNS3
234257_at	TNS3
218876_at	TPPP3
215111_s_at	TSC22D1
235315_at	TSC22D1
243133_at	TSC22D1
222220_s_at	TSNAXIP1
209114_at	TSPAN1
230997_at	TTC21A
232308_at	TTC21A
205854_at	TULP3

221964_at	TULP3
200930_s_at	VCL
200931_s_at	VCL
237755_s_at	WDR16
239916_at	WDR16
217734_s_at	WDR6
233573_s_at	WDR6
218173_s_at	WHSC1L1
221248_s_at	WHSC1L1
222544_s_at	WHSC1L1
224076_s_at	WHSC1L1
224077_at	WHSC1L1
201020_at	YWHAH
236559_at	YWHAH
242325_at	YWHAH
1557953_at	ZKSCAN1
214670_at	ZKSCAN1
214900_at	ZKSCAN1

Table A6: Genes Down in Sca1+ Cells

Probe set	Gene Symbol	Gene Name
1423523_at	Aass	aminoadipate-semialdehyde synthase
1420157_s_at	Abcf1	ATP-binding cassette, sub-family F (GCN20), member 1
1416947_s_at	Acaa1a	acetyl-Coenzyme A acyltransferase 1A /// acetyl-Coenzyme A acyltransferase 1B
1428146_s_at	Acaa2	acetyl-Coenzyme A acyltransferase 2 (mitochondrial 3-oxoacyl-Coenzyme A thiolase)
1428145_at	Acaa2	acetyl-Coenzyme A acyltransferase 2 (mitochondrial 3-oxoacyl-Coenzyme A thiolase)
1434185_at	Acaca	acetyl-Coenzyme A carboxylase alpha
1424183_at	Acat1	acetyl-Coenzyme A acetyltransferase 1
1456728_x_at	Aco1	aconitase 1
1449065_at	Acot1	acyl-CoA thioesterase 1
1439478_at	Acot2	acyl-CoA thioesterase 2
1424654_at	Acp2	acid phosphatase 2, lysosomal
1418402_at	Adam19	a disintegrin and metallopeptidase domain 19 (meltrin beta)
1418403_at	Adam19	a disintegrin and metallopeptidase domain 19 (meltrin beta)
1456307_s_at	Adcy7	adenylate cyclase 7
1440801_s_at	Adrbk2	adrenergic receptor kinase, beta 2
1449383_at	Adssl1	adenylosuccinate synthetase like 1
1420428_at	Ager	advanced glycosylation end product-specific receptor
1441958_s_at	Ager	advanced glycosylation end product-specific receptor
1425354_a_at	Aggf1	angiogenic factor with G patch and FHA domains 1
1422184_a_at	Ak1	adenylate kinase 1
1456590_x_at	Akr1b3	aldo-keto reductase family 1, member B3 (aldose reductase)
1421324_a_at	Akt2	thymoma viral proto-oncogene 2
1455247_at	Amotl1	angiomotin-like 1
1416906_at	Anapc5	anaphase-promoting complex subunit 5
1428063_at	Ankrd46	ankyrin repeat domain 46
1438090_x_at	Ankrd54	ankyrin repeat domain 54
1418858_at	Aox3	aldehyde oxidase 3
1418847_at	Arg2	arginase type II
1438841_s_at	Arg2	arginase type II
1426027_a_at	Arhgap10	Rho GTPase activating protein 10
1455166_at	Arl5b	ADP-ribosylation factor-like 5B
1428138_s_at	Arl8b	ADP-ribosylation factor-like 8B
1428137_at	Arl8b	ADP-ribosylation factor-like 8B

1423511_at	Asf1a	ASF1 anti-silencing function 1 homolog A (S. cerevisiae)
1434014_at	Atg4c	autophagy-related 4C (yeast)
1460639_a_at	Atox1	ATX1 (antioxidant protein 1) homolog 1 (yeast)
1428340_s_at	Atp13a2	ATPase type 13A2
1433562_s_at	Atp5f1	ATP synthase, H+ transporting, mitochondrial F0 complex, subunit B1
1417632_at	Atp6v0a1	ATPase, H+ transporting, lysosomal V0 subunit A1
1450634_at	Atp6v1a	ATPase, H+ transporting, lysosomal V1 subunit A
1422508_at	Atp6v1a	ATPase, H+ transporting, lysosomal V1 subunit A
1430306_a_at	Atp6v1c2	ATPase, H+ transporting, lysosomal V1 subunit C2
1449712_s_at	Atp6v1e1	ATPase, H+ transporting, lysosomal V1 subunit E1
1420038_at	Atp6v1e1	ATPase, H+ transporting, lysosomal V1 subunit E1
1421166_at	Atrn	attractin
1449435_at	B4galt3	UDP-Gal:betaGlcNAc beta 1,4-galactosyltransferase, polypeptide 3
1429432_at	Bat2l2	HLA-B associated transcript 2-like 2
1419004_s_at	Bcl2a1a	B-cell leukemia/lymphoma 2 related protein A1a /// B-cell leukemia/lymphoma 2 related protein A1b /// B-cell leukemia/lymphoma 2 related protein A1d
1420631_a_at	Blcap	bladder cancer associated protein homolog (human)
1436960_at	Brd3	bromodomain containing 3
1448521_at	Brd7	bromodomain containing 7
1437345_a_at	Bscl2	Bernardinelli-Seip congenital lipodystrophy 2 homolog (human)
1449007_at	Btg3	B-cell translocation gene 3 /// B-cell translocation gene 3 pseudogene
1459900_at	C79468	expressed sequence C79468
1436489_x_at	C85492	expressed sequence C85492
1437537_at	Casp9	caspase 9
1419803_s_at	Ccdc12	coiled-coil domain containing 12
1429150_at	Ccdc77	coiled-coil domain containing 77
1448919_at	Cd302	CD302 antigen
1425519_a_at	Cd74	CD74 antigen (invariant polypeptide of major histocompatibility complex, class II antigen-associated)
1428092_at	Cdc5l	cell division cycle 5-like (S. pombe)

1425262_at	Cebpg	CCAAT/enhancer binding protein (C/EBP), gamma
1420579_s_at	Cftr	cystic fibrosis transmembrane conductance regulator homolog
1428466_at	Chd3	chromodomain helicase DNA binding protein 3
1433684_at	Chmp6	chromatin modifying protein 6
1425455_a_at	Churc1	churchill domain containing 1
1417458_s_at	Cks2	CDC28 protein kinase regulatory subunit 2
1416616_s_at	Clpp	caseinolytic peptidase, ATP-dependent, proteolytic subunit homolog (E. coli)
1421861_at	Clstn1	calsyntenin 1
1451052_at	Cog8	component of oligomeric golgi complex 8 /// peptide deformylase (mitochondrial)
1440911_at	Col23a1	collagen, type XXIII, alpha 1
1423245_at	Cops7a	COP9 (constitutive photomorphogenic) homolog, subunit 7a (Arabidopsis thaliana)
1451825_a_at	Copz1	coatomer protein complex, subunit zeta 1
1428134_at	Coq9	coenzyme Q9 homolog (yeast)
1450895_a_at	Cox16	COX16 cytochrome c oxidase assembly homolog (S. cerevisiae)
1417607_at	Cox6a2	cytochrome c oxidase, subunit VI a, polypeptide 2
1423095_s_at	Crbn	cereblon
1452901_at	Creb1	cAMP responsive element binding protein 1
1436983_at	Crebbp	CREB binding protein
1450667_a_at	Cs	citrate synthase
1422510_at	Ctdspl	CTD (carboxy-terminal domain, RNA polymerase II, polypeptide A) small phosphatase-like
1416382_at	Ctsc	cathepsin C
1431145_a_at	Cuedc2	CUE domain containing 2
1451153_a_at	Cyhr1	cysteine and histidine rich 1
1419070_at	Cys1	cystin 1
1420129_s_at	D10Wsu52e	DNA segment, Chr 10, Wayne State University 52, expressed
1449118_at	Dbt	dihydrolipoamide branched chain transacylase E2
1436680_s_at	Ddb2	damage specific DNA binding protein 2
1417516_at	Ddit3	DNA-damage inducible transcript 3
1415915_at	Ddx1	DEAD (Asp-Glu-Ala-Asp) box polypeptide 1
1426832_at	Ddx26b	DEAD/H (Asp-Glu-Ala-Asp/His) box polypeptide 26B
1417875_at	Ddx50	DEAD (Asp-Glu-Ala-Asp) box polypeptide 50
1428728_at	Ddx51	DEAD (Asp-Glu-Ala-Asp) box polypeptide 51
1451363_a_at	Dennd2d	DENN/MADD domain containing 2D

1435927_at	Dennd3	DENN/MADD domain containing 3
1425228_a_at	Dguok	deoxyguanosine kinase
1453487_at	Dhdh	dihydrodiol dehydrogenase (dimeric)
1416144_a_at	Dhx15	DEAH (Asp-Glu-Ala-His) box polypeptide 15
1438969_x_at	Dhx30	DEAH (Asp-Glu-Ala-His) box polypeptide 30
1416918_at	Dlg3	discs, large homolog 3 (Drosophila)
1449939_s_at	Dlk1	delta-like 1 homolog (Drosophila)
1434944_at	Dmpk	dystrophia myotonica-protein kinase
1421032_a_at	Dnajb12	DnaJ (Hsp40) homolog, subfamily B, member 12
1425135_a_at	Dnm2	dynamin 2
1425136_x_at	Dnm2	dynamin 2
1437437_x_at	Dnpep	aspartyl aminopeptidase
1439452_x_at	Dnpep	aspartyl aminopeptidase
1438557_x_at	Dnpep	aspartyl aminopeptidase
1416697_at	Dpp4	dipeptidylpeptidase 4
1453731_a_at	Dram2	VDNA-damage regulated autophagy modulator 2
1449929_at	Dynlt3	dynein light chain Tctex-type 3
1418286_a_at	Efnb1	ephrin B1
1460432_a_at	Eif3e	eukaryotic translation initiation factor 3, subunit E
1439268_x_at	Eif3e	eukaryotic translation initiation factor 3, subunit E
1423220_at	Eif4e	eukaryotic translation initiation factor 4E
1419556_at	Elf5	E74-like factor 5
1450208_a_at	Elmo1	engulfment and cell motility 1, ced-12 homolog (C. elegans)
1452157_at	Eprs	glutamyl-prolyl-tRNA synthetase
1433514_at	Etnk1	ethanolamine kinase 1
1437712_x_at	Exosc4	exosome component 4
1416888_at	Fadd	Fas (TNFRSF6)-associated via death domain
1431002_x_at	Fahd2a	fumarylacetoacetate hydrolase domain containing 2A
1431189_a_at	Fahd2a	fumarylacetoacetate hydrolase domain containing 2A
1431190_x_at	Fahd2a	fumarylacetoacetate hydrolase domain containing 2A
1428540_at	Fam115a	family with sequence similarity 115, member A
1434010_at	Fam117b	family with sequence similarity 117, member B
1418474_at	Fam158a	family with sequence similarity 158, member A
1425323_a_at	Fam173a	family with sequence similarity 173, member A
1451668_at	Fam20b	family with sequence similarity 20, member B
1454621_s_at	Fam73b	family with sequence similarity 73, member B
1438036_x_at	Fam82a1	family with sequence similarity 82, member A1

1430986_at	Farsb	phenylalanyl-tRNA synthetase, beta subunit
1423828_at	Fasn	fatty acid synthase
1447878_s_at	Fgfrl1	fibroblast growth factor receptor-like 1
1444075_at	Filip1	filamin A interacting protein 1
1454935_at	Fitm2	fat storage-inducing transmembrane protein 2
1435221_at	Foxp1	forkhead box P1
1455843_at	Fut4	fucosyltransferase 4
1449410_a_at	Gas5	growth arrest specific 5
1423271_at	Gjb2	gap junction protein, beta 2
1424108_at	Glo1	glyoxalase 1
1451121_a_at	Gltscr2	glioma tumor suppressor candidate region gene 2
1435335_a_at	Gnptab	N-acetylglucosamine-1-phosphate transferase, alpha and beta subunits
1449390_at	Gpatch4	G patch domain containing 4
1437436_s_at	Grk6	G protein-coupled receptor kinase 6
1433824_x_at	Grsf1	G-rich RNA sequence binding factor 1
1438858_x_at	H2-Aa	histocompatibility 2, class II antigen A, alpha
1435290_x_at	H2-Aa	histocompatibility 2, class II antigen A, alpha
1450648_s_at	H2-Ab1	histocompatibility 2, class II antigen A, beta 1
1451721_a_at	H2-Ab1	histocompatibility 2, class II antigen A, beta 1
1425477_x_at	H2-Ab1	histocompatibility 2, class II antigen A, beta 1
1449580_s_at	H2-DMb1	histocompatibility 2, class II, locus Mb1 /// histocompatibility 2, class II, locus Mb2
1418638_at	H2-DMb1	histocompatibility 2, class II, locus Mb1 /// histocompatibility 2, class II, locus Mb2
1417025_at	H2-Eb1	histocompatibility 2, class II antigen E beta
1415743_at	Hdac5	histone deacetylase 5
1424522_at	Heatr1	HEAT repeat containing 1
1425937_a_at	Hexim1	hexamethylene bis-acetamide inducible 1
1435967_s_at	Hibadh	3-hydroxyisobutyrate dehydrogenase
1448183_a_at	Hif1a	hypoxia inducible factor 1, alpha subunit
1455014_at	Hint3	histidine triad nucleotide binding protein 3
1448239_at	Hmox1	heme oxygenase (decycling) 1
1416399_a_at	Hmox2	heme oxygenase (decycling) 2
1454898_s_at	Iah1	isoamyl acetate-hydrolyzing esterase 1 homolog (S. cerevisiae)
1429119_at	Iah1	isoamyl acetate-hydrolyzing esterase 1 homolog (S. cerevisiae)
1451412_a_at	Ift20	intraflagellar transport 20 homolog (Chlamydomonas)
1455048_at	Igsf3	immunoglobulin superfamily, member 3
1448496_a_at	Ing1	inhibitor of growth family, member 1
1450760_a_at	Ing3	inhibitor of growth family, member 3
1433464_at	Ipo13	importin 13

1451983_at	Irx1	Iroquois related homeobox 1 (Drosophila)
1420860_at	Itga9	integrin alpha 9
1450029_s_at	Itga9	integrin alpha 9
1422157_a_at	Itgb1bp1	integrin beta 1 binding protein 1
1431808_a_at	Itih4	inter alpha-trypsin inhibitor, heavy chain 4
1415961_at	Itm2c	integral membrane protein 2C
1426900_at	Jmjd1c	jumonji domain containing 1C
1420056_s_at	Jmjd6	jumonji domain containing 6
1450185_a_at	Kcnj15	potassium inwardly-rectifying channel, subfamily J, member 15
1426810_at	Kdm3a	lysine (K)-specific demethylase 3A
1436056_at	Kif13b	kinesin family member 13B
1416350_at	Klf16	Kruppel-like factor 16
1435086_s_at	Klhdc2	kelch domain containing 2
1448269_a_at	Klhl13	kelch-like 13 (Drosophila)
1417812_a_at	Lamb3	laminin, beta 3
1417057_a_at	Lamp3	lysosomal-associated membrane protein 3 /// peptidylprolyl isomerase D (cyclophilin D)
1427011_a_at	Lancl1	LanC (bacterial lantibiotic synthetase component C)-like 1
1434418_at	Lass6	LAG1 homolog, ceramide synthase 6
1440246_at	Lass6	LAG1 homolog, ceramide synthase 6
1460546_at	Lgi3	leucine-rich repeat LGI family, member 3
1456377_x_at	Limd2	LIM domain containing 2
1429104_at	Limd2	LIM domain containing 2
1417627_a_at	Limk1	LIM-domain containing, protein kinase
1418232_s_at	Lims1	LIM and senescent cell antigen-like domains 1
1450872_s_at	Lipa	lysosomal acid lipase A
1451359_at	Lpcat1	lysophosphatidylcholine acyltransferase 1
1431394_a_at	Lrrk2	leucine-rich repeat kinase 2
1438312_s_at	Ltbp3	latent transforming growth factor beta binding protein 3
1451490_at	Lyplal1	lysophospholipase-like 1
1455928_x_at	Lztr1	leucine-zipper-like transcriptional regulator, 1
1426409_at	Lzts2	leucine zipper, putative tumor suppressor 2
1416212_at	Magoh	mago-nashi homolog, proliferation-associated (Drosophila)
1434354_at	Maob	monoamine oxidase B
1423667_at	Mat2a	methionine adenosyltransferase II, alpha
1433576_at	Mat2a	methionine adenosyltransferase II, alpha
1427040_at	Mdfic	MyoD family inhibitor domain containing
1421528_a_at	Med22	mediator complex subunit 22
1417844_at	Med4	mediator of RNA polymerase II transcription, subunit 4 homolog (yeast)
1419377_at	Med9	mediator of RNA polymerase II transcription,

		subunit 9 homolog (yeast)
1439380_x_at	Meg3	maternally expressed 3
1452905_at	Meg3	maternally expressed 3
1460050_x_at	Mettl13	Methyltransferase like 13
1456736_x_at	Mff	mitochondrial fission factor
1452037_at	Mgat2	mannoside acetylglucosaminyltransferase 2
1415897_a_at	Mgst1	microsomal glutathione S-transferase 1
1416733_at	Mkln1	muskelin 1, intracellular mediator containing kelch motifs
1430635_at	Mlana	melan-A
1448139_at	Mlc1	megalencephalic leukoencephalopathy with subcortical cysts 1 homolog (human)
1433811_at	Mllt6	myeloid/lymphoid or mixed-lineage leukemia (trithorax homolog, Drosophila); translocated to, 6
1420092_at	Morc3	Microrchidia 3
1432216_s_at	Mpp7	membrane protein, palmitoylated 7 (MAGUK p55 subfamily member 7)
1455179_at	Mpp7	membrane protein, palmitoylated 7 (MAGUK p55 subfamily member 7)
1437622_x_at	Mrpl28	mitochondrial ribosomal protein L28
1427158_at	Mrps30	mitochondrial ribosomal protein S30
1453030_at	Msl2	male-specific lethal 2 homolog (Drosophila)
1436704_x_at	Mthfd1	methylenetetrahydrofolate dehydrogenase (NADP+ dependent), methenyltetrahydrofolate cyclohydrolase, formyltetrahydrofolate synthase
1419272_at	Myd88	myeloid differentiation primary response gene 88
1424933_at	Myo5c	myosin VC
1423590_at	Napsa	napsin A aspartic peptidase
1444086_at	Nckap5	NCK-associated protein 5
1448934_at	Ndufa10	NADH dehydrogenase (ubiquinone) 1 alpha subcomplex 10
1417285_a_at	Ndufa5	NADH dehydrogenase (ubiquinone) 1 alpha subcomplex, 5
1448427_at	Ndufa6	NADH dehydrogenase (ubiquinone) 1 alpha subcomplex, 6 (B14)
1447919_x_at	Ndufab1	NADH dehydrogenase (ubiquinone) 1, alpha/beta subcomplex, 1
1455911_x_at	Ndufb11	NADH dehydrogenase (ubiquinone) 1 beta subcomplex, 11
1451109_a_at	Nedd4	neural precursor cell expressed, developmentally down-regulated 4
1428248_at	Nfx1	nuclear transcription factor, X-box binding 1
1448465_at	Nipsnap1	4-nitrophenylphosphatase domain and non-

		neuronal SNAP25-like protein homolog 1 (C. elegans)
1417278_a_at	Nkd1	naked cuticle 1 homolog (Drosophila)
1429819_at	Nmnat1	nicotinamide nucleotide adenylyltransferase 1
1456573_x_at	Nnt	nicotinamide nucleotide transhydrogenase
1455768_at	Npc2	Niemann Pick type C2
1434270_at	Npcd	neuronal pentraxin chromo domain /// neuronal pentraxin receptor
1452107_s_at	Npnt	nephronectin
1421429_a_at	Npnt	nephronectin
1424412_at	Ogfrl1	opioid growth factor receptor-like 1
1418529_at	Osgep	O-sialoglycoprotein endopeptidase
1450969_at	Pccb	propionyl Coenzyme A carboxylase, beta polypeptide
1435741_at	Pde8b	phosphodiesterase 8B
1437989_at	Pde8b	phosphodiesterase 8B
1423648_at	Pdia6	protein disulfide isomerase associated 6
1427550_at	Peg10	paternally expressed 10
1449442_at	Pex11a	peroxisomal biogenesis factor 11 alpha
1448995_at	Pf4	platelet factor 4
1451149_at	Pgm2	phosphoglucomutase 2
1428714_at	Pgrmc2	progesterone receptor membrane component 2
1435003_at	Pi4ka	phosphatidylinositol 4-kinase, catalytic, alpha polypeptide
1437999_x_at	Pigq	phosphatidylinositol glycan anchor biosynthesis, class Q
1438652_x_at	Pigq	phosphatidylinositol glycan anchor biosynthesis, class Q
1435596_at	Pion	pigeon homolog (Drosophila)
1416387_at	Pip4k2c	phosphatidylinositol-5-phosphate 4-kinase, type II, gamma
1421834_at	Pip5k1b	phosphatidylinositol-4-phosphate 5-kinase, type 1 beta
1424442_a_at	Pja2	praja 2, RING-H2 motif containing
1448786_at	Plbd1	phospholipase B domain containing 1
1423372_at	Pole4	polymerase (DNA-directed), epsilon 4 (p12 subunit)
1449648_s_at	Polr1c	polymerase (RNA) I polypeptide C
1417041_at	Polr1c	polymerase (RNA) I polypeptide C
1452596_at	Polr2k	polymerase (RNA) II (DNA directed) polypeptide K
1448379_at	Pot1a	protection of telomeres 1A
1452831_s_at	Ppat	phosphoribosyl pyrophosphate amidotransferase
1454848_at	Ppp1r12c	protein phosphatase 1, regulatory (inhibitor)

		subunit 12C
1440285_at	Ppp1r9a	protein phosphatase 1, regulatory (inhibitor) subunit 9A
1425542_a_at	Ppp2r5c	protein phosphatase 2, regulatory subunit B (B56), gamma isoform
1452788_at	Ppp2r5e	protein phosphatase 2, regulatory subunit B (B56), epsilon isoform
1418036_at	Prim2	DNA primase, p58 subunit
1439549_at	Prrg3	proline rich Gla (G-carboxyglutamic acid) 3 (transmembrane)
1418320_at	Prss8	protease, serine, 8 (prostasin)
1450696_at	Psmb9	proteasome (prosome, macropain) subunit, beta type 9 (large multifunctional peptidase 2)
1433503_at	Ptgr2	prostaglandin reductase 2
1423414_at	Ptgs1	prostaglandin-endoperoxide synthase 1
1436448_a_at	Ptgs1	prostaglandin-endoperoxide synthase 1
1438670_at	Ptpn1	protein tyrosine phosphatase, non-receptor type 1
1450819_at	Pvrl1	poliovirus receptor-related 1
1437993_x_at	Qdpr	quinoid dihydropteridine reductase
1417829_a_at	Rab15	RAB15, member RAS oncogene family
1423083_at	Rab33b	RAB33B, member of RAS oncogene family
1416591_at	Rab34	RAB34, member of RAS oncogene family
1424331_at	Rab40c	Rab40c, member RAS oncogene family
1424188_at	Rabgap1	RAB GTPase activating protein 1
1443877_a_at	Rapgef6	Rap guanine nucleotide exchange factor (GEF) 6
1422449_s_at	Rcn2	reticulocalbin 2
1450107_a_at	Renbp	renin binding protein
1451236_at	Rerg	RAS-like, estrogen-regulated, growth-inhibitor
1427580_a_at	Rian	RNA imprinted and accumulated in nucleus
1426504_a_at	Rnf121	ring finger protein 121
1452769_at	Rnf145	ring finger protein 145
1429321_at	Rnf149	ring finger protein 149
1426414_a_at	Rnf7	ring finger protein 7
1438626_x_at	Rpl14	ribosomal protein L14
1448398_s_at	Rpl22	ribosomal protein L22
1439780_at	Rpl7l1	ribosomal protein L7-like 1
1422552_at	Rprm	reprimo, TP53 dependent G2 arrest mediator candidate
1455364_a_at	Rps7	ribosomal protein S7
1417096_at	Rrp15	ribosomal RNA processing 15 homolog (S. cerevisiae)
1415823_at	Scd2	stearoyl-Coenzyme A desaturase 2
1449686_s_at	Scp2	sterol carrier protein 2, liver

1429446_at	Sdccag1	serologically defined colon cancer antigen 1
1456120_at	Secisbp2l	SECIS binding protein 2-like
1450642_at	Secisbp2l	SECIS binding protein 2-like
1448110_at	Sema4a	sema domain, immunoglobulin domain (Ig), transmembrane domain (TM) and short cytoplasmic domain, (semaphorin) 4A
1449202_at	Sema4g	sema domain, immunoglobulin domain (Ig), transmembrane domain (TM) and short cytoplasmic domain, (semaphorin) 4G
1448903_at	Sep15	selenoprotein
1449040_a_at	Sephs2	selenophosphate synthetase 2
1420010_at	Serinc4	serine incorporator 4
1455546_s_at	Sf3a2	splicing factor 3a, subunit 2
1418639_at	Sftpc	surfactant associated protein C
1417560_at	Sfxn1	sideroflexin 1
1415892_at	Sgpl1	sphingosine phosphate lyase 1
1457867_at	Sgpp2	sphingosine-1-phosphate phosphotase 2
1417600_at	Slc15a2	solute carrier family 15 (H+/peptide transporter), member 2
1424730_a_at	Slc15a2	solute carrier family 15 (H+/peptide transporter), member 2
1416854_at	Slc34a2	solute carrier family 34 (sodium phosphate), member 2
1416949_s_at	Slc39a7	solute carrier family 39 (zinc transporter), member 7
1416832_at	Slc39a8	solute carrier family 39 (metal ion transporter), member 8
1460565_at	Slc41a1	solute carrier family 41, member 1
1435008_at	Slc9a6	solute carrier family 9 (sodium/hydrogen exchanger), member 6
1425108_a_at	Smagp	small cell adhesion glycoprotein
1424760_a_at	Smyd2	SET and MYND domain containing 2
1433674_a_at	Snhg1	small nucleolar RNA host gene (non-protein coding) 1
1436040_at	Snhg12	small nucleolar RNA host gene 12
1417695_a_at	Soat1	sterol O-acyltransferase 1
1417696_at	Soat1	sterol O-acyltransferase 1
1423215_at	Spcs2	signal peptidase complex subunit 2 homolog (S. cerevisiae)
1460243_at	Sptlc2	serine palmitoyltransferase, long chain base subunit 2
1435937_at	Sptlc2	serine palmitoyltransferase, long chain base subunit 2
1427902_at	Srrm2	serine/arginine repetitive matrix 2
1439095_at	Srsf11	serine/arginine-rich splicing factor 11

1427333_s_at	Srsf15	serine/arginine-rich splicing factor 15
1452616_s_at	Ssbp1	single-stranded DNA binding protein 1
1420928_at	St6gal1	beta galactoside alpha 2,6 sialyltransferase 1
1418075_at	St6galnac4	ST6 (alpha-N-acetyl-neuraminyl-2,3-beta-galactosyl-1,3)-N-acetylgalactosaminide alpha-2,6-sialyltransferase 4
1460700_at	Stat3	signal transducer and activator of transcription 3
1428917_at	Stx17	syntaxin 17
1415891_at	Suclg1	succinate-CoA ligase, GDP-forming, alpha subunit
1427896_at	Suds3	suppressor of defective silencing 3 homolog (S. cerevisiae)
1424604_s_at	Sumf1	sulfatase modifying factor 1
1422457_s_at	Sumo3	SMT3 suppressor of mif two 3 homolog 3 (yeast)
1424255_at	Supt5h	suppressor of Ty 5 homolog (S. cerevisiae)
1441927_at	Syt7	synaptotagmin VII
1440819_s_at	Szt2	seizure threshold 2
1434238_at	Taf2	TAF2 RNA polymerase II, TATA box binding protein (TBP)-associated factor
1455733_at	Taok3	TAO kinase 3
1420196_s_at	Tbc1d14	TBC1 domain family, member 14
1449772_at	Tbc1d14	TBC1 domain family, member 14
1416060_at	Tbc1d15	TBC1 domain family, member 15
1426644_at	Tbc1d20	TBC1 domain family, member 20
1434224_at	Tbl2	transducin (beta)-like 2
1451838_a_at	Tc2n	tandem C2 domains, nuclear
1439045_x_at	Tc2n	tandem C2 domains, nuclear
1437463_x_at	Tgfbi	transforming growth factor, beta induced
1428521_at	Thap3	THAP domain containing, apoptosis associated protein 3
1448517_at	Timm22	translocase of inner mitochondrial membrane 22 homolog (yeast)
1439454_x_at	Tm2d2	TM2 domain containing 2
1424707_at	Tmed10	transmembrane emp24-like trafficking protein 10 (yeast)
1427314_at	Tmed7	transmembrane emp24 protein transport domain containing 7
1426436_at	Tmem159	transmembrane protein 159
1451133_s_at	Tmem168	transmembrane protein 168
1453480_at	Tmem213	transmembrane protein 213
1417611_at	Tmem37	transmembrane protein 37
1421127_at	Tmem42	transmembrane protein 42
1424042_at	Tmem5	transmembrane protein 5
1418124_at	Tmem85	transmembrane protein 85

1417866_at	Tnfaip1	tumor necrosis factor, alpha-induced protein 1 (endothelial)
1422924_at	Tnfsf9	tumor necrosis factor (ligand) superfamily, member 9
1435055_a_at	Tom1	target of myb1 homolog (chicken)
1417754_at	Topors	topoisomerase I binding, arginine/serine-rich
1436049_at	Tox4	TOX high mobility group box family member 4
1423602_at	Traf1	TNF receptor-associated factor 1
1416170_at	Trap1	TNF receptor-associated protein 1
1456225_x_at	Trib3	tribbles homolog 3 (Drosophila)
1424611_x_at	Trub2	TruB pseudouridine (psi) synthase homolog 2 (E. coli)
1424610_at	Trub2	TruB pseudouridine (psi) synthase homolog 2 (E. coli)
1416908_s_at	Tsn	translin
1430310_at	Tspan11	tetraspanin 11
1416484_at	Ttc3	tetratricopeptide repeat domain 3
1452782_a_at	Txn2	thioredoxin 2
1417202_s_at	Uba3	ubiquitin-like modifier activating enzyme 3
1426398_at	Ube2w	ubiquitin-conjugating enzyme E2W (putative)
1453097_a_at	Ubtf	upstream binding transcription factor, RNA polymerase I
1425020_at	Ubxn2a	UBX domain protein 2A
1450968_at	Uqcrfs1	ubiquinol-cytochrome c reductase, Rieske iron-sulfur polypeptide 1
1423817_s_at	Use1	unconventional SNARE in the ER 1 homolog (S. cerevisiae)
1455812_x_at	Vasn	vasorin
1452770_at	Vkorc1	vitamin K epoxide reductase complex, subunit 1
1430801_at	Vps13b	vacuolar protein sorting 13B (yeast)
1422634_a_at	Vsig2	V-set and immunoglobulin domain containing 2
1451754_a_at	Wdr45	WD repeat domain 45
1459985_at	Wdr61	WD repeat domain 61
1423923_a_at	Wdr8	WD repeat domain 8
1438709_at	Wipi1	WD repeat domain, phosphoinositide interacting 1
1433676_at	Wnk1	WNK lysine deficient protein kinase 1
1427196_at	Wnk4	WNK lysine deficient protein kinase 4
1417437_at	Xrcc6	X-ray repair complementing defective repair in Chinese hamster cells 6
1424196_at	Yipf1	Yip1 domain family, member 1
1420668_a_at	Yipf2	Yip1 domain family, member 2
1434277_a_at	Ypel2	yippee-like 2 (Drosophila)
1435824_at	Yy1	YY1 transcription factor
1438443_at	Zbtb20	zinc finger and BTB domain containing 20

1452084_at	Zcchc17	zinc finger, CCHC domain containing 17
1423646_at	Zdhhc3	zinc finger, DHHC domain containing 3
1436081_a_at	Zfp414	zinc finger protein 414
1447775_x_at	Zfp622	zinc finger protein 622
1436537_at	Zfp629	zinc finger protein 629
1417849_at	Zfp704	zinc finger protein 704
1434682_at	Zfp770	zinc finger protein 770
1453140_at	Zfp871	zinc finger protein 871

Table A7: Genes Down in shTaz Cells

F.p.value	Name	CK1750 shGFP	CK1750 shTaz	SC241 shGFP	SC241 shTaz	Tmet shGFP	Tmet shTaz
0.03788	Wwtr1	8.73	8.02	8.06	6.92	8.28	6.08
0.01116	Zfp442	5.29	4.88	6.06	4.99	6.24	4.66
0.03684	BC003266	6.09	5.30	6.48	6.08	6.45	4.70
0.01137	Rps6ka2	7.56	6.97	8.20	7.32	7.97	6.54
0.00139	Scara3	8.69	7.97	9.01	7.66	8.76	8.01
0.02016	Ltbp4	6.96	6.37	7.38	6.40	6.71	5.71
0.0464	Mrm1	4.00	3.55	4.97	4.06	5.13	3.95
0.0021	Snord111	3.13	2.52	3.57	2.60	3.40	2.50
0.00561	Mbnl2 // Mbnl2	5.35	5.00	5.62	4.75	5.88	4.71
0.04965	Abcd4	5.71	5.28	6.17	5.59	5.81	4.48
0.04085	Aldh7a1	7.45	7.47	7.88	6.88	7.76	6.41
0.017	Kctd5	7.31	6.70	7.56	7.04	7.39	6.26
0.01783	Rpl37	4.42	3.93	4.80	4.28	4.83	3.59
0.04609	Mapk12	5.55	5.57	6.25	5.48	6.47	5.04
0.04859	D17Wsu104e	5.93	5.84	6.48	5.92	6.68	5.19
0.01877	Nudt21	8.53	8.29	8.77	8.21	9.10	7.81
0.04542	Agpat4	4.89	4.76	4.80	4.32	5.40	3.95
0.04748	Sgsh	6.26	6.26	6.30	5.41	6.67	5.50
0.04068	Ero1l // Ero1l	5.88	5.93	6.58	5.41	6.20	5.29
0.03014	Tanc1	6.65	6.58	6.91	6.14	6.94	5.78
0.01177	Trim62	3.62	3.09	3.89	3.11	3.44	2.76
0.04005	Gm8894	7.87	7.05	8.09	7.69	8.44	7.68
0.03504	Hgsnat	7.34	7.12	7.23	6.76	7.59	6.33
0.02248	Irak4	6.32	5.60	6.12	5.90	6.19	5.18
0.04403	Rxrb	6.15	5.52	6.28	6.03	6.16	5.09
0.01623	S100a13	7.05	6.06	6.79	6.43	7.14	6.57
0.03185	Rps5 // Rps5	8.08	7.96	8.61	7.85	8.87	7.86
0.03451	Farsa	7.68	7.27	7.54	7.22	8.32	7.15
0.01561	Madd	5.77	5.31	6.03	5.61	6.12	5.13
0.03882	Mrpl38	8.93	8.65	9.26	8.81	9.21	8.08
0.02796	Fzd4	5.32	4.75	5.50	5.13	5.33	4.41
0.04361	Slc35c2	7.02	6.64	6.88	6.66	7.14	5.93
0.04353	Klk1b26	3.00	2.27	3.44	3.01	3.22	2.57
0.04365	Clcn3	5.73	5.53	5.65	5.28	6.02	4.80
0.03656	Fbxw4	6.05	5.83	6.48	5.81	6.14	5.28
0.03817	Rps7	6.65	6.36	6.63	6.39	7.14	5.92

0.04879	Zscan21	5.16	4.82	5.00	4.64	5.05	4.01
0.03277	Tmem38a	5.40	5.02	5.38	5.05	6.02	4.99
0.04888	Telo2	5.44	5.08	5.81	5.52	6.02	4.95
0.01691	E4f1	5.42	5.17	5.73	4.81	5.40	4.84
0.02097	Snord66	4.81	4.63	4.93	4.08	4.89	4.23
0.02038	Fbxl4	5.07	4.47	5.29	4.82	4.98	4.38
0.03229	Rap2c	6.96	6.45	6.97	6.82	7.37	6.36
0.02385	Shroom4	5.62	5.53	5.98	5.30	6.05	5.16
0.0457	Mir1249	3.07	2.84	3.76	2.93	3.23	2.65
0.02639	Olfr1337	3.94	3.35	4.27	3.70	3.84	3.38
0.02649	Kcnk9	3.54	2.79	3.61	2.95	3.58	3.36
0.0202	Flt4	4.02	3.41	3.97	3.58	4.32	3.75
0.02806	Ywhag // Ywhag	6.90	6.45	6.98	6.67	6.92	6.10
0.03018	Gm5124	4.02	3.62	3.93	3.16	4.07	3.69
0.01981	Hcrtr1	3.55	3.18	3.88	3.42	3.87	3.16
0.04182	Sys1 // Sys1	4.27	3.70	4.44	3.75	3.83	3.57
0.02145	Wdr4	4.79	4.52	5.04	4.61	5.03	4.26
0.04116	Fbxo44	4.12	3.50	4.10	3.82	3.84	3.28
0.03681	Gm19316	6.04	5.64	5.91	5.60	6.47	5.72
0.02812	Phb	4.72	4.23	4.81	4.60	4.92	4.17
0.01787	Cyp4a10	2.58	2.20	2.67	2.36	2.79	2.04
0.01648	Mir5102 // Mir5102	5.19	4.64	5.14	4.90	5.38	4.74
0.04247	Fdxr	4.22	4.15	4.77	3.93	4.47	3.96
0.03302	Timm8a1	5.52	4.73	5.45	5.22	5.39	5.03
0.02533	Igfbp2	4.21	3.88	4.24	3.95	4.29	3.59
0.02112	Tnfrsf10b	7.61	7.27	7.50	7.13	7.80	7.19
0.03774	Cdk6	8.65	8.40	8.56	8.32	8.94	8.13
0.02075	Piga	4.77	4.40	4.89	4.49	4.74	4.22
0.0452	Gm13558	2.70	2.13	2.67	2.08	2.25	2.15
0.04835	Zdhhc21	6.04	5.41	6.06	5.88	5.95	5.53
0.03407	Mir684-1	5.77	5.53	6.01	5.55	6.12	5.62
0.03718	Fam96b	5.72	5.55	6.05	5.56	5.91	5.41
0.0396	Kif1a	3.36	2.92	3.22	2.85	3.05	2.69
0.04105	Bbs10	3.98	3.56	4.20	3.89	4.16	3.72
0.04815	Hoga1	4.27	3.74	4.39	4.16	4.39	3.98
0.04988	Asph	6.62	6.05	6.28	6.20	6.41	5.90
0.0441	Zbtb6	5.76	5.34	5.91	5.61	6.02	5.60
0.04751	LOC100504825	5.12	4.94	5.09	4.76	5.42	4.80
0.02345	Spats2	7.44	7.03	7.56	7.19	7.50	7.15
0.04856	Sowahc	5.92	5.49	5.71	5.55	6.11	5.58

0.03853	Opn4	4.02	3.89	4.26	3.78	4.19	3.69
0.04701	Cntnap5b	2.45	2.35	2.79	2.26	2.74	2.28
0.03746	Wdr36	8.47	8.23	8.38	7.96	8.43	7.99
0.049	Atp13a2	5.72	5.44	5.62	5.41	5.72	5.11
0.04178	Fzd5	6.31	5.97	6.32	6.15	6.45	5.86
0.04749	Mtmr9	8.22	7.92	8.28	8.10	8.46	7.86
0.04929	Lrrc10	4.11	3.91	4.46	3.98	4.29	3.91
0.03425	Igkv1-133	2.14	1.87	2.25	1.89	2.38	1.94
0.04982	Chsy1 // Chsy1	4.89	4.52	4.90	4.70	5.10	4.66
0.03873	Il17a	3.26	2.94	3.18	2.88	3.29	2.96
0.04701	DXBay18	3.68	4.01	3.75	3.98	3.72	4.04
0.04649	DXBay18	2.89	3.27	2.89	3.17	2.93	3.17
0.03987	Xlr5b	2.17	2.53	2.27	2.52	2.18	2.50
0.04519	Olfr1358	2.52	2.77	2.45	2.69	2.39	2.86
0.04631	Rasgrp4	2.16	2.53	2.14	2.45	2.30	2.59
0.03346	Gpr158	2.33	2.67	2.28	2.56	2.26	2.62
0.04079	Opn5	2.31	2.66	2.47	2.69	2.37	2.79
0.0479	Rcsd1	2.06	2.26	2.11	2.40	1.89	2.41
0.04099	Otos	3.34	3.69	3.45	3.62	3.23	3.73
0.0382	Beta-s // Hbb-b2 // Hbb-b1	1.93	2.35	1.94	2.13	1.83	2.24
0.04229	Grin3a	2.60	2.94	2.64	2.90	2.70	3.16
0.04698	Krt6b	2.85	3.14	2.97	3.21	2.90	3.44
0.04863	Zfp354b	1.85	2.29	2.14	2.28	1.99	2.46
0.03856	Pdzd4	3.70	4.07	3.50	3.87	3.61	3.95
0.03549	Adam26a	1.73	2.12	1.86	2.07	1.82	2.28
0.03241	Rcsd1	3.92	4.19	4.00	4.39	3.97	4.38
0.03367	Cd4	2.58	3.03	2.81	3.15	2.70	3.01
0.04312	Gm13871	3.23	3.36	3.00	3.40	3.02	3.59
0.04545	Hsf4	4.48	4.88	4.78	4.96	4.57	5.08
0.04192	Barx2	2.99	3.59	3.31	3.56	3.22	3.48
0.03751	Sds // Sds	2.37	2.77	2.53	2.79	2.55	3.00
0.03434	Atp1b2	2.88	3.41	2.94	3.12	2.91	3.32
0.0395	Ms4a10	3.57	3.79	3.66	3.97	3.37	3.96
0.02482	Olfr466	2.12	2.55	2.26	2.46	2.14	2.64
0.04009	Olfr919	2.27	2.78	2.48	2.80	2.61	2.94
0.04883	Slc44a5	2.06	2.63	2.38	2.41	2.11	2.67
0.04536	LOC100861890	2.54	2.94	2.81	3.13	2.79	3.24
0.04037	Pstpip2 // Pstpip2	2.43	2.90	2.49	2.87	2.74	3.07
0.01649	Rpe65	2.12	2.50	2.04	2.50	2.14	2.48

0.03319	B4galt4	4.34	4.84	4.25	4.81	4.53	4.65
0.04148	Gm8777	2.02	2.42	2.32	2.58	2.18	2.69
0.01992	BC106175	3.20	3.64	3.19	3.47	3.15	3.62
0.03683	Mir5100	3.75	3.93	3.79	4.17	3.57	4.21
0.03143	Vmn1r234	2.37	2.65	2.53	2.90	2.38	2.93
0.03637	Mettl7a3	2.17	2.48	2.31	2.84	2.26	2.62
0.03003	Gm12108	3.41	3.63	3.44	3.79	3.19	3.83
0.0457	Ugt2b1	2.54	2.79	2.30	2.67	2.10	2.70
0.02516	Gm6362	2.10	2.68	2.34	2.70	2.36	2.62
0.02561	Vmn1r24	2.06	2.59	2.14	2.37	2.17	2.64
0.01934	Klrb1c	1.99	2.44	2.06	2.55	2.20	2.48
0.0303	Tmem217	2.37	2.82	2.37	2.98	2.65	2.83
0.03951	Gm20599	2.26	2.76	2.59	2.70	2.18	2.79
0.04715	AY358078	4.68	4.91	4.35	4.74	4.49	5.11
0.04732	Olfr119	1.98	2.29	2.06	2.26	1.97	2.70
0.03487	Ighg	4.33	4.57	4.20	4.51	3.93	4.63
0.01568	Adcy4	3.09	3.61	3.23	3.58	3.09	3.49
0.02543	Ucp3	3.18	3.35	3.06	3.58	3.10	3.67
0.03939	Oas1f	2.13	2.66	2.38	2.58	2.39	2.94
0.04261	Unc93a	3.58	3.75	3.53	3.90	3.48	4.23
0.04552	Psmb11	2.74	2.95	2.67	2.95	2.58	3.39
0.03074	Tmem215	2.80	3.15	2.75	3.08	2.84	3.47
0.03036	Mcpt9	2.20	2.54	2.29	2.67	2.35	2.94
0.03059	Gsdmd // Gsdmd	3.67	4.38	3.88	4.22	4.08	4.36
0.03305	Gm5576	3.33	3.53	3.05	3.47	2.90	3.60
0.02832	Vmn1r72	2.06	2.35	1.90	2.23	1.89	2.60
0.04367	Gm5329	2.99	3.55	2.74	3.44	3.05	3.13
0.03192	Arhgef6	1.92	2.25	1.98	2.35	2.04	2.68
0.04234	Mir3098 // Mir3098	2.13	2.53	2.18	2.83	2.53	2.82
0.02413	Olfr448	1.72	2.23	1.95	2.21	1.92	2.51
0.02239	Gm3591	2.64	3.02	2.64	3.06	2.78	3.36
0.02201	Slc29a3	3.88	4.23	3.84	4.11	3.68	4.44
0.02496	Kcnj16	2.67	3.00	2.71	3.04	2.66	3.39
0.01173	Lypd6	3.29	3.75	3.45	3.76	3.22	3.86
0.01412	Gm15688	3.07	3.71	3.01	3.44	3.13	3.48
0.01605	Mir1905	3.78	4.16	3.89	4.21	3.71	4.44
0.03432	Ccdc62	3.00	3.37	2.85	3.08	2.71	3.54
0.04842	Pomc	2.59	3.20	2.64	3.46	2.99	2.99
0.01666	Vmn1r78	1.90	2.59	1.86	2.28	2.00	2.32
0.03009	Gm6531	2.93	3.28	3.01	3.39	3.05	3.77
0.02956	Mir713	2.66	3.36	3.04	3.26	3.01	3.57
0.03385	Gm10139	4.85	5.20	4.88	5.10	4.71	5.61

	// Gm10139						
0.02289	Olfr429	2.43	2.81	2.30	2.58	2.07	2.90
0.03084	Gm5325	6.36	6.92	6.35	6.53	6.32	7.08
0.01736	Epha5	2.88	3.10	2.80	3.36	2.76	3.49
0.04574	Gckr	2.53	2.89	2.73	2.96	2.58	3.49
0.02395	Snhg11	3.34	3.59	2.84	3.65	3.16	3.60
0.02956	Ighg	2.62	3.40	2.55	2.97	2.88	3.20
0.04761	Lce1a2	3.14	3.81	3.22	3.52	3.53	4.10
0.03797	Gm10166	4.79	5.26	4.60	4.93	4.25	5.00
0.0497	Isg15	3.59	4.19	3.26	3.57	3.38	4.03
0.02733	Gm4559	3.96	4.31	4.15	4.75	3.82	4.42
0.04153	Oca2	2.82	3.30	2.82	3.03	2.84	3.71
0.04818	Xpnpep2	3.68	3.90	3.90	4.33	3.33	4.24
0.03085	Olfr113	2.64	3.02	2.90	3.42	2.46	3.13
0.0424	Mycs	2.74	3.04	2.69	3.22	2.93	3.68
0.04904	Yy2	5.65	5.89	5.23	5.63	5.31	6.24
0.04738	Gm5751	2.36	3.03	1.98	2.45	2.07	2.52
0.03643	AU021034	3.97	4.48	3.89	4.21	4.09	4.84
0.03953	Gm10125	3.60	4.21	3.23	3.63	3.34	3.93
0.01267	Zfp352	2.69	3.33	2.86	3.08	2.69	3.44
0.04138	Acnat1	2.60	2.87	2.75	3.10	2.56	3.54
0.04336	Ipo4	3.75	4.28	3.35	3.93	3.89	4.41
0.02641	Dkk1	3.41	3.63	3.49	3.94	3.10	4.06
0.03129	Rab4a	3.70	4.09	3.51	3.79	3.42	4.39
0.04716	Gm6337	2.26	2.56	2.57	3.19	2.45	3.17
0.01189	Ggt5	2.55	2.88	2.51	3.00	2.44	3.27
0.03251	Vmn2r5	2.26	2.48	2.08	2.65	2.24	3.10
0.03376	Gm10827	3.57	3.90	3.54	3.96	3.62	4.53
0.00967	Slc22a2	3.14	4.01	3.37	3.80	3.42	3.79
0.04602	Gm4701	2.21	3.11	2.66	2.76	2.68	3.35
0.03724	Npm1	5.78	6.17	5.39	6.00	5.84	6.54
0.02261	Tnfaip8l3	3.36	3.67	3.31	3.85	3.39	4.25
0.02687	Mir1960	2.80	3.23	2.89	3.30	2.94	3.82
0.04059	Mir212	4.16	4.79	3.63	4.27	4.09	4.54
0.03401	Cox6a2	3.33	4.16	3.56	3.57	3.23	4.12
0.02923	Exoc7	2.14	2.60	2.08	2.46	2.20	3.12
0.04435	Fbxw28	2.07	2.49	1.82	2.22	2.05	2.99
0.02517	Ffar1	3.19	3.44	2.96	3.45	2.96	3.98
0.01448	Atp5j2	3.10	3.57	3.15	3.46	2.69	3.70
0.03415	Setbp1	5.47	6.38	5.36	5.87	5.90	6.28
0.01045	Sh3rf3	2.78	3.38	2.59	3.08	2.78	3.50
0.04049	Zp3	3.38	3.59	3.20	3.66	3.19	4.33
0.01514	Mir669h // Mir669h	2.43	2.63	2.09	3.06	2.12	2.78

0.02798	Foxb1	3.42	3.45	3.09	3.87	2.95	3.98
0.01765	Timm8a2	4.75	5.17	4.40	4.95	4.58	5.46
0.00463	Gvin1 // Gvin1	3.50	4.33	3.68	4.09	3.66	4.27
0.0259	Islr	3.20	3.61	3.50	4.23	3.12	3.86
0.02854	Rnase11	2.30	3.11	2.59	2.73	2.52	3.44
0.01203	Tmem90a	3.51	4.28	3.56	3.91	3.21	3.96
0.0345	Zcchc7	6.58	6.99	6.14	6.54	6.04	7.13
0.03878	Tpsab1	2.27	2.83	2.56	3.48	2.28	2.71
0.01755	Svop	3.31	3.67	3.55	4.12	3.16	4.14
0.04184	Galr3	3.50	3.54	3.23	4.28	3.48	4.30
0.02265	Mir669m-1 // Mir669m-1	4.40	5.22	4.65	4.73	4.24	5.28
0.01503	Gm10503 // Gm10503	3.13	3.93	3.33	3.56	3.23	4.19
0.04265	Gm6613	3.27	3.48	3.10	3.88	3.39	4.40
0.02625	F2rl3	2.99	4.15	3.59	3.90	3.67	4.19
0.03744	Tgtp2 // Tgtp1	2.21	2.91	2.39	2.62	2.43	3.51
0.00377	Vmn2r41 // Vmn2r40	3.08	3.69	2.93	3.78	3.28	3.84
0.02935	Olfr488	1.95	2.53	1.70	2.06	1.80	2.90
0.04933	Aph1c	4.19	4.19	3.52	4.88	4.13	4.82
0.00662	Gm19451	3.79	4.61	4.08	4.39	3.86	4.81
0.02197	Figf	3.82	4.77	4.02	4.17	3.45	4.48
0.02823	Phf11	3.86	4.11	3.12	3.89	3.04	4.28
0.01408	Apol7e	2.21	3.17	2.14	2.61	2.42	3.34
0.02622	Ppnr	5.17	5.68	4.43	5.27	4.92	5.97
0.0099	Gm609 // Gm609	1.96	2.78	2.23	2.95	2.45	3.38
0.03977	Fcrl1	2.82	3.20	3.22	4.34	2.88	3.86
0.01712	Stk39	5.28	6.23	5.22	5.48	4.80	6.19
0.01341	Sgk3	4.72	4.88	3.98	5.18	4.01	5.30
0.04852	Gm17783	2.62	3.07	2.81	3.62	2.99	4.50
0.02882	Olfr310	4.11	4.35	3.18	4.66	3.49	6.01
0.00136	Gfra2	4.08	5.90	3.86	5.22	3.81	5.02

Table A8: GSEA in shGFP vs shTaz Cells

NAME	SIZE	ES	NES	NOM p-val	FDR q-val
MITOCHONDRION	315	-0.58	-2.48	0.00	0.00
MITOCHONDRIAL_PART	137	-0.61	-2.41	0.00	0.00
MITOCHONDRIAL_ENVELOPE	93	-0.65	-2.37	0.00	0.00
MITOCHONDRIAL_MEMBRANE_PART	50	-0.71	-2.36	0.00	0.00
MITOCHONDRIAL_INNER_MEMBRANE	63	-0.67	-2.34	0.00	0.00
ORGANELLE_INNER_MEMBRANE	71	-0.65	-2.31	0.00	0.00
MITOCHONDRIAL_MEMBRANE	82	-0.64	-2.31	0.00	0.00
ENVELOPE	164	-0.58	-2.31	0.00	0.00
ORGANELLE_ENVELOPE	164	-0.58	-2.30	0.00	0.00
ORGANELLE_MEMBRANE	289	-0.54	-2.29	0.00	0.00
LIGASE_ACTIVITY	93	-0.59	-2.19	0.00	0.00
INTRACELLULAR_TRANSPORT	268	-0.52	-2.19	0.00	0.00
MITOCHONDRION_ORGANIZATION_AND_BIOGENESIS	44	-0.68	-2.18	0.00	0.00
BIOSYNTHETIC_PROCESS	445	-0.50	-2.17	0.00	0.00
CELLULAR_BIOSYNTHETIC_PROCESS	304	-0.51	-2.16	0.00	0.00
HELICASE_ACTIVITY	50	-0.63	-2.13	0.00	0.00
ENDOMEMBRANE_SYSTEM	214	-0.52	-2.13	0.00	0.00
ENDOPLASMIC_RETICULUM	271	-0.51	-2.14	0.00	0.00
NUCLEOBASENUCLEOSIDE_AND_NUCLEOTIDE_METABOLIC_PROCESS	48	-0.63	-2.10	0.00	0.00
RESPONSE_TO_OXIDATIVE_STRESS	44	-0.64	-2.11	0.00	0.00
ATP_DEPENDENT_HELICASE_ACTIVITY	26	-0.72	-2.12	0.00	0.00
GOLGI_APPARATUS	213	-0.51	-2.12	0.00	0.00
RNA_PROCESSING	164	-0.51	-2.05	0.00	0.00
GOLGI_APPARATUS_PART	96	-0.55	-2.04	0.00	0.00
ORGANIC_ACID_METABOLIC_PROCESS	166	-0.51	-2.05	0.00	0.00
TRANSLATION	173	-0.50	-2.03	0.00	0.00
RNA_BINDING	245	-0.49	-2.03	0.00	0.00
ELECTRON_CARRIER_ACTIVITY	70	-0.57	-2.02	0.00	0.00
CARBOXYLIC_ACID_METABOLIC_PROCESS	164	-0.51	-2.02	0.00	0.00
NUCLEOSIDE_TRIPHOSPHATASE_ACTIVITY	198	-0.49	-2.01	0.00	0.00
CELLULAR_LOCALIZATION	352	-0.47	-2.01	0.00	0.00

VESICLE_MEMBRANE	30	-0.66	-2.01	0.00	0.00
ESTABLISHMENT_OF_CELLULAR_LOCALIZATION	334	-0.47	-2.01	0.00	0.00
LIGASE_ACTIVITY_FORMING_CARBON_NITROGEN_BONDS	65	-0.57	-2.01	0.00	0.00
NUCLEOLUS	110	-0.53	-2.00	0.00	0.00
NUCLEOTIDE_METABOLIC_PROCESS	38	-0.62	-2.00	0.00	0.00
PROTEASOME_COMPLEX	22	-0.70	-1.98	0.00	0.00
RRNA_METABOLIC_PROCESS	16	-0.76	-1.98	0.00	0.00
MITOCHONDRIAL_RESPIRATORY_CHAIN	23	-0.69	-1.98	0.00	0.00
AMINO_ACID_AND_DERIVATIVE_METABOLIC_PROCESS	98	-0.53	-1.97	0.00	0.00
PYROPHOSPHATASE_ACTIVITY	211	-0.48	-1.96	0.00	0.00
PROTEIN_FOLDING	53	-0.59	-1.97	0.00	0.00
ORGANELLE_ORGANIZATION_AND_BIOGENESIS	449	-0.45	-1.96	0.00	0.00
CELLULAR_CATABOLIC_PROCESS	196	-0.48	-1.97	0.00	0.00
TRANSLATION_FACTOR_ACTIVITY_NUCLEIC_ACID_BINDING	36	-0.62	-1.96	0.00	0.00
PROTON_TRANSPORTING_TWO_SECTOR_ATPASE_COMPLEX	15	-0.76	-1.96	0.00	0.00
NUCLEOBASENUCLEOSIDENUCLEOTIDE_KINASE_ACTIVITY	25	-0.67	-1.96	0.00	0.00
CYTOPLASMIC_VESICLE_PART	28	-0.65	-1.94	0.00	0.00
CYTOPLASMIC_VESICLE_MEMBRANE	28	-0.65	-1.94	0.00	0.00
HYDROLASE_ACTIVITY_ACTING_ON_ACID_ANHYDRIDES	213	-0.47	-1.94	0.00	0.00
MEMBRANE_ENCLOSED_LUMEN	427	-0.45	-1.94	0.00	0.00
ALCOHOL_METABOLIC_PROCESS	81	-0.53	-1.93	0.00	0.00
ORGANELLE_LUMEN	427	-0.45	-1.93	0.00	0.00
RRNA_PROCESSING	15	-0.77	-1.93	0.00	0.00
MEMBRANE_COAT	17	-0.71	-1.92	0.00	0.00
AMINO_ACID_METABOLIC_PROCESS	77	-0.53	-1.93	0.00	0.00
CATABOLIC_PROCESS	206	-0.47	-1.93	0.00	0.00
ATP_DEPENDENT_RNA_HELICASE_ACTIVITY	16	-0.73	-1.92	0.00	0.00
LIPID_BIOSYNTHETIC_PROCESS	92	-0.52	-1.92	0.00	0.00
MACROMOLECULE_BIOSYNTHETIC_PROCESS	308	-0.45	-1.92	0.00	0.00

RIBONUCLEOPROTEIN_COMPLEX_BIOGENESIS_AND_ASSEMBLY	83	-0.52	-1.91	0.00	0.00
STRUCTURAL_CONSTITUENT_OF_RIBOSOME	78	-0.54	-1.91	0.00	0.00
NITROGEN_COMPOUND_BIOSYNTHETIC_PROCESS	23	-0.67	-1.91	0.00	0.00
TRANSLATION_INITIATION_FACTOR_ACTIVITY	23	-0.68	-1.91	0.00	0.00
GTPASE_ACTIVITY	88	-0.52	-1.90	0.00	0.00
CYTOSOL	190	-0.47	-1.91	0.00	0.00
CELLULAR_RESPONSE_TO_STIMULUS	18	-0.71	-1.91	0.00	0.00
PROTEIN_TRANSPORT	152	-0.48	-1.90	0.00	0.00
NITROGEN_COMPOUND_METABOLIC_PROCESS	149	-0.48	-1.90	0.00	0.00
RNA_HELICASE_ACTIVITY	23	-0.67	-1.90	0.00	0.00
NUCLEOTIDE_BIOSYNTHETIC_PROCESS	16	-0.73	-1.90	0.00	0.00
MACROMOLECULE_LOCALIZATION	221	-0.46	-1.89	0.00	0.00
NUCLEAR_MEMBRANE_PART	42	-0.58	-1.89	0.00	0.00
INTRACELLULAR_PROTEIN_TRANSPORT	141	-0.48	-1.89	0.00	0.00
COATED_MEMBRANE	17	-0.71	-1.89	0.00	0.00
LIPID_METABOLIC_PROCESS	284	-0.45	-1.89	0.00	0.00
PROTEIN_COMPLEX_ASSEMBLY	156	-0.47	-1.89	0.00	0.00
VESICLE_MEDIATED_TRANSPORT	180	-0.47	-1.89	0.00	0.00
RNA_DEPENDENT_ATPASE_ACTIVITY	17	-0.70	-1.88	0.00	0.00
COATED_VESICLE_MEMBRANE	17	-0.69	-1.88	0.00	0.00
MACROMOLECULAR_COMPLEX_ASSEMBLY	265	-0.45	-1.88	0.00	0.00
CELLULAR_COMPONENT_ASSEMBLY	283	-0.44	-1.87	0.00	0.00
PHOSPHOLIPID_BIOSYNTHETIC_PROCESS	37	-0.60	-1.87	0.00	0.00
NUCLEAR_ENVELOPE_ENDOPLASMIC_RETICULUM_NETWORK	90	-0.51	-1.87	0.00	0.00
ENDOPLASMIC_RETICULUM_PART	91	-0.50	-1.87	0.00	0.00
TRANSLATION_REGULATOR_ACTIVITY	37	-0.58	-1.87	0.00	0.00
CELLULAR_LIPID_METABOLIC_PROCESS	224	-0.45	-1.87	0.00	0.00

RNA_EXPORT_FROM_NUCLEUS	18	-0.70	-1.87	0.00	0.00
MEMBRANE_LIPID_BIOSYNTHETIC_PROCESS	45	-0.58	-1.87	0.00	0.00
NUCLEAR_LUMEN	360	-0.44	-1.86	0.00	0.00
APOPTOTIC_NUCLEAR_CHANGES	19	-0.68	-1.85	0.00	0.00
MITOCHONDRIAL_TRANSPORT	19	-0.69	-1.86	0.00	0.00
VITAMIN_METABOLIC_PROCESS	17	-0.70	-1.85	0.00	0.00
ESTABLISHMENT_OF_PROTEIN_LOCALIZATION	180	-0.46	-1.86	0.00	0.00
HYDROLASE_ACTIVITY_HYDROLYZING_O_GLYCOSYL_COMPOUNDS	32	-0.61	-1.85	0.00	0.00
UNFOLDED_PROTEIN_BINDING	41	-0.58	-1.86	0.00	0.00
OXIDOREDUCTASE_ACTIVITY	255	-0.45	-1.86	0.00	0.00
HYDROLASE_ACTIVITY_ACTING_ON_GLYCOSYL_BONDS	41	-0.58	-1.85	0.00	0.00
PROTEIN_LOCALIZATION	202	-0.45	-1.85	0.00	0.00
REGULATION_OF_I_KAPPAB_KINASE_NF_KAPPAB_CASCADE	88	-0.50	-1.85	0.00	0.00
GOLGI_MEMBRANE	44	-0.56	-1.85	0.00	0.00
COATED_VESICLE	45	-0.56	-1.84	0.00	0.00
CARBOHYDRATE_METABOLIC_PROCESS	168	-0.46	-1.85	0.00	0.00
VESICLE_COAT	16	-0.72	-1.84	0.00	0.00
ENZYME_BINDING	169	-0.46	-1.84	0.00	0.01
RIBONUCLEOPROTEIN_COMPLEX	139	-0.47	-1.84	0.00	0.01
PROTEIN_TARGETING	107	-0.48	-1.84	0.00	0.01
GLYCEROPHOSPHOLIPID_BIOSYNTHETIC_PROCESS	28	-0.62	-1.84	0.00	0.01
NUCLEOBASENUCLEOSIDENUCLEOTIDE_AND_NUCLEIC_ACID_TRANSPORT	29	-0.60	-1.84	0.00	0.01
CARBON_CARBON_LYASE_ACTIVITY	17	-0.69	-1.83	0.00	0.01
ENDOPLASMIC_RETICULUM_MEMBRANE	81	-0.51	-1.83	0.00	0.01
GOLGI_VESICLE_TRANSPORT	48	-0.55	-1.83	0.00	0.01
POSITIVE_REGULATION_OF_I_KAPPAB_KINASE_NF_KAPPAB_CASCADE	83	-0.50	-1.83	0.00	0.01
CELLULAR_CARBOHYDRATE_METABOLIC_PROCESS	120	-0.47	-1.82	0.00	0.01
CYTOPLASM_ORGANIZATION_A	15	-0.71	-1.82	0.00	0.01

ND_BIOGENESIS					
PROGRAMMED_CELL_DEATH	402	-0.42	-1.82	0.00	0.01
POSITIVE_REGULATION_OF_TRANSPORT	22	-0.65	-1.81	0.00	0.01
ENERGY_DERIVATION_BY_OXIDATION_OF_ORGANIC_COMPOUNDS	36	-0.57	-1.81	0.00	0.01
REGULATION_OF_APOPTOSIS	319	-0.43	-1.81	0.00	0.01
DNA_METABOLIC_PROCESS	242	-0.43	-1.80	0.00	0.01
AROMATIC_COMPOUND_METABOLIC_PROCESS	25	-0.61	-1.80	0.00	0.01
APOPTOTIC_PROGRAM	57	-0.52	-1.80	0.00	0.01
ATPASE_ACTIVITY	109	-0.47	-1.79	0.00	0.01
RIBOSOME_BIOGENESIS_AND_ASSEMBLY	18	-0.67	-1.79	0.00	0.01
COFACTOR_BIOSYNTHETIC_PROCESS	21	-0.64	-1.79	0.00	0.01
FATTY_ACID_OXIDATION	16	-0.67	-1.79	0.01	0.01
REGULATION_OF_PROGRAMMED_CELL_DEATH	320	-0.42	-1.79	0.00	0.01
APOPTOSIS_GO	401	-0.42	-1.79	0.00	0.01
PHOSPHOTRANSFERASE_ACTIVITY_PHOSPHATE_GROUP_AS_ACCEPTOR	18	-0.68	-1.79	0.00	0.01
RUFFLE	31	-0.59	-1.79	0.00	0.01
NUCLEAR_PORE	31	-0.58	-1.79	0.00	0.01
I_KAPPAB_KINASE_NF_KAPPAB_CASCADE	107	-0.47	-1.79	0.00	0.01
ACTIN_CYTOSKELETON	115	-0.47	-1.78	0.00	0.01
NEGATIVE_REGULATION_OF_APOPTOSIS	143	-0.46	-1.78	0.00	0.01
ENZYME_INHIBITOR_ACTIVITY	108	-0.47	-1.78	0.00	0.01
ACID_AMINO_ACID_LIGASE_ACTIVITY	54	-0.52	-1.78	0.00	0.01
TRANSFERASE_ACTIVITY_TRANSFERRING_PHOSPHORUS_CONTAINING_GROUPS	410	-0.41	-1.77	0.00	0.01
DAMAGED_DNA_BINDING	20	-0.65	-1.77	0.00	0.01
NUCLEOTIDE_EXCISION_REPAIR	19	-0.65	-1.77	0.00	0.01
NEGATIVE_REGULATION_OF_PROGRAMMED_CELL_DEATH	144	-0.45	-1.77	0.00	0.01
KINASE_ACTIVITY	356	-0.41	-1.76	0.00	0.01
NUCLEAR_MEMBRANE	50	-0.53	-1.76	0.00	0.01
LIPOPROTEIN_METABOLIC_PRO	30	-0.58	-1.76	0.00	0.01

CESS					
MRNA_PROCESSING_GO_0006397	70	-0.50	-1.76	0.00	0.01
TRANSFERASE_ACTIVITY_TRANSFERRING_ONE_CARBON_GROUPS	36	-0.56	-1.76	0.00	0.01
TRANSLATIONAL_INITIATION	37	-0.56	-1.76	0.00	0.01
REGULATION_OF_ENDOCYTOSIS	15	-0.68	-1.76	0.01	0.01
LIPID_TRANSPORT	27	-0.60	-1.75	0.00	0.01
REGULATION_OF_TRANSPORT	62	-0.51	-1.75	0.00	0.01
RESPONSE_TO_ENDOGENOUS_STIMULUS	184	-0.43	-1.75	0.00	0.01
NUCLEAR_EXPORT	31	-0.58	-1.75	0.00	0.01
GTP_BINDING	43	-0.54	-1.75	0.00	0.01
PROTEOLYSIS	176	-0.43	-1.75	0.00	0.01
DNA_HELICASE_ACTIVITY	25	-0.60	-1.75	0.01	0.01
NEGATIVE_REGULATION_OF_CELLULAR_COMPONENT_ORGANIZATION_AND_BIOGENESIS	27	-0.60	-1.75	0.00	0.01
NITROGEN_COMPOUND_CATABOLIC_PROCESS	29	-0.58	-1.75	0.00	0.01
HETEROCYCLE_METABOLIC_PROCESS	23	-0.61	-1.74	0.00	0.01
GUANYL_NUCLEOTIDE_BINDING	44	-0.52	-1.74	0.00	0.01
MEMBRANE_ORGANIZATION_AND_BIOGENESIS	127	-0.44	-1.74	0.00	0.01
GOLGI_ASSOCIATED_VESICLE	28	-0.59	-1.74	0.01	0.01
RNA_SPLICING	86	-0.47	-1.74	0.00	0.01
AMINE_METABOLIC_PROCESS	136	-0.45	-1.74	0.00	0.01
CYTOSKELETAL_PROTEIN_BINDING	151	-0.44	-1.73	0.00	0.01
MRNA_METABOLIC_PROCESS	81	-0.48	-1.73	0.00	0.01
CELLULAR_RESPIRATION	19	-0.64	-1.73	0.01	0.01
MITOCHONDRIAL_MATRIX	45	-0.53	-1.73	0.00	0.01
ACTIN_BINDING	68	-0.49	-1.73	0.00	0.01
ISOMERASE_ACTIVITY	34	-0.56	-1.72	0.00	0.01
ATPASE_ACTIVITY_COUPLED	90	-0.47	-1.73	0.00	0.01
NUCLEAR_TRANSPORT	85	-0.47	-1.72	0.00	0.01
POSITIVE_REGULATION_OF_SIGNAL_TRANSDUCTION	120	-0.45	-1.72	0.00	0.01
NUCLEOLAR_PART	18	-0.64	-1.72	0.00	0.01
AMINE_CATABOLIC_PROCESS	27	-0.57	-1.72	0.01	0.01
RIBONUCLEOTIDE_METABOLIC_PROCESS	15	-0.67	-1.72	0.01	0.01

RAS_GTPASE_BINDING	25	-0.59	-1.72	0.01	0.01
PHOSPHOINOSITIDE_BIOSYNTHETIC_PROCESS	22	-0.61	-1.71	0.00	0.02
MICROTUBULE_ASSOCIATED_COMPLEX	39	-0.53	-1.71	0.00	0.02
MITOCHONDRIAL_LUMEN	45	-0.53	-1.71	0.00	0.02
KINASE_BINDING	67	-0.49	-1.71	0.00	0.02
HYDROLASE_ACTIVITY_ACTING_ON_CARBON_NITROGEN_NOT_PEPTIDEBONDS	43	-0.53	-1.71	0.00	0.02
INORGANIC_CATION_TRANSMEMBRANE_TRANSPORTER_ACTIVITY	54	-0.50	-1.71	0.00	0.02
MACROMOLECULE_CATABOLIC_PROCESS	125	-0.45	-1.71	0.00	0.02
SMALL_NUCLEAR_RIBONUCLEOPROTEIN_COMPLEX	21	-0.61	-1.71	0.01	0.02
ACETYLGLUCOSAMINYLTRANSFERASE_ACTIVITY	16	-0.65	-1.71	0.01	0.02
REGULATION_OF_CELLULAR_PROTEIN_METABOLIC_PROCESS	156	-0.43	-1.70	0.00	0.02
OXIDOREDUCTASE_ACTIVITY_GO_0016616	47	-0.51	-1.70	0.00	0.02
UBIQUITIN_PROTEIN_LIGASE_ACTIVITY	46	-0.52	-1.70	0.00	0.02
REGULATION_OF_INTRACELLULAR_TRANSPORT	25	-0.58	-1.70	0.01	0.02
NUCLEAR_ENVELOPE	72	-0.47	-1.70	0.00	0.02
PROTEIN_AMINO_ACID_O_LINKED_GLYCOSYLATION	18	-0.63	-1.70	0.01	0.02
LYASE_ACTIVITY	53	-0.51	-1.69	0.00	0.02
NEGATIVE_REGULATION_OF_DEVELOPMENTAL_PROCESS	189	-0.42	-1.69	0.00	0.02
CELLULAR_MACROMOLECULE_CATABOLIC_PROCESS	94	-0.45	-1.69	0.00	0.02
PORE_COMPLEX	36	-0.54	-1.69	0.00	0.02
OUTER_MEMBRANE	24	-0.58	-1.69	0.01	0.02
RAS_PROTEIN_SIGNAL_TRANSDUCTION	65	-0.48	-1.69	0.00	0.02
NUCLEOCYTOPLASMIC_TRANSPORT	84	-0.46	-1.69	0.00	0.02
LIPOPROTEIN_BIOSYNTHETIC_PROCESS	24	-0.58	-1.69	0.01	0.02
GENERATION_OF_PRECURSOR_METABOLITES_AND_ENERGY	111	-0.44	-1.68	0.00	0.02

REGULATION_OF_TRANSLATIONAL_INITIATION	30	-0.55	-1.68	0.01	0.02
SIGNAL_SEQUENCE_BINDING	15	-0.67	-1.68	0.01	0.02
CHROMOSOME_ORGANIZATION_AND_BIOGENESIS	119	-0.44	-1.68	0.00	0.02
PURINE_NUCLEOTIDE_BINDING	197	-0.41	-1.68	0.00	0.02
PURINE_RIBONUCLEOTIDE_BINDING	191	-0.41	-1.68	0.00	0.02
MICROSOME	32	-0.55	-1.68	0.01	0.02
ELECTRON_TRANSPORT_GO_0006118	44	-0.52	-1.68	0.00	0.02
ORGANELLE_OUTER_MEMBRANE	24	-0.58	-1.67	0.01	0.02
VESICULAR_FRACTION	34	-0.53	-1.67	0.00	0.02
PROTEIN_HETERODIMERIZATION_ACTIVITY	74	-0.46	-1.67	0.01	0.02
CARBOXYLIC_ACID_TRANSPORT	39	-0.52	-1.67	0.01	0.02
ER_GOLGI_INTERMEDIATE_COMPARTMENT	22	-0.58	-1.67	0.01	0.02
ACTIN_FILAMENT_BINDING	22	-0.59	-1.67	0.01	0.02
REGULATION_OF_PROTEIN_METABOLIC_PROCESS	165	-0.42	-1.67	0.00	0.02
RESPONSE_TO_DNA_DAMAGE_STIMULUS	150	-0.42	-1.66	0.00	0.02
REGULATION_OF_NUCLEOCYTOPLASMIC_TRANSPORT	22	-0.59	-1.66	0.01	0.02
CELLULAR_COMPONENT_DISASSEMBLY	33	-0.54	-1.66	0.00	0.02
PROTEIN_KINASE_BINDING	59	-0.48	-1.66	0.00	0.02
NUCLEOTIDE_BINDING	209	-0.40	-1.66	0.00	0.02
SMALL_CONJUGATING_PROTEIN_LIGASE_ACTIVITY	48	-0.50	-1.66	0.00	0.02
SMALL_GTPASE_MEDIATED_SIGNAL_TRANSDUCTION	85	-0.46	-1.66	0.00	0.02
DNA_DIRECTED_RNA_POLYMERASE_COMPLEX	15	-0.64	-1.65	0.01	0.02
SECONDARY_ACTIVE_TRANSMEMBRANE_TRANSPORTER_ACTIVITY	42	-0.51	-1.65	0.00	0.02
OXIDOREDUCTASE_ACTIVITY_ACTING_ON_THE_CH_CH_GROUP_OF_DONORS	20	-0.59	-1.66	0.01	0.02
CARBOHYDRATE_KINASE_ACTIVITY	15	-0.64	-1.65	0.01	0.02

AMINO_ACID_CATABOLIC_PROCESS	25	-0.57	-1.66	0.01	0.02
GLUCOSE_METABOLIC_PROCESS	26	-0.55	-1.66	0.00	0.02
REGULATION_OF_MAP_KINASE_ACTIVITY	62	-0.47	-1.65	0.00	0.02
RNA_POLYMERASE_COMPLEX	15	-0.64	-1.65	0.01	0.02
MEMBRANE_LIPID_METABOLIC_PROCESS	95	-0.45	-1.65	0.00	0.02
UBIQUITIN_LIGASE_COMPLEX	26	-0.56	-1.65	0.01	0.02
RESPONSE_TO_UV	26	-0.56	-1.65	0.01	0.02
REGULATION_OF_DEVELOPMENTAL_PROCESS	415	-0.38	-1.65	0.00	0.02
REGULATION_OF_CELL_CYCLE	171	-0.41	-1.65	0.00	0.02
RESPONSE_TO_TEMPERATURE_STIMULUS	16	-0.63	-1.65	0.02	0.02
PHOSPHOLIPID_METABOLIC_PROCESS	70	-0.46	-1.65	0.00	0.02
ORGANIC_ACID_TRANSPORT	40	-0.51	-1.65	0.01	0.02
STEROID_METABOLIC_PROCESS	58	-0.48	-1.65	0.01	0.02
NUCLEAR_DNA_DIRECTED_RNA_POLYMERASE_COMPLEX	15	-0.64	-1.64	0.02	0.02
INTERPHASE	67	-0.47	-1.64	0.00	0.02
ENZYME_REGULATOR_ACTIVITY	308	-0.39	-1.64	0.00	0.02
NUCLEOTIDYLTRANSFERASE_ACTIVITY	47	-0.49	-1.64	0.00	0.02
NEGATIVE_REGULATION_OF_GROWTH	38	-0.52	-1.64	0.01	0.02
NUCLEAR_CHROMOSOME	51	-0.49	-1.64	0.00	0.02
GLYCOPROTEIN_METABOLIC_PROCESS	88	-0.44	-1.64	0.00	0.02
STRUCTURAL_MOLECULE_ACTIVITY	218	-0.40	-1.64	0.00	0.02
COFACTOR_BINDING	21	-0.59	-1.63	0.01	0.03
ENDOSOME	63	-0.47	-1.63	0.01	0.03
PROTEIN_KINASE_CASCADE	276	-0.39	-1.63	0.00	0.03
NEGATIVE_REGULATION_OF_CELLULAR_PROTEIN_METABOLIC_PROCESS	44	-0.49	-1.63	0.01	0.03
PHOSPHOINOSITIDE_METABOLIC_PROCESS	29	-0.54	-1.63	0.01	0.03
CELLULAR_LIPID_CATABOLIC_PROCESS	31	-0.53	-1.63	0.01	0.03
DNA_REPAIR	117	-0.42	-1.63	0.00	0.03

RIBONUCLEASE_ACTIVITY	19	-0.60	-1.62	0.02	0.03
SMALL_PROTEIN_CONJUGATING_ENZYME_ACTIVITY	48	-0.48	-1.62	0.01	0.03
PROTEOGLYCAN_METABOLIC_PROCESS	21	-0.58	-1.62	0.02	0.03
IDENTICAL_PROTEIN_BINDING	290	-0.38	-1.62	0.00	0.03
CLATHRIN_COATED_VESICLE	36	-0.52	-1.62	0.01	0.03
REGULATION_OF_ACTION_POTENTIAL	17	-0.60	-1.62	0.02	0.03
CELLULAR_PROTEIN_COMPLEX_ASSEMBLY	31	-0.54	-1.61	0.01	0.03
HOMEOSTASIS_OF_NUMBER_OF_CELLS	19	-0.59	-1.61	0.02	0.03
DNA_DIRECTED_RNA_POLYMERASEII_HOLOENZYME	63	-0.46	-1.61	0.00	0.03
POSITIVE_REGULATION_OF_CATALYTIC_ACTIVITY	155	-0.41	-1.61	0.00	0.03
ANTIOXIDANT_ACTIVITY	17	-0.60	-1.61	0.02	0.03
PROTEIN_AMINO_ACID_LIPIDATION	22	-0.57	-1.61	0.02	0.03
POSITIVE_REGULATION_OF_MAP_KINASE_ACTIVITY	42	-0.50	-1.61	0.00	0.03
INTRAMOLECULAR_OXIDOREDUCTASE_ACTIVITY	18	-0.59	-1.61	0.02	0.03
REGULATION_OF_PROTEIN_MODIFICATION_PROCESS	42	-0.49	-1.60	0.01	0.03
DNA_REPLICATION	95	-0.43	-1.60	0.00	0.03
CYTOSKELETON	329	-0.38	-1.60	0.00	0.03
POSITIVE_REGULATION_OF_TRANSFERASE_ACTIVITY	79	-0.44	-1.60	0.00	0.03
PROTEIN_RNA_COMPLEX_ASSEMBLY	64	-0.46	-1.60	0.01	0.03
AEROBIC_RESPIRATION	15	-0.64	-1.60	0.03	0.03
CELLULAR_CARBOHYDRATE_CATABOLIC_PROCESS	22	-0.58	-1.60	0.01	0.03
REGULATION_OF_PROTEIN_AMINO_ACID_PHOSPHORYLATION	29	-0.55	-1.59	0.01	0.03
INTERPHASE_OF_MITOTIC_CELL_CYCLE	61	-0.47	-1.59	0.01	0.03
OXIDOREDUCTASE_ACTIVITY_ACTING_ON_CH_OH_GROUP_OF_DONORS	53	-0.47	-1.59	0.01	0.03
OXIDOREDUCTASE_ACTIVITY_ACTING_ON_THE_ALDEHYDE_OR_OXO_GROUP_OF_DONORS	22	-0.57	-1.59	0.02	0.03

CHROMATIN_MODIFICATION	53	-0.47	-1.59	0.01	0.03
POST_TRANSLATIONAL_PROTEIN_MODIFICATION	457	-0.37	-1.59	0.00	0.03
GLYCOPROTEIN_BIOSYNTHETIC_PROCESS	72	-0.45	-1.59	0.01	0.03
GLYCEROPHOSPHOLIPID_METABOLIC_PROCESS	43	-0.49	-1.59	0.01	0.03
PHOSPHOTRANSFERASE_ACTIVITY_ALCOHOL_GROUP_AS_ACCEPTOR	322	-0.37	-1.59	0.00	0.03
NUCLEOPLASM	266	-0.38	-1.59	0.00	0.03
NEGATIVE_REGULATION_OF_PROTEIN_METABOLIC_PROCESS	46	-0.48	-1.58	0.01	0.04
PHOSPHORYLATION	297	-0.37	-1.58	0.00	0.04
REGULATION_OF_CATALYTIC_ACTIVITY	260	-0.38	-1.58	0.00	0.04
COFACTOR_METABOLIC_PROCESS	51	-0.47	-1.58	0.01	0.04
METHYLTRANSFERASE_ACTIVITY	35	-0.51	-1.58	0.01	0.04
CELL_CYCLE_GO_0007049	298	-0.37	-1.58	0.00	0.04
DRUG_BINDING	16	-0.61	-1.57	0.02	0.04
DNA_CATABOLIC_PROCESS	23	-0.56	-1.57	0.02	0.04
HISTONE_MODIFICATION	22	-0.56	-1.58	0.03	0.04
TRANSCRIPTION_FACTOR_BINDING	292	-0.37	-1.57	0.00	0.04
MITOTIC_CELL_CYCLE	151	-0.40	-1.57	0.00	0.04
LEADING_EDGE	47	-0.47	-1.57	0.01	0.04
REGULATION_OF_MOLECULAR_FUNCTION	306	-0.37	-1.57	0.00	0.04
PROTEIN_N_TERMINUS_BINDING	36	-0.50	-1.57	0.02	0.04
HYDROGEN_ION_TRANSMEMBRANE_TRANSPORTER_ACTIVITY	23	-0.55	-1.57	0.03	0.04
RESPONSE_TO_HORMONE_STIMULUS	30	-0.52	-1.57	0.01	0.04
MITOCHONDRIAL_OUTER_MEMBRANE	18	-0.58	-1.57	0.03	0.04
CELL_CYCLE_PHASE	165	-0.39	-1.57	0.00	0.04
ESTABLISHMENT_AND_OR_MAINTENANCE_OF_CHROMATIN_ARCHITECTURE	74	-0.43	-1.56	0.00	0.04
ACTIVE_TRANSMEMBRANE_TRANSPORTER_ACTIVITY	115	-0.40	-1.56	0.01	0.04
BIOPOLYMER_CATABOLIC_PRO	106	-0.41	-1.56	0.01	0.04

CESS					
REGULATION_OF_PROTEIN_IMPORT_INTO_NUCLEUS	16	-0.60	-1.56	0.04	0.04
REGULATION_OF_CELLULAR_COMPONENT_ORGANIZATION_AND_BIOGENESIS	120	-0.41	-1.56	0.00	0.04
SPLICEOSOME	49	-0.47	-1.56	0.01	0.04
MONOVALENT_INORGANIC_CATION_TRANSMEMBRANE_TRANSPORTER_ACTIVITY	30	-0.51	-1.56	0.02	0.04
POSITIVE_REGULATION_OF_PHOSPHATE_METABOLIC_PROCESS	26	-0.53	-1.56	0.03	0.04
CHROMOSOME	119	-0.41	-1.55	0.01	0.04
CARBOHYDRATE_CATABOLIC_PROCESS	23	-0.55	-1.55	0.02	0.04
TRANSITION_METAL_ION_BINDING	96	-0.42	-1.55	0.01	0.04
ADENYL_NUCLEOTIDE_BINDING	158	-0.39	-1.55	0.00	0.04
TRANSFERASE_ACTIVITY_TRANSFERRING_GLYCOSYL_GROUPS	105	-0.41	-1.55	0.00	0.04
ONE_CARBON_COMPOUND_METABOLIC_PROCESS	26	-0.53	-1.55	0.03	0.04
CELL_STRUCTURE_DISASSEMBLY_DURING_APOPTOSIS	18	-0.58	-1.55	0.03	0.04
RECEPTOR_MEDIATED_ENDOCYTOSIS	32	-0.51	-1.55	0.02	0.04
PHOSPHORIC_MONOESTER_HYDROLASE_ACTIVITY	110	-0.41	-1.55	0.01	0.04
PERINUCLEAR_REGION_OF_CYTOPLASM	50	-0.47	-1.55	0.02	0.04
REGULATION_OF_PROTEIN_KINASE_ACTIVITY	143	-0.39	-1.55	0.00	0.04
NUCLEOPLASM_PART	203	-0.39	-1.54	0.00	0.04
REGULATION_OF_SIGNAL_TRANSDUCTION	211	-0.37	-1.54	0.00	0.04
ADENYL_RIBONUCLEOTIDE_BINDING	152	-0.39	-1.54	0.00	0.05
FATTY_ACID_METABOLIC_PROCESS	52	-0.46	-1.54	0.02	0.05
PEROXISOME	45	-0.46	-1.54	0.02	0.05
REGULATION_OF_CELL_GROWTH	44	-0.47	-1.54	0.01	0.05
LIPID_CATABOLIC_PROCESS	34	-0.50	-1.54	0.02	0.05
INDUCTION_OF_APOPTOSIS_BY_EXTRACELLULAR_SIGNALS	27	-0.53	-1.53	0.04	0.05

CHROMATIN	35	-0.49	-1.53	0.02	0.05
AMINO_ACID_TRANSPORT	26	-0.51	-1.53	0.03	0.05
SECRETORY_PATHWAY	82	-0.42	-1.53	0.01	0.05
ATP_BINDING	145	-0.39	-1.53	0.00	0.05
PEPTIDYL_AMINO_ACID_MODIFICATION	60	-0.44	-1.53	0.01	0.05
RESPONSE_TO_DRUG	19	-0.55	-1.53	0.04	0.05
ACTIN_FILAMENT_BASED_PROCESS	111	-0.41	-1.53	0.01	0.05
MICROBODY	45	-0.46	-1.52	0.02	0.05
NAME	**SIZE**	**ES**	**NES**	**NOM p-val**	**FDR q-val**
CYTOKINE_ACTIVITY	93	0.51	2.15	0.00	0.00
CHEMOKINE_RECEPTOR_BINDING	32	0.65	2.16	0.00	0.00
CHEMOKINE_ACTIVITY	31	0.66	2.18	0.00	0.00
G_PROTEIN_COUPLED_RECEPTOR_BINDING	43	0.56	2.05	0.00	0.01
HEMATOPOIETIN_INTERFERON_CLASSD200_DOMAIN_CYTOKINE_RECEPTOR_BINDING	23	0.60	1.87	0.01	0.04

Transcription Factors Differentially Expressed in Lung and Lung Stem Cells

Statistical and Bioinformatics Analysis was performed by the Center for Computational Cancer Biology (CCCB) at Dana-Farber Cancer Institute.

Array quality was assessed using the R/Bioconductor package (Gentleman et al., 2004). All arrays passed visual inspection and no technical outliers were identified. Raw CEL files were processed using the robust multiarray average (RMA) algorithm (Irizarry et al., 2003). To identify genes correlating with the phenotypic groups, we used limma (Smyth, 2004) to fit a statistical linear model to the data and then tested for differential gene expression in the contrasts of interest. Results were adjusted for multiple testing using the Benjamini and Hochberg (BH) method (Benjamini and Hochberg, 1995), and significance was determined using a False-Discovery-Rate cutoff of less than 5%.

First, transcription factors were found from the differentially expressed gene lists. Then, separate transcription factor analyses were performed by first filtering the normalized expression values based on GO annotations (Ashburner et al., 2000) to include only genes belonging to that particular class. A statistical linear model was then fit to the filtered dataset and then tested for differential gene expression in the contrasts of interest.

Next, quantitative real-time PCR was performed in wildtype lung samples of Sca1+ (BASC-enriched) and Sca1- (AT2 cell-enriched) cells, or in wildtype Sca1-low (BASC-enriched) and Sca1-high (mesenchymal-enriched) populations. Whole lung or CD31-CD45- (epithelial-enriched) cells served as controls. qPCR results shown are those that verified the array findings.

The following array comparisons from our lab's generated datasets were performed:

- WT lung Sca1+ high vs Sca1+ low
- WT lung Sca1+ vs Sca1-
- WT lung Sca1low vs Sca1-
- Kras;p53-flox Sca1+ vs Kras;p53-flox Sca1-

The following array comparisons from published datasets were performed:

- Mouse adult lung vs other adult tissues
- Mouse adult lung vs embryonic lung (E13.5)
- Human fetal lung vs other fetal tissues
- Human adult lung vs other adult tissues
- Human adult lung vs fetal lung

Mouse embryonic lung (E 13.5) (Naxerova et al., 2008): GSE11539
Mouse adult lung and other adult tissues (Thorrez et al., 2008): GSE9954
Human adult lung and other adult tissues, human fetal lung and other fetal tissues (Su et al., 2004): GSE1133

Table A9: Transcription factors up in lung vs. other organs

Gene Name	Arrays	Literature
Dmtf1	up in human adult lung vs other	deleted in NSCLCs, Myb-like, tumor suppressor, activation of Arf by Ras/Raf signaling is indirectly mediated by Dmp1, macrophage differentiation
Pa2g4 (Ebp1)	up in WT Sca1low vs neg, up in mouse adult lung vs other	enriched in lung branching regions- distal lung mesenchyme
Pou2f2 (Oct2)	up in human fetal lung vs other	lineage specificity of B cells
Six6	up in human fetal lung vs other	expressed in embryonic lung nuclear extracts

Table A10: Transcription factors up epithelial lung cells vs BASCs

Gene Name	Arrays	Literature
Etv5 (Erm)	up in wt Sca1 neg, Kras;p53 Sca1 neg	Expressed in spermatogonial stem cells, Lung AT1 and AT2 cell differentiation
Pbx2	up in wt Sca1 neg, Kras;p53 Sca1 neg	Pre B-cell leukemia TF2, forms transcription complex in myeloid cells-lineage differentiation, Up in lung cancer
Usf2	up in wt Sca1 neg, Kras;p53 Sca1 neg	Induces SP-A expression in development, Up in lung squamous cell carcinoma

Table A11: Transcription factors up in BASC populations vs. other lung populations

Gene Name	Arrays	Literature
Cbx2 (M33)	up in WT Sca1low vs neg, down in WT Sca1high vs low	In PRC1 complex with Bmi1, Polycomb gene (PRC1 complex), expansion of T and B cell precursors
Hopx (Hop)	up in WT Sca1low vs neg, down in WT Sca1high vs low	Acts downstream of Ttf-1, negatively regulates surfactant production. Loss of hopx causes defective AT2 development, increased surfactant, disrupted alveolar formation
Myb	up in Sca1 low, Kras;p53 Sca1 pos	Promotes proliferation and inhibits differentiation in hematopoietic stem and progenitor cells, regulates colon and neural stem cells, colon and breast cancer, Up in lung adenocarcinoma
Nfe2l3 (Nrf3)	up in WT Sca1low vs neg, down in WT Sca1high vs low	Role in placental gene expression and development, Reactive oxygen species balancing and in muscle precursor migration during early embryo development, Role in SMC differentiation from stem cells toward vascular lineage
Six4	up in WT Sca1low vs neg, down in WT Sca1high vs low	Differentiation of neuronal, retinal cells. Also in tooth mammary, uterine buds, limb buds
Sox2	Up in Kras;p53 Sca1pos vs neg, Down in Wt Sca1 high vs low,	
Sox21	up in Sca1 low, Wt Sca1 pos, Kras;p53 Sca1 pos	Expressed in hair follicle progenitors neural stem and progenitor cells, overlapping expression/ counteracts Sox2, Expressed in lung neuroendocrine cells, Antibodies expressed in SCLC, squamous cell carcinoma
Tbx5	up in WT Sca1low vs neg, down in WT Sca1high vs low	lung mesenchyme, induces mesenchymal Fgf10- production of branching signals, target of Hif1a, upregulated by Nkx2.5, forelimb bud formation, cardiac morphogenesis

Table A12: Additional transcription factors found using separate linear model

Gene Name	Arrays	Literature
Erg	Up in WT Sca1 pos vs neg, WT Sca1 low vs neg, down in WT Sca1 high vs low	ETS family, expressed in lung-antiinflammatory effects, overexpressed in lung tumors, regulator of differentiation of early hematopoietic cells, required for the differentiation of embryonic stem cells along the endothelial lineage, requirement in normal HSC and megakaryocyte homeostasis
Glis 3	Up in Kras;p53 Sca1pos vs neg, Down in Wt Sca1 high vs low,	Plays a role in cell lineage specification, particularly in the development of pancreatic beta cells, also regulates insulin gene expression
Hey1	Up in Kras;p53 Sca1 pos vs neg, WT Sca1 low vs Sca1 neg, Down in WT Sca1 high vs low	Inhibits myogenesis, Notch mediator, enriched in lung endothelial cells, highly expressed in lung cancer cell lines
Klf7	Up in Kras;p53 Sca1pos vs neg, WT Sca1 pos vs neg, WT Sca1 low vs Sca1 neg	Regulates differentiation of neuroectodermal and mesodermal cell lineages, mice without Klf7 die at birth and display hypoplastic olfactory bulbs which lack peripheral innervation, iportant for neuronal morphogenesis, required for TrkA gene expression
Prrx1	Up in Kras;p53 Sca1pos vs neg, WT Sca1 pos vs neg, WT Sca1 low vs Sca1 neg	Required for pulmonary vascular development, localizes to differentiating endothelial cells (ECs) within the fetal lung mesenchyme
Purb	Up in Kras;p53 Sca1 pos vs neg, WT SCa1 low vs Sca1 neg, Down in WT Sca1 high vs low	Represses smooth muscle alpha-actin gene transcription
Runx1	Up in Kras;p53 Sca1 pos vs neg, WT SCa1 low vs Sca1 neg, Down in WT Sca1 high vs low	Hematopoetic transcription factor
Sox18	Up in Kras;p53 Sca1 pos vs neg, WT SCa1 low vs Sca1 neg, Down in WT Sca1 high vs low	Very abundant in lung tissue, key regulator of murine and human blood vessel formation, directly targets and trans-activates VCAM-1 expression, expression led to the enhanced proliferation of early hematopoietic precursors while blocking their maturation

Tbx1	Up in Kras;p53 Sca1pos vs neg, Down in Wt Sca1 high vs low,	Regulates proliferation and differentiation of multipotent heart progenitors, regulates Vegfr3 and is required for lymphatic vessel development, expressed in the developing lung epithelium
Tcerg1	Up in Kras;p53 Sca1 pos vs neg, WT SCa1 low vs Sca1 neg, Down in WT Sca1 high vs low	
Tead2 (Etf)	Up in WT Sca1 pos vs neg, WT Sca1 low vs neg, down in WT Sca1 high vs low	Enriched in lung during development and adult, YAP/Hippo pathway, neural tube closure, regulates Pax3
Ttf-1 (Nkx2-1)	Down in Kras;p53 Sca1pos vs neg	Regulates differentiation of lung epithelial cells during development, lost in lung adenocarcinoma metastasis
Zeb1	Up in Kp53 pos vs neg, Up in WT Sca1pos vs neg,	EMT regulator (repressses Ecad), Knockdown suppresses anchorage-independent growth of lung cancer cell lines, associated with poor prognosis and EGFR resistance in lung cancer, promotes metastasis
Zfp423	Up in WT Sca1 pos vs neg, WT Sca1 low vs neg, down in WT Sca1 high vs low	Transcriptional regulator of preadipocyte determination, deregulated expression contributes to CML, required for normal cerebellar development, controls proliferation and differentiation of neural precursors in cerebellar vermis formation

Figure A-1: **Expression of Transcription Factors in BASCs and AT2 cells. A.** Quantitative real-time PCR analysis of relative Etv5 mRNA levels in whole lung cells, lung epithelial cells (CD31-CD45-), BASCs (CD31-CD45-Sca1+), or AT2 cells (CD31-CD45-Sca1-). Each set (1-2) represents samples from a separate sort and mouse. **B.** Quantitative real-time PCR analysis of relative Ttf-1 mRNA levels in lung epithelial cells (CD31-CD45-), BASCs (CD31-CD45-Sca1+), or AT2 cells (CD31-CD45-Sca1-). Each set (1-2) represents samples from a separate sort and mouse. **C.** Quantitative real-time PCR analysis of relative Sox21 mRNA levels in whole lung cells, lung epithelial cells (CD31-CD45-), BASCs (CD31-CD45-Sca1+), or AT2 cells (CD31-CD45-Sca1-). **D.** Quantitative real-time PCR analysis of relative Sox2 mRNA levels in whole lung cells, lung epithelial cells (CD31-CD45-), BASCs (CD31-CD45-Sca1+), or AT2 cells (CD31-CD45-Sca1-). Each set (1-2) represents samples from a separate sort and mouse. **E.** Quantitative real-time PCR analysis of relative Six4 mRNA levels in whole lung cells or BASCs (CD31-CD45-Sca1^{low}), or mesenchymal cells (CD31-CD45-Sca1^{high}). Each set (1-3) represents samples from a separate mouse. **F.** Quantitative real-time PCR analysis of relative Myb mRNA levels in whole lung cells, BASCs (CD31-CD45-Sca1^{low}), or mesenchymal cells (CD31-CD45-Sca1^{high}). Each set (1-3) represents samples from a separate mouse. Error bars represent the standard deviation of the mean.

Figure A-1: (continued)

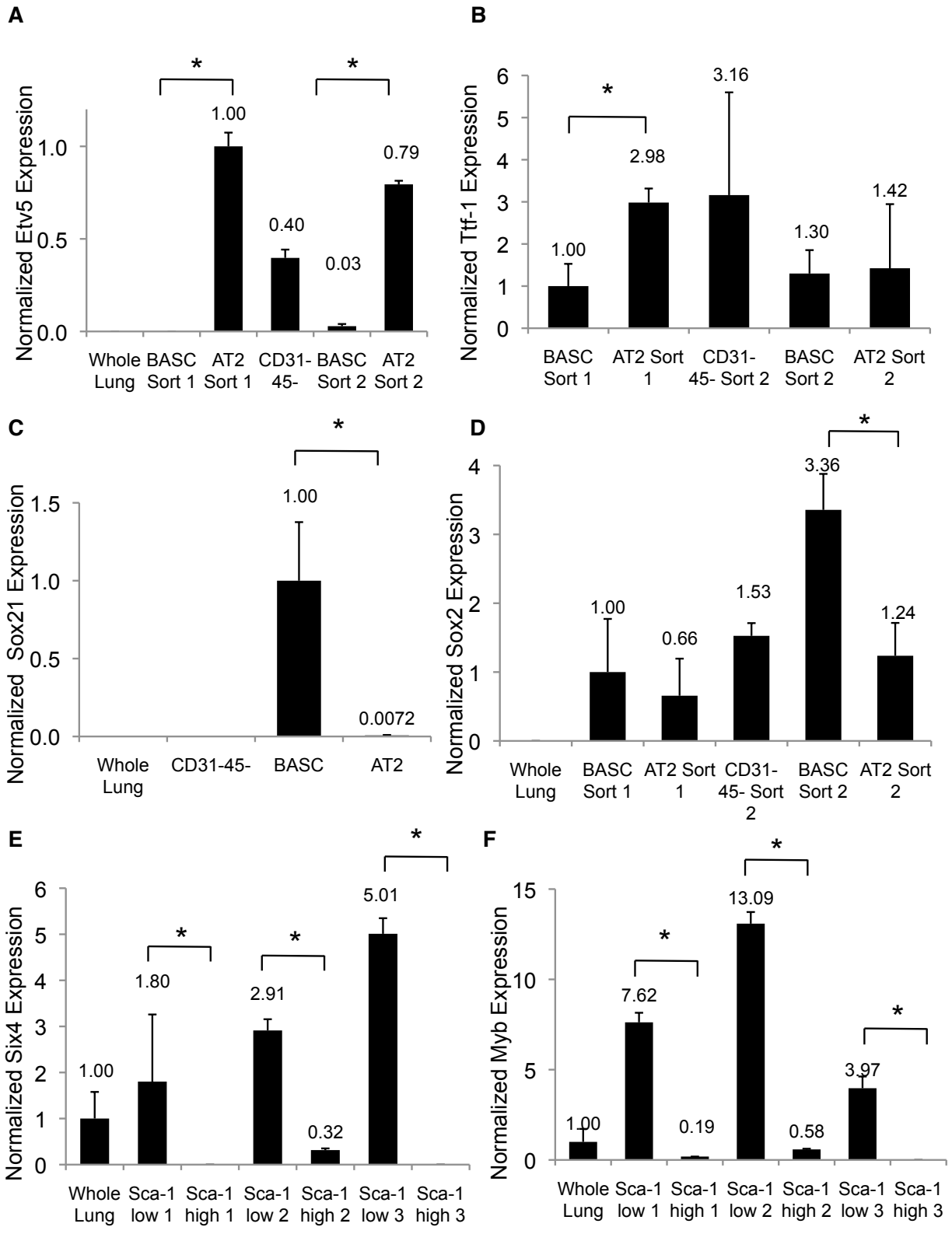

Ashburner, M., Ball, C.A., Blake, J.A., Botstein, D., and Butler, H. (2000). Gene Ontology: tool for the unification of biology. Nat. Genet. *25*, 25-29.

Benjamini, Y., and Hochberg, Y. (1995). Controlling the false discovery rate: a practical and powerful approach to multiple testing. J. R. Stat. Soc. Ser. B *57*, 289-300.

Gentleman, R.C., Carey, V.J., Bates, D.M., Bolstad, B., Dettling, M., Dudoit, S., Ellis, B., Gautier, L., Ge, Y., Gentry, J., et al. (2004). Bioconductor: open software development for computational biology and bioinformatics. Genome Biol. *5*, R80.

Irizarry, R.A., Hobbs, B., Collin, F., Beazer-Barclay, Y.D., Antonellis, K.J., Scherf, U., and Speed, T.P. (2003). Exploration, normalization, and summaries of high density oligonucleotide array probe level data. Biostatistics *4*, 249–264.

Naxerova, K., Bult, C.J., Peaston, A., and Fancher, K. (2008). Analysis of gene expression in a developmental context emphasizes distinct biological leitmotifs in human cancers. Genome Biol. *9*, R108.

Smyth, G.K. (2004). Linear models and empirical bayes methods for assessing differential expression in microarray experiments. Stat. Appl. Genet. Mol. Biol. *3*, Article3.

Su, A.I., Wiltshire, T., Batalov, S., and Lapp, H. (2004). A gene atlas of the mouse and human protein-encoding transcriptomes Proc. Natl. Acad. Sci. U.S.A. *101*, 6062-6067.

Thorrez, L., Van Deun, K., Tranchevent, L.-C., Van Lommel, L., Engelen, K., Marchal, K., Moreau, Y., Van Mechelen, I., and Schuit, F. (2008). Using ribosomal protein genes as reference: a tale of caution. PLoS ONE *3*, e1854.

Testing of CCSP and SPC knock-in mice for lineage tracing

Two mice strains were created with the intent to be able to do lineage tracing of the BASC population. The first strain uses tamoxifen-inducible Flp recombinase (Flp-ER) to restricted to Clara cells and BASCs: the “CKI 1” strain contrains a FlpER- IRES-GFP allele knocked in to the endogenous CCSP locus. For the strain named “CKI 2,” a Frt-Stop-Frt-Cre-ERT2-IRES-mCherry cassette was knocked in to the endogenous SPC locus, a BASC-specific component when used in combination with CCSP-FlpER. In mice containing both CKI 1 and CKI 2 alleles (CCSP-FlpER-IRES-GFP; SPC-Frt-Stop-Frt-CreER-IRES-mCherry mice), only SPC-expressing cells will transcribe Cre-ERT2 after Flp-mediated recombination. This would enable spatial (BASC-specific) and temporal (in adult vs. all of development) regulation of Cre expression.

In CKI 1 mice, qPCR analysis showed that knock-in mice had expression of Flp and reduced expression levels of CCSP as expected (qPCR was performed by Dave Raiser). However, after many experiments testing several doses or methods (IP injection or oral gavage) of tamoxifen delivery, both tissue staining and FACS experiments failed to show expression of Flp dependent fluorescent reporters. This indicated that the CKI 1 mice were not functioning as expected. In CKI2 mice, 1 experiment was done to test the leakiness of the SPC-FSF-CreER by giving CKI2; LSL-YFP mice (with no Flip driver) tamoxifen by IP injection. YFP expression was not detected. A final set of experiments was done combining both CKI 1 and CKI 2 alleles along with Kras and LSL-YFP. YFP expression was not detected in these mice 3-4 months after IP tamoxifen injection, and no tumors were formed, indicating that one or both knock-in alleles was not functioning properly. CKI2 mice were then further tested by Kristen Leeman using B-actin Flp mice and AdFlpO virus.

Figure A-2: **Diagrams of knock-in mice and reporters tested. A.** CKI 1: CCSP-FlpER- IRES-GFP. **B.** CKI 2: SPC-Frt-Stop-Frt -CreER- IRES-mCherry. **C.** Fela: Rosa26-Frt-Stop-Frt-LoxP-GFP-Stop-LoxP-βGal **D.** Frepe: Rosa26-Frt-Stop-Frt-LoxP-mCherry-Stop-LoxP-GFP

Figure A-2: (continued)

A

Mice tested:

CKI 1: CCSP-FlpER-IRES-GFP

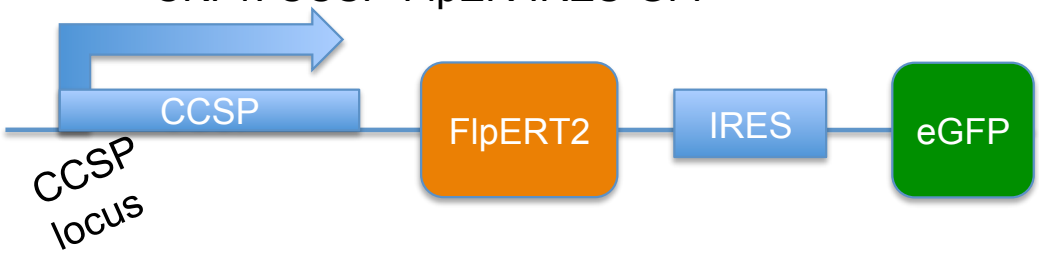

B

CKI 2: SPC-FSF-CreER-IRES-mCherry

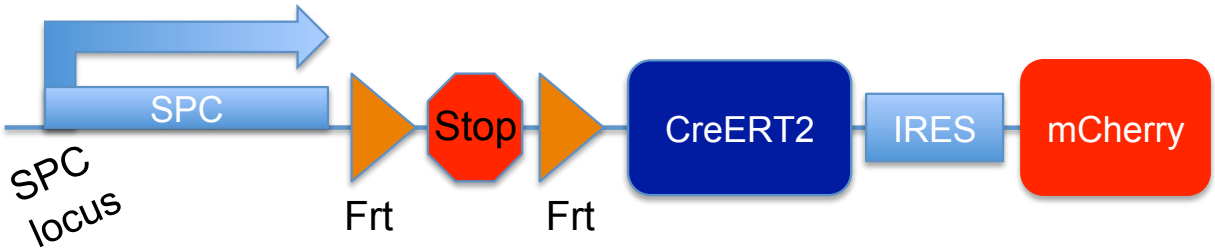

Fluorescent reporter mice:

C

Fela:

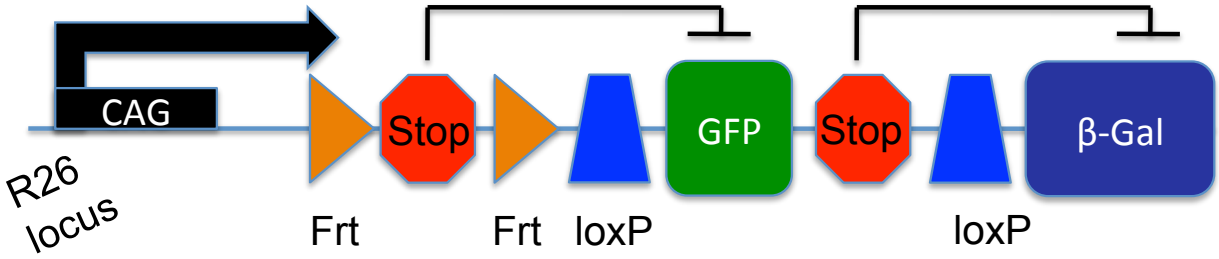

D

Frepe:

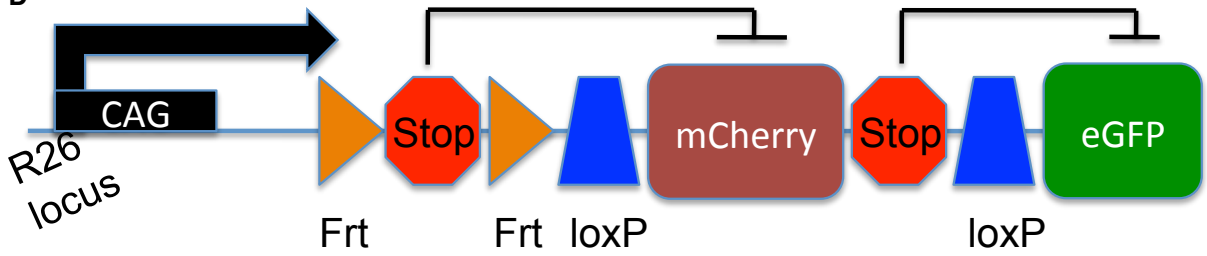

Figure A-3: **Testing CKI 1 mice. A.** Quantitative real-time PCR analysis of relative Flp mRNA levels in CKI1 mice compared to non-CKI 1littermate controls. Error bars represent the standard deviation of the mean. **B.** Quantitative real-time PCR analysis of relative CCSP mRNA levels in CKI1 mice compared to non-CKI 1 littermate controls. Error bars represent the standard deviation of the mean. **C.-E.** Immunofluorescent staining for CCSP (red) and YFP/GFP (green) in lung slides from **C.** wildtype 129 mice (negative control) **D.** CC10Cre-ER; LSL-YFP mice (positive control) **E.** tamoxifen-treated CKI 1.1; Fela mice **F.-H.** Representative FACS analysis for GFP expression in CD31-CD45- lung cells from **F.** wildtype 129 mice (negative control) **G.** B-actin-GFP mice (positive control) **H.** tamoxifen-treated CKI 1.1; Fela mice **I.** Table showing tamoxifen doses, delivery method and reporter mice tested.

Figure A-3: (continued)

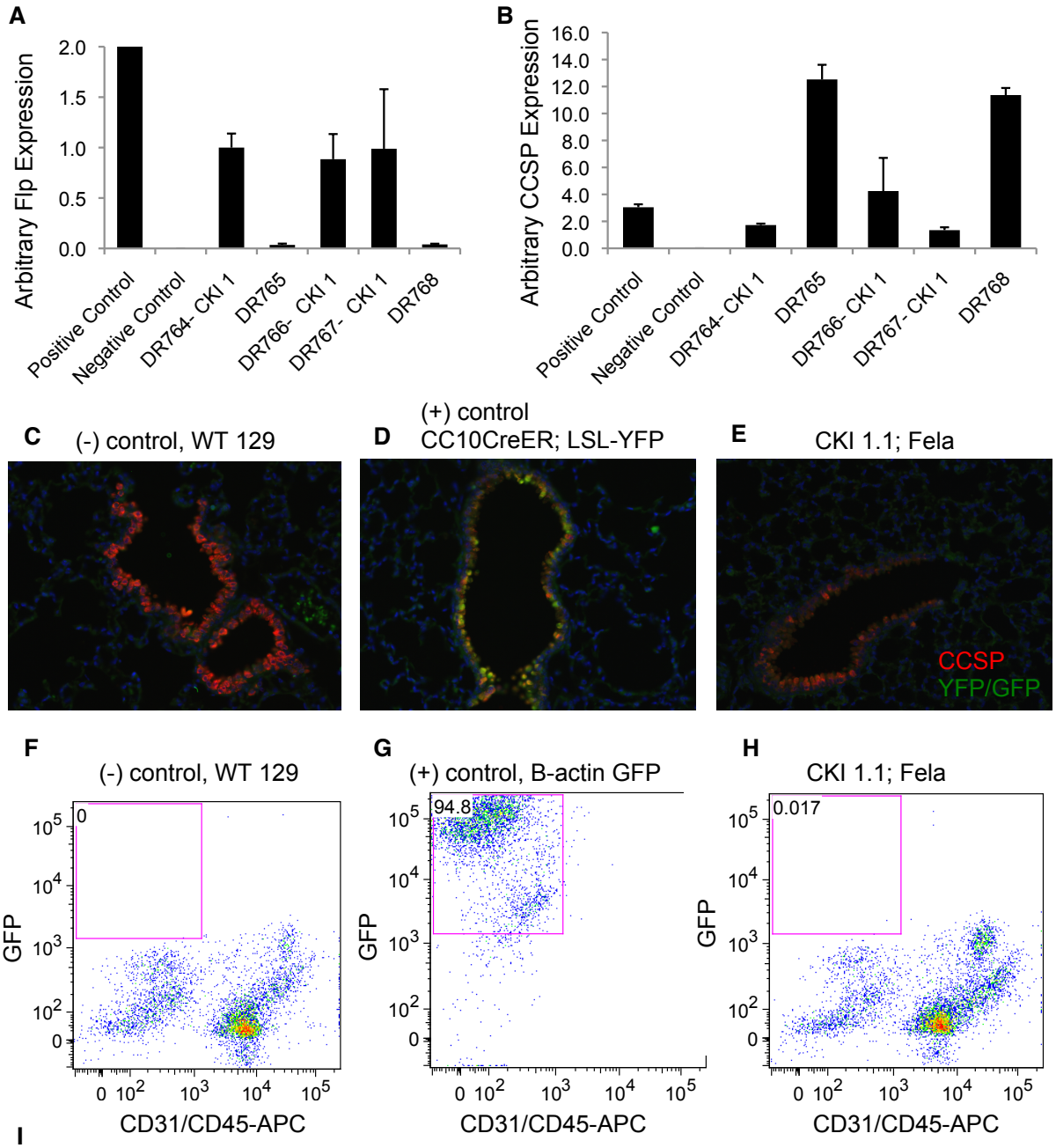

I

Doses Tamoxifen	Number of Doses	Delivery Method	Reporter mouse
0.25 mg/g	4- every other day	IP injection	Frepe
0.20 mg/g	4- every other day	Oral gavage	Frepe, Fela
0.25 mg/g, 0.35 mg/g last dose	5- three in a row, last two two days apart	Oral gavage	Fela
0.25mg/g	7- every day for 1 week	Oral gavage	Fela

Figure A-4: **Testing CKI1 and CKI2 mice. A.-E.** FACS analysis of YFP expression in CD31-CD45- EpCAM+ lung cells from **A.** untreated CKI2 mice (negative control) **B.** untreated CKI2; LSL-YFP mice (negative control) **C.** untreaed B-actin-Flp; CKI2; LSL-YFP mice (negative control) **D.** tamoxifen treated CKI2 mice (negative control for YFP) **E.** tamoxifen treated CKI2; LSL-YFP mice. Results are from one experiment. **F.-H.** FACS analysis of YFP expression in CD31-CD45- EpCAM+ lung cells from **F.** CC10-CreER; LSL-YFP mice (positive control) **G.** corn oil-treated CKI; CKI2; Kras; LSL-YFP mice (negative control) **H.** tamoxifen treated CKI; CKI2; Kras; LSL-YFP mice. Results are representative from two experiments.

Figure A-4: (continued)